IMPACT OF HYPOXIA ON HEPATITIS B VIRUS REPLICATION

NICHOLAS ROSS BAKER FRAMPTON

A thesis submitted to the University of Birmingham for the degree of

Doctor of Philosophy

Institute of Immunology and Immunotherapy

College of Medical and Dental Sciences

University of Birmingham

September 2017

ABSTRACT

Hepatitis B virus (HBV) is one of the world's unconquered diseases, with 370 million chronically infected globally. HBV replicates in hepatocytes within the liver that exist under a range of oxygen tensions from 11% in the peri-portal area to 3% in the peri-central lobules. HBV transgenic mice show a zonal pattern of viral antigen with expression in the peri-central areas supporting a hypothesis that low oxygen regulates HBV replication. We investigated this hypothesis using a recently developed *in vitro* model system that supports HBV replication. We demonstrated that low oxygen significantly increases covalently closed circular viral DNA (cccDNA), viral promoter activity and pre-genomic RNA (pgRNA) levels, consistent with low oxygen boosting viral transcription. Hypoxia inducible factors (HIFs) regulate cellular responses to low oxygen and we investigated a role for HIF-1α or HIF-2α on viral transcription. A combination of HIF inhibitors and silencing of HIF-1α and HIF-2α ablated the effect of low oxygen on cccDNA and pgRNA, suggesting a role in regulating HBV transcription. This study highlights a new role for hepatic oxygen levels to regulate multiple steps in the HBV life cycle and this may impact on future treatments for viral associated pathologies.

DEDICATION & ACKNOWLEDGEMENTS

Firstly, I'd like to thank Professor Jane McKeating for her supervision throughout my PhD and great help in preparing my thesis, her input was invaluable. I'd also like to thank everyone who has ever helped me in the lab. In particular, Peter Balfe, who taught me how to run and analyse PCRs; and Ke Hu, who helped me learn a great many techniques. I'd like to thank all my colleagues from throughout the PhD, both for the fun times and support in the lab. I'd also like to thank Dan Tennant and members of his lab who helped me during the early stages of my PhD. I'd like to thank Chunkyu Ko, Maarten van de Klundert and the Protzer Laboratory for a productive collaboration and help in developing some techniques. I'd also like to thank the Ratcliffe Laboratory for providing many of the reagents used in this study. Finally, I'd like to thank Jane and Peter for giving me the opportunity to study for this PhD and the European Commission for funding my research.

Thank you to my friends and fellow PhD students for supporting me throughout the PhD and providing great memories. Thank you to my parents Helen and Jon for their great advice during my PhD and continued financial, educational and emotional support throughout my life. Lastly, I'd like to thank my wife Rosalind, my constant companion and light of my life.

TABLE OF CONTENTS

LIST OF FIGURES

LIST OF TABLES

LIST OF COMMON ABBREVIATIONS

Akt	Protein Kinase B
ARNT	Aryl Hydrocarbon Receptor Nuclear Translocator
CBP	CREB-Binding Protein
BCP	Basal Core Promoter
cccDNA	Covalently Closed Circular DNA
DHBV	Duck Hepatitis B Virus
DMOG	Dimethyloxalylglycine
DMSO	Dimethyl sulfoxide
EnhI	Enhancer 1
EnhII	Enhancer 2
ERK	Extracellular signal–Regulated Kinases
FIH	factor inhibiting HIF-1
HBc	Hepatitis B Virus Core Protein
HBe	Hepatitis B Virus E Antigen
HBs	Hepatitis B Virus S Antigen
HBV	Hepatitis B Virus
HBx	Hepatitis B Virus X Protein
HCC	Hepatocellular Carcinoma
HIF	Hypoxia Inducible Factor
HNF4a	Hepatocyte Nuclear Factor 4 alpha
HRE	Hypoxic Responsive Element
IFN	Interferon
ISG	Interferon Stimulated Genes
LHB	Large Surface Protein
Luc	Luciferase
MAPK	Mitogen-Activated Protein Kinase
NTCP	Na^+-Taurocholate Cotransporting Polypeptide
ODD	Oxygen-dependent Degradation Domain
ORF	Open Reading Frame
PCR	Polymerase Chain Reaction
pgRNA	Pre-Genomic RNA
PHD	Prolyl Hydroxylases
PHH	Primary Human Hepatocytes
Pol	Polymerase
PTM	Post Translational Modification
rcDNA	Relaxed Circular DNA
ROS	Reactive Oxygen Species
VEGFA	Vascular Endothe
VHL	Von Hippel-Lindau Protein
WHV	Woodchuck Hepatitis Virus

1. INTRODUCTION

1.1 The Liver as the Site for Hepatitis B Infection

The liver is a specialised organ that has diverse roles in the storage and conversion of energy, blood homeostasis, chemical detoxification and immunity to microbial infections. The liver is composed of different cell types: hepatocytes are the most dominant cell type comprising up to 70% of the liver, bile duct epithelium and Kupffer cells. Hepatocytes and bile duct epithelium are unique to the liver and stem from a common progenitor (Fausto, 1990, Thorgeirsson, 1996, Fausto and Campbell, 2003). Hepatocytes are the only confirmed target for all members of the Hepatitis B virus family (Seeger and Mason, 2000) and limited evidence suggests that bile duct epithelial cells, pancreas, kidney and lymphoid cells can be infected by hepadnaviruses, however most of this data was obtained using woodchuck or duck Hepatitis B virus (HBV) (Halpern *et al*., 1983, Jilbert *et al*., 1987, Ogston *et al*., 1989, Nicoll *et al*., 1997).

1.1.1 Liver Structure

The liver can be divided into small sections called lobules, where (**Figure 1.1**) shows a schematic representation demonstrating the role of the liver in blood homeostasis (Seeger and Mason, 2000). Blood enters through the portal veins and hepatic arteries that make up the hepatic portal triad. Blood then splits into smaller vessels and into the sinusoidal spaces, which exist between rows of hepatocytes (Seeger and Mason, 2000). These rows of hepatocytes are typically one cell thick in mammals. Blood flows through spaces that are lined with endothelial cells and Kupffer cells (Kolios *et al*., 2006). These enact various functions in cleaning blood, immune responses and

breakdown of heme into bile. Blood flow continues to the hepatic central vein and exits the liver. This occurs in each lobule separately but ultimately the blood flows into one of several surrounding “central” veins (Seeger and Mason, 2000).

The liver experiences a range of oxygen concentrations from 11% at the hepatic portal triad to 3% in the hepatic central vein. This gradient can be divided into 3 zones as shown in (**Figure 1.2**) (Jungermann and Kietzmann, 2000, Adams and Eksteen, 2006, Wilson *et al*., 2014). These zones are created through the directional blood flow towards the central veins that result in a physiological oxygen gradient (Wilson *et al*., 2014). These zones can also be distinguished based upon carbohydrate metabolic functions, which are modulated through the oxygen tension (Jungermann and Kietzmann, 2000, Gebhardt *et al*., 2007). An oxygen concentration of 3% is considered a hypoxic environment; therefore, part of a healthy liver is continually exposed to low oxygen.

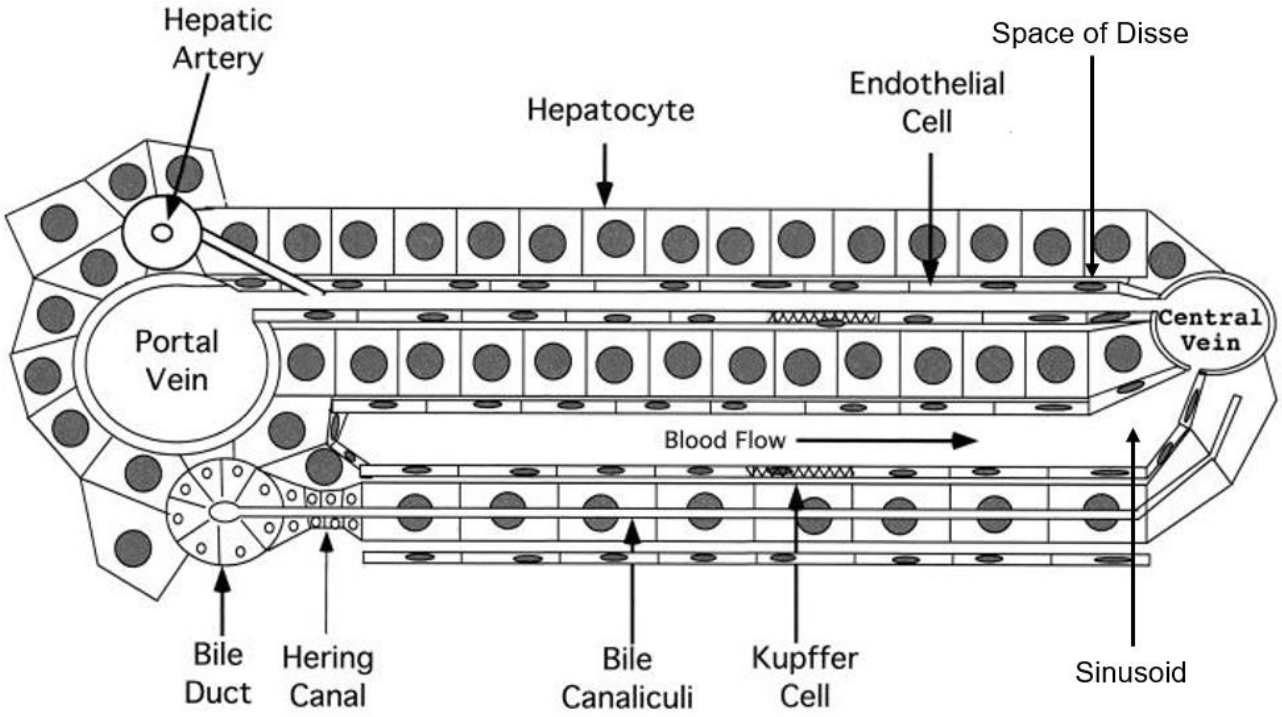

Figure 1.1 Anatomy of the liver lobule (Seeger and Mason, 2000)

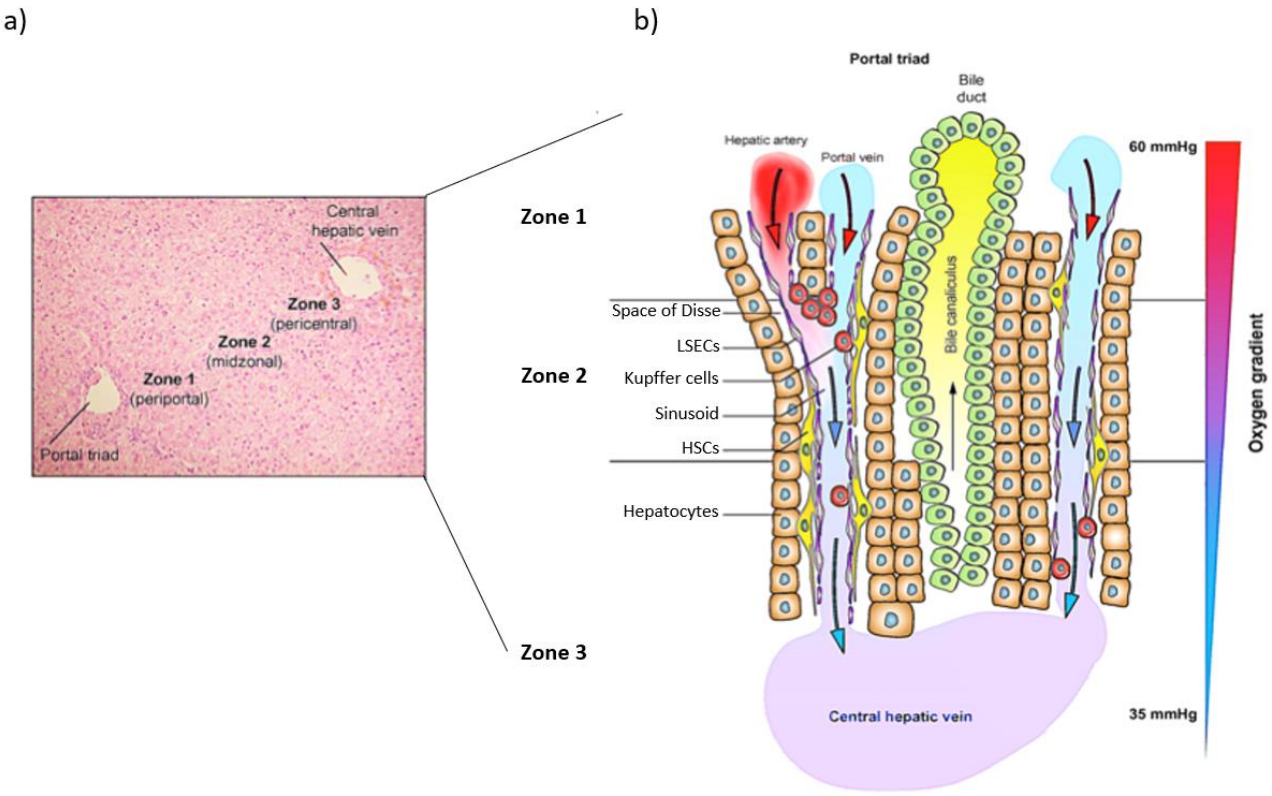

Figure 1.2 Cartoon depicting different zones within a liver lobule (Wilson *et al*., 2014)

A) A hematoxylin and eosin stain of a liver lobule, which is divided into 3 zones**. B)** Schematic representation of the oxygen gradient within the liver.

1.1.2 Liver Differentiation

Hepatocytes are considered “terminally” differentiated and will remain within the liver not dividing for up to 12 months (Seeger and Mason, 2000). However, the capacity of the liver to regenerate following injury is remarkable. Following acute injury and removal of up to 70% of liver mass, hepatocytes can replicate and generate replacements for lost cell mass (Grisham, 1962, MacDonald, 1961, Rhim *et al*., 1994). If required almost the entire cell population can proceed through the cell cycle. However, this is not the only method of regeneration. Literature shows that in circumstances of severe or chronic injury, hepatocytes can become overwhelmed; at this point the hepatic stem cells or oval cells will begin to repair damaged tissues, a process known as ductal reaction (Fausto and Campbell, 2003, Thorgeirsson *et al*., 1993, Thorgeirsson, 1996, Fausto *et al*., 2006). The literature suggests that the progenitor cells reside within the periportal region of the liver (specifically in the canal of Hering **Figure 1.1**) (Coleman *et al*., 1993, Dabeva *et al*., 1993, Evarts *et al*., 1987, Evarts *et al*., 1989, Thorgeirsson *et al*., 1993). When proliferation begins they migrate towards the central vein along the row of hepatocytes, where they will mature into bipotential cells, that proliferate into hepatocytes and finally mature hepatocytes. The cells get larger as they proceed towards the central vein (MacDonald, 1961, Fausto, 1990, Thorgeirsson *et al*., 1993, Zaret and Grompe, 2008).

It is unclear whether HBV can target and infect progenitor cells or if viral nucleic acids spread during division. One of the problems with current treatments for established HBV infections is the persistence of viral DNA in infected hepatocytes, of which up to 35% can be infected in chronically infected patients (Rodriguez-Inigo *et al*., 2003). Removing the virus requires either total elimination of viral DNA from liver cells or complete replacement of infected cells by an uninfected population of progenitor cells.

Hepatocytes provide an incredibly stable and constant environment for hosting HBV infections. The regenerative capacity of the liver is amazing, potentially able to replace all infected cells with uninfected cells, however this simply does not occur fast enough in cells with 6-12 month half life. The virus does not appear to be cytopathic so removal of an established chronic infection would be difficult (Seeger and Mason, 2015).

1.2 Hepatitis B Virus

1.2.1 HBV Epidemiology and Vaccinology

HBV is one of the most common infectious diseases globally. There are approximately 350 million people chronically infected with HBV worldwide and an estimated 2 billion people show serological evidence of a past or present HBV infection. The prevalence of HBV varies geographically; from high levels (>8%) in African regions and East Asia, to intermediate levels (2-7%) in the Middle East and Indian subcontinent and low levels (<2%) in Western Europe and North America (Hou *et al*., 2005, Saeed *et al*., 2014).

HBV infects the liver and can cause both acute and chronic disease. Of those infected more than 90% of healthy adults will recover from the infection within the first year. Approximately 5% of infected adults will develop chronic infections and of these individuals, 20-30% will progress to develop cirrhosis and/or hepatocellular carcinoma (HCC). Those at greater risk of chronic infection are children below the age of 6, with 80-90% of infants infected in the first year of life developing chronic infections (Schweitzer *et al*., 2015). HBV is transmitted through multiple routes however, in areas where HBV is highly endemic, the most common route is from mother to child. This is called perinatal transmission. The second most common route is through exposure to infected blood, called horizontal transmission. Blood is the most important vehicle for

transmission, but other bodily fluids have been implicated such as semen and saliva (Hou *et al*., 2005).

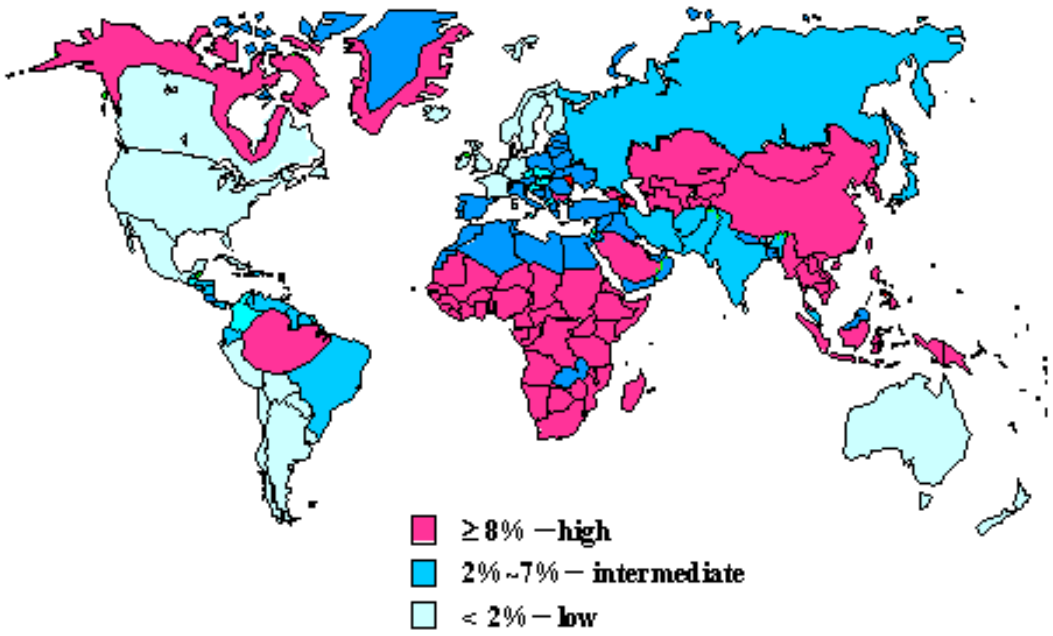

Figure 1.3 Global HBV prevalence (Hou *et al*., 2005)

Transmission from mother to child occurs during the perinatal period. Before HBV vaccination was integrated into routine immunisations, the incidence of babies becoming HBV positive was between 10-30% for mothers that were HBV S antigen (HBsAg) positive and HBV E antigen (HBeAg) negative. These values are important because clinical symptoms for HBV are indistinguishable from other forms of viral hepatitis, so diagnosis is dependent on serological testing for HBV antigens and antibodies against these antigens (Mahoney, 1999). However, transmission rates as high as 70-90% were reported in mothers positive for both HBV antigens (Hou *et al*., 2005, Kwon and Lee, 2011). There are 3 main routes of HBV transmission from mother to baby: transplacental transmission in utero, natal transmission during delivery and post-natal infection during care or breastfeeding (Kwon and Lee, 2011, Hou *et al*., 2005, Choisy *et al*., 2017, Manyahi *et al*., 2017). In many countries where 8-15% of children would develop chronic infections; the use of vaccination has reduced the rate to less than 1% (WHO, 2017, Gentile *et al*., 2014). As of 2013, 183 member states of the UN have agreed to vaccinate infants against HBV (WHO, 2017).

Sexual transmission is another common route of infection, particularly in the low endemicity regions like North America. Men who have sex with men (MSM) were considered at the highest risk of infection with 70% of homosexual men being infected within 5 years of beginning sexual activity. However, there has been an increase in the level of heterosexual transmission case, such that sexual partners of drug users, prostitutes or clients of prostitutes are considered at high risk of infection (Hou *et al*., 2005, Lu *et al*., 2010, Sharifi, 2014). The third route of transmission is through parenteral or percutaneous transmission. This includes injection drug use, transfusions, dialysis, acupuncture and working as a health worker as examples. These routes carry a low risk of developing into chronic infections (<5%) because

individuals at risk generally acquire their infections in adolescence or as early adults. Most of these patients will progress to immune clearance and spontaneous recovery (Hou *et al*., 2005, Kwon and Lee, 2011).

Interestingly HBV infection does not result in a significant host innate immune response through proinflammatory cytokine or interferon (IFN) activity. Recent studies have shown that HBV infection can result in the downregulation of antiviral effectors such as interferon stimulated genes (ISG), Toll-like receptor, and pathogen recognition receptor pathways (Lebossé *et al*., 2016, Luangsay *et al*., 2015). The lack of innate immune stimulation appears to be regulated by high level expression of HBV S antigen (Wang *et al*., 2013, Ortega-Prieto and Dorner, 2017). However, at higher HBV titres, macrophages are capable of sensing HBV and stimulating inflammatory cytokine expression (Cheng *et al*., 2017). This process remains poorly understood, because high level expression of HBV surface proteins can also act as an immune decoy. This is because surface proteins expressed at vast levels have tolerogen behaviour, which inhibits corresponding antibody activity through exhaustive binding (Ortega-Prieto and Dorner, 2017). The HBV genome is organised onto host-derived histones, which results in regulation at an epigenetic level (this will be discussed in more detail in **Section 1.2.4**). It has been shown that host factors can inhibit HBV transcription at this point through deacetylation of histones, however, HBV X protein binding to covalently closed circular DNA (cccDNA) reverses this inhibition as part of the transcriptional activation process (Riviere *et al*., 2015). This process enables a form of host mimicry that prevents activation of host immune responses (Riviere *et al*., 2015). Additionally, HBV transcripts are capped and polyadenylated similar to host mRNAs. This helps to prevent innate immune sensing via RIG-I and MDA-5 (Seeger and Mason, 2015, Ortega-Prieto and Dorner, 2017).

Following acute infection with HBV in adults there are multiple stages to infection progression. Approximately 5% of patients with acute HBV will progress into chronic HBV infection. Initial infection can result in an immune tolerance phase, in which patients demonstrate high levels of HBeAg and HBV DNA expression, however this is primarily seen in patients with perinatal or early-childhood infections (Takashima *et al*., 1992, Shi and Shi, 2009).

The next stage in HBV infection is called the immune clearance stage. This stage is characterised by high levels of HBeAg, HBV DNA, and active inflammation and fibrosis of the liver (Sharma *et al*., 2005). During this stage patients can undergo HBeAg seroconversion, resulting in the expression of anti-HBeAg antibodies (Sharma *et al*., 2005). This activity can stimulate the host immune response allowing activation of HBeAg and HBcAg specific T cell clones (Milich *et al*., 1995). This can cause a decrease in hepatic inflammation, decreased HBeAg expression, immune-mediated hepatocellular injury, and inhibition of viral replication (Sharma *et al*., 2005, Elgouhari *et al*., 2008). During the immune clearance phase, it has been demonstrated that patients can experience flare ups of acute-like HBV infection, which can precede remission of hepatitis activity, however, this can also result in cirrhosis progression and further HCC development (Furusyo *et al*., 2002, Shi and Shi, 2009).

The next phase of chronic HBV infection is the inactive carrier stage. Inactive carriers represent the largest group of chronically infected patients. Following seroconversion, patients remain negative for HBeAg expression and demonstrate low level expression of HBV DNA (Sharma *et al*., 2005). This stage of infection is usually benign. However, patients can undergo spontaneous reactivation of HBV, which results in progressive liver damage and can mimic acute HBV infections (Tsai *et al*., 1992, Shi and Shi, 2009). Progress to the reactivation stage can occur spontaneously or whilst a patient

undergoes immune suppression (Shi and Shi, 2009). Chronic HBV patients who are HBeAg negative demonstrate lower levels of HBV DNA, however long-term prognosis is poorer and spontaneous recovery is rarer (Shi and Shi, 2009). HBeAg negative patients experience the same level of necrotic inflammation but demonstrate higher levels of fibrotic activity than patients who are HBeAg positive (Shi and Shi, 2009).

Currently there is no cure for chronic HBV infections, however there are treatments that limit viral replication and reduce the risk of developing complications such as cirrhosis, liver failure and HCC. The main treatments recommended by the WHO are Entecavir and Tenofovir, particularly when treating infections in high endemic, low-income areas because the treatments are easy to implement, just a single pill per day, and represent a low risk for developing resistance (Chang *et al*., 2006, Jenh *et al*., 2009, Chang *et al*., 2010, Gane, 2017). Entecavir is a selective guanosine analogue that has significant activity against HBV, specifically through inhibition of reverse transcription, DNA synthesis and viral transcription (Chang *et al*., 2006, Sims and Woodland, 2006). Entecavir can suppress viral DNA and maintain normal alanine transaminase (ALT) levels in infected individuals over 5 years of therapy (Chang *et al*., 2010, WHO, 2017). Tenofovir is a nucleotide analogue that inhibits HBV reverse transcriptase activity and reduces viral replication; it is also regularly used in the treatment of HIV (Jenh *et al*., 2009, Gentile *et al*., 2014, Isorce *et al*., 2015). The two drugs mentioned above can be used in concert to prevent the development of drug resistance.

Despite the effectiveness of nucleotide analogues, some literature suggests peginterferon as a first-line treatment (Isorce *et al*., 2015). This is due to reportedly higher off-treatment response rates due to the added immune-modulatory effects. The literature suggests that treatment can result in the development of an inactive HBsAg carrier state in 30% of patients (Rijckborst and Janssen, 2010), this represents

chronically infected patients that demonstrate no HBeAg expression, anti-HBe antibodies and low or undetectable levels of HBV DNA (Rijckborst and Janssen, 2010, Sharma *et al*., 2005). However, this treatment is expensive and only recommended by the WHO for high income, low endemic areas (Perrillo, 2009, Rijckborst and Janssen, 2010, WHO, 2017).

As there is no cure and these treatment options are costly and lifelong, the best method of controlling HBV is through prevention. One method is simple behaviour modifications; practicing safe sex and improving blood-screening practices. However, in developing countries where the greatest risk of infection occurs in early childhood; the use of immunoprophylaxis and active immunisation are recommended. Immunoprophylaxis involves treating patients with Hepatitis B Immune Globulin (HBIG): a preparation of anti-HBV Ig isolated from the donors with high levels of anti-HBV immunity. This is typically given in 4 instances: to new-borns with infected mothers; after needle stick exposures; after sexual exposure and following a liver transplantation (Hou *et al*., 2005). The primary method of prevention is through immunisation using a HBV vaccine that comprises high concentrations of Hepatitis B Surface antigen (HBsAg), with small alterations that prevented spontaneous aggregation into 20nm particles. The first generation of vaccines consisted of an inactive plasma-derived vaccine. A second-generation vaccine is a DNA recombinant HBV vaccine. Both are effective at inducing protective antibody levels in 95% of infants, children and young adults. Evidence suggests that vaccination against HBV can reduce HCC incidence in HBV endemic area. One study showed that the annual incidence in children from Taiwan aged 6-14 dropped 0.70 per 100,000 to 0.57 over a 4 year period (Chang *et al*., 1997). It is suggested that protection lasts for up to 20 years, perhaps lifelong in some cases. Studies have shown that protection remains

even when anti-HBs levels begin to drop or are undetectable. This suggests long term B-cell memory continues to provide protection against HBV (WHO, 2017). Despite the existence of the vaccines, of which more than 1 billion doses have been given, HBV is responsible for 500,000 to 1.2 million people deaths annually due to HBV related morbidity and mortality. HBV represents a substantial portion of the global disease burden and warrants further study (Hou *et al*., 2005).

1.2.2 HBV Morphology

Hepatitis B virus (HBV) is a small DNA virus of the Hepadnaviridae family and is classified into 7-8 genotypes A-G (and recently described H) with distinct geographical locations (Hou *et al*., 2005, Song *et al*., 2005). As mentioned briefly, there are related viruses that exist within woodchucks, squirrels, ducks and herons. HBV has 3 well characterised types of particles that can be visualised using electron microscopy (Gerlich, 2013). These are differentiated by the size of the particle and include: 22nm spherical non-infectious structures that comprise HBV Surface (S) protein and host derived lipids; non-infectious filaments consisting of HBs and host derived lipids, however they also contain HBV M and L proteins; finally, infectious HBV virions also called Dane particles that are 42nm in diameter, spherical in shape and double shelled. This double shell consists of a lipid envelope studded with HBV S proteins (Urban *et al*., 2014, Gerlich, 2013). This contains an inner nucleocapsid of HBV core proteins, which are complexed with a viral polymerase and DNA genome. **Figures 1.4** and **1.5** represent the 3 viral particles and a schematic of the HBV genome respectively.

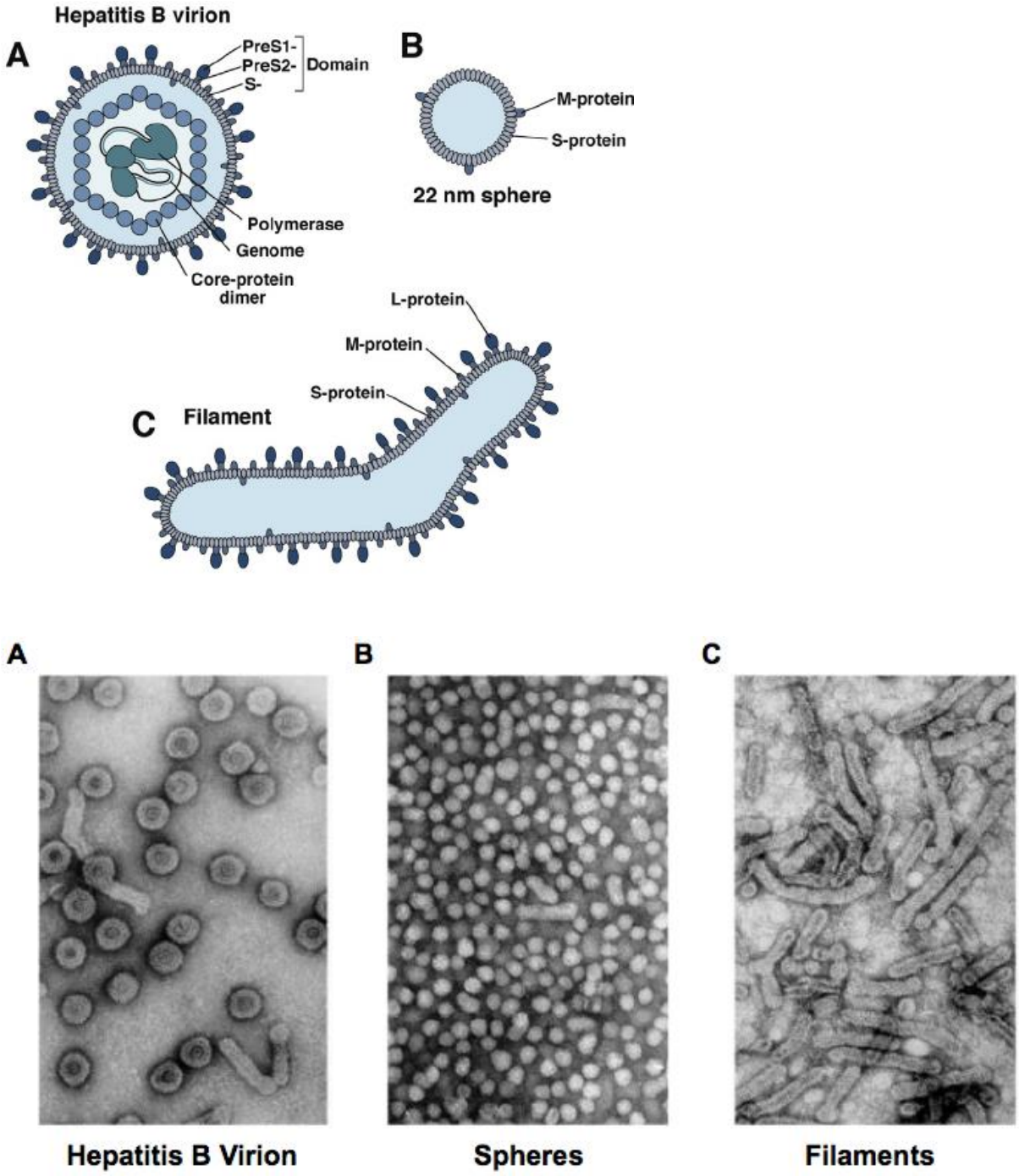

Figure 1.4 Hepatitis B viral particles (Gerlich, 2013, Urban *et al*., 2014)

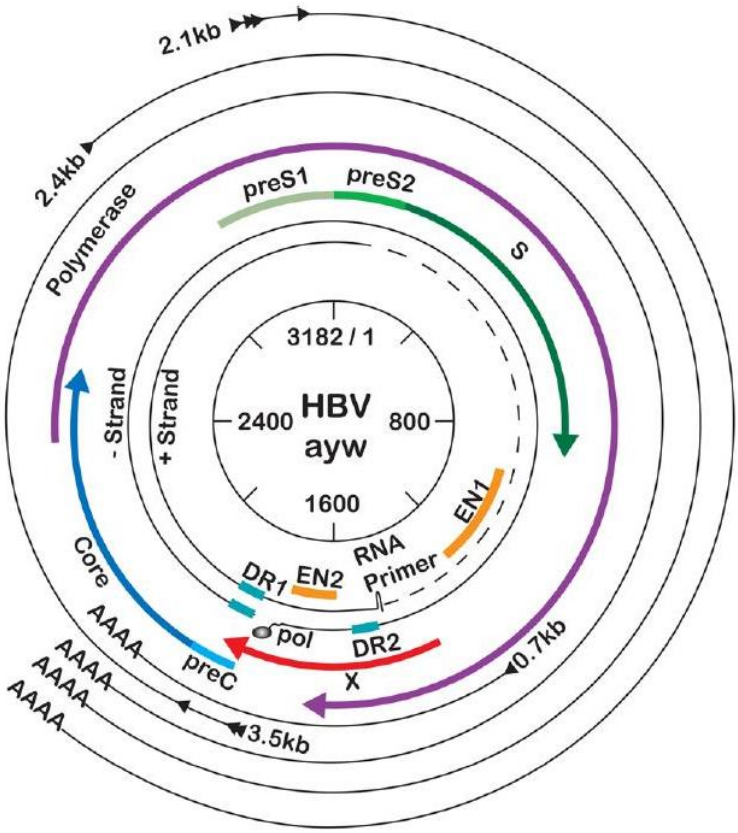

Figure 1.5 Hepatitis B virus DNA genome (adapted from (Lamontagne *et al*., 2016)

A schematic of HBV genotype D, subtype ayw. This figure shows the partially double-stranded genome and the positions of attached RNA primer and polymerase protein. Coloured arrows represent the HBV open reading frames. The outer black lines represent viral transcripts of different sizes that share a polyadenylation site.

The HBV genome is partially double stranded circular DNA called relaxed circular DNA (rcDNA). This genome is approximately 3.2kb in size. The viral polymerase is covalently attached to the 5' end of the minus strand on DNA. The viral genome encodes 4 overlapping open reading frames (ORFs); these are Surface (S), Core (C), Polymerase (P) and Hepatitis B X protein (X). The S ORF encodes the viral surface proteins S, M and L; these are represented by the S, preS2 and preS1 regions on the ORF respectively (Liang, 2009). The C ORF encodes the viral core proteins or nucleocapsid and Hepatitis B e antigen (HBeAg) (Milich and Liang, 2003). The P ORF encodes the viral polymerase. The X ORF encodes a non-structural protein called HBx, this is a multifunctional protein involved in many aspects of the HBV lifecycle. Each of these proteins will be discussed in more detail later. In addition to these ORFs, the HBV genome includes two direct repeats in the 5' end of the plus strand called DR1 and DR2; these are essential for strand specific DNA synthesis. There are also two enhancer elements called EnhI and EnhII involved in regulating viral gene expression and a glucocorticoid responsive element (GRE). (Su and Yee, 1992, Hatton *et al*., 1992, Seeger *et al*., 1986, Yee, 1989, Tur-Kaspa *et al*., 1986, Liang, 2009). The viral lifecycle has been well studied and is represented in **Figure 1.6** and will be discussed in more detail in the following sections.

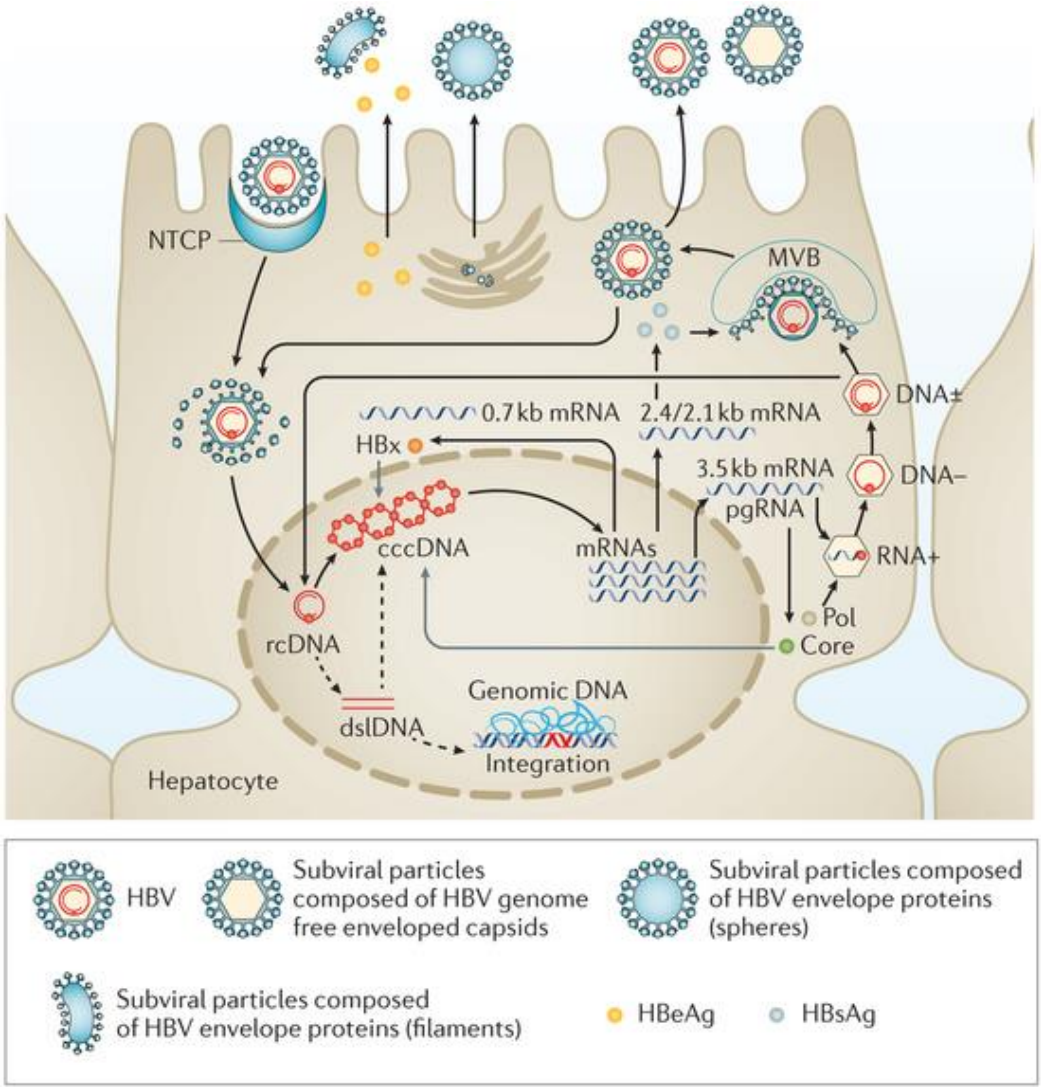

Figure 1.6 Hepatitis B lifecycle (Thomas and Liang, 2016)

1.2.3 HBV Entry and Nuclear Import

1.2.3.1 Entry into Hepatocytes

HBV entry into hepatocytes is the first step on the infection cycle. Until very recently this area of the lifecycle was poorly understood and difficult to study with limited cell lines available that supported HBV replication. Primary human hepatocytes (PHHs) and a specialised and highly differentiated pluripotent stem cell line HepaRG (Glebe and Urban, 2007) provided the only successful *in vitro* model systems (Glebe and Urban, 2007, Schulze *et al*., 2012, Schulze *et al*., 2007). In addition infection of PHH cells could be dependent on source and time since being obtained (Schulze *et al*., 2012). Human hepatoma cell lines such as Huh7 and HepG2 cells showed minimal evidence of viral replication (Schulze *et al*., 2012, Li and Urban, 2016).

However, in 2012, Yan and colleagues identified the bile salt transporter called sodium taurocholate co-transportation polypeptide (NTCP), as a binding and entry receptor for HBV and by association HDV as well (Ni *et al*., 2014, Yan *et al*., 2012, Watashi *et al*., 2014, Urban *et al*., 2014). This receptor is expressed on the basolateral surface of hepatocytes and is encoded by the SLC10A1 gene. It belongs to the SLC10 family of carrier proteins. While the structure of this transporter has not been fully characterised, 9 transmembrane domains have been found, these are demonstrated in **Figure 1.7** (Yuen and Lai, 2015). This receptor has been identified as an HBV specific receptor and is expressed in PHH cells and DMSO-differentiated HepaRG cells, it is highly tissue specific and provides an explanation for the liver tropism of HBV. Importantly, expression of NTCP in hepatoma cell lines such as Huh-7 and HepG2 enabled infection with both HBV and HDV (Ni *et al*., 2014, Yan *et al*., 2014). This discOvary

provided the cell culture system to enable effective study of HBV lifecycle *in vivo* using *de novo* infections (Li and Urban, 2016).

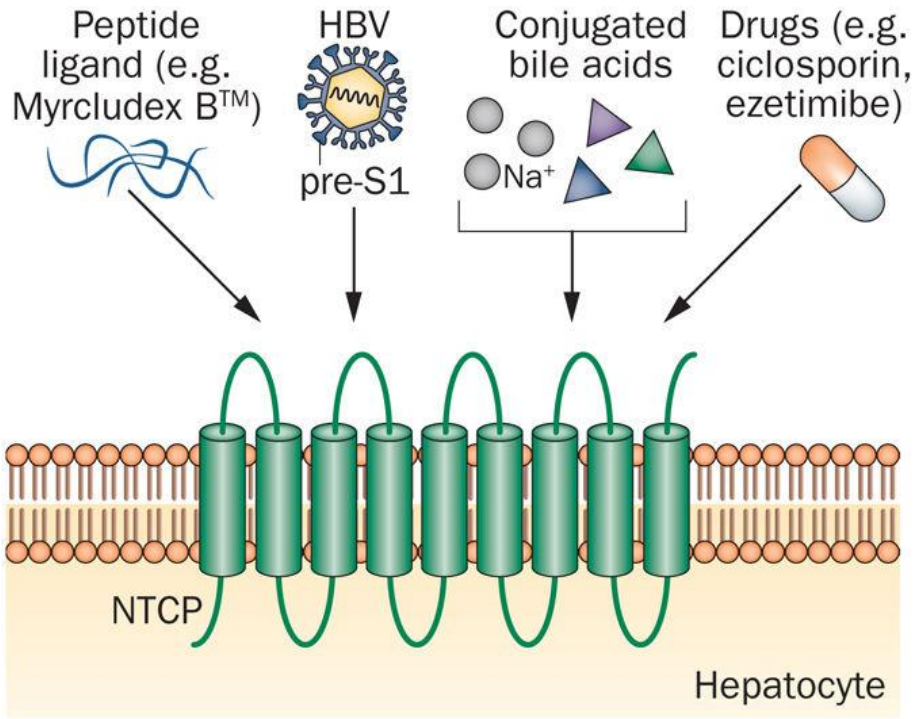

Figure 1.7 Cartoon of Sodium Taurocholate Cotransporting Polypeptide (NTCP) (Yuen and Lai, 2015)

A schematic representation of NTCP bile acid transporter, which is involved in transporting conjugated bile acids across membranes into Hepatocytes. This transporter behaves as a receptor for HBV entry. NTCP receptor function is blocked by a variety of different agents such as Myrcludex B™, a synthetic N-acylated preS1-derived lipopeptide that inhibits HBV entry in vitro and in vivo with high efficacy, or ciclosporin and ezetimibe which are known to inhibit membrane transporter activity.

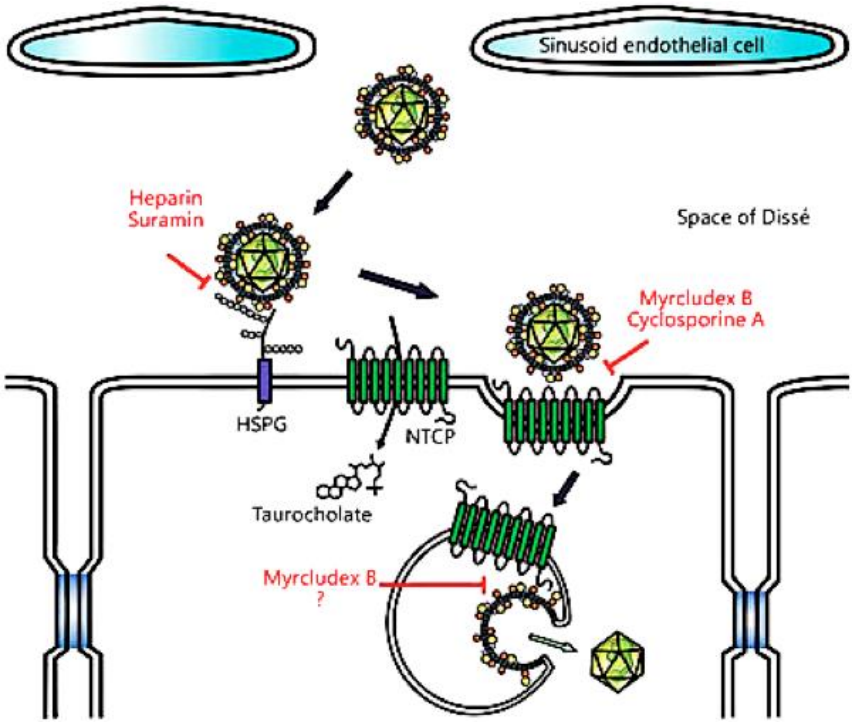

Figure 1.8 Cartoon of HBV entry (adapted from (Lempp and Urban, 2014)

A cartoon of HBV entry showing HBV initial binding to HSPGs before transitioning to the high-affinity entry receptor NTCP. NTCP facilitates the endocytosis of HBV along the basolateral surface of hepatocytes. Drugs such as Heparin, Suramin, Myrcludex B^{TM}, and Cyclosporin A can inhibit HBV infection by binding to the surface proteins and preventing viral interaction.

Initial interaction between HBV and hepatocytes occurs via binding cell surface expressed heparin sulfate proteoglycans (HSPGs). These are cell surface glycoproteins that are ubiquitously expressed on the surface of adherent cells and in the extracellular matrix (ECM); they primarily function as coreceptors by regulating ligand encounters with receptors. This occurs through high expression of heparin sulfate chains binding ligands and increasing concentration around specific signalling receptors (Chen *et al*., 2008). HSPGs have been shown to interact with proteases, behave as endocytic receptors, coreceptors for tyrosine-kinase like growth factor receptors and as proteoglycans that integrate with integrins and other cell adhesion molecules to facilitate cell-cell interactions and motility (Sarrazin *et al*., 2011). It has been demonstrated that numerous microbes including viruses utilise these to bind to multiple cell types (Chen *et al*., 2008). There are approximately 17 different HSPGs that can be divided into 3 groups determined by their location. The first of these are membrane HSPGs such as syndecans and glycosylphosphatidylinositol-anchored proteoglycans (glypicans), evidence suggests that these are some of the initial contact receptors for HBV (Verrier *et al*., 2016a). The second type of HSPGs are secreted extracellular HSPGs such as agrin and perlecan (Chen *et al*., 2008). The last type of HSPG is the secretory vesicle proteoglycan serglycin (Sarrazin *et al*., 2011).

HBV infection requires an initial interaction with the carbohydrate side chains of hepatocyte specific HSPGs and this is mediated via the viral encoded PreS1 (Sureau and Salisse, 2013). **Figure 1.8** is a cartoon representation of initial binding of the HBV particle on HSPGs and subsequent internalisation (Lempp and Urban, 2014). The PreS2 domain is not essential for HBV infection and can be removed (Urban *et al*., 2014). This was demonstrated with soluble heparin as well as other known inhibitors of duck hepatitis infections such as suramin and highly sulfated dextran sulfate that inhibit

HBV infection by competitively binding HSPGs (Schulze *et al*., 2007, Leistner *et al*., 2008). This binding provides the initial step to HBV infection, the viral glycoproteins recognise specific patterns of hepatic proteoglycans (Schulze *et al*., 2007, Leistner *et al*., 2008). Using a combination of siRNA treatments against HSPG families, glypican 5 (GPC5) was shown to bind HBV (Verrier *et al*., 2016a). This was confirmed through the use of anti-GPC5 monoclonal antibodies and soluble recombinant GPC5, both of which could neutralise HBV infection . GPC5 is so called because it uses 5 insertion sites into the extracellular surface to anchor itself (Li *et al*., 2011).

Binding to GPC5 as well as other HSPGs initiates a multistep process of entry depicted in **Figure 1.8** (Lempp and Urban, 2014); after initial binding, HBV moves to the higher affinity receptor NTCP. NTCP is a transporter residing in the basolateral membrane of hepatocytes and is involved in the uptake of conjugated bile salts and has been shown to be essential for efficient HBV infection, this has been demonstrated using specific siRNAs and drugs such as cyclosporin A and Myrcludex B (**Figure 1.8**) that inhibit virus and receptor interactions (Lempp and Urban, 2014, Volz *et al*., 2013, Lutgehetmann *et al*., 2012). Evidence shows that the PreS1 region of HBV surface protein L binds with high specificity to NTCP extracellular loops (Yan *et al*., 2012, Volz *et al*., 2013, Urban *et al*., 2014, Colpitts *et al*., 2015, Li and Urban, 2016). Following binding to NTCP, HBV is internalised through endocytosis, although the pathways are not defined (Watashi *et al*., 2014, Cooper and Shaul, 2006).

1.2.3.2 Nuclear Import

Following entry into the hepatocyte the mature capsid needs to translocate from the cytoplasm into the nucleus. This occurs through interaction with the nuclear pore complex (NPC). HBV hijacks the host cellular transportation factors; these facilitate

interaction with the NPCs and aid nuclear import. NPCs are macromolecular complexes that consist of approximately 30 proteins, called nucleoporins (Nups). Together these form a complex with octagonal rotation symmetry that spans the nuclear envelope and forms a pore through which HBV can traverse (Gallucci and Kann, 2017). There are additional Nups that form asymmetric structures on either side of the NPC. Nup358 and Nup214 are examples that have been shown to form part of the cytoplasmic filaments around the cytoplasmic face of the NPC (Lim *et al*., 2007, Tran and Wente, 2006, von Appen and Beck, 2016, Gallucci and Kann, 2017). A similar structure called the nuclear basket is found on the inside of the nuclear envelope. These are formed by numerous Nups; well characterised examples include Nup153 and Tpr (Lim *et al*., 2007, Tran and Wente, 2006). The distribution of Nups varies significantly, but they are essential for nuclear import and export, as well as for differentiation during other cell cycle, chromatin distribution and embryogenesis processes. Nups collectively form a passive diffusion barrier inside the nuclear pore, this is characterised by phenylalanine-glycine repeats (FG-repeats) in approximately 30% of the Nups (Gallucci and Kann, 2017).

Small molecules with diameters of 5nm or less can passively diffuse through the NPC (Ghavami *et al*., 2016), however larger macromolecules require active transport across the nuclear envelope. The channel formed by the NPC is approximately 40nm in diameter. This restricts the entry and exit of larger viral capsids. HBV viral capsids are approximately 36nm in diameter, which means that they can pass through the NPC. This occurs through interaction of the macromolecule nuclear localisation signal (NLS) for import or the nuclear export signal (NES) for export, with the nuclear transport receptors; these are collectively called importins or exportins (Rabe *et al*., 2003, Li *et al*., 2010a, Gallucci and Kann, 2017).

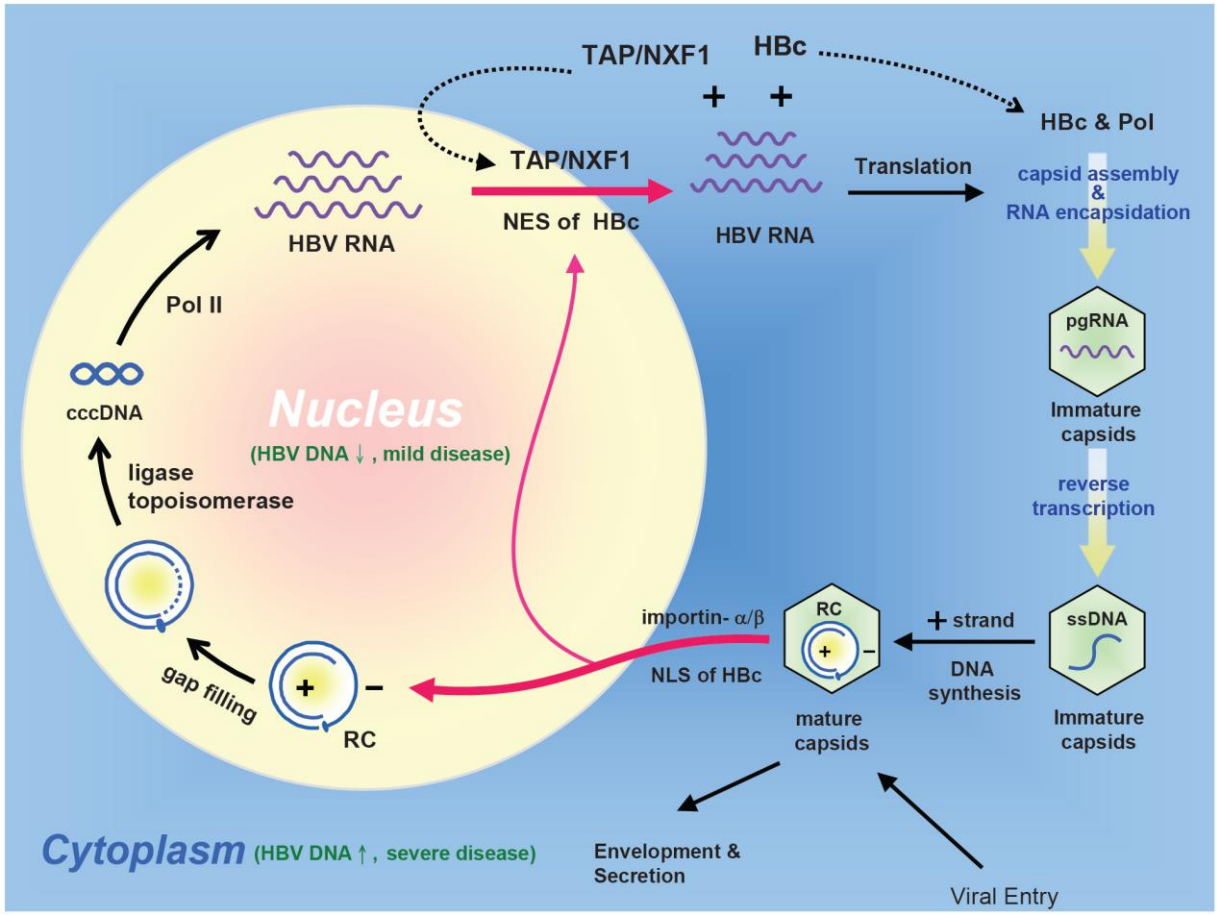

Figure 1.9 HBV import and export as part of viral lifecycle (Li *et al*., 2010a)

The pathway regulating HBV import to the nucleus and role of NPC is not well understood; currently there are 2 models for transport of the HBV genome. The first of these is mediated by binding of the HBV polymerase (Pol) to HBV core (HBc) protein dimers and importin α/β at the NPC. In contrast, the second model focuses on whole capsid transport through the NPC followed by disassembly while in the nuclear basket (Gallucci and Kann, 2017). When considering each of these models it is important to discuss the diversity of HBV capsids with mature virions comprising 240 copies of HBc that form T4 icosehedral symmetry. Capsid assembly begins with the formation of HBc dimers; these form hexamers; which piece together into full capsids. These structures are dynamic with HBc subunits able to dissociate and re-associate and had been dubbed capsid breathing (Zlotnick *et al*., 1997).

Aside from the structure of the capsid, virions can be distinguished by their nucleic acid content as shown in **Figure 1.9**. Mature capsids contain mature rcDNA or double stranded linear DNA (dslDNA), these are both enveloped and secreted at later stages in the lifecycle or imported into the nucleus. Non-enveloped capsids contain HBV pregenomic RNA (pgRNA) and polymerase. The last form of the HBV capsid contains all of the HBV genome intermediates from pgRNA to rcDNA and are defined as immature virions (Li *et al*., 2010a). The mature capsids undergo nuclear import, it has been reported that capsids are predominantly found in the nucleus (Rabe *et al*., 2003), whereas others (Cui *et al*., 2015) suggest more cytoplasmic localisation. Evidence suggests that both can be true, but that the severity of HBV disease may be determined by this localisation (Li *et al*., 2010a). A more nuclear-based localisation is associated with milder disease because there is a higher viral load, but less hepatocellular injury. The first model for HBV genome nuclear transport is based on interaction of NLS importin α/β with the viral polymerase. This model suggests that

mature capsids will destabilise into HBc dimers; releasing the rcDNA-polymerase complex at the cytoplasmic face of the NPC. Following destabilisation, the NLS importin α/β will bind to the HBV polymerase or the HBc dimers independently and they will pass through the NPCs by interacting with nuclear import receptors. The transport factors finally dissociate from core protein and HBV polymerase and this can be followed by capsid re-assembly. The second model involves the transport of the intact capsid via interactions with Importin α/β and Nup153. At this point the capsid destabilises into HBc dimers and the rcDNA-polymerase complex is released (Li *et al*., 2010a, Li and Urban, 2016, Gallucci and Kann, 2017).

1.2.4 cccDNA Formation

Following nuclear import, the HBV genome uses host cell factors to 'repair' the rcDNA and form covalently closed circular DNA (cccDNA): the viral mini chromosome that forms a reservoir for continual replication. Due to the long hepatocyte half-life and lack of initiating immune responses, the cccDNA can persist for long periods of time (Moraleda *et al*., 1997, Lutgehetmann *et al*., 2010, Nassal, 2015). Current treatments suppress HBV polymerase activity and reduce viral rcDNA levels but have no impact on cccDNA. Therefore, treatment for an established chronic infection is lifelong (Quasdorff and Protzer, 2010, Seeger and Mason, 2015). HBV cccDNA formation is the first step in the HBV DNA replication process and conversion of rcDNA to cccDNA can be detected within the first 24 hours of infection and is indicative of successful initiation of viral replication. This process utilises cellular enzymes to repair the DNA and complete the rcDNA; however the exact enzymes used are still unknown (Qi *et al*., 2016). Two models for cccDNA formation have been suggested; the first model proposes that cellular endonucleases remove short terminally redundant sequences from the minus strand copy of rcDNA along with the viral DNA polymerase from the 5'

terminus and RNA primer from the plus strand. This is followed by a ligation reaction to fill the gaps in each strand of rcDNA. This model is based on the observation that nucleotide analogues inhibit reverse transcriptases and do not prevent cccDNA formation in duck hepatitis B (DHBV) (Fourel *et al*., 1994). This would indicate that rcDNA is the direct precursor to cccDNA (Qi *et al*., 2016). Current understanding of the model suggests that host cellular DNA repair enzymes catalyse each of these reactions. However, the identity of these enzymes is not well understood. An example enzyme that has been shown to target rcDNA is tyrosyl-DNA-phosphodiesterase 2 (Tdp2), however knockout of this gene reduces cccDNA formation in DHBV and has minimal impact on cccDNA formation in HBV infection of HepG2 cells (Cortes Ledesma *et al*., 2009, Hu and Seeger, 2015). Tdp2 cleaves tyrosyl-5' DNA linkages found between topoisomerase II and cellular DNA (Cortes Ledesma *et al*., 2009) and has been reported to release covalently linked reverse transcriptase from the 5' end of rcDNA minus strand and cleave the tyrosyl-minus strand DNA linkage of HBV (Cortes Ledesma *et al*., 2009, Jones *et al*., 2012). Another previously studied example is Ku80, a component of the DNA repair pathway, which is involved in non-homologous end joining of DNA. In Duck HBV, Ku80 has been shown to be essential for cccDNA formation from a dslDNA intermediate but not from rcDNA (Guo *et al*., 2012). This is relevant because it has been demonstrated that cccDNA can be formed from dslDNA rather than rcDNA (Yang and Summers, 1995). An alternative model proposes polymerase extension of 3' ends of both plus and minus DNA strands, followed by "DNA strand displacement synthesis" that forms a dslDNA containing large terminal redundancies. These would span the overlap regions in rcDNA. These would then combine through homologous recombination to form cccDNA, however, the evidence for this model is limited (Yang *et al*., 1996, Seeger and Mason, 2015).

Using DHBV and woodchuck hepatitis virus (WHV) and viral DNA polymerase inhibitors it has been demonstrated that viral DNA polymerases are not essential for cccDNA formation . The implication is that viral polymerases are not essential for plus strand DNA synthesis (Kock and Schlicht, 1993, Moraleda *et al*., 1997, Delmas *et al*., 2002, Qi *et al*., 2016); rather the virus utilises host cell DNA polymerases. Qi and colleagues utilised *de novo* infections in HepG2-NTCP cells with HBV deficient in HBc production to demonstrate that the viral polymerase is not required for cccDNA formation. In addition they used an RNAi screening process to identify the host cell DNA polymerase K (POLK) as a crucial factor in HBV cccDNA formation (Qi *et al*., 2016). Qi and colleagues confirmed that cccDNA formation occurs within 24 hours of infection and demonstrated that approximately 3 copies of cccDNA can be found per cell. Further confirmation of cccDNA synthesis being independent of the viral DNA polymerase comes from Sohn and colleagues, who showed that a host cell DNA polymerase will fill in the 3' end of both strands (Sohn *et al*., 2009). However, they also observed that inhibiting the polymerase caused a modest reduction in cccDNA levels. This implies that either the viral polymerase has a small contributing effect in cccDNA formation or that off-target inhibitory effects may have occurred. Qi and colleagues also demonstrated that cellular DNA polymerases L and H (POLL/ POLH) may play a minor role in cccDNA formation (Qi *et al*., 2016). Qi and colleagues suggest that POLL and POLH might have roles distinct from POLK depending on the size of the plus strand gap. Alternatively, the polymerase used could be dependent upon the size of precursor rcDNAs. However, different polymerase activities could simply be due to redundancy (Qi *et al*., 2016).

A previous study by Yeh and colleagues demonstrated that cccDNA synthesis could be enhanced by arresting cells in G1 phase (Yeh *et al*., 1998). Qi and colleagues also

demonstrated an increased infection efficiency that associated with the number of G0 and G1 phases in HepG2-NTCP cultures. This observation supports the theory that HBV preferentially infects non-dividing cells and then forms cccDNA (Werle-Lapostolle *et al*., 2004). This is an important observation because POLK activity is at least partly regulated by the growth state of cells. Maximal activity of POLK is observed in non-dividing cells with low levels of deoxynucleotide expression (Qi *et al*., 2016). Current *de novo* infection protocols treat HepG2-NTCP cells with DMSO to increase expression of differentiation markers essential for infection. A by-product of DMSO treatment is to arrest the cell cycle, suggesting that DMSO could boost infection through slowing of cell cycles.

Although currently unknown, it is possible that other host cell DNA repair proteins are involved in HBV plus-strand DNA synthesis. Qi and colleagues suggest that HBV may hijack cellular endonucleases and exonucleases to cleave capped RNA primers on the 5’ end of the plus strand. They also suggest that other proteins in the host nucleotide excision repair (NER) pathway might be involved; XRCC1-hig3 is required for ligation in repairing DNA breaks within quiescent cells (Qi *et al*., 2016). HBV cccDNA formation is a complex process, but once complete the cccDNA functions as a mini chromosome for HBV and enables the maintenance of chronic HBV infection (Qi *et al*., 2016).

The HBV genome is able to integrate into the host genome. This occurs throughout the host genome at double strand DNA breaks (Bill and Summers, 2004). The roles and clinical implications for this process are unclear because the HBV genome in this form is considered replication incompetent. This is because HBV pgRNA cannot be transcribed from HBV double stranded linear DNA (dslDNA) (Tu *et al*., 2017). However, it has been demonstrated that dslDNA derived cccDNA can revert back into wild type cccDNA, possibly via homologous recombination (Yang and Summers, 1998). The

arrangement of the HBV genome following integration can affect the expression of viral ORFs. This is due to the position of viral promoters to drive transcription. Whilst HBV polymerase, HBeAg and HBV core ORFs typically remain intact, they are separated from their corresponding promoters, which prevents expression (Tu *et al*., 2017). Interestingly the HBV surface proteins ORF typically remains intact and expression of surface proteins can still occur using the native HBs promoter (Tu *et al*., 2017). The integrated form of HBV is still able to produce transcripts from the HBx ORF through activity of Enhancer 1, but the HBx protein is likely to be truncated (Shamay *et al*., 2001). However, it has been demonstrated that truncated HBx is still functional in transcriptional activations (Kumar *et al*., 1996).

1.2.5 cccDNA Transcription and Translation

1.2.5.1 Transcription and Translation

HBV cccDNA is assembled in combination with host cell histone proteins; this forms the mini chromosome, which is an episomal form of the genome. This structure is regulated through post-translational modification (PTM) of the histone proteins in a similar manner to that observed with cellular chromatin. These modifications are important because they enable access of HBV DNA to host transcriptional machinery (Tropberger *et al*., 2015). HBV cccDNA forms the template for viral mRNA synthesis. The episomal form of the genome includes 4 overlapping ORFs that encode 7 proteins; these are represented in **Figure 1.10**. These proteins are translated from the 5 viral mRNAs transcribed from HBV cccDNA (**Figure 1.10**), which are regulated by 4 promoters called Core, PreS, S and X. Pre-genomic RNA (pgRNA) transcription is directed by the core promoter and M/S is regulated by the S promoter. PreS and X are regulated by their respective promoters (Seeger and Mason, 2015). Two additional

mRNAs are reported to be transcribed from initiation start sites up and downstream of an AUG in the Core and S promoters that begin from staggered start sites (Morikawa *et al*., 2016).

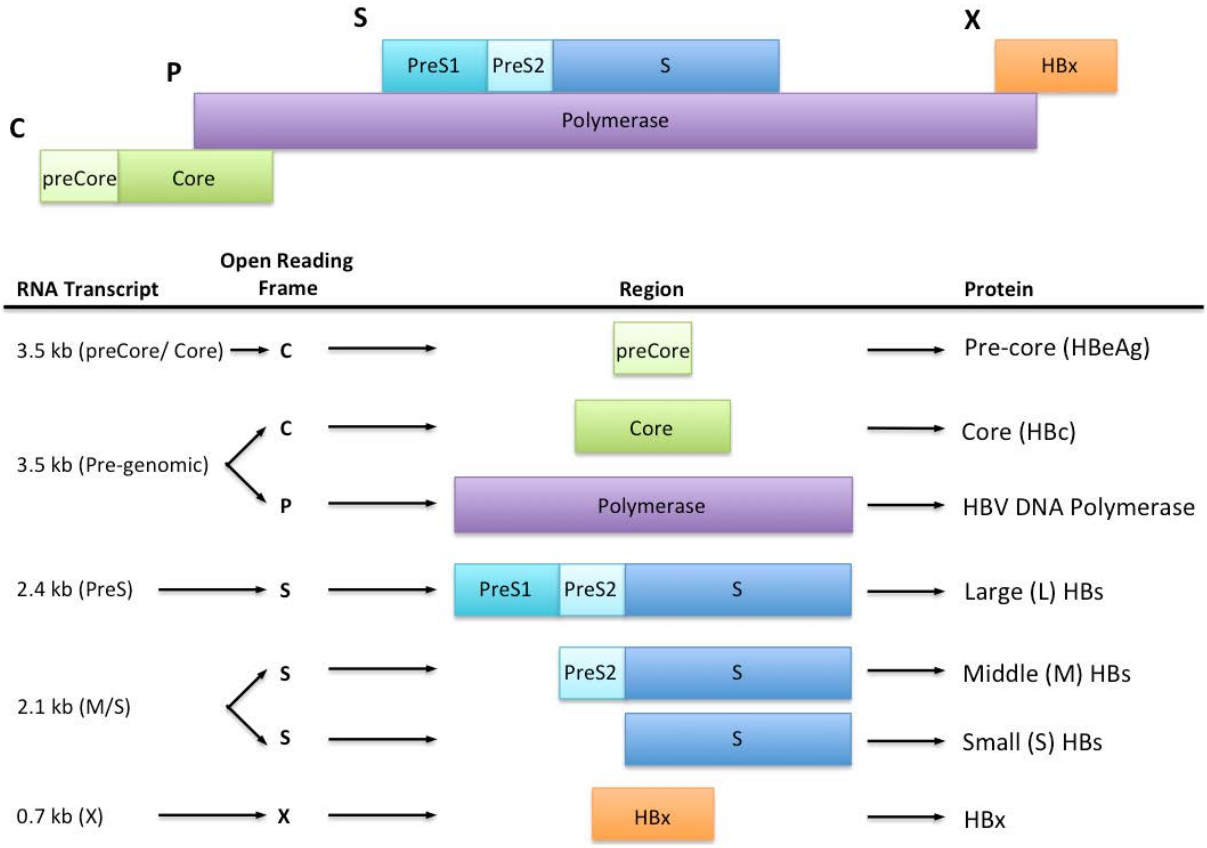

Figure 1.10 Linear cartoon representation of HBV open reading frames

HBV cccDNA serves as the template for mRNA synthesis by host polymerase II. Each of the HBV promoters controls the synthesis of specific viral transcripts. HBV mRNAs transcribed from cccDNA translate into 7 viral proteins. However, it is important to note that HBx is required for efficient transcription of cccDNA (Seeger and Mason, 2015). It has been demonstrated that HBx binds directly to cccDNA (Belloni *et al*., 2009). However, interaction of HBx with cccDNA has also been demonstrated via the DNA damage binding protein 1 (DDB1) and Cullin4A-RING-DDB1 ubiquitin ligase (Li *et al*., 2010b). Specifically, HBx could be involved in regulation of acetylation of histones to activate transcription (Seeger and Mason, 2015). Viral mRNAs are transported to the host ribosomes and translated into viral proteins. This process relies on post-transcriptional cis-acting regulatory elements (PREs), which overlap with the HBx coding sequence. HBx is translated from the X transcripts; however, unlike other viral RNAs it might be produced immediately following cccDNA formation. This is due to the previously mentioned activity for HBx in binding to cccDNA, through Cullin4A-DDB1 interaction with the histones of the mini chromosome (Seeger and Mason, 2015). HBV pgRNA forms the template for viral replication by acting as a template for reverse transcription; pgRNA is translated to produce the core and viral polymerase proteins; the latter is the result of a separate internal initiation of translation. In addition, pgRNA acts as a template for genomic DNA formation inside the viral nucleocapsid. PreCore RNA is translated into preCore protein or HBeAg, this RNA is colinear with pgRNA with the exception of a small 5’ extension which enables translation from an independent AUG codon. The M and S surface proteins are translated from the PreS1 and M/ S mRNAs (2.4kb and 2.1kb respectively). These also exhibit a colinear relationship with a distinct 5’ end on the AUG codon of M mRNA. The L surface protein is translated from

the PreS1 mRNA and X is translated from the X transcript (Doitsh and Shaul, 2003, Liang, 2009).

1.2.5.2 HBV Transcription Factor Interactions

As mentioned previously the HBV promoter regions include the enhancers EnhI and EnhII; these are located upstream of the X promoter and Core promoters respectively. These enhancers enable the binding of liver specific transcription factors required for promoter activity. cccDNA transcription is regulated in multiple ways. Evidence suggests that regulation of this transcriptional activity occurs through host transcription factors and some epigenetic factors (Levrero *et al*., 2009, Quasdorff and Protzer, 2010, Belloni *et al*., 2009). Some of these transcription factors are shown in **Figure 1.11**, this is a linear representation of the HBV genome indicating reported transcription factor binding sites. It is interesting to note a mix of ubiquitous and liver specific transcription factors actively bind to the HBV genome (Quasdorff and Protzer, 2010). The literature suggests that the Nuclear Factor 1 (NF1) family of transcription factors regulates HBV transcription. In particular, binding sites for NF1 transcription factors were found at three sites in the HBV genome: a site upstream of the S promoter was shown to be essential for optimal activity (Shaul *et al*., 1986, Quasdorff and Protzer, 2010); two additional binding sites in EnhI suppress enhancer activity (Spandau and Lee, 1992) and a third binding site within EnhI regulates transcription of HBV RNA; specifically, inhibiting this site through mutation reduced 3.5kb HBV mRNA (pgRNA) levels (Ori *et al*., 1994).

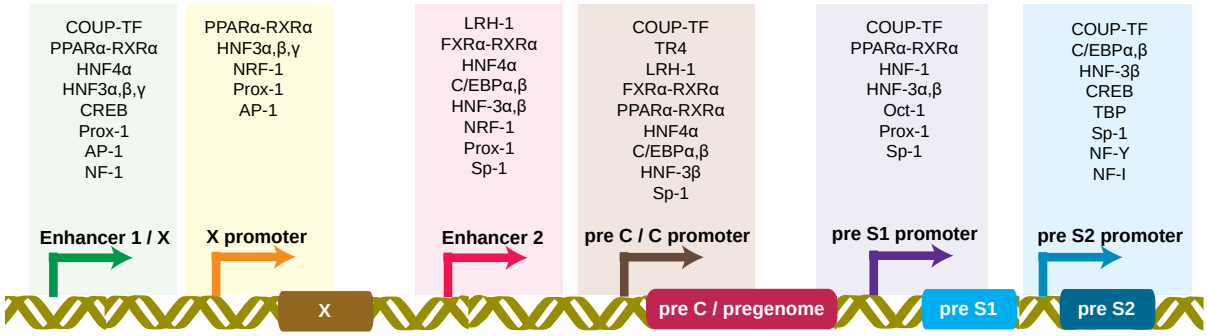

Figure 1.11 Linear HBV genome and transcription factor interactions (Lai, A. 2017)

HNF-1, HNF3α,β,γ, and HNF4α are liver specific transcription factors. Each of these transcription factors has demonstrated roles in a number of host cell transcriptional pathways.

Other transcription factors include specificity protein 1 (SP1), that binds guanine-cytosine rich DNA and has been shown to bind within the PreS2/ S, PreS1 and Core promoters as well as the EnhII element (Krainc *et al*., 1998, Raney *et al*., 1992, Raney and McLachlan, 1995, Zhang *et al*., 1993). Binding to EnhII induced mRNA levels of all HBV genes, whereas binding sites in S and X genes resulted in negative regulation of each gene (Li and Ou, 2001). This difference in activity supports a regulatory role for both NF1 and SP1 at different stages in the HBV lifecycle (Quasdorff and Protzer, 2010). It has been demonstrated that NF1 inhibits SP1 interaction with the promoter (Rafty *et al*., 2002). Other well-studied transcription factors shown to interact with HBV include Activator Protein 1 (AP1); TATA binding protein (TBP), C-AMP response element binding protein (CREB) and Nuclear Factor – kappa B (NF-κB) (Ren *et al*., 2014, Trierweiler *et al*., 2016, Tanaka *et al*., 2005, Tsai *et al*., 2015, Bogomolski-Yahalom *et al*., 1997, Herzig *et al*., 2003, Herzig *et al*., 2001, Gilmore, 2006, Lin *et al*., 2009, Kim *et al*., 2010a, Quasdorff and Protzer, 2010). AP1 shows activity in HBx regulation (Choi *et al*., 1998, Hess *et al*., 2004, Tanaka *et al*., 2005); TBP binds to TATA sequences in the PreS2 promoter and promotes activity (Bogomolski-Yahalom *et al*., 1997). CREB reportedly binds to a region in EnhI that is highly conserved amongst HBV genotypes; this factor is involved in glucose and lipid metabolism, as well as hepatocyte proliferation (Herzig *et al*., 2003, Herzig *et al*., 2001, Tacke *et al*., 2005, Cougot *et al*., 2007, Kim *et al*., 2008). NF-κB appears to play a negative regulatory role through its family members p50 and p65. These form a heterodimer that reportedly causes a reduction in all viral mRNAs. This is due to p65 activity in inhibiting SP1 and its binding to the HBV genome (Sirma *et al*., 1998, Lin *et al*., 2009, Lin *et al*., 2017).

These ubiquitous transcription factors are essential to HBV promoter and enhancer activity; however, they do not account for the hepatocyte tropism observed by HBV. This is the result of liver specific transcription factors. Hepatocyte Nuclear Factor 3 (HNF3) is shown to bind DNA in hepatocyte regulatory regions with roles in carbohydrate metabolism and β-oxidation of lipids (Costa *et al*., 2003). It is shown to increase activity of both HBV enhancers and promote PreS1 promoter activity (Chen *et al*., 1994, Li *et al*., 1995, Raney *et al*., 1995). HNF3 has been demonstrated to bind to chromatin and open nucleosomal domains in the absence of ATP-dependent enzymes. Quasdorff and Protzer reasoned that this activity might mean that HNF3 can bind to the HBV mini chromosome and enable access to other transcription regulators (Quasdorff and Protzer, 2010). Hepatocyte Nuclear Factor 1 (HNF1) is an important factor in regulating glucose and amino acid homeostasis (Pontoglio *et al*., 1996). In addition it maintains normal liver structure by regulating hepatocyte differentiation and polarisation (Kimata *et al*., 2006). HNF1 increased PreS1 promoter activity, however this activity was dependent on interaction with another ubiquitous transcription factor Octamer transcription factor (Oct1) (Raney *et al*., 1991, Zhou and Yen, 1991). PreS1 is part of the L surface envelope protein, suggesting a role for HNF1 in regulating viral release.

Hepatocyte Nuclear Factor 4 alpha (HNF4α) is another host transcription factor with important functions in the HBV lifecycle. HNF4α is a nuclear receptor and along with retinoic X receptor α (RXRα) can form homo- or heterodimers that regulate many hepatocyte functions; these include lipid, carbohydrate, cholesterol and amino acid homeostasis (Schrem *et al*., 2002, Odom *et al*., 2004). As with HNF1, this transcription factor has a role in the development and maintenance of normal liver structure (Kimata *et al*., 2006). HNF4α can promote HBV promoter activity, with increases in PreS1,

PreS2/ S and Core promoter activity having been demonstrated (Raney *et al*., 1997). Despite not boosting EnhI and X promoter activity it was shown that HNF4α could bind within this region and transactivate the core promoter (Garcia *et al*., 1993, Raney *et al*., 1997). HNF4α was shown to increase the synthesis of pgRNA, possibly linked to evidence showing it increased transcription from the pgRNA promoter (Yu and Mertz, 1997, Yu and Mertz, 1996, Yu and Mertz, 2003). HNF4α plays an essential role in regulating the genesis of pgRNA and therefore is important in the production of HBV core and polymerase. Quasdorff *et al* have also demonstrated that high expression levels of HNF4α in differentiated hepatocytes increased HBV replication efficiency; in addition, they demonstrate that HNF1α regulates expression of HNF4α and therefore regulates HBV replication (Quasdorff *et al*., 2008). As discussed previously, this is important to viral replication, these factors are linked to hepatocyte differentiation and together have been shown to regulate the efficiency of pgRNA transcription (Tang and McLachlan, 2002, Quasdorff and Protzer, 2010).

The other liver transcription factor that can bind to RXRα and form heterodimers is called Peroxisome proliferator-activated receptors (PPARα). PPARα is expressed in numerous locations including the heart, kidneys and liver. It plays a significant role in regulating cellular development, differentiation and metabolism (Michalik *et al*., 2006). It is know that PPARα-RXRα dimers increase the activity of HBV Core, Pres1 and EnhI/ X promoters (Raney *et al*., 1997). In addition, it has been shown that expression of these dimers increases HBV pgRNA expression (Yu and Mertz, 1997, Tang *et al*., 2001, Tang and McLachlan, 2001, Quasdorff and Protzer, 2010). Together these ubiquitous and hepatocyte specific transcription factors play an important role in the viral lifecycle; these represent a small number of a large group of factors that can

directly interact with and regulate the HBV genome and replication activity (see **Figure 1.11**).

1.2.5.3 Epigenetic Regulation of cccDNA

Tropberger *et al* demonstrated that cccDNA chromatin structure is highly organised and regulated by post-translational modifications (PTMs) such as acetylation and methylation. The authors identified specific regions at which PTM activity modifies cccDNA and showed that PTMs could predict the transcriptional state of viral promoters (Tropberger *et al*., 2015). Four PTMs are known to be involved in active transcription; these include H3K4me3, H3K27me3, H3k27ac and H3K122ac (Santos-Rosa *et al*., 2002, Tropberger *et al*., 2013, Creyghton *et al*., 2010, Tropberger *et al*., 2015). H3K4me3 modifications are found at transcription start sites (TSS) of actively transcribed genes. Acetylation marks (ac) indicate active TSS and gene enhancers. H3K36me3 is also a marker for active transcription, but this marker is located at the 3' end of the host genome. H3K4me3, H3K27ac and H3K122ac PTMs were found highly expressed in cccDNA chromatin; however, H3K36me3 expression was lower than controls. Two well-characterised PTMs are involved in transcriptional silencing; these are H3K9me3 and H3K27me3 (Beisel and Paro, 2011, Tropberger *et al*., 2015). PTM markers for silencing transcriptional activity both had low levels of expression (Tropberger *et al*., 2015). Tropberger and colleagues demonstrated that EnhII and basal core promoter regions showed minimal expression of these PTMs. However, a spike in expression for H3K4me3, H3K27ac and H3K122ac were found located in the precore and pregenomic TSS (Tropberger *et al*., 2015). This pattern of expression closely matches that seen in cellular chromatin. An additional spike in PTMs was observed around the EnhI region (Tropberger *et al*., 2015). This data was gathered using *de novo* infections; a subsequent comparison of PTM expression profiles in PHH

cells and HBV positive liver tissue demonstrated different profiles of activity and distributions of PTMs. The author suggests that this means cccDNA chromatin is not solely regulated by the virus and might adapt to the cellular environment (Tropberger *et al*., 2015). It has been shown that inflammation can play a role in epigenetic regulation of gene silencing through the NF-κB pathway and trimethylation of H3K9 (Chen *et al*., 2009, Bayarsaihan, 2011, Beisel and Paro, 2011). This pathway has also been linked to the acetylation and activation of histones in the promoter regions of inflammatory genes (Bayarsaihan, 2011). In addition, a number of pro-inflammatory cytokines are regulated through acetylation by CBP/p300 (Villagra *et al*., 2010). Both pathways have been demonstrated to interact with HBV and could therefore modulate the HBV epigenome (Cougot *et al*., 2007, Kim *et al*., 2010a, Xiang *et al*., 2015). In addition to inflammation, evidence suggests that hypoxia can regulate chromatin and DNA modifications through multiple chromatin modifiers such as CBP/p300 and HDACs (Tsai and Wu, 2014), however the evidence is limited. Prickaerts and colleagues demonstrate that methylation of H3K4me3 and H3K27me3 can be mediated by low oxygen and 2-oxoglutarate dioxygenase enzymes (Prickaerts *et al*., 2016, Hancock *et al*., 2015); the result demonstrated that low oxygen can regulate histone methylation. Like inflammation, hypoxic environments within the liver could modulate the HBV epigenome.

It has been demonstrated that interferon alpha (IFNα) can suppress HBV replication by targeting the epigenetic regulation of cccDNA transcription (Belloni *et al*., 2012). Specifically, evidence suggests that regulation occurs through modifications to histones bound to cccDNA by chromatin-modifying enzymes histone deacetylases (HDACs) (Pollicino *et al*., 2006); these modulate the acetylation status of histones H3 and H4. Palumbo and colleagues demonstrate the treatment of infected HepG2-NTCP cells

with interleukin-6 (IL6) inhibit viral transcription by reducing HNF1a and 4a interaction with cccDNA and subsequent reduction of histone acetylation resulting in reduced pgRNA transcription (Palumbo *et al*., 2015).

1.2.6 HBV Protein Roles and Functions

1.2.6.1 HBV Core and Polymerase

Translation of core and viral polymerase proteins is carefully regulated to ensure the correct balance of core subunits to polymerase proteins. The icosahedral shape of the HBV capsid is made up of 240 core subunits and contains a single polymerase covalently bound to pgRNA (Patel *et al*., 2017). This interaction between pgRNA and viral polymerase is mediated through a specific signal called epsilon (or ε); this signal is required for specific packaging of the pgRNA into viral nucleocapsids (Ryu *et al*., 2008, Chen and Brown, 2012, Jones *et al*., 2012, Patel *et al*., 2017). This signal is a stemloop structure found on the 5' terminal of pgRNA as shown in **Figure 1.12** (Chen and Brown, 2012). The epsilon structure is represented at both the 5' and 3' ends of the pgRNA, but only the 5' epsilon signal is utilised in the packaging process (Seeger and Mason, 2015). This binding triggers packaging and begins the DNA replication process in a host-chaperone dependent manner. Evidence suggests that heatshock proteins might stabilise the binding (Hu and Seeger, 1996, Hu *et al*., 1997). Once bound to pgRNA, the HBV polymerase initiates the process of reverse transcription by using itself as a protein primer and the epsilon signal as a template (Jones *et al*., 2014, Seeger and Mason, 2015). The viral polymerase is made up of 4 separate domains; these are the terminal protein (TP) domain, space domain, reverse transcriptase (RT) and RNaseH. HBV polymerase primes the reverse transcription process from a tyrosine residue in the TP domain. The hydroxyl group of tyrosine Y63 is used to

initiate the DNA synthesis. Additionally, the polymerase behaves as a catalyst for synthesis. The reverse transcriptase region of polymerase forms a phosphotyrosyl linkage between Y63 and the first nucleotide residue of the HBV minus strand DNA (Jones *et al*., 2014).

Figure 1.12 Schematic representation of pgRNA including *Cis* RNA elements adapted from (Chen and Brown, 2012)

Refer to section 1.2.6.1 for details.

The Core subunits translated from pgRNA form a nucleocapsid structure. This capsid consists of 183-185 amino acids depending on the genotype. These individual subunits form homodimers by linking cysteine residues via disulfide bridges (Bruss, 2007). These dimers form larger oligomers, via a poorly understood process that results in the formation of 2 types of capsid. The first of these is a 30nm structure with T=3 symmetry containing 90 core dimers. The second structure is larger at 34nm and consists of a T=4 symmetry icosahedral structure comprising 120 core dimers (Patel *et al*., 2017, Zlotnick *et al*., 1997). While both structures can be found in infectious liver samples, the T=4 structure is found in infectious virions. The core protein consists of 2 different domains: the N-terminal region between 149-151 amino acids in length and forms the primary assembly domain and is sufficient for capsid self-assembly (Bruss, 2007). The C-terminal domain is involved in packaging of the pgRNA and RT; this structure is 34 amino acids in size and is not essential for capsid formation (Gallina *et al*., 1989). Viral DNA synthesis occurs in the lumen of the viral capsid through reverse transcription of the pregenome into double stranded DNA, this forms a mature nucleocapsid.

During the synthesis of viral DNA, the capsid structure becomes a mature nucleocapsid containing double stranded DNA. These structures develop the ability to bud following envelopment with viral surface proteins. However, another outcome involves the re-import of the mature nucleocapsid into the nucleus and amplification of cccDNA. This occurs using the import mechanisms previously described. This was demonstrated by Tuttleman and colleagues using DHBV (Bruss, 2007, Tuttleman *et al*., 1986, Seeger and Mason, 2015). This process has been dubbed intracellular recycling (Schreiner and Nassal, 2017) and results in a pool of cccDNA within the nucleus that acts as a reservoir for viral persistence and this process can be blocked with nucleotide analogues (Hu and Seeger, 2015, Schreiner and Nassal, 2017).

1.2.6.2 Reverse Transcription and DNA Synthesis

Reverse transcription is utilised by HBV through the action of the viral polymerase to convert pgRNA into rcDNA for packaging into mature virions (Jones *et al*., 2012). The HBV polymerase has reverse transcriptase activity that initiates the process of binding the first nucleotide residue (Ryu *et al*., 2008, Jones and Hu, 2013). This enzyme is capable of catalysing both RNA and DNA dependent DNA polymerisation. HBV DNA synthesis can be broken down into roughly 3 processes (Jones and Hu, 2013). These include the initial protein priming discussed previously, in which the terminal protein domain of viral polymerase binds to pgRNA through interaction with the 5' epsilon signal (Hu and Boyer, 2006, Boregowda *et al*., 2012, Wang and Seeger, 1992). It has been demonstrated that this step inhibits translation of proteins from pgRNA (Ryu *et al*., 2008). The method of repression is not well understood, but the literature suggests that polymerase interaction with the epsilon signal prevents ribosomal binding (Ryu *et al*., 2008, Ryu *et al*., 2010). Following initial protein priming is the DNA polymerisation stage, this involves the addition of 2 deoxy-adenosine monophosphate (dAMP) residues to the deoxy-guanosine monophosphate (dGMP) attached to the terminal protein domain of HBV polymerase (Jones and Hu, 2013, Jones *et al*., 2012, Boregowda *et al*., 2012). This process is followed by DNA elongation. Protein priming results in a three-nucleotide long oligomer attached to the viral polymerase. The synthesis of HBV minus strand DNA occurs following transfer of the polymerase complex onto the direct repeat 1 (DR1) region at the 3' end of pgRNA (shown in **Figure 1.12** with the dotted line) (Abraham and Loeb, 2006, Loeb and Tian, 1995, Rieger and Nassal, 1996, Jones and Hu, 2013, Hu and Seeger, 2015).

Minus strand DNA synthesis begins and simultaneously as pgRNA is degraded by the RNaseH domain of the viral polymerase (Radziwill *et al*., 1990, Chen and Marion,

1996, Jones and Hu, 2013). HBV plus strand DNA synthesis then occurs in the opposite direction and begins at direct repeat 2 (DR2); this utilises an RNaseH resistant fragment of the 5' end of pgRNA for protein priming (Loeb *et al*., 1991). This process all occurs within the viral nucleocapsid, evidence suggests that the nucleocapsid regulates the reverse transcription process by phosphorylation activities that might regulate the HBV polymerase (Perlman *et al*., 2005, Basagoudanavar *et al*., 2007, Jones and Hu, 2013).

1.2.6.3 Envelope glycoproteins

Mature virions that are not imported into the nucleus become enveloped in viral surface proteins through a host derived lipid bilayer acquired through budding into the lumen of an intracellular membrane thought to represent multivesicular bodies (MVBs) that accumulate at late endosomal membranes (Watanabe *et al*., 2007, Bruss, 2007). Viral surface proteins are translated from the PreS1 and M/ S mRNAs. These become infectious HBV virions or Dane particles that are subsequently secreted from the cell (Watanabe *et al*., 2007). The S, M and L surface proteins are encoded from a single ORF that includes 3 different "in frame" ATG codons for initiation of translation, resulting in 3 different proteins that differ in length at the N-terminal region (**Figure 1.10**). These proteins are not evenly distributed amongst HBV particles. The major component of Dane particles is the S proteins (HBs); L protein is found on the surface of both filamentous particles and infectious virions. The M protein is more evenly distributed between all types of viral particle. These membrane proteins are synthesised at the rough endoplasmic reticulum (Bruss, 2007, Patient *et al*., 2009). **Figure 1.13** is a representation of each surface protein and their assembly.

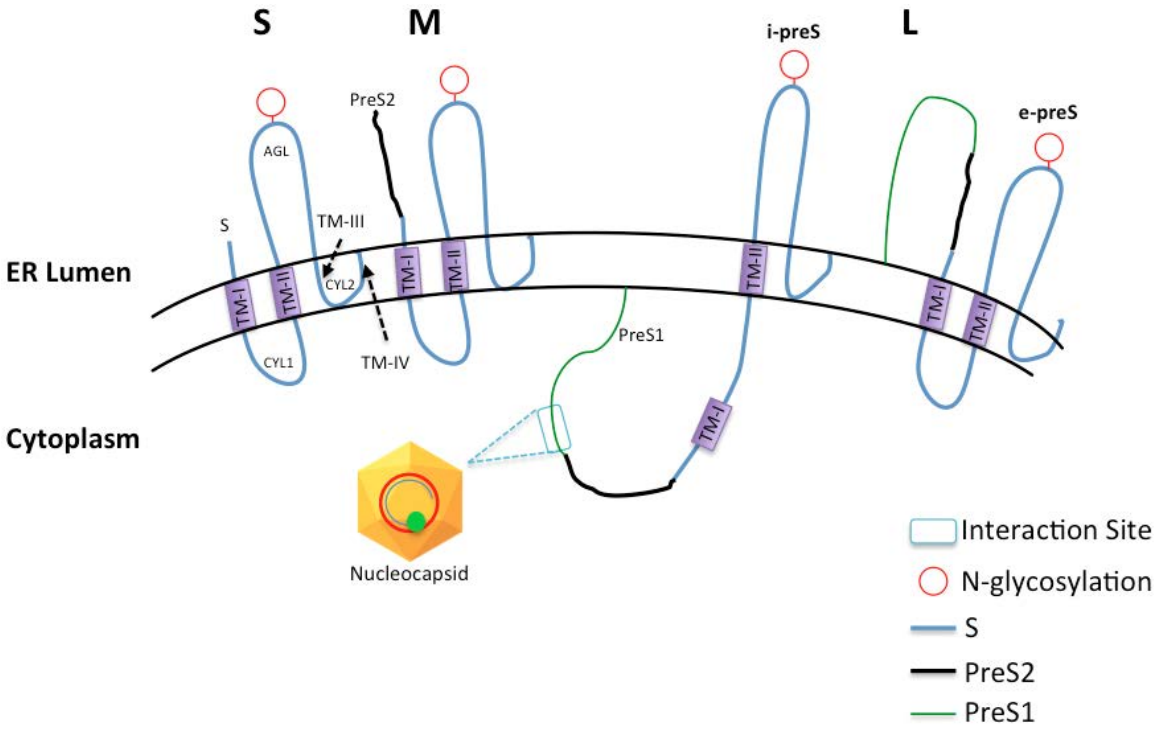

Figure 1.13 Cartoon representation of HBV surface proteins

HBs is translocated at the ER through activity of the N-terminal first transmembrane domain (TM-I), which is directed into the ER lumen (Patient *et al*., 2009). A combination of a cytosolic loop (CYL1) and second transmembrane domain are found further downstream; together these behave as a type II signal/ anchor domain (TM-II) (Patient *et al*., 2009). TM-II C-terminal domain directs an antigenic loop (AGL)(Peterson *et al*., 1982); this is composed of two transmembrane α-helices (TM-III and TM-IV); which are separated by a short cytosolic sequence (CYL2) (Persson and Argos, 1994). This structure contains a large number of cysteine residues involved in the formation of disulfide bridges to form a regulated structure. Evidence suggests these cysteine residues undergo post-translational modifications by a range of host ER chaperones such as protein disulfide isomerase (PDI) (Helenius and Aebi, 2001, Huovila *et al*., 1992). Each of the antigenic loops described earlier contains a single N-glycosylation site (Bruss, 2007, Schädler and Hildt, 2009). The production of M and L proteins is similar with the addition of a 55-amino acid and 108 amino acid sequences onto the N-terminal end of HBs respectively. The 55-amino acid sequence is called PreS2 and is found in both M and L proteins. This is co-translationally translocated into the nucleus by the TM-I sequence (Eble *et al*., 1990, Heermann *et al*., 1984). The L protein has an additional 108 sequence called PreS1 and the N-terminus of M (Persing *et al*., 1987, Bruss, 2007, Patient *et al*., 2009). The exact role of the M protein is currently unknown because it is not essential to envelop mature virions or subsequent secretion. Both S and L are required for envelopment and secretion (Patient *et al*., 2009). L has two possible conformations (**Figure 1.13**) called i-preS (Hildt *et al*., 1996, Bruss, 2007) and e-preS (Urban and Gripon, 2002, Gripon *et al*., 2005). The first conformation i-preS has internal PreS1 and PreS2 chains within the virion and contacts the viral nucleocapsid; this has been demonstrated to activate promoter elements (Hildt

et al., 1996, Bruss, 2007). The second conformation e-preS has PreS1 and PreS2 chains exposed on the surface of virions and participates in virus receptor binding (Urban and Gripon, 2002, Gripon *et al*., 2005, Bruss, 2007, Glebe and Urban, 2007).

1.2.6.4 Envelopment and Secretion

Other structures called HBsAg spheres and filaments are also formed by the surface proteins. These are capsid free subviral particles lacking a viral genome that are secreted far in excess of the infectious virions (Gilbert *et al*., 2005, Patient *et al*., 2007). S protein aggregations can self assemble into 22nm spheres within the ER lumen, these then progress through the ER-Golgi intermediate compartment (ERGIC) and are released through the general secretory pathway (Patient *et al*., 2009, Patient *et al*., 2007). The incorporation of L protein into these particles forms the filamentous subviral particles (Heermann *et al*., 1984, Roingeard and Sureau, 1998); the secretion of these particles and mature virions is a more complex process. The filaments and Dane particles utilise a more complex pathway that involves multivesicular bodies (MVBs) of the late endosomal pathway and the endosomal sorting complexes required for transport (ESCRT)(Patient *et al*., 2009, Stieler and Prange, 2014, Jiang *et al*., 2016). The mature nucleocapsids acquire host-derived lipid bilayers that are studded with viral proteins. These are formed by viral particles budding into the lumen of the late endoplasmic compartments (Ueda *et al*., 1991, Patzer *et al*., 1986). Dane particles are enveloped by a combination of S, M and L proteins; however, L is only found on the mature particle and the filaments (Heermann *et al*., 1984, Patient *et al*., 2009). The N-terminal region of PreS1 domain “i-preS” on L proteins is thought to recognise mature particles. The process by which this occurs has not been confirmed, but it has been suggested that the nucleotide content of the virion (i.e. dsDNA) causes slight

conformational changes in the nucleocapsid that act as a maturation signal that recruits surface proteins (Hildt *et al*., 1996, Bruss, 2007).

Mature virions utilise the ESCRT machinery for secretion and do so through α-taxilin; this mediates an interaction between viral surface protein L and ESCRT component tsg101 (Jiang *et al*., 2016, Hoffmann *et al*., 2013). ESCRT-MVB complex is comprised of many subunits; ESCRT I, ESCRT II and ESCRT III. The last component is the core complex, this recruits vacuolar protein sorting 4A and 4B (Vsp4A/ 4B). These proteins constrict membranes and mediate the splitting off of vesicles (Bishop and Woodman, 2000, Fujita *et al*., 2003, Watanabe *et al*., 2007, Patient *et al*., 2009). Other literature suggests that the endosomal sorting and trafficking adaptor γ2-adaptin and the ubiquitin ligase Nedd4 are involved in HBV secretion (Rost *et al*., 2006, Lambert *et al*., 2007); specifically, through interaction with L protein. γ2-adaptin was later shown to interact with L protein and it was shown that this interaction was involved in MVB dependent release of HBV (Lambert *et al*., 2007). This applies to L protein in the filamentous sub viral particles as well. MVBs are endosomal compartments that contain exosomes and, in this case, viral particles. These MVBs facilitate secretion of exosomes and viral particles through fusion with the host plasma membrane (Watanabe *et al*., 2007).

1.2.6.5 Hepatitis B X Protein

HBx is translated from the X mRNA, which is transcribed from the X ORF (Urban *et al*., 2010). It is 17kDa in size and is conserved amongst mammalian hepadnaviruses (van Hemert *et al*., 2011). HBx is essential for the expression of other viral proteins, but HBx is not packaged into virions during assembly. A couple of possible hypotheses might apply here. First, HBx mRNA is transcribed immediately and then acts to increase

transcription of the remaining mRNAs. The second model suggests that HBx is not essential for early infection, and is instead expressed alongside each of the other viral proteins. In this instance HBx behaves as an inhibitor of cellular responses that would control HBV transcription (Lucifora, 2012). HBx is a multifunctional protein and the only regulatory protein for HBV. HBx interactions with host proteins have been well studied to try and define its role within viral replication (Murakami, 2001, Murakami, 1999). It has been demonstrated that HBx is essential for viral replication both *in vivo* and (Tsuge *et al*., 2010, Lucifora *et al*., 2011).

Literature suggests that this regulation of replication occurs through epigenetic regulation of cccDNA (Pollicino *et al*., 2006, Guo *et al*., 2009, Koumbi and Karayiannis, 2015). HBV cccDNA is subject to H3 and H4 acetylation during replication in an HBx dependent manner. HBx is recruited alongside histone acetyltransferases and deacetylases (Belloni *et al*., 2009, Pollicino *et al*., 2006) and activates genes on episomal templates regardless of promoter or enhancer sequences (Colgrove *et al*., 1989); this is because HBx is a non-specific transactivator (Twu and Schloemer, 1987, Spandau and Lee, 1988). However, it does not transactivate chromosomal genes (van Breugel *et al*., 2012, Decorsiere *et al*., 2016). HBx has demonstrated a regulatory role over HBV promoter activity by transactivation of EnhI; this occurs despite a lack of binding to DNA, through interaction with host transcription factors (NF-κB, AP1, e-EBP, ATF/CREB, SP1 etc) (Quasdorff and Protzer, 2010). HBx has also demonstrated multiple interactions with host proteins; such as the UV-damaged-DNA-binding protein (Sitterlin *et al*., 1997), mitochondrial hsp60 and hsp70 (Zhang *et al*., 2005) and the mitochondrial antiviral signalling protein (Wei *et al*., 2010). Research has also demonstrated host proteins that bind with HBx and negatively regulate viral transcription, such as methyltransferase PRMT1 (Benhenda *et al*., 2013).

However, the HBx interaction with DDB1-Cul4 ubiquitin ligase machinery is of interest because inhibition of this interaction negatively regulates HBV infection (Sitterlin *et al*., 2000a, Sitterlin *et al*., 2000b, Li *et al*., 2010b). DNA binding protein 1 (DDB1) binds to Cullin4 (Cul4) as a component of the E3 ubiquitin ligase complex; which is utilised by multiple viruses such as HIV-1 or Influenze A virus, to degrade proteins that inhibit viral replication, through proteasomal degradation. It has been shown that HBx transactivator activity is dependent on interaction between HBx and DDB1-Cul4 (van Breugel *et al*., 2012). This interaction occurs through an H-box binding motif near the C-terminal of HBx, which selectively replaces a subset of DCAF proteins in DDB1; this has been shown to be essential for HBx function (Yoo *et al*., 2008).

Recent evidence has demonstrated that HBx activates episomal gene expression by promoting the degradation of the Structural Maintenance of Chromosomes (SMC) complex Smc5/6 (**Figure 1.14**), through DDB1-Cul4 ubiquitin ligase activity (Livingston *et al*., 2017, Murphy *et al*., 2016). The Smc5/6 subunits of the complex are putative HBx substrates and HBx has been demonstrated to reduce expression of the complex (Livingston *et al*., 2017, Murphy *et al*., 2016). This is important for viral replication because the Smc5/6 complex has been shown to bind to cccDNA and silence transcription (Livingston *et al*., 2017, Murphy *et al*., 2016). It is unclear how Smc5/6 detects cccDNA; but it is sequence independent and it has been demonstrated that Smc5/6 can bind to and block transcription from multiple forms of episomal DNA, including plasmids (Kanno *et al*., 2015). It has been suggested that Smc5/6 interacts with components of the Nuclear Domain bodies 10 (ND10) in the nucleus of primary human hepatocytes, which traffic towards incoming DNA genomes (Adler *et al*., 2011, Full *et al*., 2014) and co-localise to repress cccDNA (Everett, 2006, Niu *et al*., 2017). This interaction is inhibited by HBx (Niu *et al*., 2017).

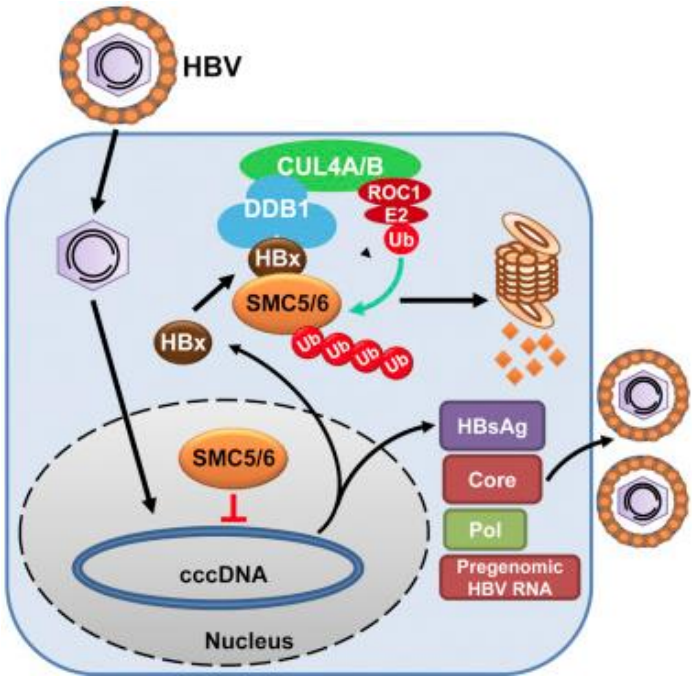

Figure 1.14 Cartoon representation of Smc5/6 pathway (Murphy *et al*., 2016)

1.3 Hypoxia Inducible Factors

Hypoxia inducible factors (HIFs) are a group of transcription factors that enable the host stress responses and are responsible for regulating the adaptation to low oxygen environments. They are found within most cell types and tissues. Typically, stabilisation of the transcription factor occurs under low oxygen and indicates that the protein is no longer being degraded. There are situations under which the protein may be stabilised under normal oxygen, for example mitochondrial stress and the generation of reactive oxygen species (Zhao *et al*., 2014, Solaini *et al*., 2010, Wilson *et al*., 2014, Guzy *et al*., 2005). Currently there are three known isoforms of HIFs; 1α, 2α and 3α. The last of these has a number of different splice variants and is not well studied (Maynard *et al*., 2003). HIF1α is ubiquitously expressed in cells and tissues around the body. The other isoforms HIF2α and 3α are more tissue-specific. All HIF isoforms are expressed in liver parenchymal cells (Nath and Szabo, 2012). Under normal oxygen HIFα subunits are degraded through proteosomal degradation. Prolyl-hydroxylases (PHDs) hydroxylate two-conserved proline residues found in the oxygen dependent degradation domain (ODD)(Berra *et al*., 2003, Nath and Szabo, 2012). Hydroxylation results in the recruitment of the Von Hippel Lindau protein (VHL) protein, which is an E3 ubiquitin ligase complex (Wilson *et al*., 2014). This in turn results in the polyubiquitination of the HIFα subunit and targeting to proteasome (Aragones *et al*., 2008, Kaelin and Ratcliffe, 2008, Schofield and Ratcliffe, 2004, Tennant *et al*., 2009, Carroll and Ashcroft, 2006).

Under hypoxic conditions the HIFα subunit for each isoform binds to a common HIFβ subunit, also called ARNT. This subunit is continuously expressed and not regulated through oxygen concentrations. This forms a heterodimer that translocates to the nucleus and binds hypoxic response elements (HREs) in the promoter regions of target genes (Carroll and Ashcroft, 2006). Reportedly, this action enables the regulation of

numerous stress response genes (Kaelin and Ratcliffe, 2008, Bertout *et al*., 2008). HIF activity is controlled under hypoxia due to a negative feedback system that upregulates PHD1-3 expression and subsequent VHL activity resulting in transient HIF expression (Schofield and Ratcliffe, 2004, Aragones *et al*., 2008, Tennant *et al*., 2009). Under hypoxic conditions the activities of these 2 hydroxylases is inhibited, that results in the stabilisation of HIF1α, following which, the protein accumulates and translocates to the nucleus where it dimerises with its HIFβ counterpart. This heterodimer can bind co-activators p300/CBP and bind the HREs found within the regulatory regions of target genes, stimulating a wide range of stress responses (Carroll and Ashcroft, 2006, Wilson *et al*., 2014). Evidence suggests that while each isoform may exist within the same tissue, these are differentially regulated through multiple mechanisms (Majmundar *et al*., 2010). The different isoforms can control a range of different genes at the same time, but have also been shown to enact different responses upon the same genes. This may indicate that each isoform regulates the others activities or performs opposing functions where required (Majmundar *et al*., 2010).

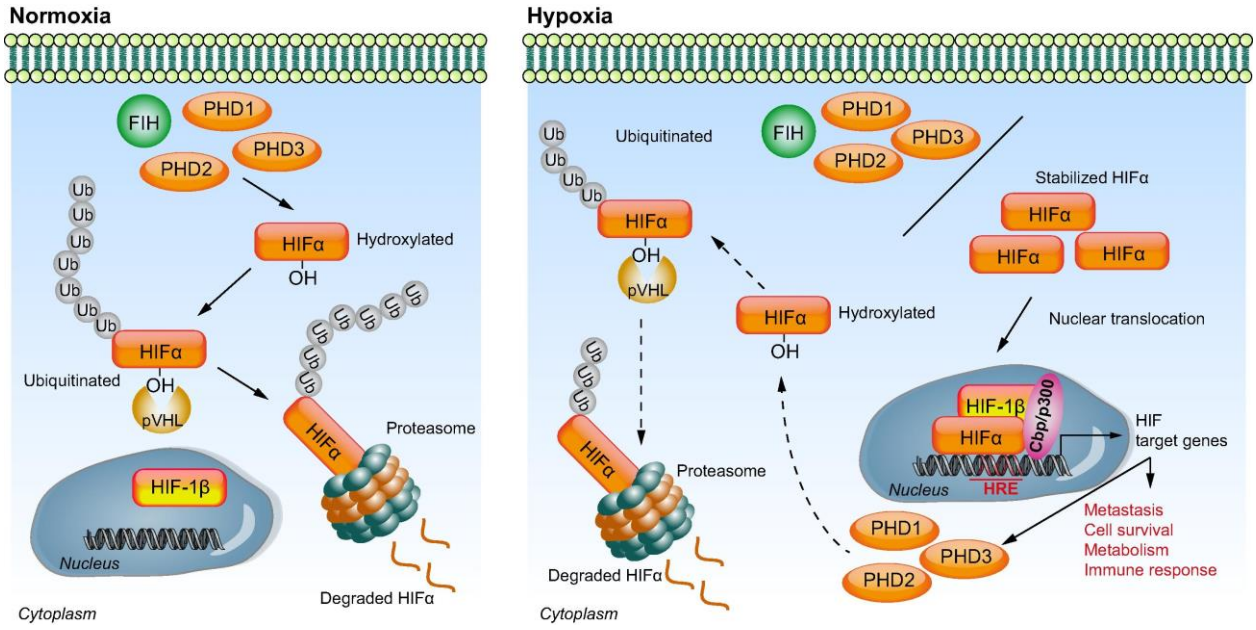

Figure 1.15 Hypoxia inducible factors, Oxygen dependent and independent regulation (Wilson *et al*., 2014)

There is another oxygen sensitive hydroxylase that regulates the activity of HIF1α; this is called the factor inhibiting HIF (FIH). FIH activity occurs through hydroxylation of an asparaginyl residue in the C-terminal domain of HIF1α. This hydroxylation prevents the binding of HIF1α to the transcriptional coactivator p300 (Wilson *et al*., 2014). HIFs can also be stabilised in the absence of a low oxygen environment; this occurs through cell surface receptor activity such as G protein-coupled receptors or receptor tyrosine kinases promoting HIF1α mRNA translation (Wilson *et al*., 2014). The phosphatidylinositol-3-kinase (PI3K) pathway uses the binding of growth factors to its receptors to activate downstream serine/ threonine kinase Akt and mTOR and HIF signalling (Agani and Jiang, 2013). Growth factors binding to receptors can activate ERK and p70S6K1, two factors important in regulating HIF1α mRNA translation (Semenza, 2003, Agani and Jiang, 2013). The ERK can also activate the MAPK signalling pathway (Sang *et al*., 2003). Reactive oxygen species generated through mitochondrial dysfunction can also result in HIF1α stabilisation through inhibiting the activity of PHDs (Chandel *et al*., 2000, Guzy *et al*., 2005, Wilson *et al*., 2014). Data obtained using HIF1 knockout mice models and an ethanol diet suggests that HIFs play a regulatory role in hepatic lipogenesis, the results showed an increase in lipid accumulation following HIF1 inhibition (Nishiyama *et al*., 2012). This implies that HIF1 plays a role in protection against alcoholic liver disease (ALD). Moon and colleagues demonstrated that HIF1 deficient mice showed increased levels of liver fibrosis and hypothesised that during chronic liver injury, continued expression of HIF1 results in increased expression of profibrotic proteins (Moon *et al*., 2009). This was tested using mice subjected to bile duct ligation (BDL) and animal model of fibrosis (Moon *et al*., 2009). Another study by Scortegagna and colleagues demonstrated the effect of HIF2 knockout in mice models; these also demonstrated an increase in lipid accumulation

and development of steatosis (Scortegagna *et al*., 2003). HIFs are involved in regulating a number of pathways.

1.3.1 HIF1α

HIF1α is involved in glucose metabolism, regulation of lipid metabolism, liver injury and tumour-associated angiogenesis, metastasis and inflammation. While under low oxygen conditions, this transcription factor regulates the conversion of oxygen-dependent ATP production to glycolysis. This is achieved by increasing glycolytic enzyme activity and lactate dehydrogenase A (LDHA) expression, which leads to increased NAD^+ production for glycolysis under hypoxia (Shim *et al*., 1997, Gordan *et al*., 2007b). In addition, PDK1 is up regulated, which enables pyruvate conversion to acetyl-CoA and reduces the oxygen consumption within cells (Kim *et al*., 2006a, Papandreou *et al*., 2006, Simon, 2006). HIF1α uses the pentose phosphate pathway to convert glycolytic intermediates into RNA and DNA. These metabolic changes play an important role in facilitating cell survival and growth under low oxygen conditions (Simon, 2006, Gordan *et al*., 2007b, Goda and Kanai, 2012).

Evidence suggests that HIF1α plays a role in cancer metabolism, metastasis and invasion. Mutations that inactivate fumerate hydratase (FH) and succinate dehydrogenase (SDH) enzymes result in increased ROS generation in tumours after fumerate and succinate accumulation (King *et al*., 2006, Selak *et al*., 2005, Isaacs *et al*., 2005). This increased inactivation of PHDs, which in turn increases HIF1α stabilisastion (King *et al*., 2006). HIF1α expression can result in a loss of E-cadherin (Evans *et al*., 2007, Krishnamachary *et al*., 2006, Esteban *et al*., 2006, Kaelin, 2008). Evidence suggests that HIF1α expression is also linked to epithelial to mesenchymal transition (EMT)(Yang *et al*., 2008). However, the mechanism differs between cancers

(Kaelin, 2008, Mak *et al*., 2010). Accumulation of HIF1α is important for the stimulation of angiogenesis, glycolysis, erythropoiesis and other targets already discussed. These are all involved in cellular tolerance to hypoxia and increasing tissue vascularity. This process is commonly utilised by host cells to heal injured tissues. However, deregulation of these pathways is commonly used by cancers. Wang and colleagues suggest that HIF1α regulates apoptosis via autophagy to destroy compromised cells (Wang *et al*., 2017). Cursio and colleagues demonstrate that HIF1α induces apoptosis in liver cells following ischemia-reperfusion injury (Cursio *et al*., 2008).

1.3.2 HIF2α

HIF2α is also responsible for regulating stress response genes in an oxygen dependent manner. These include glucose and lipid metabolism, angiogenesis, inflammation and redox homeostasis (Leek *et al*., 2002, Imtiyaz *et al*., 2010, Qu *et al*., 2011, Majmundar *et al*., 2012). HIF2α can interact with Cytochrome C oxidase to increase the electron transport chain efficiency (Gordan *et al*., 2007b). In addition, inhibition of HIF2α results in increased p53 pathway activity and this is linked to increased apoptosis of tumour cells; this is regulated through accumulation of ROS by anti-oxidant enzyme SOD2 activity (Scortegagna *et al*., 2003, Gordan *et al*., 2007a, Bertout *et al*., 2009). HIF2α is essential for pro-inflammatory cytokine expression and regulates macrophage migration or chemotaxis in models of acute and tumour inflammation (Imtiyaz and Simon, 2010, Imtiyaz *et al*., 2010), unlike HIF1α this is not regulated through ROS (Imtiyaz *et al*., 2010). High levels of HIF2α expression are observed in tumour-associated macrophages (TAMs) (Talks *et al*., 2000), with expression associated with increased tumour grade and vascularity as well as a poorer prognosis (Leek *et al*., 2002, Murdoch *et al*., 2004, Kawanaka *et al*., 2008). There is an overlap in the genes regulated through action of transcription factors HIF1α and HIF2α,

suggesting complementary or opposing functions. It has been shown that knock down of one HIFα subunit results in the up regulation of the other (Hu *et al*., 2003, Kim *et al*., 2009, Keith *et al*., 2011).

HIF2α regulates EPO production and erythropoiesis and plays a role in regulating hepatic lipid metabolism (Scortegagna *et al*., 2003, Mastrogiannaki *et al*., 2009). It has been demonstrated that continual activation of HIF2α results in severe hepatic steatosis; this is combined with impaired fatty acid β-oxidation, decreased lipogenic gene expression and an increase in lipid storage capacity(Scortegagna *et al*., 2003). This demonstrated the importance of HIF2α as a lipid metabolism regulator (Rankin *et al*., 2009). HIF2α regulates the expression of liver-enriched gene 1 (leg1), a secretory protein involved in hepatogenesis at the final stage called 'hepatic outgrowth' (Lin *et al*., 2014).

1.3.3 HIF3α

The third known isoform is HIF3α. This is the least well-studied isoform, although previous studies have shown expression in kidneys and lung epithelial cells. Expression has been reported in the liver; however, the number of studies is limited. Most experiments looking into HIF3α activity have been conducted in Chinese Hamster Ovary cells (ChoK1). It has been shown that HIF3α is regulated in an oxygen dependent manner similar to HIF1α and HIF2α. Unlike the other 2 HIFα subunits, HIF3α has 7 identified splice variants, which can be separated by size (Maynard *et al*., 2003). It has been reported that HIF3α interaction with the other HIFα subunits can prevent nuclear translocation; this suggests a regulatory role over the other HIFα subunits (Heikkila *et al*., 2011). The 3α4 splice variant in particular has been shown to interact with HIF1α, HIF2α and HIFβ and act as a negative regulator (Heikkila *et al*.,

2011, Ando *et al*., 2013). HIF3α enacts its negative regulation of HIF1α through inhibition of nuclear translocation. In addition, down regulation of HIF3α has been shown to reduce HIF target gene expression; perhaps indicating that HIF3α is not limited to a negative regulatory role (Augstein *et al*., 2011, Heikkila *et al*., 2011). There is some evidence to suggest that HIF3α might be a target of HIF2α, it is demonstrated that hypoxia does not stimulate HIF3α expression, rather its linked to the expression of HIF2α (Liu *et al*., 2016).

1.4 HBV and Hypoxia

Having discussed the HBV lifecycle in detail and talked about HIFs and low oxygen in the liver; it is important to discuss how these tow topics intersect. As mentioned previously HBV reportedly interacts with a range of ubiquitous and liver specific transcription factors (Quasdorff and Protzer, 2010). These interactions occur through direct interaction with HBV promoters and enhancers or through binding of the HBx protein. As discussed HIFs and HIF1α are associated with regulating a range of stress response genes as well as playing roles in glucose and lipid metabolism. These transcription factors have been linked to oncogenesis for several cancers such as bladder, breast, liver, ovarion, pancreatic, prostate and renal cancers (Harris *et al*., 2002, Pilarsky *et al*., 2004, Bardos and Ashcroft, 2004, Franovic *et al*., 2009, Semenza, 2003). Studies have shown that HIF1α is linked to HCC progression and that HIFs might be the link to HBV associated HCC pathogenesis. HIF1α activity can be induced in a couple of ways, through disruption of oxygen-dependent degradation or through an increase in growth factor signalling. Previous studies indicate that this interaction between HBV and HIF1α primarily occur through the HBx protein. Interactions have primarily been shown through co-immunoprecipitation of HBx and HIFs following transfection of HBV or overexpression of HBx and treatment with HIF stabilising agents

such as Dimethyloxalylglycine (DMOG) or cobalt chloride ($CoCl_2$). The following section will detail some of these previously observed interactions (**Figure 1.16**).

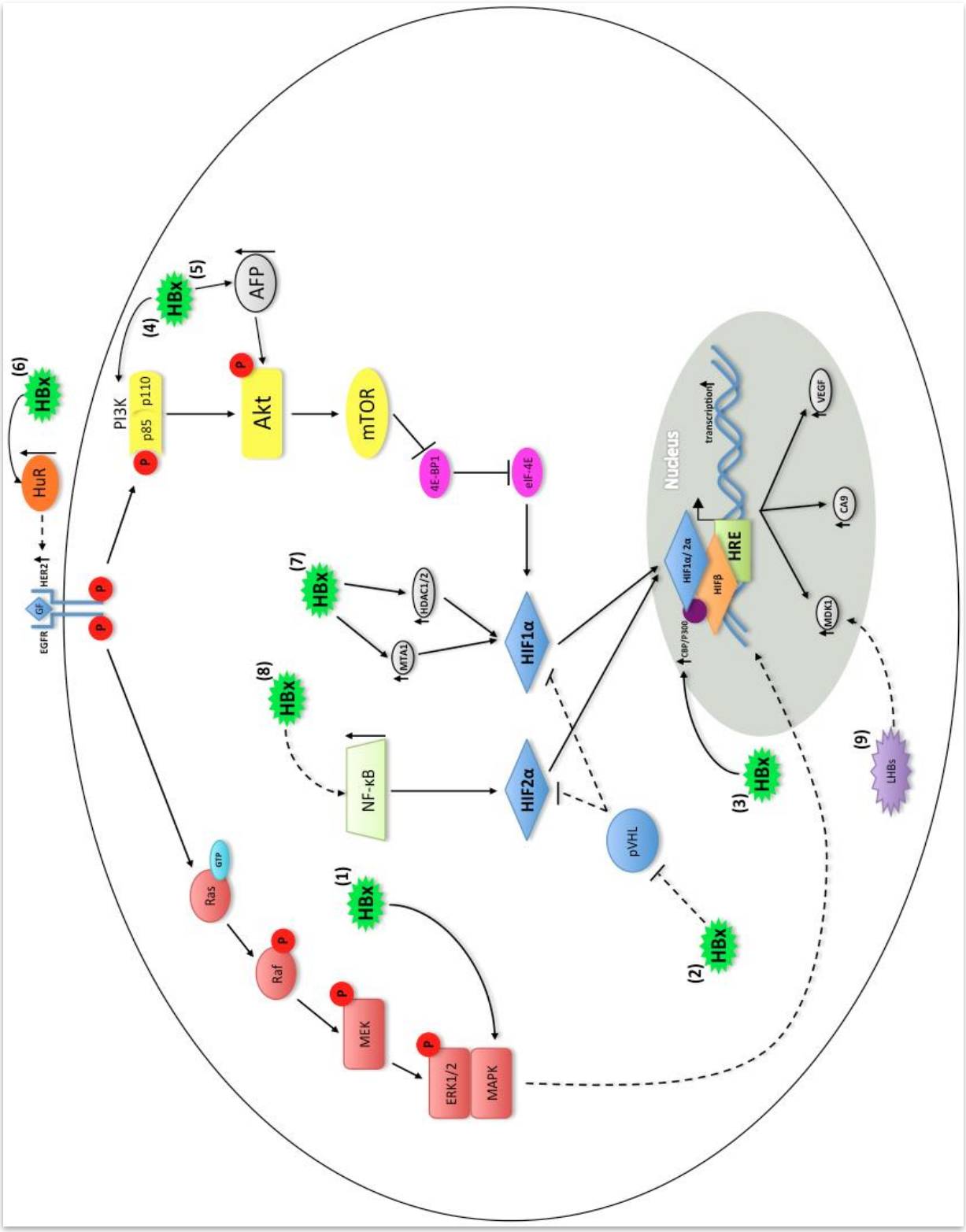

Figure 1.16 Cartoon representation of reported HBV-HIF interactions

HBx has been identified as a major contributing factor in the development of HBV associated HCC (Fallot *et al*., 2012). Yoo and colleagues showed that HBx induced genetic instability and disrupts the normal cell cycle; this occurred simultaneous to increased translation of HIF1α mRNA and increased HIF target gene activity. This study demonstrated that HBx activation of MAPK signalling may activate HIF1α transcription (**Figure 1.16 (1)**) (Yoo *et al*., 2003). Yoo and colleagues also demonstrated that the C-terminus domain of HBx increased the stability of HIF1α in HBx transfected liver and non-liver cells (Yoo *et al*., 2004). In addition they demonstrated that the C-terminus of HBx increased the transactivation function of HIF1α by enhancing its association with CBP/p300 (**Figure 1.16 (3)**) (Yoo *et al*., 2004). The authors showed that the C-terminus of HBx interacts and binds the bHLH/ PAS, ODD and C-TAD domains of HIF1α and suggest that this could interfere with PHD and VHL interactions with HIFs, thereby preventing proteasomal degradation (**Figure 1.16 (2)**) (Yoo *et al*, 2004). Moon and colleagues reported the same observation and suggested that HBx stabilisation of HIFs lead to angiogenesis during hepatocarcinogenesis (Moon *et al*., 2004). Holotnakova and colleagues also showed that HBx binding to the bHLH/PAS region stimulated HIF1α interaction with its target promoters and resulted in increased carbonic anhydrase 9 (CA9) expression (Holotnakova *et al*., 2010). CA9 is known for roles in pH regulation, which enables survival in cells with intracellular acidosis and hypoxia like conditions (Holotnakova *et al*., 2010).

Liu and colleagues reported that HBx could stabilise HIF1α via activating the human epidermal growth factor receptor 2 (HER2) signalling pathway via increased activation of PI3K and Akt pathway (**Figure 1.16 (4)**) (Liu *et al*., 2009). Hung and colleagues have demonstrated that HBx interacts with RNA-binding protein HuR and increases

stabilisation of HER2, which could result in increased activation of the PI3K pathway (**Figure 1.16 (6)**) (Hung *et al*., 2014). Zhu and colleagues also demonstrated that the HBx increases alpha-fetoprotein (AFP) expression that activates PI3K/ Akt signalling and promotes mTOR stimulation of HIF expression (**Figure 1.16 (5)**) (Zhu *et al*., 2015a, Zhu *et al*., 2015b), possibly through inhibition of 4E-BP1 (Gingras *et al*., 1998, Uniacke *et al*., 2012). HBV has been shown to interact with eIF-4E previously, through HBV polymerase and incorporation into the nucleocapsid (Montero *et al*., 2015, Kim *et al*., 2010b). Yoo and colleagues demonstrated that HBx induced expression of metastasis associated protein 1 (MTA1) and histone deacetylase (HDAC) at transcriptional levels. These have been shown to physically associate with HIF1α in the presence of HBx. HBx interaction with HDAC stimulates deacetylation of the ODD region in HIF1α, this prevents hydroxylation by PHDs and subsequent ubiquitination by VHL (**Figure 1.16 (7)**) (Yoo *et al*., 2008). This interaction could be inhibited through siRNA treatment against MTA1 (Yoo *et al*., 2008).

Hu and colleagues demonstrate the HBx can stimulate the stabilisation of HIF2α, this occurs through HBx binding to VHL to prevent alpha subunit degradation and simultaneous stimulation of NF-κB, which upregulated expression HIF2α (**Figure 1.16 (8)**) (Hu *et al*., 2016). Alternatively, Li *et al* recently suggested a new role for HIF1α in HBV infections. They demonstrate that HBV L protein can increase the expression of multi-drug resistance protein 1 (MDR1) in a HIF1α dependent manner (**Figure 1.16 (9)**) (Li *et al*., 2017). They argued that this contributed to the pathogenic changes in chronic HBV and contributed to chemotherapeutic resistance in HCC. Another argument suggests that this activation of MDR1 occurs following accumulation of HBsAg (including L protein), which could cause cellular stress responses. Li *et al*, suggest that LHBs might stimulate HIF1α more strongly than HBx (Li *et al*., 2017).

It is clear that there is a relationship between HBV and HIF1α, however the exact mechanism of interaction and impact of the interaction requires further study. The use of HBx over-expression systems has limited many of the conclusions reached in the reports.

1.5 Aims

The aim of this study was to further our understanding of the role hypoxia plays in HBV viral lifecycle and to expand upon current research using current gold standards for modelling native infections and examining the effect of hypoxia at different stages of replication. Most studies to date used artificial models of infection and stimulated hypoxic responses with drugs rather than true low oxygen environments. First, we examined the kinetics of HIF stabilisation and activity in hepatoma cell lines known to support HBV infection. We also studied the impact of differentiation status on cellular responses to low oxygen. Next, we examined the kinetics of HIF stabilisation and activity in chronically infected producer cell lines and artificial transfections of HBV genomes. We also studied the effect of differentiation on viral nucleic acids and HIF responses in the producer cells. Lastly, we examined the effects of low oxygen on viral replication using a *de novo* infection model that utilises mature Dane particles. Taken together these aims provided the basis for experiments that aided in understanding low oxygen effects on HBV replication. We hypothesised that low oxygen was promoting viral replication.

2. MATERIALS AND METHODS

2.1 Tissue Culture

All cells used in this study are described in **Table 2.1** Cells were maintained in Dulbecco's modified Eagles medium (DMEM) (Gibco, USA) supplemented with 10% foetal bovine serum (FBS), 1% v/v penicillin-streptomycin (pen/strep) and 1% L-Glutamine; from here on referred to as growth media. For normoxic experiments cells were incubated at 37ºC with 20% O_2 and 5% CO_2. For hypoxia cells were grown under 1% O_2 or 3% O_2 in a humidified sealed hypoxystation (Don Whitely Scientific, UK) calibrated to 5% CO_2 and 95% N_2. For Non-DMSO differentiation cells were maintained in William's E Medium (Gibco, USA) supplemented with 10% FBS, 1% v/v pen/strep, 1% L-Glutamine, inosine 10 µg/ml, 25 mM Glucose, 4.9 µg/ml Hydrocortisone and 1µg/ml insulin; from here on referred to as differentiation media.

2.2 Transfections

Target cells were seeded into 6-well plates in 10% FBS growth media. Prior to transfection the media was removed and replaced with penicillin/streptomycin free DMEM containing 3% FBS. Cells were transfected with Fugene6 (Promega, USA) according to the manufacturer's instructions. siRNA transfections were performed with Lipofectamine® RNAiMax (Thermo Fisher Scientific, USA) according to the manufacturer's instructions. After transfection in some protocols, cells were reseeded into 96 well plates as described in **Section 2.3**. All plasmids used in this study are listed in **Table 2.2**.

Table 2.1 Cell lines used in this study

Table detailing the cell lines used throughout this project, including the name of each cell line, tissue of origin, a brief description of the cell line, and the source from which we obtained the cell lines.

Name	Tissue of origin	Description	Source
Huh-7	Human Hepatoma	Well differentiated hepatocyte derived cellular carcinoma cell line taken from a 57-year-old Japanese male in 1982.	Dr Charles Rice, Rockefeller University, New York, USA
Huh-7.5	Subclone of Huh-7	Derived from Huh-7 cells, highly permissive to HCV infection.	Dr Charles Rice, Rockefeller University, New York, USA
HepG2	Human Hepatoma	Well differentiated hepatocellular carcinoma derived cell line taken from a 15-year-old Caucasian male.	ATCC
HepG2-NTCP	HepG2 with over expressed NTCP	HepG2 cells overexpressing bile acid transporter NTCP.	Dr Ulrike Protzer, Technische Universität München, Munich, Germany
HepG2-NTCP K7	Subclone of HepG2-NTCP	-	Dr Ulrike Protzer, Technische Universität München, Munich, Germany
HepG2.2.15	HepG2-derived cell line	Derived from HepG2 cells and characterised by having stable HBV expression derived from four tandem repeats of HBV genotype D.	Dr Ulrike Protzer, Technische Universität München, Munich, Germany
HepAD38	HepG2-derived cell line	Derived from HepG2 cells and characterised by having stable HBV expression under the control of a CMV promoter and inducible with tetracycline.	Dr Ulrike Protzer, Technische Universität München, Munich, Germany

Table 2.2 Plasmids used in this study

Table detailing the plasmids used throughout this project including the vector, specific insert, the working concentration and the source from which we obtained the plasmid.

Vector	Insert	Plasmid Source	Working Concentration
pGL3	HRE Luciferase	Professor Margaret Ashcroft, University of Cambridge, Cambridge, UK	2µg/ml
pCDNA3	HIF-1α-FLAG	Professor Margaret Ashcroft, University of Cambridge, Cambridge, UK	10µg/ml
pCDNA3	HIF-2α-Myc	Professor Margaret Ashcroft, University of Cambridge, Cambridge, UK	10µg/ml
pCDNA3	HIF-1α wild type	Dr Norma Masson, University of Oxford, Oxford, UK	1µg/ml
pCDNA3	HIF-2α wild type	Dr Norma Masson, University of Oxford, Oxford, UK	1µg/ml
pCDNA3	HIF-1α double proline mutation	Dr Norma Masson, University of Oxford, Oxford, UK	1µg/ml
pCDNA3	HIF-2α double proline mutation	Dr Norma Masson, University of Oxford, Oxford, UK	1µg/ml
pGEM-4Z	HBV Genotype C	Dr Ulrike Protzer, Technische Universität München, Munich, Germany	1µg/ml
pGEM-4Z	HBV Genotype D	Dr Ulrike Protzer, Technische Universität München, Munich, Germany	1µg/ml and 10^{10} copies for PCR standards
pGEM-4Z	Genotype D (X-)	Dr Ulrike Protzer, Technische Universität München, Munich, Germany	1µg/ml
pGEM-4Z	Genotype D (L-)	Dr Ulrike Protzer, Technische Universität München, Munich, Germany	1µg/ml
pGEM-4Z	Genotype D (X- / L-)	Dr Ulrike Protzer, Technische Universität München, Munich, Germany	1µg/ml
PGL3	HBV EnhI/II + BCP promoter	Dr Chunkyu Ko, Technische Universität München, Munich, Germany	500ng/ml
PGL3	HBV Enh1/X promoter	Dr Chunkyu Ko, Technische Universität München, Munich, Germany	500ng/ml
PGL3	HBV S1 Promoter	Dr Chunkyu Ko, Technische Universität München, Munich, Germany	1µg/ml
PGL3	HBV S2 Promoter	Dr Chunkyu Ko, Technische Universität München, Munich, Germany	1µg/ml
PGL3	HBV X protein	Dr Maarten van de Klundert, Technische Universität München, Munich, Germany	1µg/ml
PGL3	HBV X protein mutant (R96E)	Dr Maarten van de Klundert, Technische Universität München, Munich, Germany	1µg/ml
-	HIF-1α siRNA	Dharmacon, USA	1µg/ml
-	HIF-2α siRNA	Dharmacon, USA	1µg/ml

2.3 HRE Luciferase Assay

This assay is performed to ascertain the kinetics of HRE activation in cells exposed to hypoxic conditions representing HIF activity. Hepatoma cells were seeded at $2x10^5$ per $9.6cm^2$ in 10% FBS growth media. The cells were transfected with 2µg of HRE luciferase reporter plasmid. Twenty-four hours after transfection, the cells were trypsinised and $2x10^4$ cells were re seeded into each well of 96-well plates for each time point and condition in triplicate. The cells are then placed into either normoxic (20% O2) or hypoxic (1-3% O2) incubation. A T0 time point is taken at this point. The media is removed from each well in the 96-well plate. Samples are lysed using 1x luciferase lysis buffer (25mM Tris-phosphate (pH 7.8), 2mM DTT, 2mM 1,2-diaminocyclohexane-N,N,N´,N´-tetra acetic acid, 10% glycerol, 1% Triton X-100) added to each well, the plates are then frozen at -20ºC until ready for reading. Following lysis of all samples, plates are removed from the freezer and thawed. The lysis buffer and lysed cells are transferred to the 96 well luminometer plates. Luciferase assay substrate (Promega, USA) is added to each well. The plate is read using a luminometer (Centro LB 960 Microplate Luminometer) kinetics operation. Data demonstrated in graphs represents raw relative light units (RLU) from 3-4 technical repeats normalised against cell counts. Data is also represented as relative values of hypoxic samples against normoxic controls.

2.4 Generation of HBV

This protocol is used to generate full-length genotype D HBV particles from the producer cell line HepG2.2.15s. These cells are chronically infected with Hepatitis B. HepG2.2.15 cells were seeded into T175 flasks (Corning, USA) coated with collagen (Sigma, USA). These cells are maintained in DMEM with 10% FBS and 1% pen/strep.

After 72 hours, the media is changed to DMEM with 5% FBS, 2% DMSO and 1% pen/strep to DMSO differentiate the cells over an additional 72 hours. Following differentiation, discard the media and change to serum free DMEM containing 2% DMSO and 1% pen/strep. The media is harvested and replaced every 24 hours. Conditioned media contains un-concentrated HBV particles. Virus is concentrated using Vivaspin columns (25 mL a time) at 4,000G for 15 minutes in centrifuge. Concentrated virus is aliquoted into 1ml Eppendorfs. DNA levels are quantified using qPCR (Section 2.9). Dane particles are purified using HiTrap Heparin HP affinity columns (GE Healthcare Life Sciences, UK). Concentrated virus was applied to the column and washed 5x with wash buffer (20 mM phosphate buffer, 50 mM NaCl, pH 7) to remove non-infectious sub viral particles. The virus was then eluted with elution buffer (20 mM phosphate buffer, 2 M NaCl, pH 7). Following elution the virus was aliquoted into 1mL cryovial tubes and frozen at -80^{o}C. The virus was shipped from Munich by secure courier using appropriate containment measures in dry ice. Upon receiving the virus, cryovial tubes were stored at -80^{o}C.

2.4.1 Category 3 containment

All cell culture and experiments using HBV or chronically infected producer cell lines were performed under Category 3 containment. This involved two layers of containment. The safety equipment and the laboratory itself. Entry to catergory 3 laboratory was prohibited until safety training was completed.

2.5 De Novo Infections

HepG2-NTCP K7 cells are seeded at 5x10^{4} cells per well in DMEM containing 10% FBS, 2% DMSO, 1% pen/strep. The cells are DMSO differentiated over 72 hours in this media. Concentrated HBV (MOI of 100) is combined with infection media, DMEM

containing 5% FBS, 2% DMSO, 5% PEG8000 and 1% pen/strep. Following combination, the virus and media should be mixed for 5 minutes before being added to cells. Twenty-four hours later, remove the infection media and wash cells 3x with serum-free DMEM (Gibco, USA). Retain the final wash as a T0 time point. This can be used as a negative control. The sample can be frozen at -20^{o}C. Replace the serum-free DMEM with DMEM containing 5% FBS, 2% DMSO and 1% pen/strep. After 96 hours (5 days post infection), collect the media and replace with fresh media that is DMSO free. Store the sample at -20^{o}C. After 24 hours the samples can be treated with drugs or transfected. Dependent of whether treatments were applied, infections can be placed into hypoxic or normoxic conditions 5-6 days post infection. Collected supernatants can be used in HBsAg and HBeAg ELISAs to detect HBV infections. HBV RNA and DNA levels quantified by PCR (Sections 2.8 and 2.9).

2.6 HBV E and S antigen ELISAs

Following completion of infection HBV E and S antigen can be detected in the conditioned media removed at time points throughout infection using ELISA kits (Abnova, USA). Samples were collected as described in section 2.5 and the assays performed as per manufacturer's instructions. Briefly for S antigen ELISAs, add 50 µL of sample supernatants into wells of the ELISA plates. Add 50 µL of Anti-HBs Peroxidase Solution to each well except the blank. Incubate the reaction plate at 37^{o}C in a water bath or incubator for 80 minutes. For E antigen ELISAs, add 100 µL of sample supernatants into wells of the ELISA plates. Incubate the reaction plate at 37^{o}C in a water bath or incubator for 1 hour. Follow the "plate washing procedure". Add 100 µL of Anti-HBe Peroxidase Solution to each well except the blank. Incubate the reaction plate at 37^{o}C in a water bath or incubator for 1 hour. Repeat washing procedure. Add 100 µL of TMB substrate solution and incubate at room temperature for 30 minutes. Stop the reaction by adding 100 µL of 2 N H_2SO_4 to each well except the blanks. Following incubations and colour development the plates are read at 490nm using a spectrophotometer to determine an OD reading. This is compared to blank wells along with positive and negative control samples. The OD readings are expressed relative to a cut-off value (s/ c off) (as described in manufacturer's instructions). This value is determined by combining the uninfected cell sample mean and two standard deviations around the mean. Any value above the cut-off value is considered a true infection.

2.7 Western Blotting

2.7.1 Lysate preparation and sodium dodecyl sulphate polyacrylamide gel electrophoresis (SDS-PAGE)

Cell lysates were prepared from target cells harvested after exposure to hypoxic (1% O_2) or normoxic conditions (20% O_2) using 8M urea lysis buffer (H_2O, 8M urea, 8% glycerol, 20% sodium dodecyl sulphate [SDS], 1M Tris-HCL, pH7.5) and then 1x reducing laemmli buffer (H_2O, 30% glycerol, 6% SDS, 0.02% bromophenol blue, 10% 2-β-mercaptoethanol and 0.2M Tris-HCL; pH6.8) was added at a ratio of 1:3. Protein concentration was determined using the NanoDrop 2000 spectrophotometer; thereafter, lysates were denatured at 95^{o}C for 10 minutes. Proteins were separated on 8% SDS polyacrylamide gels using the Mini Protean 3 system (Bio-Rad, USA) according to the manufacturer's instruction. Briefly, 10-20µg of protein was loaded onto gels and ran at 350 mAmps constant for 45 minutes in running buffer (0.25M Tris base, 1.92M glycine, pH 8.4) (National Diagnostics, USA). Proteins were transferred to polyvinylidene membranes (Millipore, USA) using a Mini Trans-Blot Electrophoresis transfer system (Bio-Rad, USA). Polyvinylidene membranes were activated with methanol for 2 minutes followed by incubation in transfer buffer (National Diagnostics, USA) for 5 minutes at room temperature. SDS gels were also equilibrated in transfer buffer to prevent shrinking and transfer was performed at 350mAmps for 70-80 minutes at room temperature.

2.7.2 Immuno-blotting and chemiluminescent detection of proteins

After transfer, membranes were incubated in antibody buffer (PBS, 0.1% Tween-20 and 5% Marvel Dry Milk) for 45 minutes at room temperature to prevent non-specific antibody binding. The blocking buffer was removed and membranes incubated in

primary antibodies for HIF-1α (BD Biosciences, USA), HIF-2α (Ratcliffe Laboratory, University of Oxford) or β-actin (Thermo Fisher Scientific, USA), diluted in antibody buffer at 4°C overnight with gentle agitation on a tube roller (Barloworld Scientific, UK). The following day membranes were washed in washing buffer (PBS, 0.1% Tween-20) 4 times for 5 minutes. Incubation with horseradish peroxidase (HRP) conjugated secondary antibodies (Dako, Agilent Technologies, USA) was carried out for 60 minutes at room temperature in antibody buffer followed by excess washing. Chemiluminescent detection of HRP-conjugates was achieved with an ECL detection system called SuperSignal™ West Dura Extended Duration Substrate (Thermo Fisher Scientific, USA). Briefly, membranes were incubated in ECL reagent for 1 minute and proteins detected using the PXi Touch Gel Imaging System (Syngene, UK).

2.8 Quantitative RT-PCR

RNA was prepared from target cells. The growth medium was removed and samples were washed with PBS, the cells were then lysed using RLT+ lysis buffer (Qiagen, Germany). Cellular RNA purification was performed using the Allprep DNA and RNA purification kit (see **Figure 8.2**) (Qiagen, Germany). RNA was amplified using the TaqMan™ primers (Applied Biosystems, USA) listed in **Table 2.3**. Reaction master-mix was designed using components of the Cells Direct Kit (Invitrogen, USA) according to the manufacture's instructions. Quantitative reverse-transcription PCR (qRT-PCR) was carried out in a microAmp 96 well optimal reaction plate (Applied Biosystems, USA) using a Mx3000P qPCR system (Agilent Technologies, USA) and data analysed with the MXpro software. The PCR cycling conditions are as follows: 30 minutes at 50ºC, 5 minutes at 95ºC followed by 50 cycles of 95ºC for 15 seconds and 60ºC for 60 seconds. HBV pgRNA data represents copies as determined by a standard curve produced using a 10-fold dilution series of concentrated HBV genome (Genotype D – plasmid H1.3). Copies are normalized against Beta-2 Microglobulin (B2M) endogenous control for extraction efficiency. HIF target genes data represents relative mRNA expression as determined by the $2^{-\Delta\Delta Ct}$ method for relative quantification; samples are normalized against B2M endogenous control.

2.9 SYBR Green PCR to amplify HBV nucleic acids

DNA was prepared from target cells. The growth medium was removed and samples were washed with PBS, the cells were then lysed using RLT+ lysis buffer (Qiagen, Germany). Cellular DNA purification was performed using the Allprep DNA and RNA purification kit (Qiagen, Germany). Quantitative PCR (qPCR) performed using SYBR green master mix (Life Technologies, USA) as per manufacturer's instructions. DNA

amplification was performed using primer pairs listed in **Table 2.4**. The PCR cycling conditions are as follows for HBV rcDNA: 5 mins at 95°C; 50 cycles at 95°C for 3s and 60°C for 60s. The PCR cycling conditions are as follows for HBV cccDNA: 5 mins at 95°C; 60 cycles at 95°C for 3s, 60°C for 60s and 72°C for 15s. The PCR cycling conditions are as follows for ChIP assay: 10 mins at 95°C; 45 cycles at 95°C for 30s and 58°C for 30s and 72°C for 30s. HBV rcDNA and cccDNA data represents copies as determined by a standard curve produced using a 10 fold dilution series of concentrated HBV genome (Genotype D – plasmid H1.3). Copies are normalized against cellular prion protein (PrPc) endogenous control. Representative dissociation curves for HBV SYBR Green PCRs are displayed in **Figure 2.1**.

Table 2.3 TaqMan™ primers used in study

Table detailing the TaqMan™ primers used throughout this project including the name of each primer, the source, and the sequence information if available.

Primers	Source	Sequence
AFP	Applied Biosystems	Non-disclosed sequences
ALB	Applied Biosystems	Non-disclosed sequences
BNIP3	Applied Biosystems	Non-disclosed sequences
CYP3A4	Applied Biosystems	Non-disclosed sequences
EPAS1 (HIF2α)	Applied Biosystems	Non-disclosed sequences
EPO	Applied Biosystems	Non-disclosed sequences
HIF1α	Applied Biosystems	Non-disclosed sequences
HNF4α	Applied Biosystems	Non-disclosed sequences
PDK1	Applied Biosystems	Non-disclosed sequences
pgRNA	Applied Biosystems	Custom-made primers (Sequences Obtained from Dr Chunkyu Ko TUM). HBV2270F: 5′-GAGTGTGGATTCGCACTCC-3′ HBV2392R: 5′-GAGGCGAGGGAGTTCTTCT-3′
SLC16A3	Applied Biosystems	Non-disclosed sequences

Table 2.4 SYBR Green primers used in this study

Table detailing the SYBR Green primers used throughout this project including the name of each primer, the source, and the sequence information if available.

Primer Pairs	Source	Sequences (Forward [F] and Reverse [R])	
HBV Genome Pair 1	Applied Biosystems	HBV178F	5'-TTCCTAGGACCCCTTCTCGT-3'
		HBV307R	5'-GGCCAAGACACACGGTAGTT-3'
HBV Genome Pair 2	Applied Biosystems	HBV346F	5'-TCCTGTCCTCCAACTTGTCC-3'
		HBV422R	5'-AGCAGCAGGATGAAGAGGAA-3'
HBV Genome Pair 3	Applied Biosystems	HBV518F	5'-GCCGAACCTGCATGACTACT-3'
		HBV653R	5'-GCCCACTCCCATAGGAATTT-3'
HBV Genome Pair 4	Applied Biosystems	HBV718F	5'-CCCACTGTTTGGCTTTCAGT-3'
		HBV801R	5'-CAGCGGTAAAAAGGGACTCA-3'
HBV Genome Pair 5	Applied Biosystems	HBV995F	5'-ACGAATTGTGGGTCTTTTGG-3'
		HBV1108R	5'-GTTGGCGAGAAAGTGAAAGC-3'
HBV Genome Pair 6	Applied Biosystems	HBV1089F	5'-GCTTTCACTTTCTCGCCAAC-3'
		HBV1154R	5'-AACGGGGTAAAGGTTCAGGT-3'
HBV Genome Pair 7	Applied Biosystems	HBV1581F	5'-GTGCACTTCGCTTCACCTCT-3'
		HBV1693R	5'-GGTCGTTGACATTGCAGAGA-3'
HBV Genome Pair 8	Applied Biosystems	HBV1738F	5'-GGAGTTGGGGGAGGAGATTA-3'
		HBV1837R	5'-GGCAGAGGTGAAAAAGTTGC-3'
HBV Genome Pair 9	Applied Biosystems	HBV2112F	5'-CTGGGTGGGTGTTAATTTGG-3'
		HBV2297R	5'-TAAGCTGGAGGAGTGCGAAT-3'
HBV Genome Pair 10	Applied Biosystems	HBV2279F	5'-TTCGCACTCCTCCAGCTTAT-3'
		HBV2392R	5'-GAGGCGAGGGAGTTCTTCTT-3'
HBV Genome Pair 11	Applied Biosystems	HBV2983F	5'-ACAAGGTAGGAGCTGGAGCA-3'
		HBV3133R	5'-GTAGGCTGCCTTCCTGTCTG-3'
cccDNA	Applied Biosystems	cccDNA92F	5'-GCCTATTGATTGGAAAGTATGT-3'
		cccDNA2251R	5'-AGCTGAGGCGGTATCTA-3'
rcDNA	Applied Biosystems	rcDNA1844F	5'-GTTGCCCGTTTGTCCTCTAATTC-3'
		rcDNA1745R	5'-GGAGGGATACATAGAGGTTCCTTGA-3'
PrPc	Applied Biosystems	PrPc F	5'-TGCTGGGAAGTGCCATGAG-3'
		PrPc R	5'-CGGTGCATGTTTTCACGATAGTA-3'

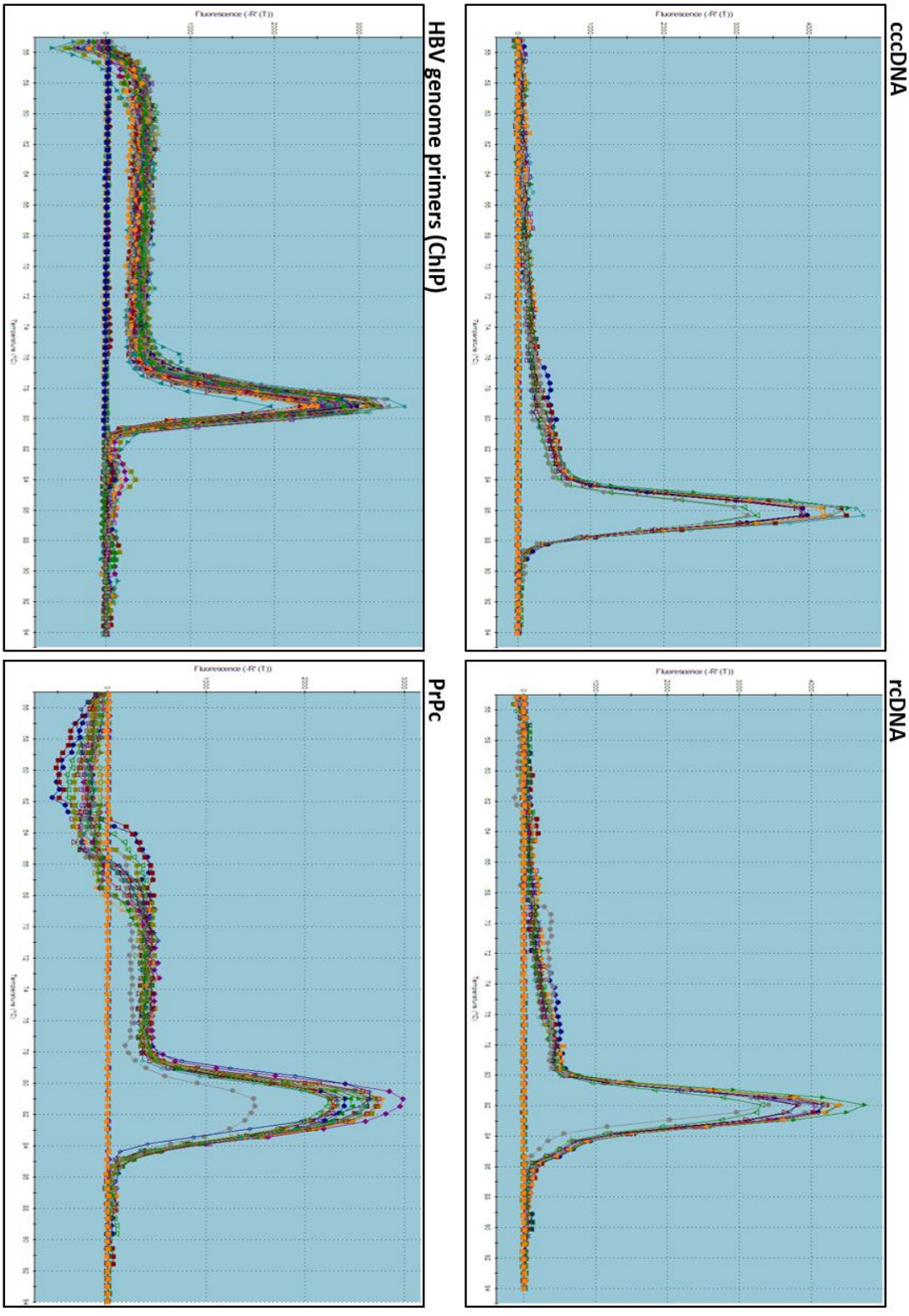

Figure 2.1 Representative dissociation curves for HBV SYBR Green PCRs

2.10 PCR Array

Selected hypoxia signalling PCR arrays consisting of 84 hypoxia regulated genes were purchased from (SABiosciences, USA) and performed as per the manufacture's instructions. Briefly, cDNA was synthesized from purified cellular RNA using the RT^2 First Strand Kit components listed in **Table 2.5**. Followed by reverse transcription of cDNA products using the SYBR Green Reverse Transcriptase mix (Qiagen, Germany). Reaction mix was added to profiler array 384 well plates and PCR cycling achieved with the Applied Biosystems 7900HT machine using the following conditions, 10mins at 95°C, 40 cycles of 15s at 95°C, and 1 minute at 60°C. Data analysed via the SABiosciences online PCR array portal.

Table 2.5 PCR array components

Table detailing reaction components and required volumes for 4 reactions using selected hypoxia signalling PCR arrays.

Components	Volumes for 4 reactions
5x Buffer BC3	16µL
Control P2	4µL
RE3 Reverse Transcriptase Mix	8µL
RNase-free water	12µL
Total Volume	40µL

2.11 Immunofluorescent Staining of HBV S Antigen

Following completion of infection, it is possible to stain for the presence of HBV S antigen, which is indicative of infection. HepG2.2.15 and uninfected HepG2 NTCP cells are used as positive and negative controls in this experiment. After the infection is complete the cells are fixed for 25 minutes in 6% paraformaldehyde (PFA) (Sigma, USA). The fixative is removed and cells washed with PBS. The cells are permeabilized for 10 minutes using a solution of 0.01% Triton X-100 (Sigma, USA) diluted in PBS. Following permeabilization, the solution is aspirated and cells washed 3x with PBS. The cells are blocked for 30 minutes in PBS containing 0.5% bovine serum albumin (BSA). This prevents non-specific antibody binding. The primary antibody (Anti-Hepatitis B Virus Surface Antigen (ab8636), Abcam, UK) is diluted in PBS containing 0.5% BSA and 0.5% Saponin. After adding primary antibody to the cells (1:100 or 2µg/ml), incubate at room temperature for 1 hour. The antibody is removed and cells washed 3x in diluent solution. Add the secondary antibody (Goat anti-Mouse Alexa Fluor 488, Life Technologies, USA – 1:500 dilution in diluent solution). The cells are incubated at room temperature for 1 hour in the dark, wrapped in foil. Following incubation, the cells are washed 3x with diluent solution. DAPI (Life Technologies, USA) is added to the cells for 1 minute, the cells are subsequently rinsed and can be maintained in PBS until imaging. Coverslips are mounted onto microscope slides using ProLong® Gold Antifade Reagent (Life Technologies, USA). Images captured using a Leica D6000 fluorescence microscope using a 10x and 40x objective.

2.12 Chromatin Immunoprecipitation (ChIP)

HepG2.2.15 cells were grown to 80% confluency in T75 culture flasks. After reaching 80% confluency flasks are placed under 20% and 1% oxygen for 24 hours. Samples

are fixed in 1% formaldehyde for 5 minutes at room temperature to cross-link protein to DNA. Fixed cells are washed 1x with ice-cold PBS. Fixation is stopped using Glycine Stop-Fix solution (Active Motif, USA). Cells are washed 1x with ice-cold PBS. Cells are harvested by addition cell scraping solution (Active Motif, USA) and scraping using rubber policeman. Harvested cells are pelleted by centrifugation at 2,500 rpm for 10 minutes at 4^{o}C. The supernatant is discarded. The pellet is resuspended in 1ml of ice-cold Lysis Buffer (Active Motif, USA) and incubated on ice for 30 minutes. The cells are transferred to an ice-cold dounce homogenizer; cells are homogenized with 10 strokes to aid nuclei release. Homogenized cells are transferred to microcentrifuge tubes and the nuclei are pelleted by centrifugation at 5,000 rpm for 10 minutes at 4^{o}C. Supernatants are carefully removed and discarded. Nuclei pellets are resuspended in Shearing Buffer (Active Motif, USA). The DNA is sheared by sonication at 25% power using 10 pulses of 20 seconds. Sonicated samples are centrifuged at 15,000 rpm for 10 minutes at 4^{o}C. The supernatants are carefully transferred to fresh tubes. This is the sheared chromatin. Chromatin immunoprecipitation (ChIP) is performed as per manufacturer's instructions using ChIP-IT® Express Chromatin Immunoprecipitation kit including Protein G Magnetic Beads (Active Motif, USA). Primary antibodies for HIF-1α (Ratcliffe Laboratory, University of Oxford) and FLAG (Active Motif) are used in this experiment. Following immunoprecipitation, samples amplified by PCR using the protocol detailed in section 2.10. Graph represents relative binding as determined by the $2^{-\Delta\Delta Ct}$ method for relative quantification against negative control FLAG antibody.

2.13 Statistical Analysis

Statistical analyses were performed using One-Way and Two-Way ANOVAs or Multiple t tests on grouped data in Prism 7.0 (GraphPad, USA) with $P<0.05$ being considered statistically significant. Significance shown using standardised star rating as follows

(*<0.05, **<0.01, ***<0.001, ****<0.0001). Tukey's multiple comparisons tests were used in conjunction with ANOVAto find means that are significantly different from each other. This test compares all possible pairs of means. This test identifies any difference between two means greater than the expected standard error. Sidak's multiple comparisons tests are also used in conjunction with ANOVA to control the familywise error rate that can occur in multiple comparisons tests. The test is designed to correct for type 1 errors when performing multiple hypotheses tests. We used the Welch's correction in conjunction with Multiple t tests. This correction is used to test the hypothesis that two or more sample means have equal means. This correction is considered more reliable than a Student's t test when samples have unequal sample sizes or variance.

3. EXAMINING THE HEPATOMA CELL RESPONSE TO LOW OXYGEN

3.1 Introduction

The majority of hepatocytes within the liver are terminally differentiated (Fausto, 1990, Fausto *et al*., 2006) and exist as part of an oxygen gradient from 11% oxygen at the hepatic portal vein to 3% at the hepatic central veins (Jungermann and Kietzmann, 2000, Adams and Eksteen, 2006). The major cell type in the liver that supports HBV infection is the hepatocyte and recent studies show that the hepatocyte derived HepG2 cell line supports efficient HBV replication *in vitro* (Meredith *et al*., 2016, Verrier *et al*., 2016b). We therefore studied the response of uninfected HepG2, Huh-7, and Huh-7.5 human hepatoma lines to low oxygen. Initially we studied the response of Huh-7.5 cells to low oxygen; these are derivatives of the parent cell line Huh-7 that contain a single point mutation in the dsRNA sensor retinoic acid inducible gene-I (RIG-I); these were originally used to study HCV infection because they were highly permissive to infection (Blight *et al*., 2002). Huh-7 cells are an immortalized cell line of epithelial-like, tumorigenic cells originally derived from carcinoma cells of differentiated hepatocytes (Vecchi *et al*., 2010). *In vitro* studies highlight the importance of hepatocellular differentiation status for HBV replication and current infection protocols require differentiation of the target cells to establish infection. We were therefore interested to examine how the differentiation status of hepatoma cells regulated their response to low oxygen.

In this chapter, we examined the hypoxic responses of hepatoma cell lines and study the kinetics of HIF activation using a combination of Western blotting, quantitative PCR and an HRE luciferase (HRE-Luc) reporter assay. The HRE reporter assay utilises 5

tandem repeats of the HIF binding site HRE in the promoter region for luciferase gene (**Figure 3.1**); exposure to low oxygen stabilises HIFα that binds their cognate HRE and stimulate transcription and luciferase expression. In addition, we used this model system to evaluate the effect of drugs targeting different steps in the HIF degradation and signalling pathway for future evaluation in HBV infection systems.

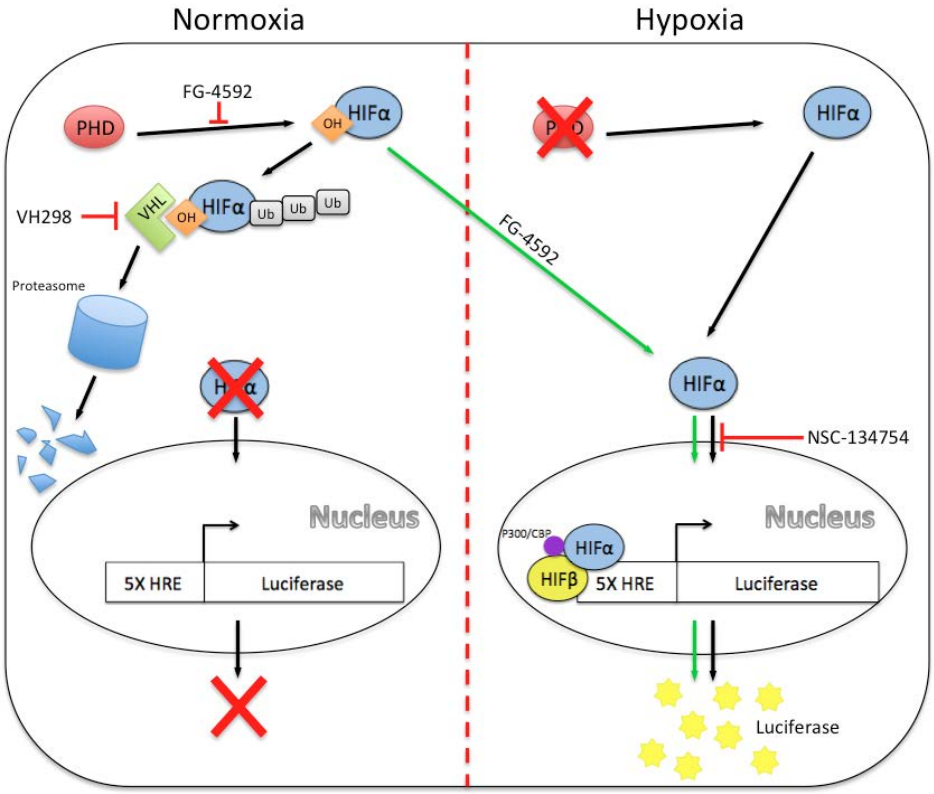

Figure 3.1 HRE Luciferase assay for HIF activity

HRE-Luc reporter plasmid is transfected into the target cell. The cells are exposed to normoxic or hypoxic conditions. Under normoxia the alpha subunit is degraded and we observed minimal luciferase expression. Under hypoxia, the alpha subunit translocates to the nucleus, forms a heterodimer with the beta subunit and binds the co-activator P300/CBP. This complex binds to the HRE repeats within the promoter and activates transcription and luciferase expression. Inhibiting the prolyl-hydroxylases with FG-4592 stabilises the alpha subunit and promotes luciferase expression. NSC-134754 treatment inhibits the HIF signalling pathway, although the method of inhibition is currently unknown.

Results

3.2 Huh-7.5 cell response to low oxygen

We initially focus on 1% oxygen because this oxygen tension is most often used in the literature to represent a 'hypoxic' environment, this is due to the high K_m value for PHDs; the lower the oxygen tension, the greater the inhibition of PHD activity (Schofield and Ratcliffe, 2004, Jokilehto and Jaakkola, 2010). PHDs are highly sensitive oxygen sensors and tightly control HIF-α expression whilst active (Stolze *et al*., 2006). Additionally, 1% oxygen reflects changes in oxygen tension induced during viral hepatitis, inflammation and carcinogenesis (Jungermann and Kietzmann, 2000, Wilson *et al*., 2014). We examined the pattern of HIF-1α and HIF-2α expression in Huh-7.5 cells over 72 hours of exposure to 1% oxygen using Western blotting (**Figure 3.2a**). This demonstrated that both HIF-1α and HIF-2α were expressed within this cell type and expression occurred over an extended time period. Additionally, 1% oxygen significantly promotes HRE-Luc activity in Huh-7.5s (**Figure 3.2c**). This data demonstrated that the HRE activation continues to increase up to 25 hours compared to normoxic controls (**Figure 3.2d)**.

In addition, we examined the effect of exposure to 3% oxygen, which reportedly represents the lower end of the physiological oxygen gradient in healthy liver (Wilson *et al*., 2014).Here we observed a similar pattern of HIF expression with significant increases under 3% oxygen over 25 hours (**Figure 3.2e**), with a peak of activity at 15 hours post exposure to 3% oxygen (**Figure 3.2f**). It is important to note that under 1% oxygen, the increases in relative HRE activity are higher than those observed under 3% oxygen. We used a GRE-Luc reporter as a control to demonstrate 1% oxygen does not activate luciferase expression in non HRE reporter systems (**Figure 3.2b**).

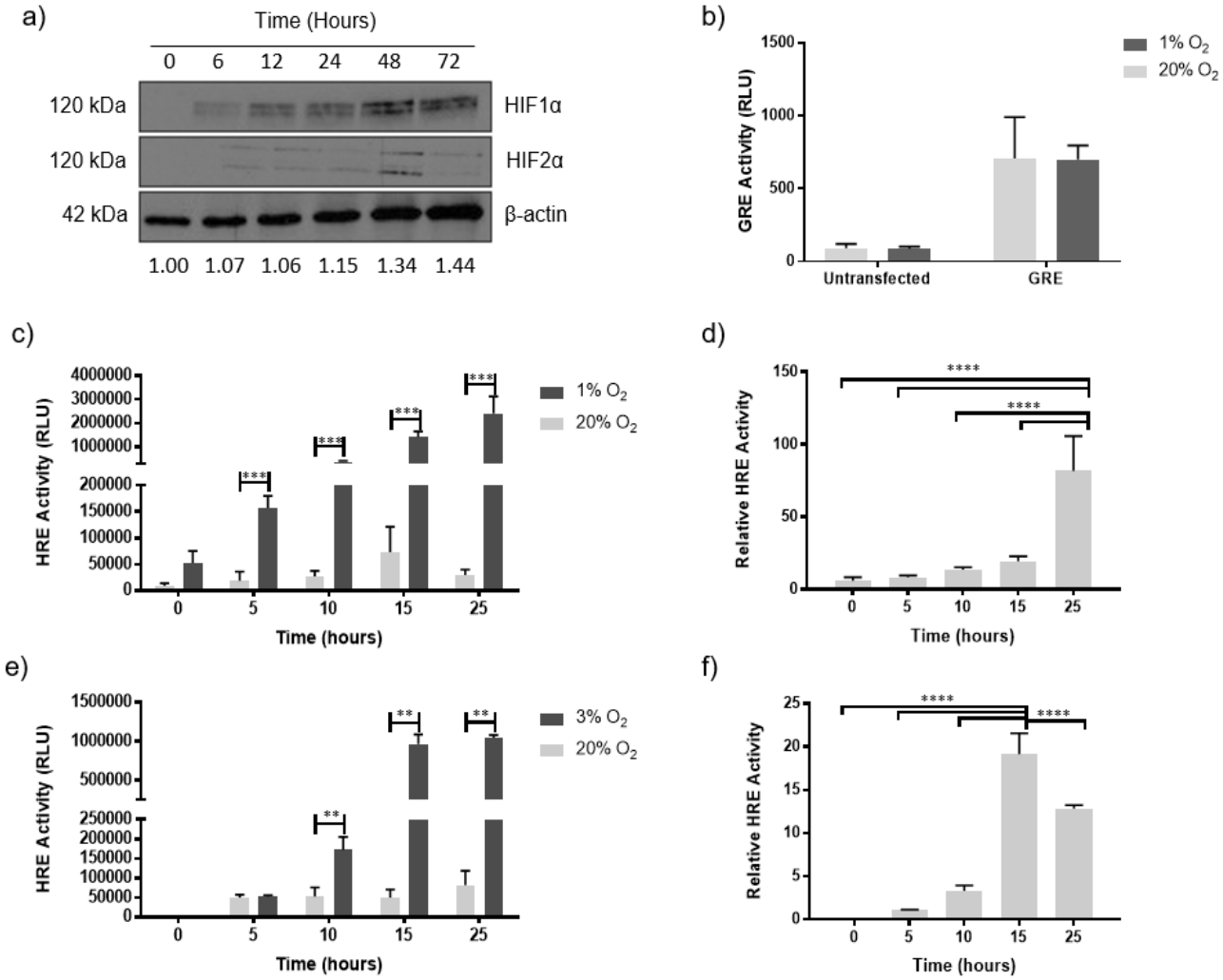

Figure 3.2 Huh-7.5 response to low oxygen

Huh-7.5 cells were transfected with a plasmid encoding an HRE-Luc or GRE-Luc reporter. Following transfection the cells were reseeded into 96 well plates and placed into hypoxic or normoxic conditions. **A)** A western blot demonstrating HIF-1α and HIF-2α stabilisation in Huh-7.5 cells over 72 hours. Numbers under actin represent relative densitometry. **B)** GRE-Luc reporter control results demonstrating raw RLU values for GRE activation under 1% for 24 hours **C)** HRE-Luc reporter results demonstrating the raw RLU values for HRE activation over 25 hours under 1% oxygen. **D)** HRE-Luc reporter results represented as 1% oxygen values relative to normoxic controls. **E)** HRE-Luc reporter results demonstrating the raw RLU values for HRE activation over 25 hours under 3% oxygen. **F)** HRE-Luc reporter results represented as 3% oxygen values relative to normoxic controls. Data shows means of 3 biological repeats. Multiple T Tests used for raw RLU data and One-Way ANOVA with Tukey's multiple comparisons test for relative HRE activity.

3.3 HepG2 cell response to low oxygen

After demonstrating the effects of two different low oxygen tensions on Huh-7.5 cells; it is important to examine the effect in another hepatoma cell line to determine whether the observed activity is cell line specific or can be generalized to multiple hepatocyte derived lines. HepG2 cells are an immortalized cell line derived from a well-differentiated hepatocellular carcinoma that exhibits epithelial-like morphology, however unlike Huh-7.5 cells they are non-tumorigenic (Costantini *et al*., 2013, Donato *et al*., 2015). Using the HRE-Luc reporter assay we demonstrated the kinetics of HRE activity under 1% oxygen over 25 hours (**Figure 3.3a**). As observed in Huh-7.5 cells, this data demonstrated that exposure to 1% oxygen significantly increases HRE activity relative to normoxic controls (**Figure 3.3b**). Using 3% oxygen we demonstrated the kinetics of HRE activation in HepG2 cells (**Figure 3.3c**) and compared the expression relative to normoxic controls (**Figure 3.3d**). This data shows that 3% oxygen is also able to increase HRE activation over the 25 hour time course. However, as observed in Huh-7.5 cells the relative activity is increased under 1% oxygen compared to 3% oxygen.

Both cell lines demonstrate a greater relative induction under 1% oxygen compared to 3% oxygen (**Figure 3.4a-b**). Importantly the pattern of expression is similar between each of the cell lines under both oxygen tensions, although HepG2 cells express higher signals under both oxygen tensions. The Huh-7.5 cells demonstrated a greater difference in relative fold induction between oxygen tensions (**Figure 3.4c**). These results indicate there is less variance in HRE activity between 1% and 3% oxygen tensions in HepG2 cells. Coupled to the fact that HepG2 cells are the basis for many of the current model systems used to study HBV, we decided to primarily focus on this cell line for infection models.

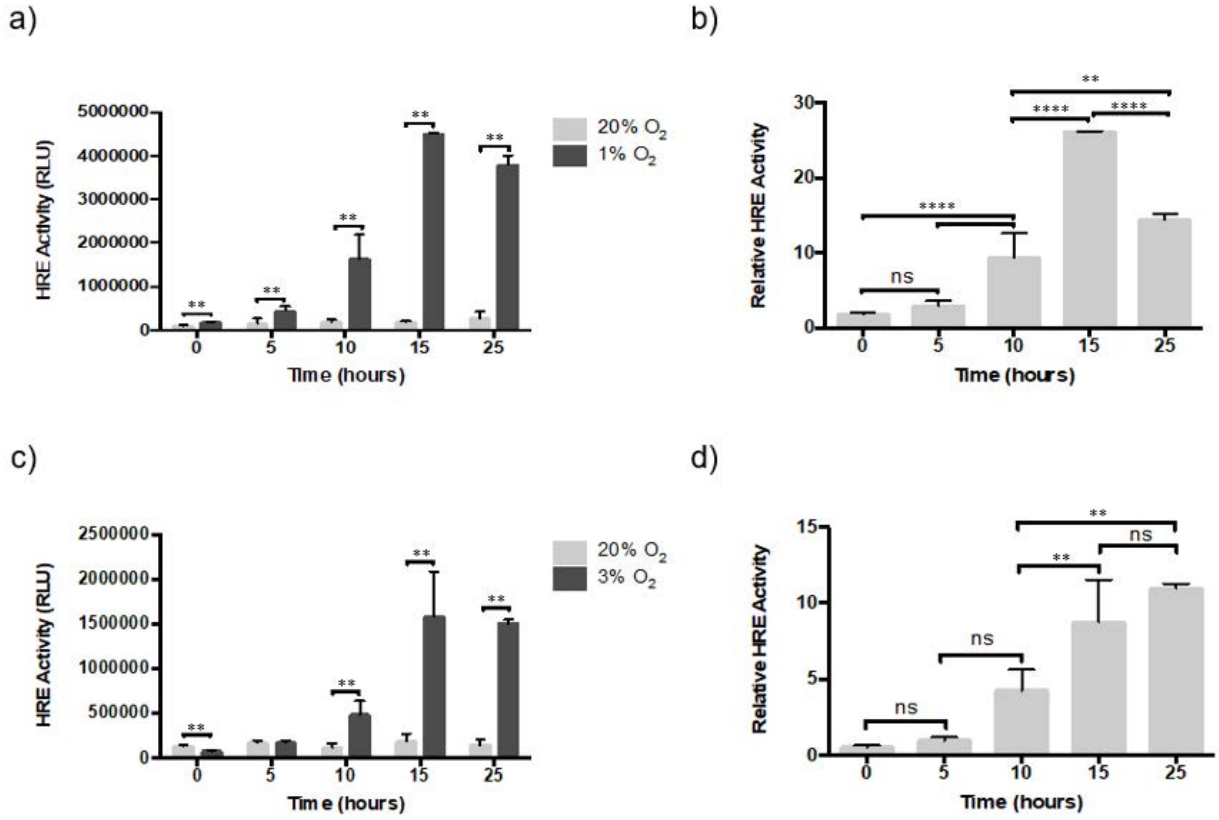

Figure 3.3 HepG2 response to low oxygen

HepG2 cells were transfected with an HRE-Luc reporter, then reseeded into 96 well plates. The cells were then placed into hypoxic or normoxic conditions and lysed every 5 hours with 1x Luciferase lysis buffer. **A**) HRE-Luc reporter results demonstrating the raw RLU values for HRE activation over 25 hours under 1% oxygen. **B**) HRE-Luc reporter results represented as 1% oxygen values relative to normoxic controls. **C**) HRE-Luc reporter results demonstrating the raw RLU values for HRE activation over 25 hours under 3% oxygen. **D**) HRE-Luc reporter results represented as 3% oxygen values relative to normoxic controls. Each graph shows means of 3 biological repeats. Multiple T Tests used for raw RLU data and One-Way ANOVA with Tukey's multiple comparisons test for relative HRE activity.

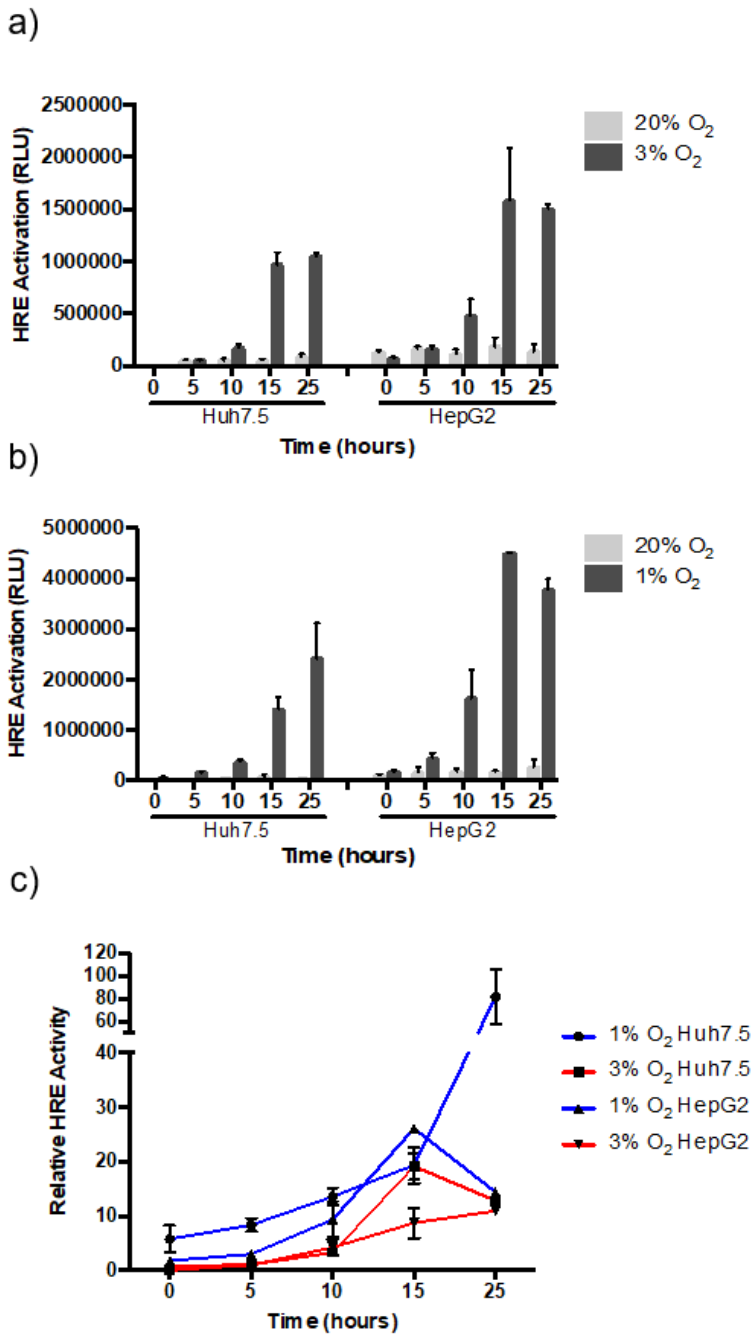

Figure 3.4 Comparing Huh-7.5 and HepG2 responses to low oxygen

A) Comparison of raw RLU values for HRE activation in Huh-7.5 and HepG2 cells under 3% oxygen. **B)** Comparison of raw RLU values for HRE activation in Huh-7.5 and HepG2 cells under 1% oxygen. **C)** Graph representing the relative increases for each oxygen tension in both of the hepatoma cell lines relative to their respective normoxic controls. Each graph shows the means of 3 biological repeats per cell line. Error bars show SE of 9 technical repeats.

3.4 The effect of HIF targeting drugs on hepatoma cell lines

We had access to three different drugs that regulate the expression and function of HIFs. The first of these is called NSC-134754 (NSC) and was kindly provided by Margaret Ashcroft (University of Cambridge) and the second is FG-4592. Reports show that NSC is a small-molecule HIF pathway inhibitor that prevents the expression of HIFs under low oxygen conditions; it has been demonstrated that NSC induces metabolic alterations and reduces the expression of a number of downstream HIF targets (Baker *et al*., 2012). The exact mode of action has not been reported, but this could provide a useful tool to study the role of HIFs in HBV replication. The second drug is called FG-4592 that targets the prolyl-hydroxylases that regulate HIF expression under normoxia. Literature shows that this inhibitor can stabilize the expression of HIFs under normal oxygen conditions and boost downstream HIF activity; with observed increases in erythropoiesis and regulation of iron metabolism (Maxwell and Eckardt, 2016, Provenzano *et al*., 2016, Chen *et al*., 2017). The third drug is called VH298 that inhibits von Hippel-Lindau (VHL) E3 ubiquitin ligase complex. The inhibitor behaves as a competitive inhibitor by binding with high affinity to VHL, this results in the accumulation of HIFα (Frost *et al*., 2016). In this chapter, we demonstrated HIF expression and HRE-Luc reporter activity in HepG2 cells; however, the primary use of this drug is found in chapter 5.

We investigated the effect of NSC on each of the hepatoma lines using a combination of Western blotting and the HRE-Luc reporter assay. Initially we examined the effect of NSC on HIF protein expression under 20% and 1% oxygen by performing a dose response from 0.1μM to 1μM NSC in both hepatoma lines and Western blotting (**Figure3.5a,b**). Despite a 10% difference in the loading of the Western blot lanes, we selected the 1μM dosage for future experiments because lower doses did not appear

to inhibit HIF expression efficiently. We confirmed this result in Huh-7.5 cells by treating with 1μM NSC for 24 hours alongside untreated controls. These results demonstrate that NSC significantly reduces HRE activation under 1% oxygen (**Figure 3.6a**). We then demonstrated reduced HRE activity in HepG2 cells under 1% oxygen following drug treatment (**Figure 3.6b**). Both cell lines respond to NSC inhibition of HIF in a similar way.

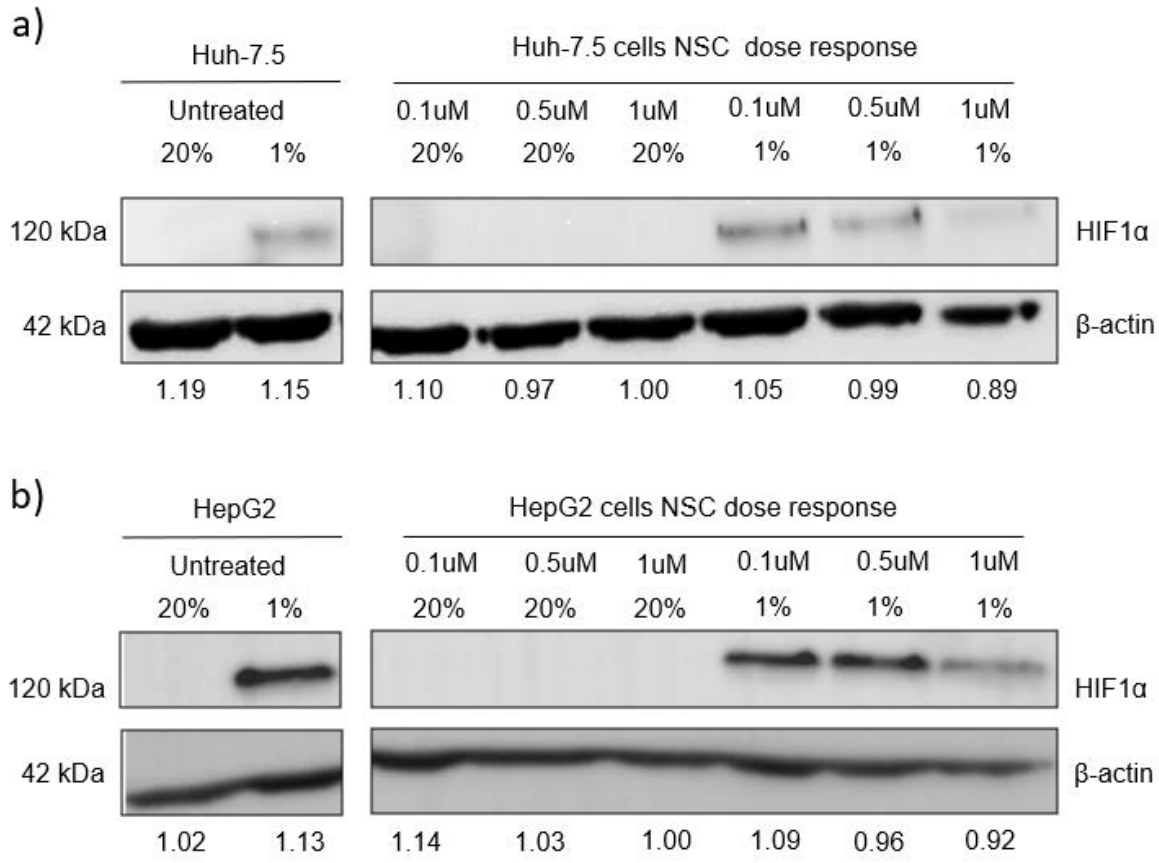

Figure 3.5 Comparing the effect of NSC on hepatoma HIF expression

Huh-7.5 and HepG2 cells were were treated with a range of NSC doses. The cells were placed into 1% or 20% oxygen for 24 hours, samples lysed with 8M Urea lysis buffer. **A)** A western blot demonstrating a HIF-1α dose response for expression in Huh-7 cells. Numbers under actin demonstrate the relative densitometry between loading in each lane relative to 1μM 20% lane. **B)** A western blot demonstrating a HIF-1α dose response for expression in HepG2 cells. Numbers under actin demonstrate the relative densitometry between loading in each lane relative to 1μM 20% lane. Western blots representative of 3 biological repeats.

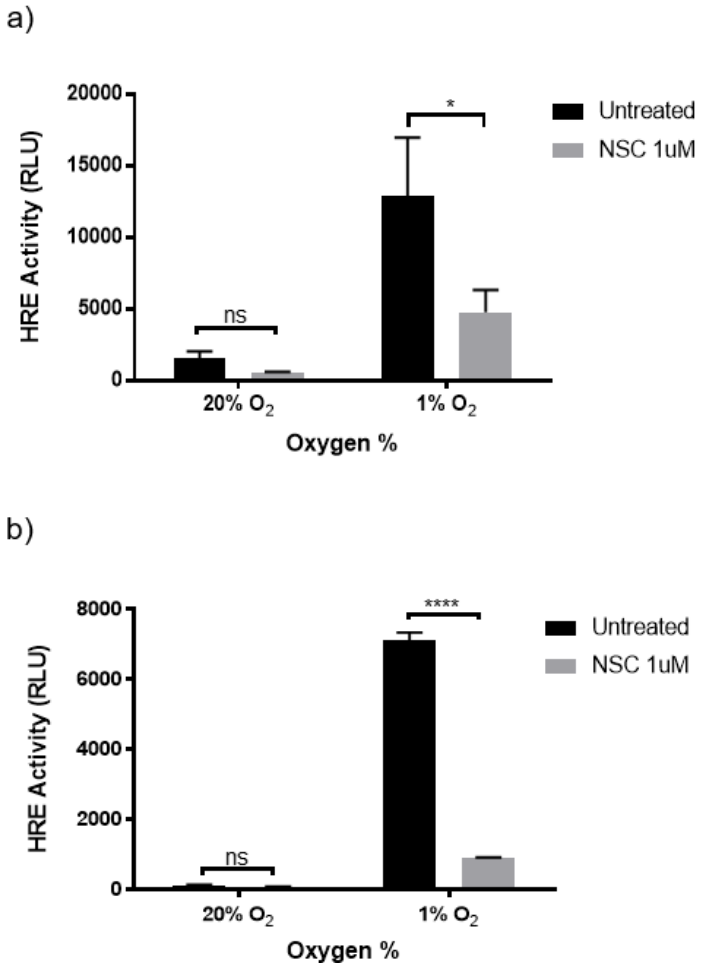

Figure 3.6 HRE activity following NSC treatment in hepatoma cells

Huh-7.5 and HepG2 cells were transfected with an HRE-Luc reporter then reseeded into 96 well plates. The cells were then placed into hypoxic or normoxic conditions and treated with 0.1μM or 1μM NSC or untreated for 24 hours. Samples were lysed with 1x Luciferase lysis buffer. **A**) HRE-Luc reporter activation in Huh-7.5 cells under 20% and 1% oxygen. **B**) HRE-Luc reporter activation in HepG2 cells under 20% and 1% oxygen. Each graph shows means of 2 biological repeats and error bars represent SE of 6 technical repeats. Two-Way ANOVA with Tukey's multiple comparisons test for HRE activity.

Next, we tested the efficacy of FG-4592 treatment on HIF stabilisation over a 72 hour time course in HepG2 cells (**Figure 3.7a**). Following demonstration of protein expression, we tested the effect of FG-4592 stabilised HIF transcriptional activity using our HRE-Luc reporter assay and demonstrate HRE activity similar to that observed in 1% oxygen controls in both cell types (**Figure 3.7b**). We followed these data with a comparison of FG-4592 stabilisation of HIF-1α expression in both Huh-7 and HepG2 cells under 20% oxygen conditions following treatment for 24 hours (**Figure 3.7c-e**). FG-4592 treatment up-regulates HRE activation under 20% oxygen. However, activation is slightly lower than under 1% oxygen, perhaps reflecting that proteasomal degradation is not completely inhibited by treatment with the drug. We demonstrated similar results following treatment with VH298. This drug stabilises HIF-1α and HIF-2α expression in HepG2 cells for 72 hours (**Figure 3.8a**). In addition, we demonstrated that accumulated HIFα expression results in significantly increased HRE activity using the HRE-Luc reporter assay (**Figure 3.8b**).

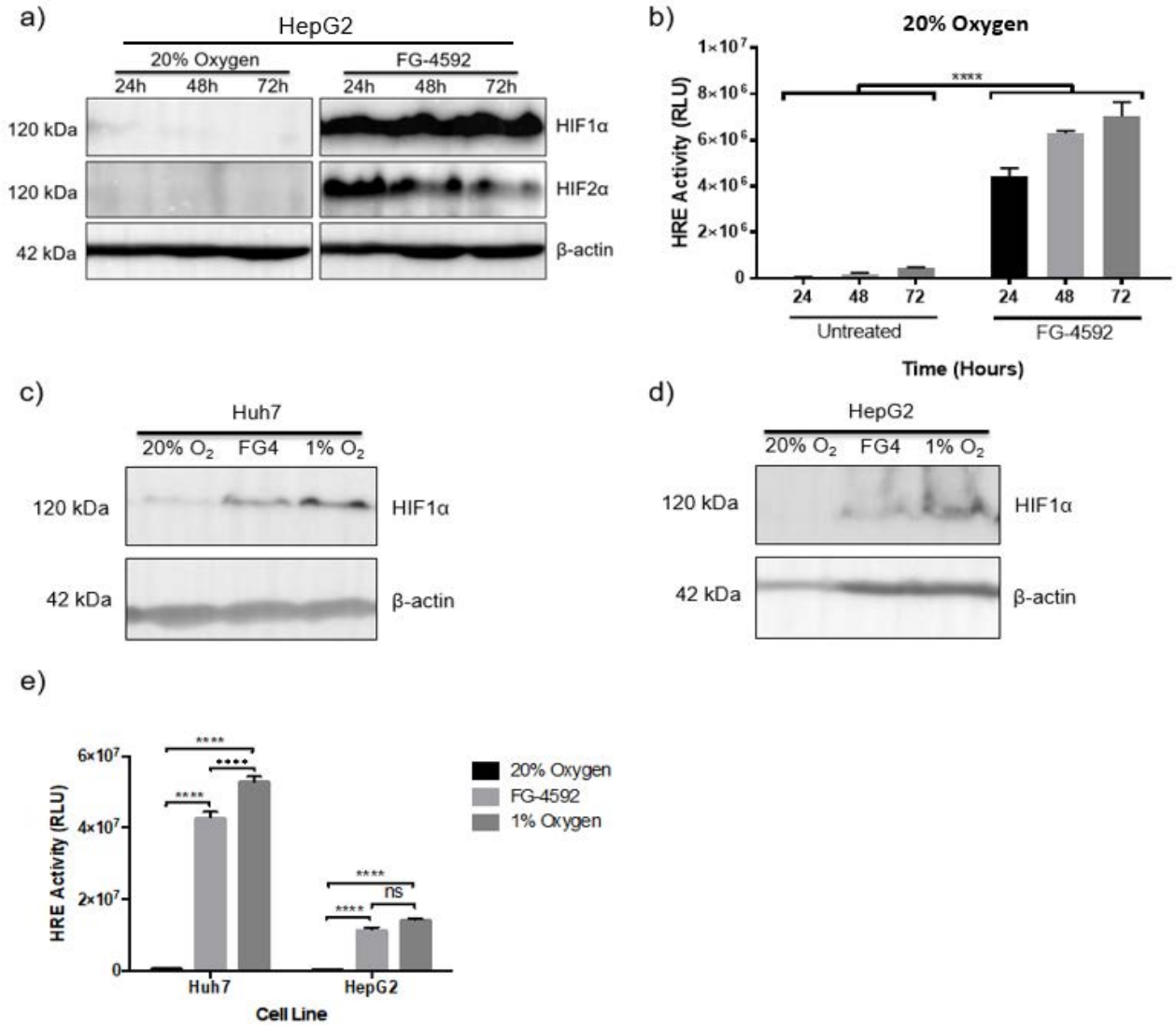

Figure 3.7 The effect of PHD inhibitor on hepatoma cells

Huh-7 and HepG2 cells were transfected with an HRE-Luc reporter then reseeded into 96 well plates. The cells were then placed into 1% or 20% oxygen or treated with 1μM FG-4592 for 24 hours. **A)** Western blot demonstrating HIF-α stabilisation in HepG2 cells with FG-4592. **B)** HRE-Luc reporter activation in HepG2 cells over 72 hour with FG-4592 and untreated controls under 20% oxygen. **C/D)** Western blots demonstrating HIF-1α stabilisation in Huh-7 cells (**C**) and HepG2 cells (**D**) following exposure to 1% oxygen and treatment with FG-4592. **E)** HRE-Luc reporter activation in Huh-7 and HepG2 cells over 24 hours following various treatments. Each graph shows means of 4 biological repeats (**B**) and 2 biological repeats (**E**). Error bars represent SE of 6 technical repeats. Two-Way ANOVA with Tukey's multiple comparisons test for HRE-Luc reporter data. (NB, this experiment and the one shown in **Figure 3.8** were done together and therefore share a negative control in Western blots **3.7a** and **3.8a**).

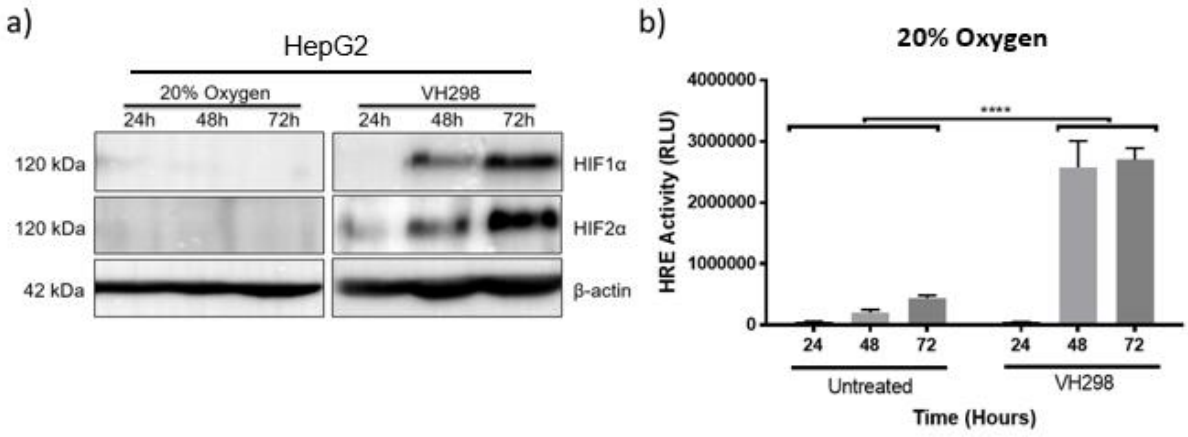

Figure 3.8 The effect of VHL inhibitor on HepG2 cells

HepG2 cells were transfected with an HRE-Luc reporter, then reseeded into 96 well plates (B)**.** The cells were then placed into 20% oxygen and treated with 100μM VH298 for 72 hours. **A)** Western blot demonstrating HIF-α stabilisation in HepG2 cells over 72 hours treatment with VH298 under 20% oxygen, samples were lysed every 24 hours post treatment. **B)** HRE-Luc reporter activation in HepG2 cells over 72 hour treatment with VH298 under 20% oxygen, compared against untreated controls. Each graph shows means of 4 biological repeats. Error bars show SE of 12 technical repeats. Two-Way ANOVA with Tukey's multiple comparisons test.

3.5 HIF over expression in hepatoma cells

After demonstrating the effect of the HIF-regulating drugs on HIF stabilisation and HRE activation, it was important to observe the effect of over expressed HIF-1α and HIF-2α using plasmids pHIF-1α-FLAG and pHIF-2α-Myc kindly provided by Margaret Ashcroft (University of Cambridge). Transfection of these plasmids into target cells results in the over expression of HIF-1α and HIF-2α under normoxic conditions. We demonstrated that transfection results in protein expression in a dose dependent manner (**Figure 3.9a**). Based on the Western blot results we determined the concentration required for subsequent HRE-Luc reporter assays. Following transfection with each of the over expression plasmids we demonstrated that tagged HIFs are transcriptionally active over a 72 hour time course. HIF-1α-FLAG expression increases HRE activity over 72 hours (**Figure 3.9c**), demonstrating that the HIF-1α-FLAG is functional and can activate downstream HIF signalling. HIF-1α-FLAG causes a significant increase in HRE activity under 20% oxygen at 24 hours when compared against 0 hour time point.

HIF-2α-Myc over expression is also functional and activates downstream HIF signalling. Interestingly, the expression of HIF-2α activates the HRE-Luc reporter, but exposure to low oxygen only minimally increases the observed HRE activation (**Figure 3.9d**). HIF-2α-Myc causes a significant increase in HRE activity under 20% oxygen at 24 hours when compared against 0 hour time point. HRE is activated by each plasmid under normoxia up to 72 hours; both plasmids demonstrate peaks of expression at 24-48 hours at 20% oxygen that begins to decrease by 72 hours. Perhaps due to the loss of transient transfection. These data demonstrate that over expression plasmids can be used to examine HIF responses in target cells.

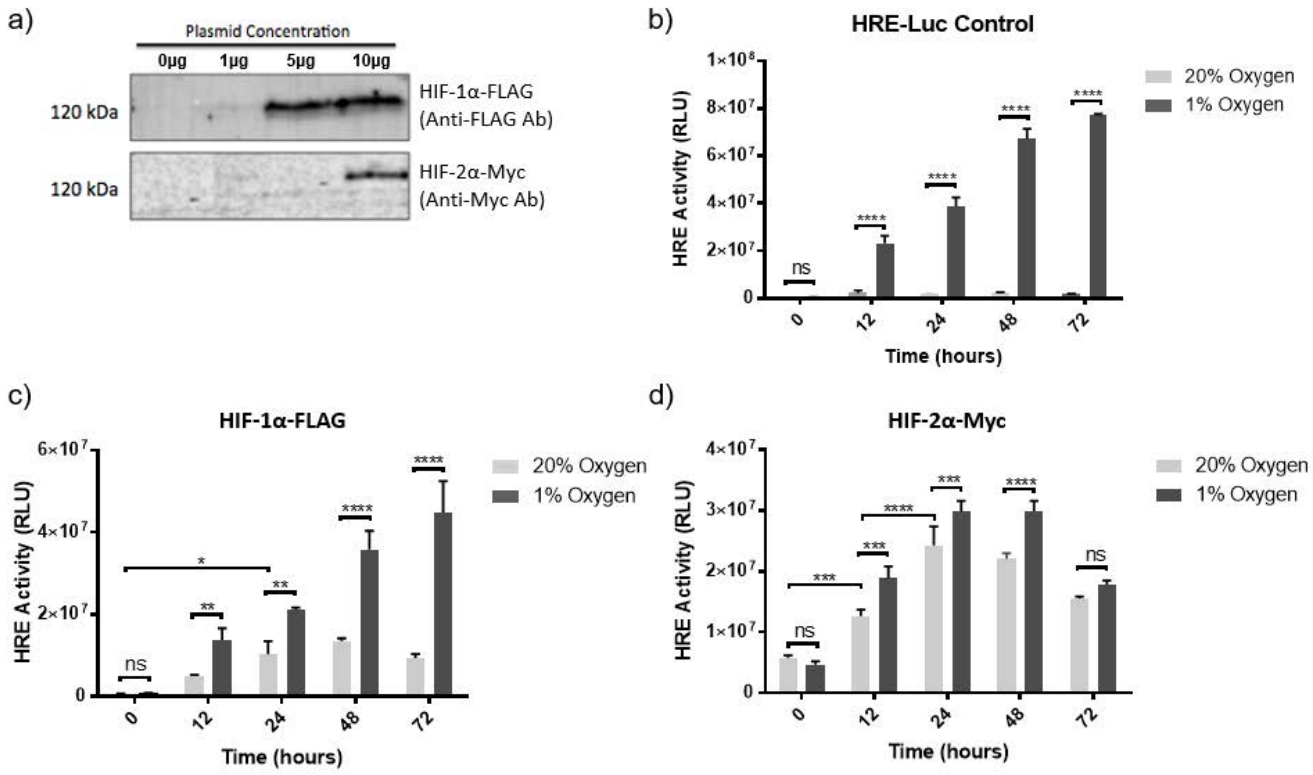

Figure 3.9 HIFα over expression and HRE activation

Huh-7.5 cells were transfected with a dose response of pHIF-1α-FLAG or pHIF-2α-Myc. **A)** Western blot demonstrating over expression under normoxic conditions. Huh-7.5 cells were seeded and transfected with an HRE-Luc reporter **(B)** and co-transfected with either pHIF-1α-FLAG **(C)** or pHIF-2α-Myc **(D).** The cells were then placed into 1% or 20% oxygen for 72 hours. Graph (B) represents means of 2 biological repeats. Graphs (C-D) represent means of 3 biological repeats. Error bars show SE of 9 technical repeats. Data analysed using Two-Way ANOVA with Sidak's multiple comparisons test.

3.6 HIF target gene activation in hepatoma cells

Having demonstrated the effects of over expression and HIF regulating drugs in two different hepatoma cell lines, we decided to examine any differences in activity caused by these different mechanisms for HIF expression and compare these against a normoxic control that demonstrated the transcriptional activity of hepatoma cells under 20% oxygen. This provides a baseline for comparison when examining HBV stabilised HIF. This was achieved using the RT2 profiler PCR array by Qiagen that contains a panel of 84 genes commonly associated with the HIF pathway and responses to low oxygen. Using this array in combination with the over expression plasmids and HIF targeting drugs allowed us to further demonstrate that the observed HIFs can be functional and examine any differences in the profile of activated genes.

The first array compares the activity of HIF target genes in Huh-7.5 samples following over expression via plasmid transfection (**Figure 3.9**). These are compared against Normoxic and Hypoxic (1% oxygen) controls (**Figure 3.10a**). Interestingly, transfecting the cells with a HIF-1α and HIF-2α over expression plasmid does not result in the same pattern of gene expression (**Figure 3.11**), perhaps reflecting other activity of other low oxygen activated pathways. This heat map demonstrated that the tested hepatoma cells exhibit up-regulation of common hypoxic response markers such as solute carrier family 2 member 1 (SLC2A1) and solute carrier family 2 member 3 (SLC2A3), carbonic anhydrase 9 (CA9) and vascular endothelial growth factor A (VEGFA), making them a suitable model for studying infection.

We organised the expression of genes in the 1% oxygen control samples from highest expression to lowest and then compared the expression profile of pHIF-1α-FLAG and pHIF-2α-Myc against this (**Figure 3.11a,b**). These graphs highlight that the expression

profile is altered through over expression of pHIF-α, perhaps reflecting the lack of hypoxic involvement in HIF-α stabilisation. We compared the transcript up-regulation for four different conditions; which are displayed in this heat map. There is a correlation between Hypoxic samples and over expressed HIF-1α up-regulated genes indicated by the box. A number of these are involved in carbohydrate metabolism, such as glycogen synthase (GYS1), glucose-6-phosphate isomerase (GPI), and SLC2A3 (also called glucose transporters 3 (GLUT3)). The second heat map represents the HIF transcriptional profile for Huh-7 cells treated with the PHD inhibitor FG-4592 and 1% oxygen (**Figure 3.10b**). When comparing the fold change for each gene independently we saw a similar profile of activated HIF target genes following FG-4592 treatment compared to the 1% oxygen control (**Figure 3.12a, b**). Artificial stabilisation of HIFs demonstrated different profiles of gene expression, however FG-4592 treatment exhibits similar levels of regulation. This is an important observation to consider when using these drug in future experiments in the context of HBV infection.

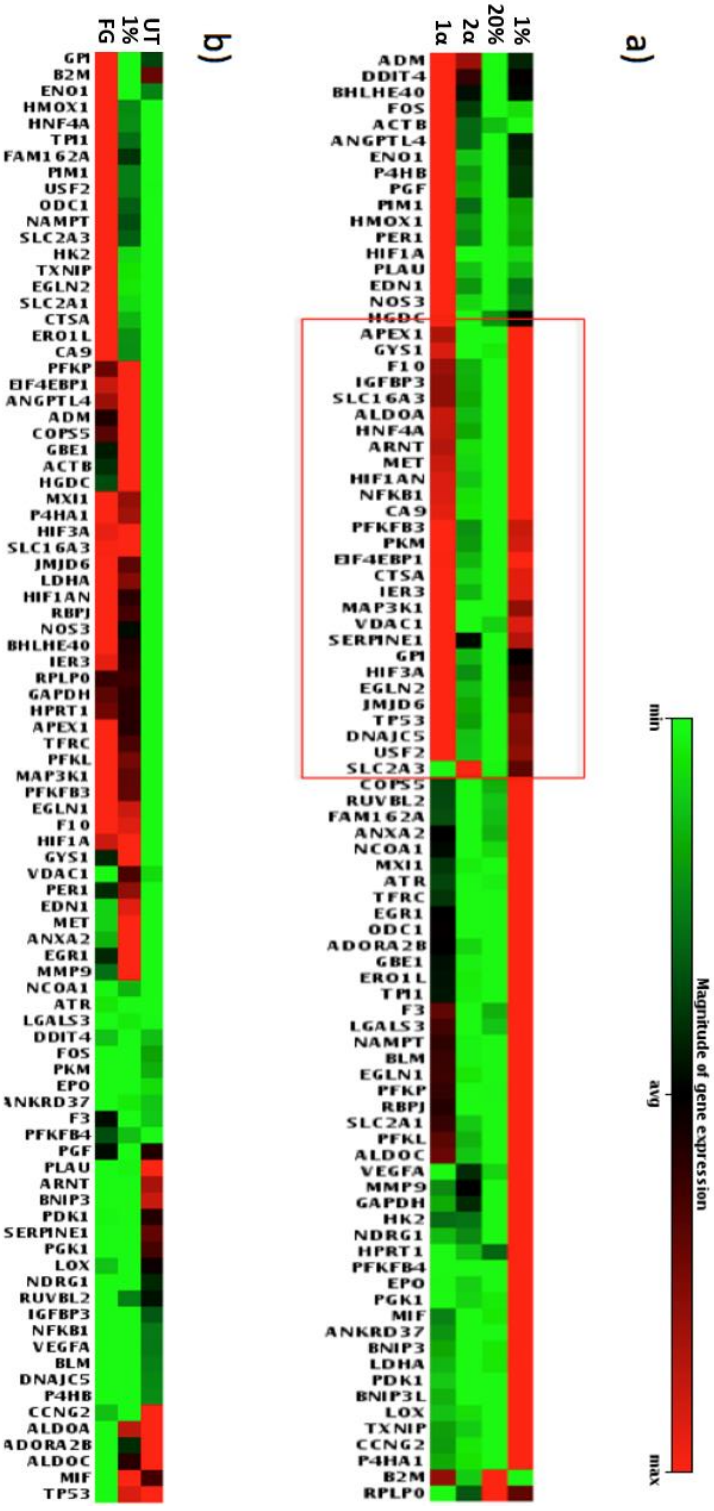

Figure 3.10 Heatmap of hypoxic gene regulation following HIF stabilising treatments

Legend on following page.

Figure 3.10 Heatmap of hypoxic gene regulation following HIF stabilising treatments (Cont.)

A) Huh-7.5 cells were transfected with either HIF-1α-FLAG or HIF-2α-Myc over expression constructs over 24 hours under 20% oxygen. Control cells exposed to 20% and 1% oxygen for 24 hours were also prepared. Groups are as follows: 20% (normoxia), 1% (hypoxia – 1%), 1α (pHIF-1α-FLAG plasmid) and 2α (pHIF-2α-Myc plasmid) The red box indicates a region of overlap between hypoxic group and overexpression of HIF-1α-FLAG. **B)** Huh-7 cells were either placed under 1% oxygen or treated with FG-4592 (1 μM) for 24 hours. Control cells exposed to 20% oxygen for 24 hours were also prepared. Groups are as follows: UT (normoxia), 1% (hypoxia – 1% oxygen, 24 hours), FG (FG-4592 - 1 μM, 24 hours). Each condition represents 3 technical repeats.

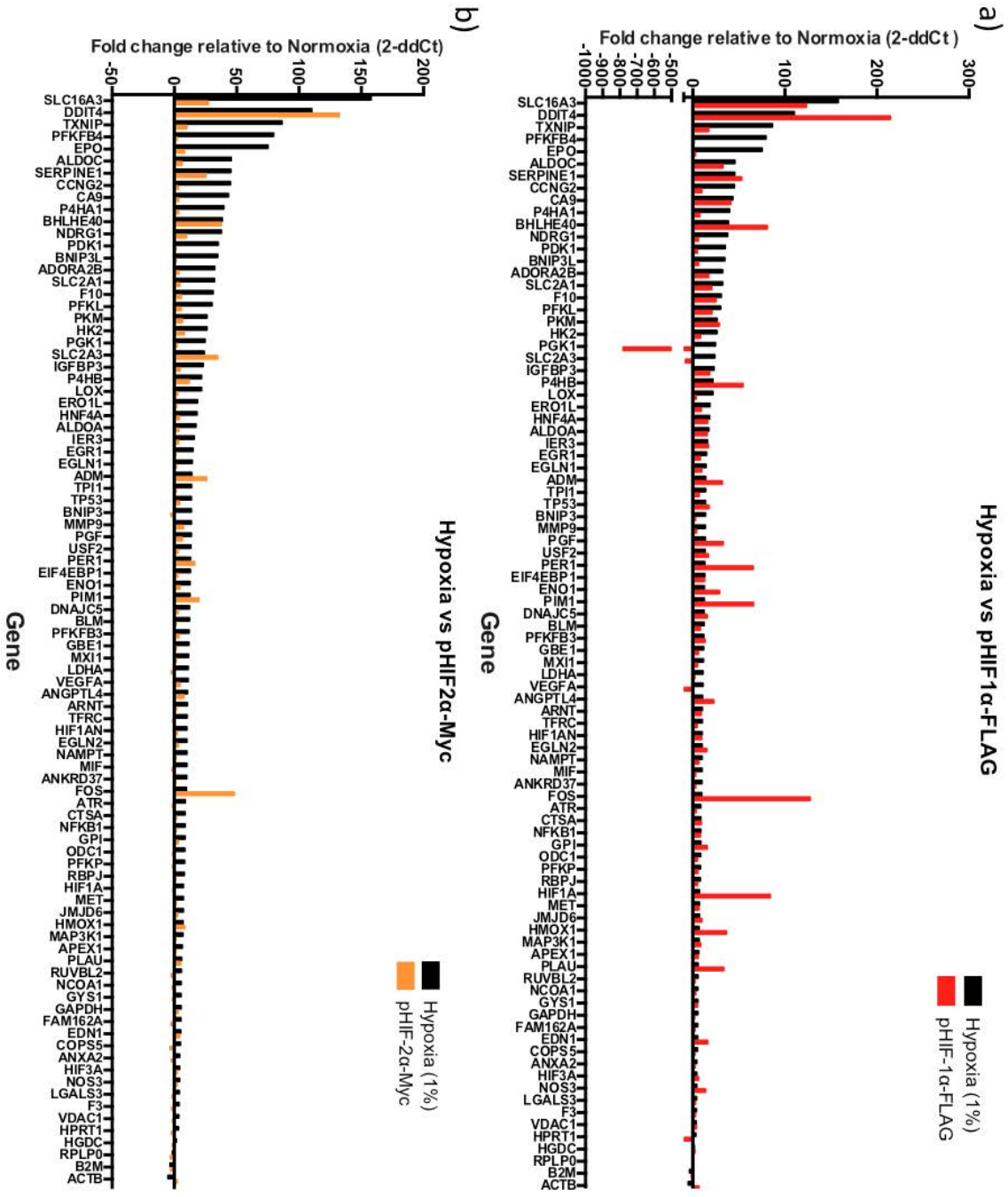

Figure 3.11 Comparing transcript activity following over expression of HIF-1 and HIF-2

Huh-7.5 cells were transfected with either HIF-1α-FLAG or HIF-2α-Myc over expression constructs over 24 hours under 20% oxygen. Control cells exposed to 20% and 1% oxygen for 24 hours were also prepared. Graphs demonstrate RT2 hypoxic gene array results sorted by highest expression for 1% oxygen controls. **A)** Expression profile for hypoxic genes following transfection with pHIF-1α-FLAG. **B)** Expression profile for hypoxic genes following transfection with p HIF-2α-Myc.

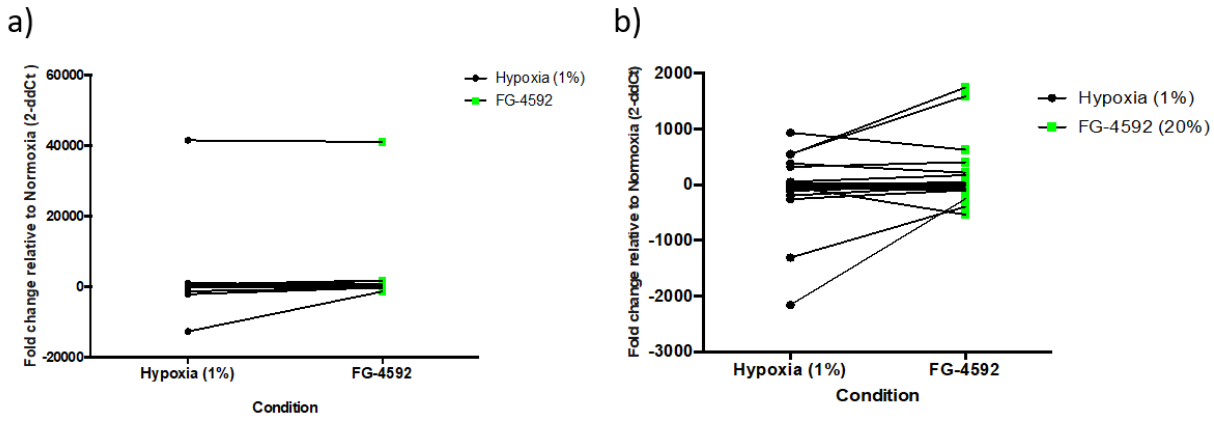

Figure 3.12 Comparing transcript activity following FG-4592 and hypoxic treatment

Huh-7.5 cells were either placed under 1% oxygen or treated with FG-4592 (1 μM) for 24 hours. Control cells exposed to 20% oxygen for 24 hours were also prepared. **A)** Graph demonstrates comparison of individual gene expression under 1% oxygen and FG-4592 treatment. **B)** Graph demonstrates comparison of individual gene expression under 1% oxygen and FG-4592 treatment with outliers excluded.

3.7 Hepatoma cell lines and differentiation

Current protocols for *de novo* HBV infections utilise Dimethyl sulfoxide (DMSO) to differentiate target cells to enable efficient infection (Huang *et al*., 2012, Schulze *et al*., 2012). Therefore, it is important to study the effect of this differentiation protocol on the cellular response to low oxygen. We examined the effect of DMSO differentiation on each of the cell lines by examining mRNA transcript levels of four liver specific differentiation markers (**Figure 3.13a,b**): albumin (ALB), alpha fetoprotein (AFP), hepatocyte nuclear factor 4 alpha (HNF4α) and cytochrome P450 3A4 (CYP3A4) (Hay *et al*., 2008, Olsavsky Goyak *et al*., 2010, Holtzinger *et al*., 2015). DMSO increased the expression of all differentiation markers in both cell lines (**Figure 3.13**).

For comparison, we utilised an alternative method of differentiation that involved culturing the cells with glucose, hydrocortisone and insulin for four weeks and showed a similar up-regulation of differentiation markers (**Figure 3.13c**). Unfortunately, the HepG2 cells could not survive this process beyond 2 weeks and the data represented in (**Figure 3.13c**) only demonstrates the process in Huh-7 cells. DMSO differentiation increases expression of all four markers in both Huh-7 and HepG2-NTCP cells, these cells are HepG2 cells over expressing the bile acid transporter NTCP. This enables more efficient HBV infections and so became the cell line of choice for further experimentation. Non-DMSO differentiation also causes increases in expression of each marker. CYP3A4 and AFP expression are significantly increased using this method. However, the increased difficulty and risks of long term culture coupled with an inefficient way of maintaining cells for infection makes DMSO protocol a preferable method. Considering that HepG2 cells are the primary cells used to study HBV infections, this effectively removed the use of this protocol for future study in *de novo* infections.

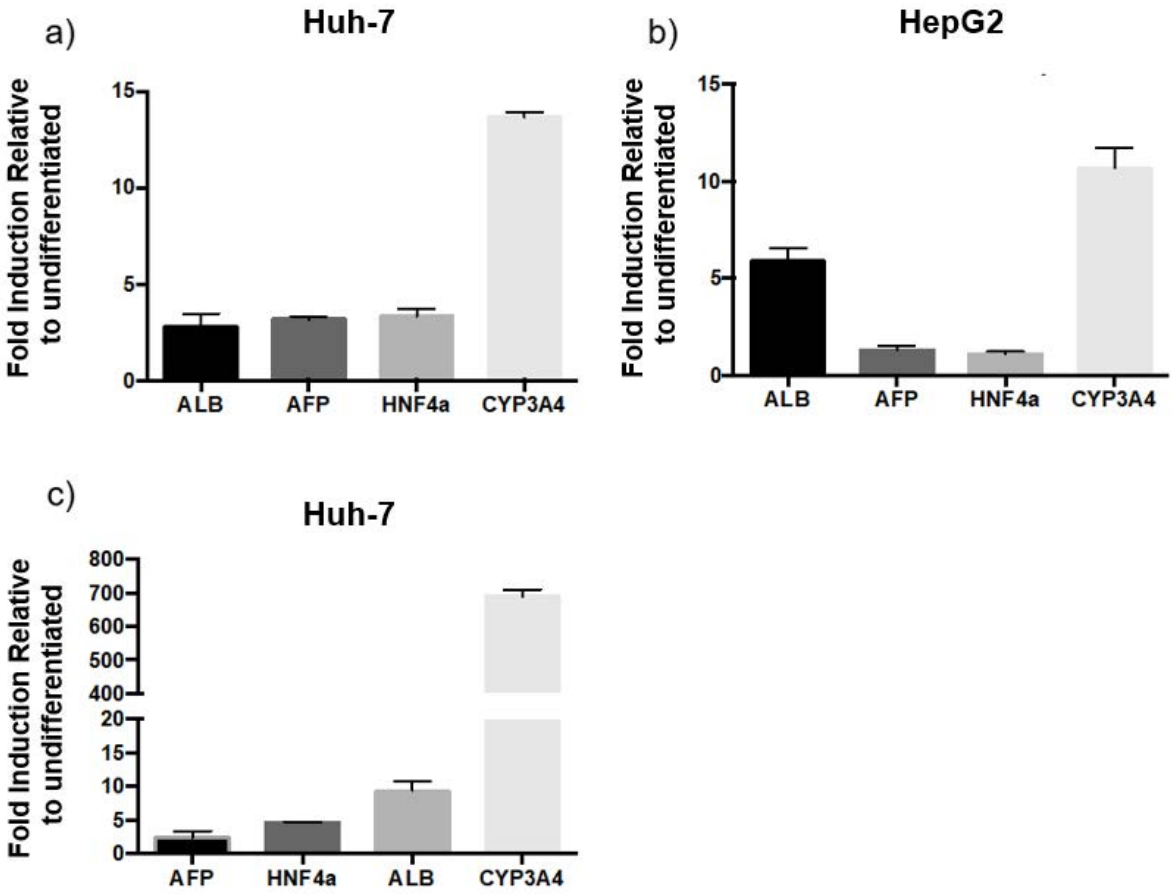

Figure 3.13 Differentiation marker expression in hepatoma cells

Graphs displays PCR result comparing expression levels of common hepatoma differentiation markers relative to un-differentiated Huh-7 and HepG2-NTCP cells. **A)** DMSO differentiated Huh-7 cells. **B)** DMSO differentiated HepG2-NTCP cells. Differentiation status of cells compared using panel of hepatocyte differentiation markers. **C)** Non-DMSO differentiated Huh-7 cells. Each graph represents the means of 3 biological repeats. Error bars show SE of 9 technical repeats.

3.8 Cellular differentiation status and response to low oxygen

When considering the effect of differentiation on hypoxic responses we decided that it was important to understand how differentiation affects cellular response to low oxygen and HIF expression. We evaluated HIF-1α expression over a 96-hour time in differentiated and undifferentiated HepG2 cells under normoxic conditions. Dimethyloxalylglycine (DMOG) is a competitive inhibitor of PHDs that is widely used to stabilize HIFs under normoxic conditions and was used as a positive control (Zhang *et al*., 2016). Differentiated cells do not express HIF under normoxic conditions over the time period studied, however, non-differentiated cells express HIF-1α after 96 hours under normoxic conditions (**Figure 3.14**). This is probably due to cell over-growth that limits oxygen availability, whereas DMSO differentiation is known to arrest cell proliferation by arresting in G1 phase of the cell cycle (Fiore *et al*., 2002, Huang *et al*., 2004). This data is important to consider when planning HBV infection experiments, which typically have a long protocol for infection over 7 days and highlights the importance of cell seeding density in subsequent experiments.

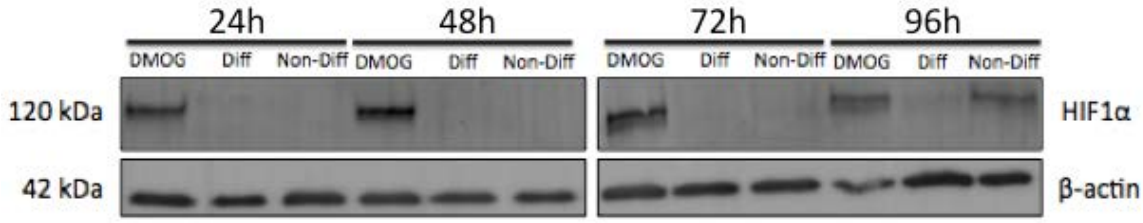

Figure 3.14 HIF expression in differentiated vs non-differentiated hepatoma cells

HepG2-NTCP cells were either differentiated with 2% DMSO or left untreated and incubated at 37ºC for 96 hours. Control cells were treated with DMOG (1µM) at T0 and lysed every 24 hours. Cells were counted and equal amount of protein lysate were analysed by SDS PAGE and screened for HIF-1α expression.

3.9 Cell density, differentiation and HIF responses

After demonstrating HIF expression in over confluent cells we decided to examine the effect of cell seeding density and DMSO differentiation on HIF expression and downstream signalling more closely. HepG2 cells were seeded at multiple densities to reflect a range of confluencies (**Figure 3.15a**) and we compared HIF-1α expression under normoxic and hypoxic conditions in DMSO differentiated and non-differentiated HepG2-NTCP cells. DMSO mediated differentiation of HepG2 cells blunts HIF-1α expression (**Figure 3.15b**) under 1% oxygen independent of cell density. The use of the HRE-Luc reporter assay enables us to determine whether the reduced levels of HIF-1α result in a blunted transcriptional response. HRE-Luc reporter activity is independent of cell seeding density in non-differentiated cells. However, following DMSO treatment the cells show a blunted HRE-Luc reporter activation that is density dependent, consistent with reduced HIF-1α expression by western blotting (**Figure 3.15c**). We examined the effect of DMSO differentiation and cell density on HIF-1α regulated target genes: PDK1 and SLC16A3 (**Figure 3.16**). Differentiated cells show a blunted HIF gene expression response that is independent of cell density. This builds upon the previous result and provides a justification for removing DMSO from our HBV infection protocol.

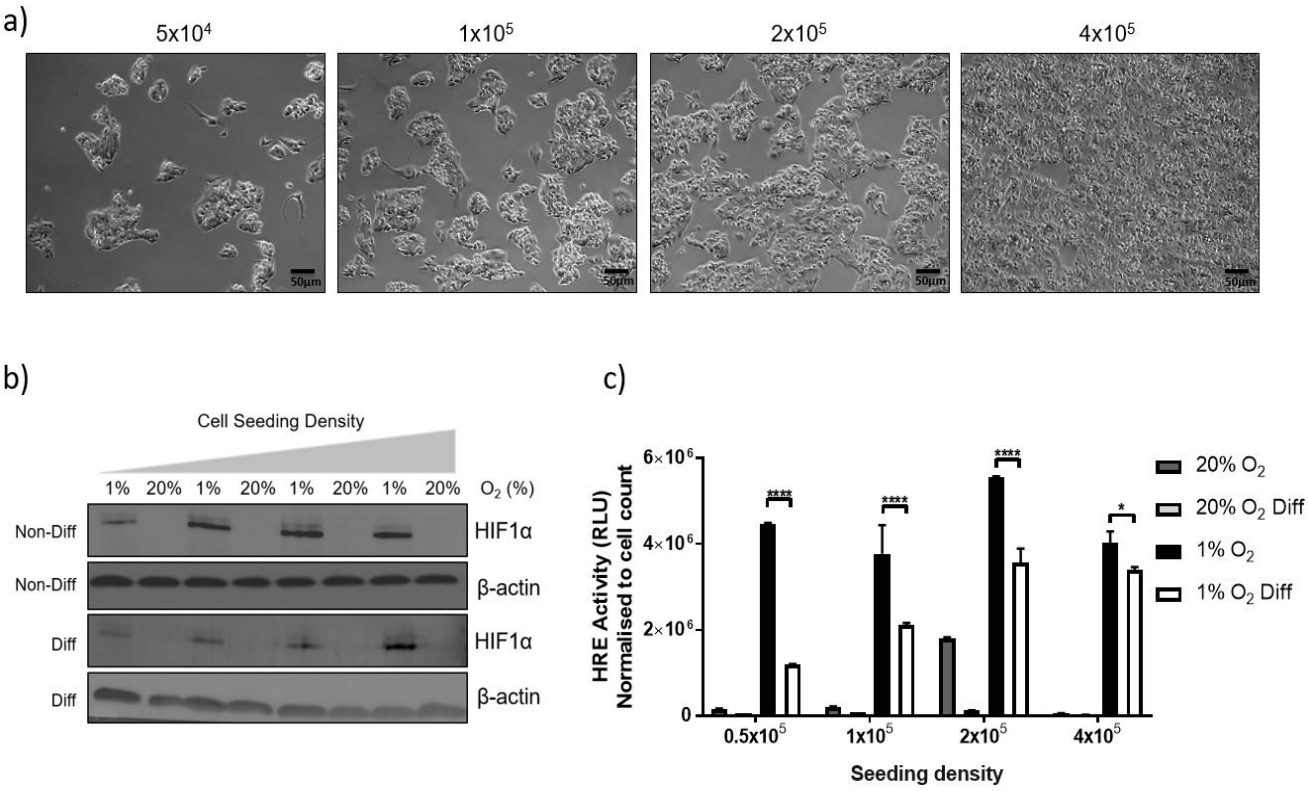

Figure 3.15 Hepatoma differentiation blunts HIF-1α expression and transcriptional activity

A) Brightfield microscopy images of HepG2-NTCP cell seeding densities per 1.9cm^2 under 20% oxygen. Western blot (**B**) and HRE activity (**C**) of HIF-1α expression in HepG2-NTCP cells at a range of densities incubated with DMSO (2%) or untreated for 72 hours. Cells were cultured under normoxic (20% O_2) or hypoxic (1% O_2) conditions for 24 hours, counted to normalise cell lysates before loading or luciferase measurement. Hypoxic-dependent RLU activity per 100,000 cells is shown. Two-Way ANOVA with Tukey's multiple comparisons test was used. Graph represents the mean of 2 biological repeats. Error bars show SE of 4 technical repeats.

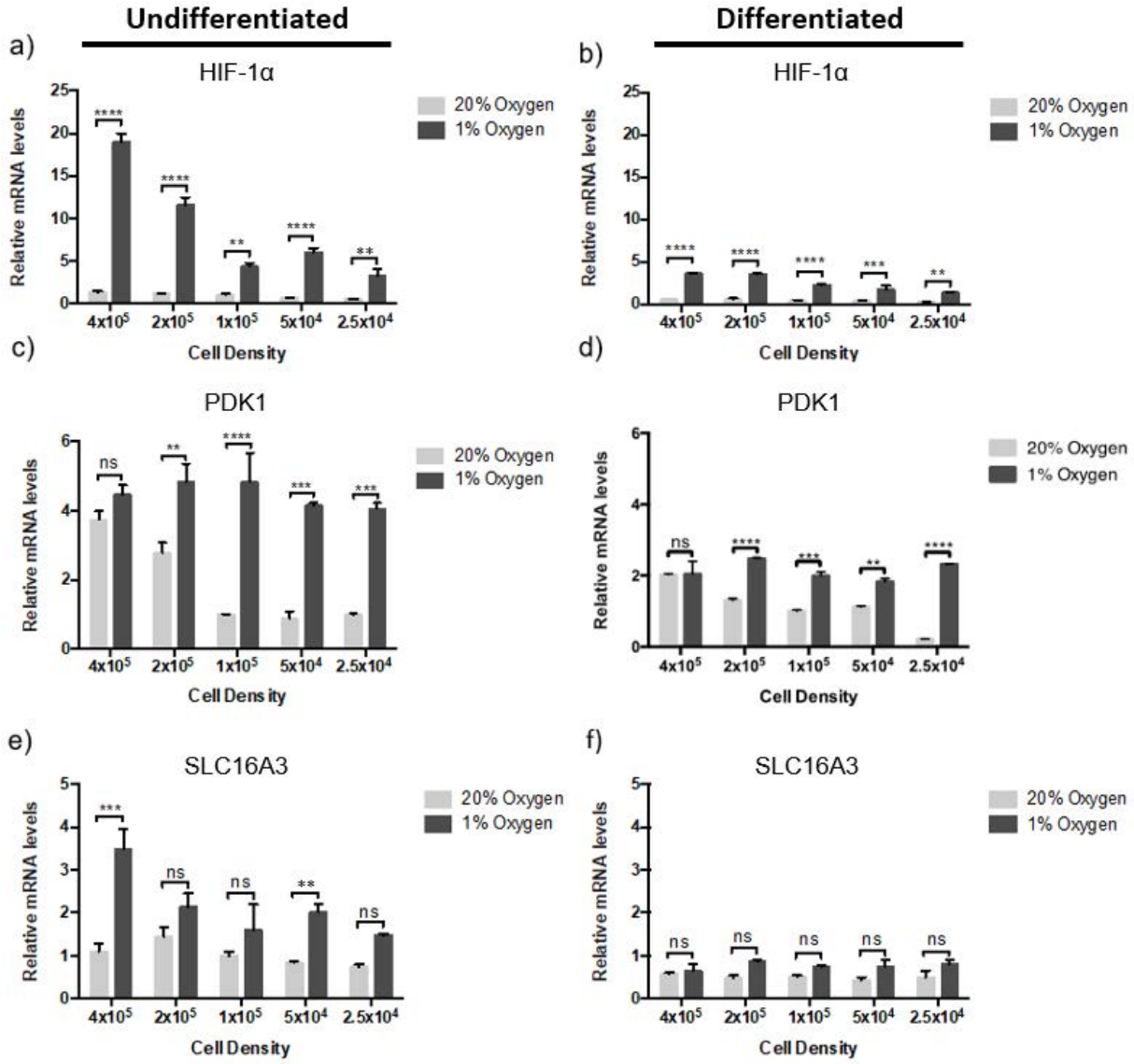

Figure 3.16 Effect of HepG2 differentiation status on HIF-1α and target gene RNA levels

HepG2-NTCP cells were seeded at a range of densities and incubated with DMSO (2%) or untreated for 72 hours. Cells were then cultured under normoxic (20% O_2) or hypoxic (1% O_2) conditions for 24 hours. **A/B)** qRT-PCR result for HIF-1α mRNA levels in un-differentiated (**A**) and DMSO differentiated (**B**) HepG2-NTCP cells. **C/D)** qRT-PCR result for PDK1 mRNA levels in un-differentiated (**C**) and DMSO differentiated (**D**) HepG2-NTCP cells. **E/F)** qRT-PCR result for SLC16A3 mRNA levels in un-differentiated (**E**) and DMSO differentiated (**F**) HepG2-NTCP cells. Data analysed with Two-Way ANOVA with Sidak's multiple comparisons test. Graphs display relative mRNA levels normalised against house keeping gene B2M. Each graph represents the means of 2 biological repeats. Error bars show SE of 6 technical repeats.

Using the same 84-gene PCR array as before, we performed a comparison of common HIF-1α target genes in DMSO differentiated versus non-differentiated samples. The results are displayed from the highest to lowest gene induction of the DMSO differentiated samples. Each sample is compared with the equivalent non-differentiated sample induction. This graph clearly shows that DMSO differentiation blunts mRNA levels of a wide range of HIF target genes (**Figure 3.17a**). Plotting the data as two groups “DMSO differentiated” vs “Non-differentiated” demonstrating blunted gene expression in most genes represented on the array following differentiation (**Figure 3.17b**). This graph demonstrates that one gene on the array is up regulated significantly through DMSO differentiation, this is EGR1 and is known to be involved tendon differentiation, providing an explanation for up-regulation (Guerquin *et al.*, 2013). Important to note that the examples previously used PDK1 and SLC16A3 demonstrate the same blunted response in this array. Other important genes that typically express highly in hepatocytes exposed to low oxygen are CA9 and EPO; these are also blunted significantly in DMSO differentiated samples.

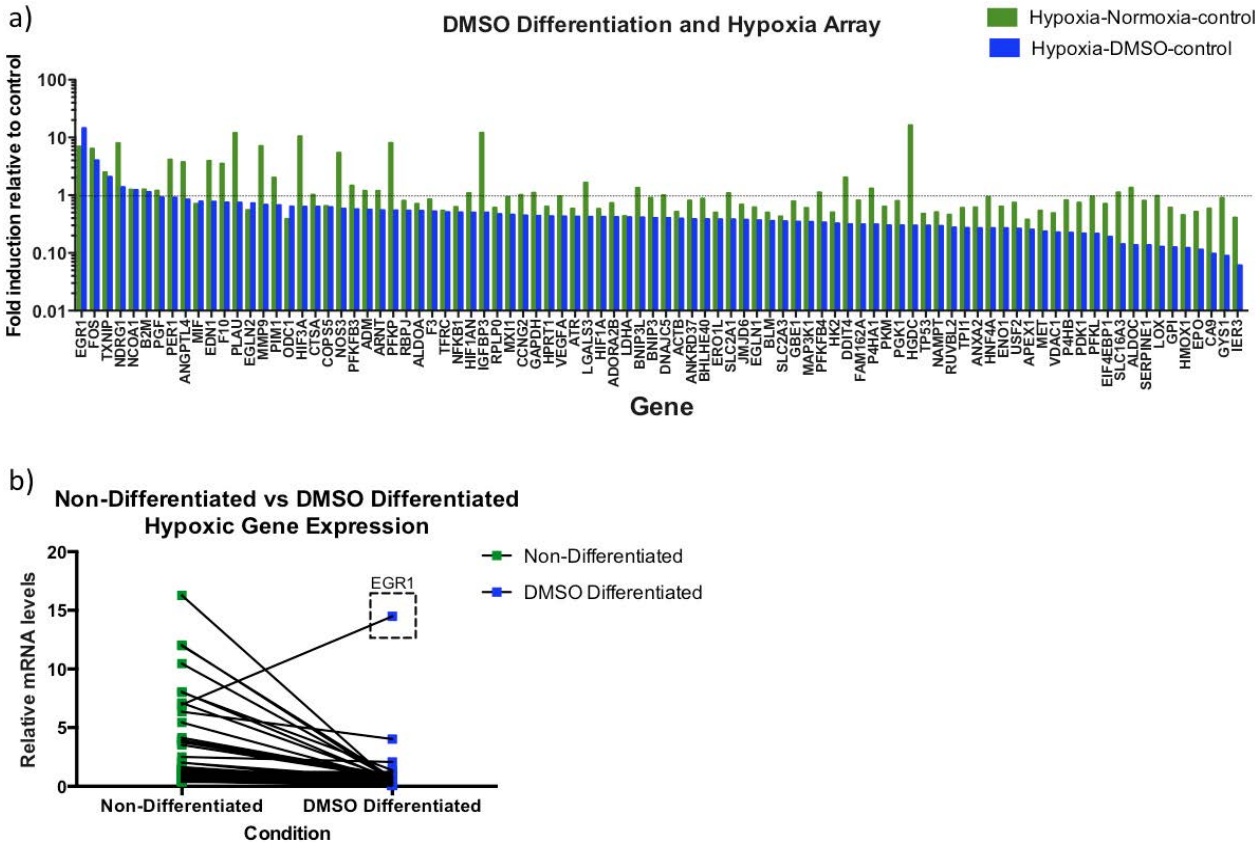

Figure 3.17 Non-differentiated vs DMSO differentiated hypoxic gene expression

Huh-7 cells were either DMSO differentiated in 2% DMSO for 72 hours or left undifferentiated. The cells were then placed under 1% and 20% oxygen for 24 hours. **A)** Expression profile for hypoxic genes in DMSO differentiated vs non-differentiated samples. **B)** Graph demonstrates comparison of individual gene expression from the hypoxic array under 1% oxygen in DMSO differentiated vs non-differentiated samples.

3.10 Discussion

The aim of this results chapter was to develop a better understanding of hepatocellular responses to low oxygen in our target cells for HBV infection. So, this chapter aimed to establish the baseline for future experiments by examining HIF expression and transcriptional activity in Huh-7 and HepG2 cells. This information was used to establish a model to examine the effect of low oxygen and HIF on HBV replication.

We examined the effect of HIFα over expression plasmids and HIF regulating drugs on each of the cell lines studied so far. Plasmids were also used to over express HIFs under normoxia with the goal of demonstrating functional HIFs in normoxic conditions and we confirmed the result demonstrated using FG-4592 treatment (**Figure 3.9**).

Using the hypoxic gene array from Qiagen we demonstrated that these treatments activate HIF target genes (**Figure 3.10**), however, the response is different compared to hypoxic cells (**Figure 3.11**). HIF target gene expression is cell context dependent and any differences noted are likely to reflect heterogeneous responses between cell types. This suggests that there are other variables involved in regulating these signalling pathways. In **Figure 3.10a** we observe a difference in gene expression between plasmid HIF-1α (under 20% oxygen) and 1% oxygen samples. Interestingly, this suggests that up-regulation of genes is occurring with no associated HIF activation, especially because pHIF-2α does not account for observed differences. This suggests that either another oxygen sensor is involved (perhaps PHDs themselves) or that the low oxygen is capable of activating these genes alone. Perhaps these are activated under different kinds of cellular stress (such as mitochondrial) or through growth factor interaction with receptors. Literature has shown that HIF-2α plays a role in lipid metabolism in particular (Rankin *et al*., 2009). Considering the genes found in this

array (many involved in carbohydrate metabolism), it is not surprising that we saw minimal pHIF-2α activation of genes.

Hepatocytes are highly differentiated (Olsavsky Goyak *et al*., 2010, Holtzinger *et al*., 2015, Meier *et al*., 2013, Alder *et al*., 2014) and this is required for efficient infection by HBV. Using two independent methods we examined the expression of some reported differentiation markers (Hay *et al*., 2008, Olsavsky Goyak *et al*., 2010, Holtzinger *et al*., 2015). We found a difference in hypoxic responses in differentiated cells; which we tested using Western blots and the HRE-Luc reporter assay (**Figure 3.14** and **Figure 3.15**).

Cell seeding density and differentiation status are important factors to consider when studying HBV infections using *de novo* infection models. This provides justification for our study of the differentiation effects on hypoxic responses. In particular **Figure 3.15b,c** suggests that the differentiation state of the cells can determine the level of HIF expression and regulate how the HIF signalling pathway responds to low oxygen stimulation. Whilst the method of regulation is unclear for HIF signalling, it has previously been demonstrated that DMSO can down regulate transcription factor activity in the liver, with studies looking at NF-κB and ATF4 (Essani *et al*., 1997, Song *et al*., 2012). Alternatively, these results could suggest that DMSO up-regulates many host genes and masks the effect of hypoxia.

Further data supporting this conclusion was obtained using PCR to examine the fold induction relative to control for HIF-1α mRNA and two genes associated with HIF-1a signalling PDK1 and SLC16A3 (**Figure 3.16**). These hinted at a blunting effect, but a further use of the 84-gene array (**Figure 3.17a**) demonstrated that this effect is observed in many genes (**Figure 3.17b**).

Current protocols for studying HBV utilise DMSO differentiation for efficient *de novo* infection. However, to study the effect of low oxygen on HBV replication we should try and work around this. We cannot be sure that this is not an off-target effect of DMSO or differentiation, the literature does not say. Therefore, we tested another method of differentiation to try and confirm this reason. However, the primary cell line for testing HBV infections (HepG2 cells) did not survive the process. Therefore, to effectively establish an infection model for examining low oxygen effects we had to try and remove DMSO from the infection process.

3.11 Summary

This chapter establishes low oxygen responses in our target cell line of choice, HepG2 cells and examines the effect of differentiation on hypoxic responses. This chapter primarily identifies tools for use in developing an effective model for infection and low oxygen.

4. STUDYING HBV AND HIF STABILISATION

4.1 Introduction

In the previous chapter we identified a range of tools to study the response of hepatoma cells. We showed that HepG2 cells express HIF-1α and HIF-2α and are responsive to low oxygen and highlighted a role for differentiation status to regulate HIF expression and transcriptional responses to low oxygen. These observations provide the foundation for studying the effects of low oxygen on HBV replication.

HBV has been previously reported to stabilize HIF via interactions with viral encoded X protein (HBx), as detailed in the main introduction (See **Figure 1.16**). However, the majority of these reports have studied HBx-HIF interactions in the absence of full replicating HBV. Our studies have been performed using a combination of different models for HBV infections, including transfections of viral genomes, the chronically infected HepG2.2.15 cells and *de novo* infections using mature HBV particles. In addition, we used multiple methods for examining HIF stabilisation and pathway activity. These include HIF stabilising agents detailed in chapter 3 and exposure to 1% oxygen conditions using specialized hypoxic incubators. These enable a study of HBV-HIF interaction under less artificial conditions.

We selected to use HepG2.2.15 cells stably expressing integrated copies of the HBV genome (Sells *et al*., 1987, Lu *et al*., 2001). These cells express HBV DNA as chromosomally integrated sequences, as well as the episomal cccDNA and rcDNA; and express the HBV ORFs under the control of wild-type HBV promoters (Sells *et al*., 1987, Lu *et al*., 2001). In addition, these cells have been shown to secrete HBV antigens HBs/ HBe and infectious Dane particles (Sells *et al*., 1987). These cells

provide an ideal model to study the effects of low oxygen on HBV replication in the absence of any DMSO treatment. In addition, we had an additional HepG2 based line that stably expresses HBV genomes - HepAD38 cells express high levels of integrated HBV DNA under the control of an artificial CMV promoter that is tetracycline-inducible and when the cells are cultured in tetracycline containing media viral transcription is inhibited (Ladner *et al*., 1997, Severi *et al*., 2006, Jia *et al*., 2017). These cells are used briefly to demonstrate comparable results between producer cell lines.

The HBV life cycle is depicted in **Figure 4.1**, the incoming particles contain rcDNA that is repaired to form cccDNA, which provides the template for pgRNA transcripts; reverse transcription of pgRNA into negative strand DNA and subsequent plus strand DNA synthesis (Seeger and Mason, 2015, Thomas and Liang, 2016). These processes have been discussed in more detail in the introduction (**section 1.2.5**). As discussed in the main introduction the liver exists under an oxygen gradient with hypoxic zones around the hepatic central veins (**Figure 4.2a**), therefore it is important to consider the impact of low oxygen on HBV. HBV core antigen stains kindly provided by the Protzer laboratory at TUM. demonstrate significant HBV core expression around the Peri-central regions of HBV transgenic mice (**Figure 4.2b**). In this chapter we aimed to confirm that HBV infection can stabilize HIFs and to show transcriptional activation of this pathway.

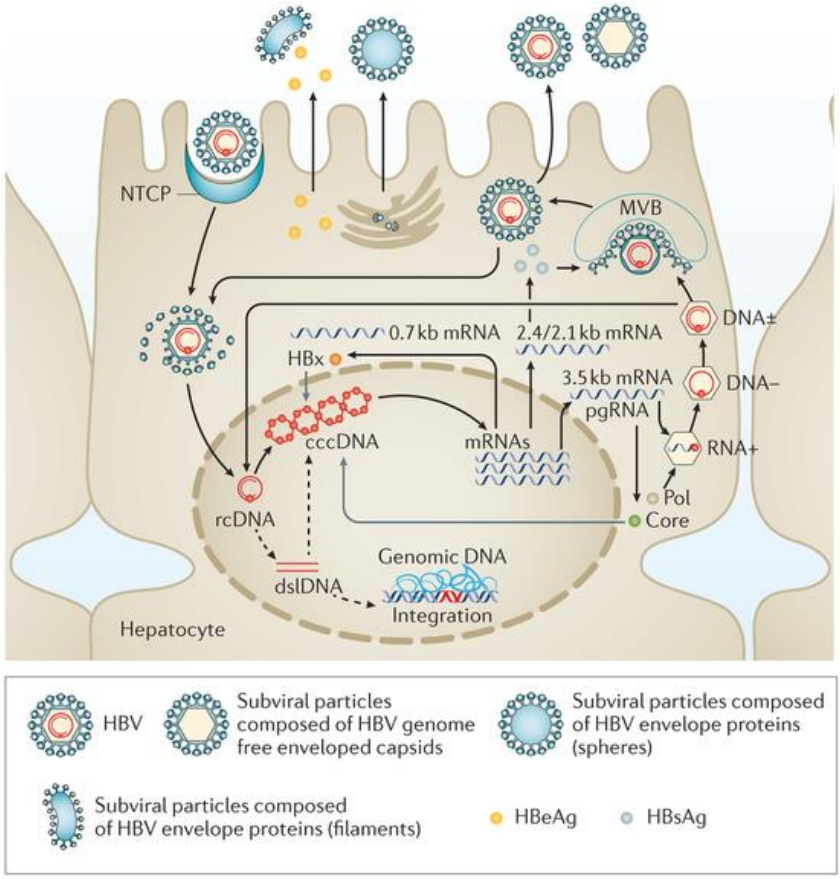

Figure 4.1 HBV life cycle (Thomas & Liang, 2016)

a)

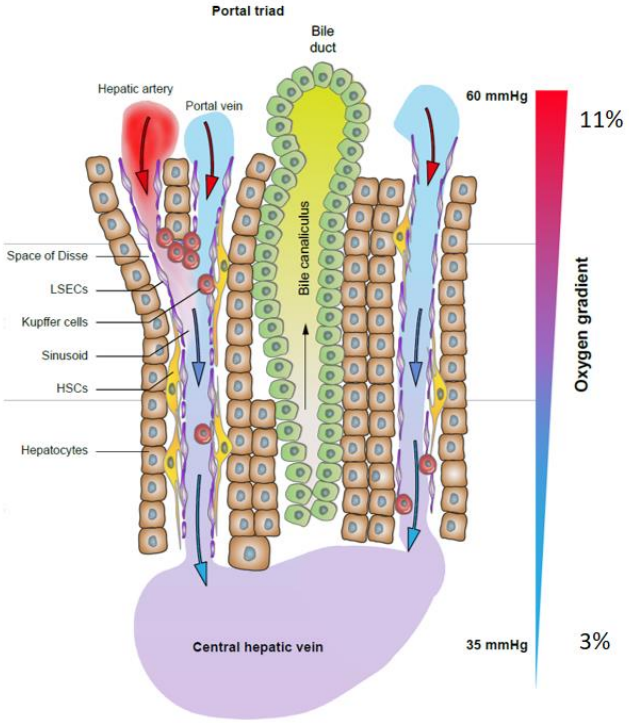

b)

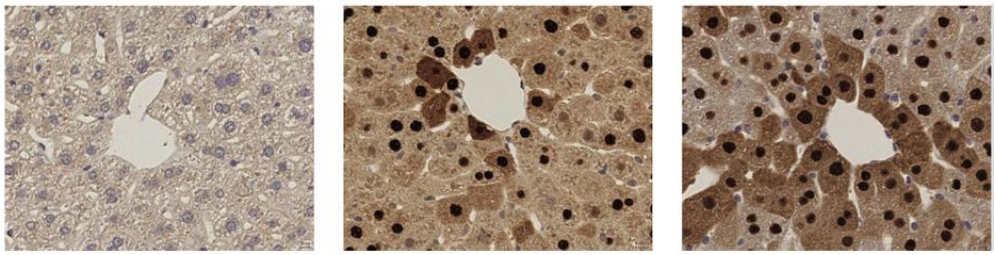

Figure 4.2 Oxygen gradient in the liver and HBV antigen expression in mice engineered to express the complete viral genome

Cartoon displaying the natural oxygen gradient found in the liver ranging from 9% at the hepatic portal triad to 3% at the area around the central hepatic vein. (B) HBV Core antigen staining around the Peri-central region in HBV transgenic mice liver slices (Kindly provided by collaborators at TUM.).

Results

4.2 HBV models and HIF expression

HBV infection has been reported to stabilize HIFs via an association between the viral encoded regulatory protein HBx, however there is no consensus on the mechanism and some of the caveats of the studies were discussed in the main introduction (**Figure 1.16**). Our initial experiments examined the effect of transfecting HBV genotypes into HepG2-NTCP target cells and assessed HIF expression by Western blotting. First, we demonstrated that delivery of full-length replication competent HBV genotypes C and D into HepG2-NTCP cells via plasmid-based transfection stabilises HIF-1α and HIF-2α under normoxic conditions (**Figure 4.3a** and **Figure 4.3b**), compared to mock transfected controls. We observed comparable levels of HIF expression in the HBV transfected cells cultured under normoxia to control cells cultured under 1% oxygen. Following this initial experiment, we demonstrated that transfecting HBV into HepG2 cells can stabilize HIFs over an extended duration using a time course experiment like those observed in chapter 3. This demonstrated stable expression of both HIF-1α and HIF-2α under normoxic conditions for up to 72 hours (**Figure 4.3c**).

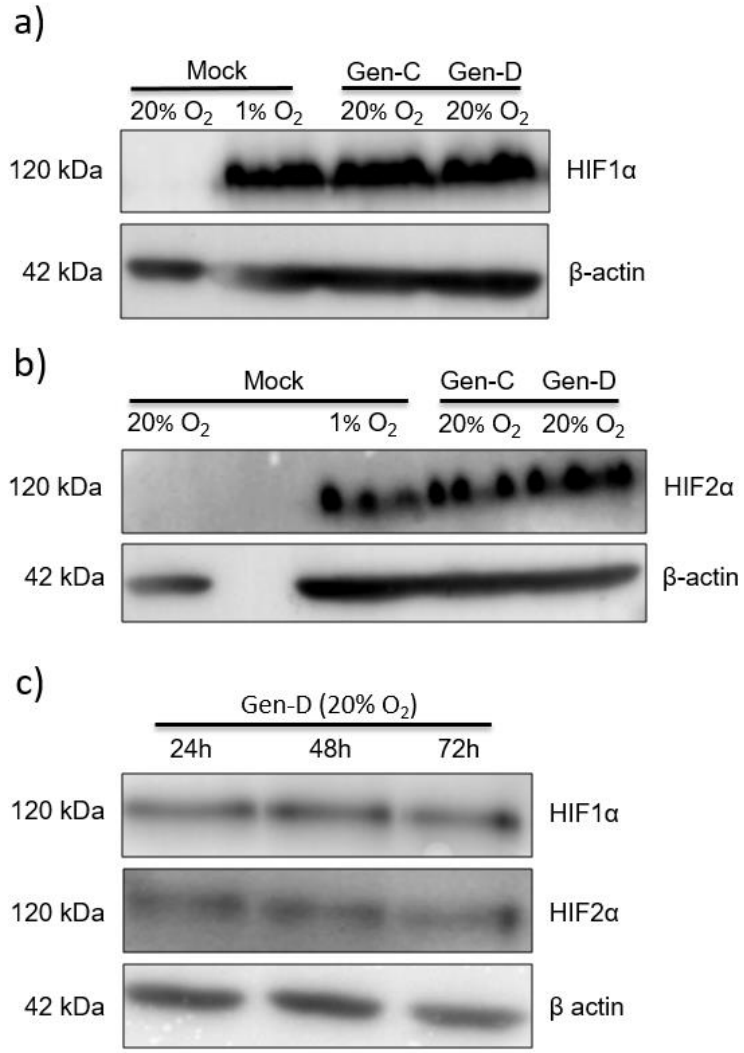

Figure 4.3 Transfection of HBV genomes into hepatoma cells stabilises HIFs

HepG2-NTCP K7 (Sub clone of HepG2-NTCP cells that express higher levels of NTCP) cells were transfected with diverse HBV genotypes (1µg per genotype) and lysed for Western blotting and PCR 24 hours post transfection. **A/B)** Western blots showing HIF-1α and HIF-2α expression in HepG2-NTCP K7 cells following transfection with HBV genotypes C (Gen-C) and D (Gen-D) under 20% oxygen compared to a 1% oxygen positive control. **C)** HepG2-NTCP K7 cells transfected with 1µg of HBV 1.3 plasmid (Genotype D) and placed under normoxia. Western blots show HIF-1α and HIF-2α expression over 72hrs following transfection.

4.3 HBV stabilisation of HIF is independent of HBx

Following the demonstration of stable HIF expression in HBV transfected cells, we wanted to confirm previous reports that suggest that the HBx protein is the primary target of interaction between the virus and host transcription factor. To achieve this, we utilised a combination of plasmid transfections for HBV genotype D. Protzer and colleagues kindly provided us with plasmids encoding HBV genotype D with selected gene deletions. These include genotype D with HBx deletion (X-), large surface antigen deletion (L-) and a double knock out of both HBx and L antigen (X/L-). We examined HIF expression following transfection using Western blotting, compared against wild-type genotype D genome and normoxic and hypoxic controls (**Figure 4.4a**). This result demonstrated that HBV stabilisation of HIF can occur independent of HBx protein. In addition, our data demonstrated that stabilisation of HIFs occur independent of the large surface antigen as well (**Figure 4.4a**), perhaps suggesting that stabilisation occurs through another HBV protein such as Core or perhaps in response to infection.

To investigate whether HBx expression cells could stabilize HIF we transfected cells with pHBx and compared the stabilisation of HIFs following transfection with HBV genotype D, the genome with X deletion and plasmid HBx (**Figure 4.4b**). Previous reports suggest that HBx primarily affects HIFs transcriptional activity, however they also suggest that HBx is involved in HIF stabilisation (Yoo *et al*., 2003, Liu *et al*., 2014, Hu *et al*., 2016). **Figure 4.4b** confirms our previous result by demonstrating a lack of stabilisation under 20% oxygen following transfection with HBx. To investigate whether HBx could affect HRE activation we transfected cells with pHBx or pR96E in combination with the HRE-luciferase reporter. R96E is a single point mutation in HBx that abrogates interaction with DDB1 and negatively regulates HBV infection by preventing HBx interaction with cccDNA and inhibiting viral transcription (Sitterlin *et al*.,

2000a, Sitterlin *et al*., 2000b, Li *et al*., 2010b), this serves as a control in our investigation of the role of HBx in HIF stabilisation and transcriptional activity. This result demonstrated that transfection with HBx does not stimulate additional HRE activity in HepG2-NTCP K7 cells (**Figure 4.4c,d**).

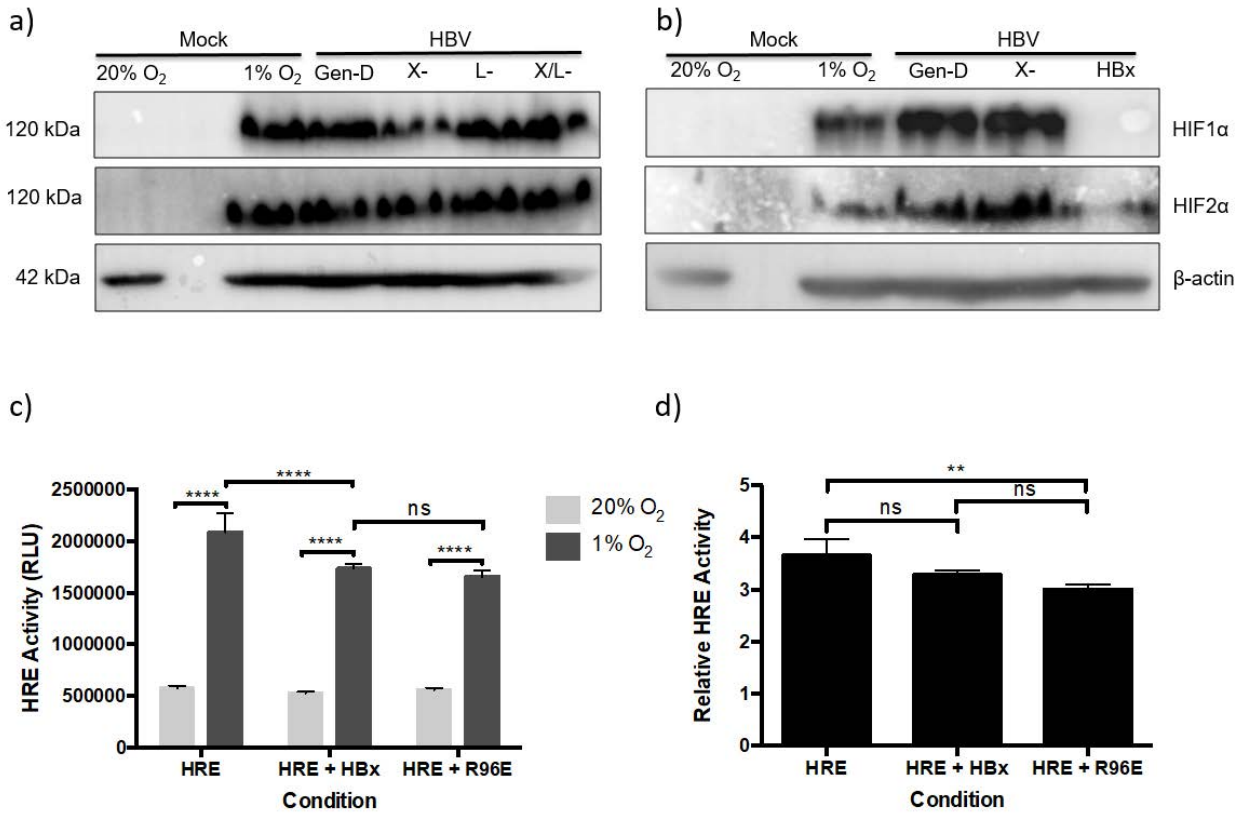

Figure 4.4 HBV stabilisation of HIF independent of HBx

HepG2-NTCP K7 cells were transfected with diverse HBV Genotype D and genotype D with HBx deletion (X-), large surface antigen deletion (L-), or double knockout of HBx and L (X/L-) and lysed for Western blotting (**A**). Additionally, HepG2-NTCP K7 cells were transfected with HBV Genotype D wild type, X deletion, and plasmid HBx, then lysed for Western blotting (**B**). **C)** HRE luciferase result demonstrating HRE activation under 20% and 1% oxygen following co-transfection of HRE and HBx or R96E mutation. **D)** Relative expression of HRE activity following co-transfection of HRE and HBx or R96E. One-Way ANOVA (D) and Two-Way ANOVA (C) with Tukey's multiple comparisons test used for analyses. Each graph shows the means of 2 biological repeats. Error bars show SE of 6 technical repeats.

4.4 HBV producer cells and HIF stabilisation

Having demonstrated that delivering HBV genomes into HepG2-NTCP cells stabilises HIF in a HBx independent manner, we wanted to confirm HIF stabilisation in cell lines stably expressing HBV and finally in *de novo* infections. HepG2.2.15 and HepAD38 cells provide a model system of chronic infection to study HBV transcription. Of note HepAD38 cells are the source of infectious HBV used by most laboratories worldwide to purify virus for *in vitro* infection studies. Both HepG2.2.15 and HepAD38 cells express HIF-1α under both 20% and 1% oxygen conditions, whereas uninfected HepG2-NTCP K7 cells only express HIF-1a under hypoxic conditions (**Figure 4.5a**), confirming our earlier observations with transfected HBV genomes. We observed increased expression of HIF-1α in both HBV expressing cells cultured under low oxygen conditions, demonstrating that the cells can still respond to low oxygen stress and consistent with additive pathways to stabilize HIF in the infected cells. Culturing the producer cells under 20% oxygen and lysing the samples for Western blotting every 24 hours demonstrated that stabilisation of HIF occurs over a prolonged period, up to 72 hours (**Figure 4.5b**).

We examined HIF target genes CA9 and VEGF expression within the cells using quantitative PCR demonstrating that the HepG2.2.15 cells still respond to low oxygen and show increased transcription of HIF target genes compared to uninfected HepG2-NTCP K7 cells (**Figure 4.5c**). Following this result, we performed PCR to determine the effect of the HIF stabilising drug FG-4592 on HBV infected cells. We examined the expression of CA9 and VEGFA following drug treatment and exposure to low oxygen (**Figure 4.5 d,e**). This result confirms the response to low oxygen in HepG2.2.15 cells and demonstrated that FG-4592 is effective at increasing HIF target gene expression in HBV infected cells relative to normoxic controls.

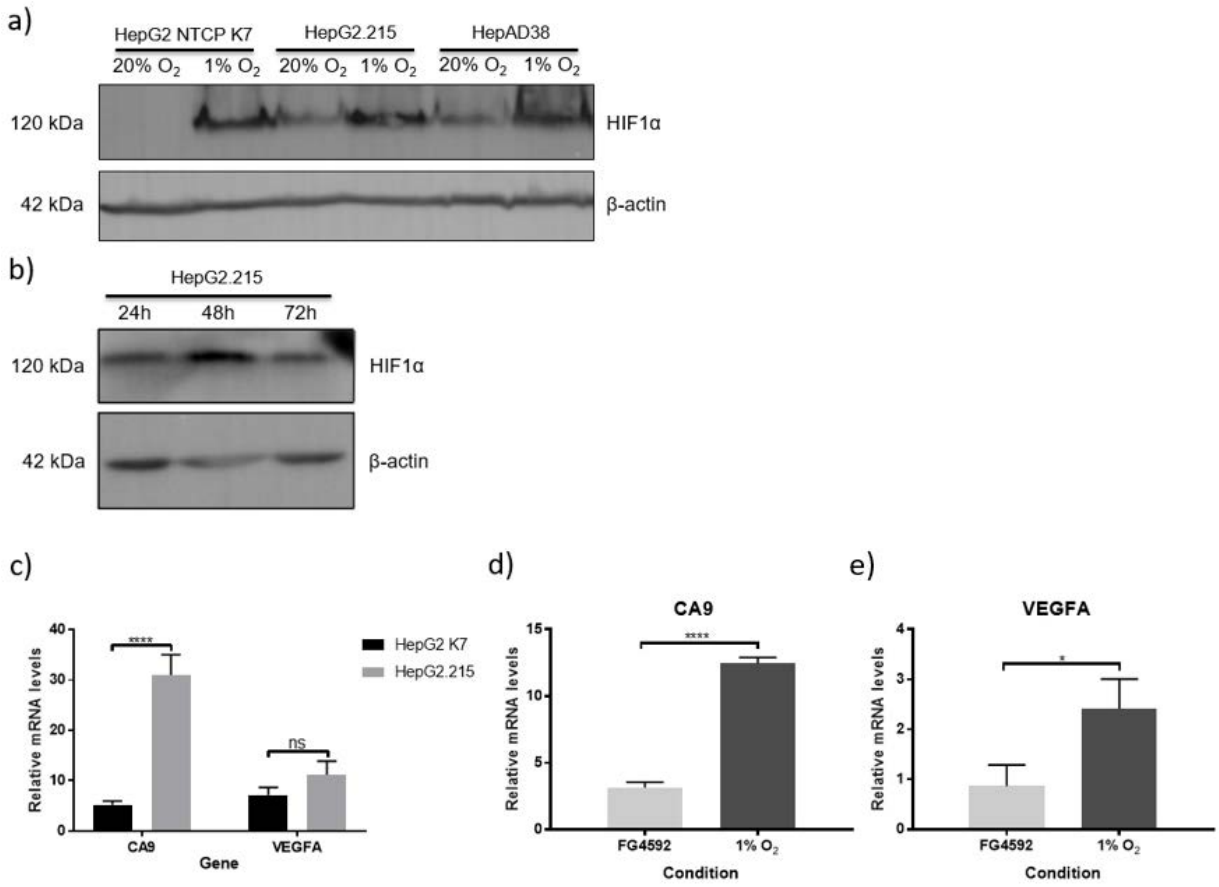

Figure 4.5 HBV and HIF stabilisation

A) HepG2-NTCP K7, HepG2.2.15 and HepAD38 cells were placed under normoxic or hypoxic conditions or treated with 1μM FG-4592 for 24 hours, samples were blotted for HIF-1α. **B)** HepG2.2.15 cells were placed under normoxic conditions for 72 hours. Cell counting of comparable wells was utilised for equal loading, samples were blotted for HIF-1α. **C)** Relative CA9 and VEGFA induction in uninfected HepG2-NTCP K7 cells and HepG2.2.15 cells under 1% oxygen, Two-Way ANOVA with Sidak's multiple comparisons test. **D)** CA9 and VEGFA up-regulation relative to uninfected cells in HepG2.2.15 cells, Unpaired t test with Welch's correction. Each graph shows the means of 4 biological repeats. Error bars show SE of 12 technical repeats.

After demonstrating increased CA9 and VEGF mRNA levels in HepG2.2.15 cells we extended these results to study additional HIF regulated genes using a selected hypoxia PCR array (**Figure 4.6**), HIF stabilisation previously confirmed in Figure 4.5a. This result demonstrated that HBV infected cells under normoxic conditions promote the expression of multiple hypoxic response genes. Of note HBV infected cells show a different profile of hypoxic gene expression compared to uninfected hypoxic HepG2-NTCP K7 cells or following treatment with FG-4592 (**Figure 4.7a,b**).

As discussed previously, FG-4592 treatment stimulates HIF expression through inhibition of PHDs (**Figure 3.1**), this result demonstrated that FG-4592 treatment stimulates a fewer genes compared to 1% oxygen incubation in HepG2-NTCP K7 cells, however for most genes demonstrated with the array, the expression is more limited (**Figure 4.8a**). A comparison of 1% oxygen and HBV stimulated gene expression demonstrated very similar levels of expression in up-regulated genes (**Figure 4.8b**). A comparison of commonly up-regulated genes in HBV positive and 1% oxygen samples reveals some differences in expression (**Figure 4.8c**). Expression is lower in HBV positive samples, this could reflect continued degradation under 20% oxygen or simply cell type specific differences. HBV positive HepG2.2.15 cells specifically demonstrate increased up-regulation of numerous genes involved in regulating cell growth, proliferation, apoptosis and cellular metabolism (**Figure 4.8c**).

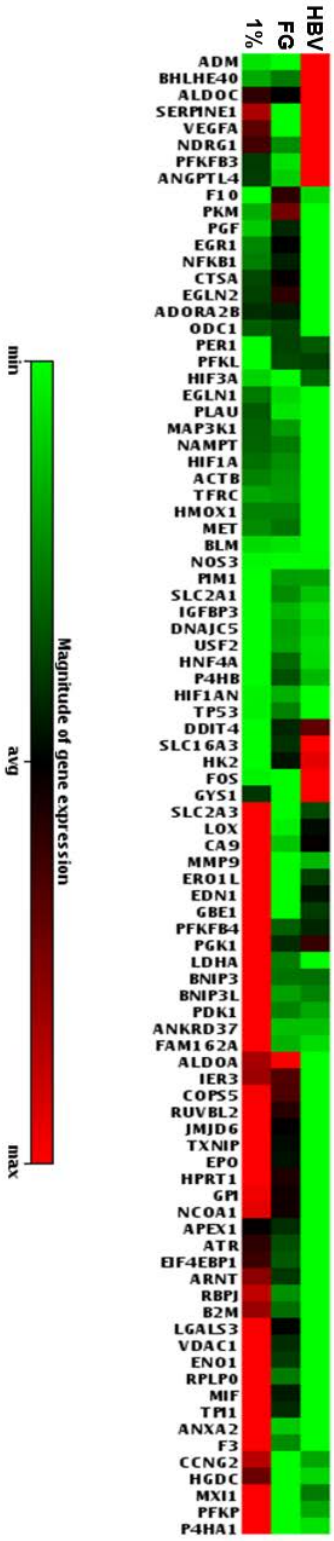

Figure 4.6 HIF transcript activity in HBV expressing HepG2 cells compared to PHD inhibitor treated HepG2 cells

Legend on following page.

Figure 4.6 HIF transcript activity in HBV expressing HepG2 cells compared to PHD inhibitor treated HepG2 cells (Cont.)

HepG2-NTCP K7 cells were treated with FG-4592 (1µM) (FG - group) under 20% oxygen or placed into 20% or 1% oxygen (1% - group) for 24 hours untreated. HepG2.2.15 cells were placed under 20% oxygen for 24 hours (HBV – group). Heatmap was generated by Qiagen RT2 software.

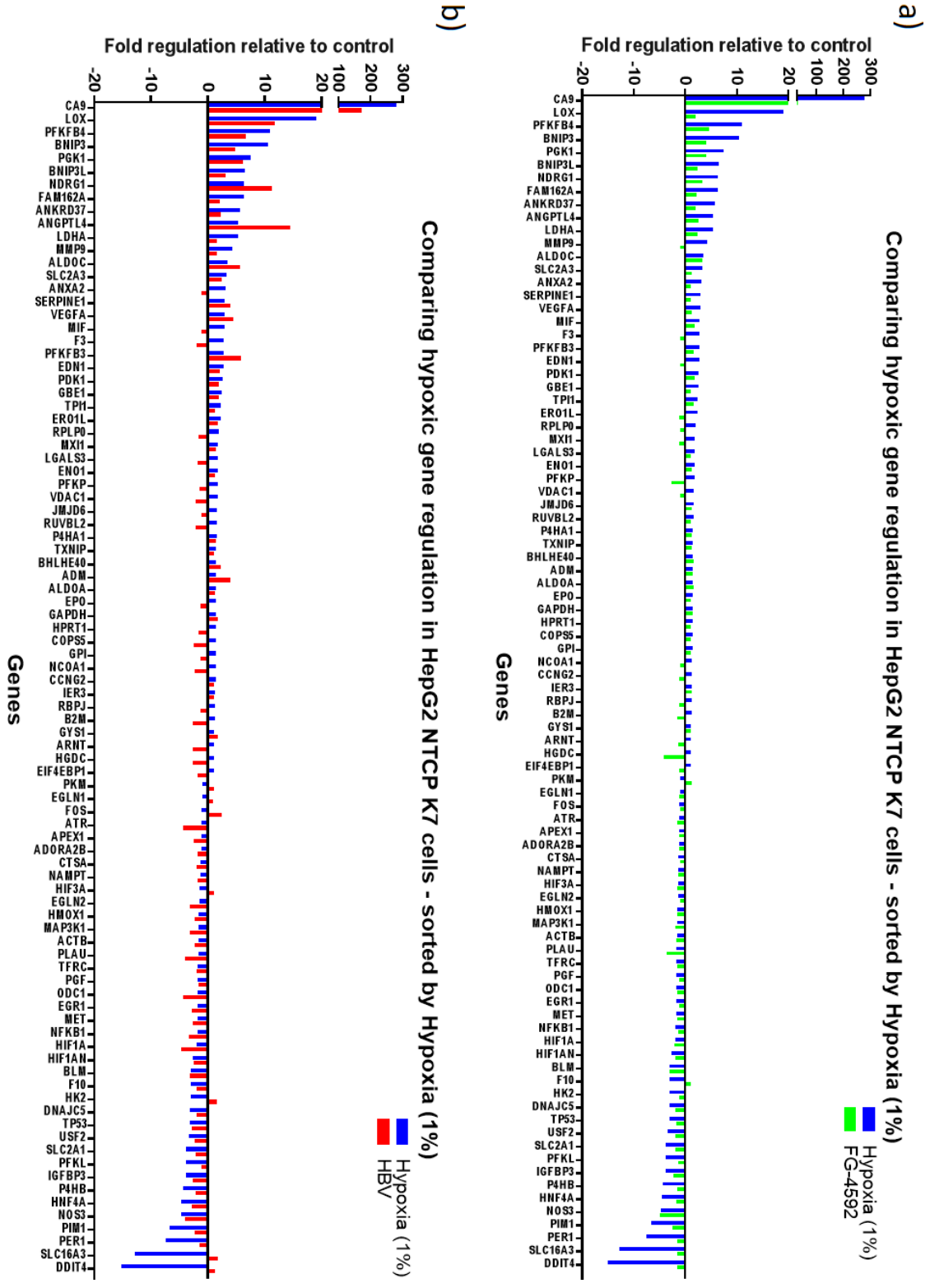

Figure 4.7 HIF transcript activity in chronic HBV producer cells compared to PHD inhibitor treated cells

Legend on following page.

Figure 4.7 HIF transcript activity in chronic HBV producer cells compared to PHD inhibitor treated cells (Cont.)

HepG2-NTCP K7 cells were treated with FG-4592 (1µM) under 20% oxygen or placed into 20% or 1% oxygen for 24 hours untreated. HepG2.2.15 cells were placed under 20% oxygen for 24 hours. **A)** Comparison of hypoxia and FG-4592 treated samples regulated genes, sorted against hypoxic samples. **B)** Comparison of hypoxia and HBV positive samples regulated genes, sorted against hypoxic samples.

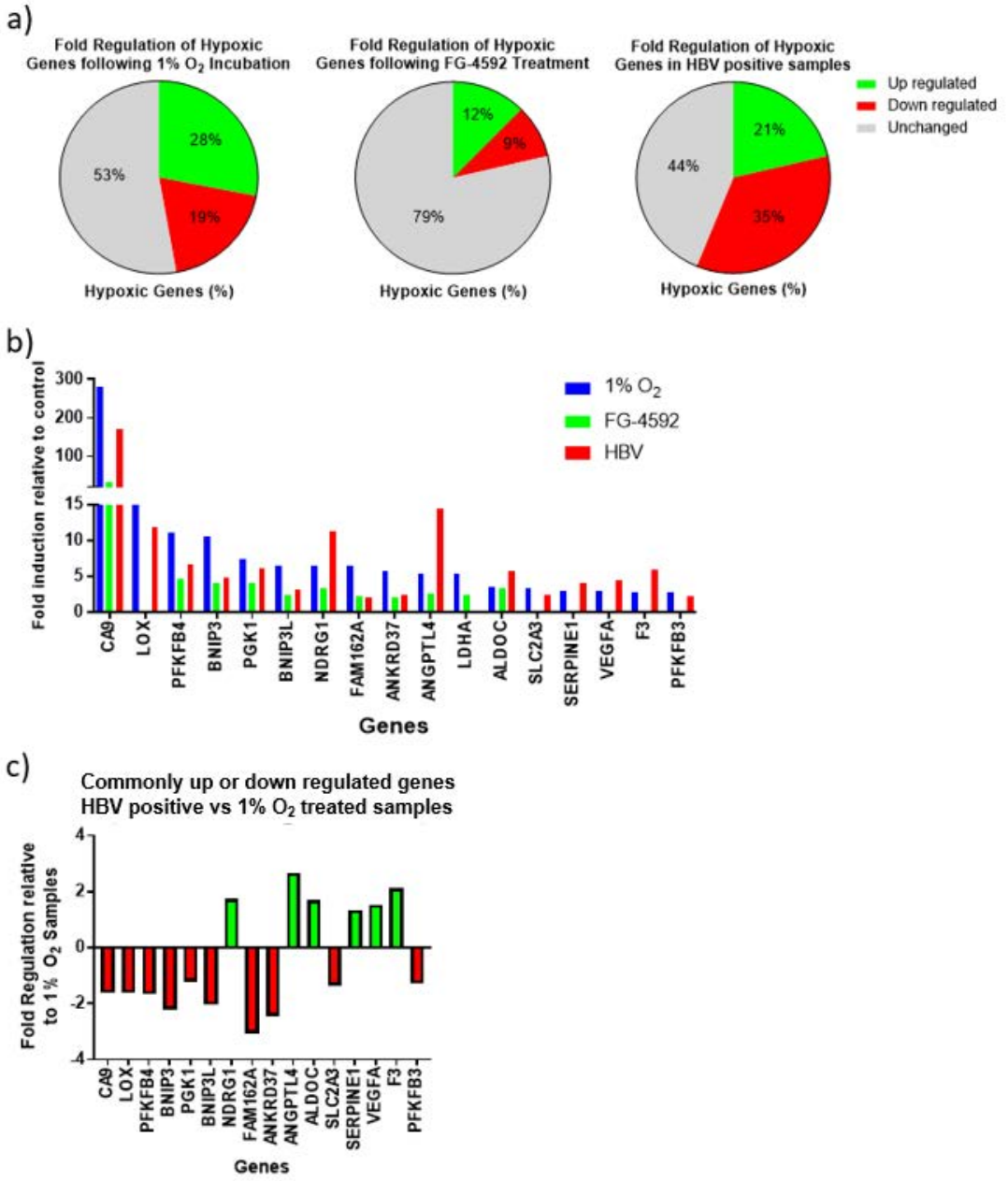

Figure 4.8 Comparing HIF transcript activity in HBV positive versus drug stabilised HIF

HepG2-NTCP K7 cells were treated with FG-4592 (10µM) under 20% oxygen for 24 hours or placed into 20% or 1% oxygen for 24 hours untreated. HepG2.2.15 cells were placed under 20% oxygen for 24 hours. **A)** Comparison of fold regulation between sample conditions. **B)** Comparison of up-regulated genes ordered highest to lowest using 1% oxygen controls. **C)** Comparison of fold difference in up-regulated genes for HBV positive and 1% oxygen samples.

4.5 HIF stabilisation in de novo infections

After demonstrating HIF stability and downstream pathway stimulation in HepG2.2.15 cells, we decided to model HBV low oxygen responses using more authentic *de novo* infection protocols. In the previous chapter we demonstrated HIF kinetics in Huh-7 and HepG2 cells; however, gold standard HBV infection protocols currently use HepG2-NTCP K7 cells that over express the viral entry receptor NTCP. Our initial experiments analysed HIF expression in HepG2-NTCP K7 cells under 20% and 1% oxygen over a 72 hour time course (**Figure 4.9a**). This result demonstrated a similar pattern of expression observed in previously tested cell lines. In addition, we examined the kinetics of HRE activation using the HRE-Luc reporter assay (**Figure 4.9b**). This cell line demonstrated a peak of HRE activity after 24 hours under 1% oxygen, which decreased by 72 hours, matching HIF protein expression. Following a *de novo* infection we examined the expression of HIF-1α and HIF-2α after 24 hours exposure to 20% and 1% oxygen conditions (**Figure 4.9c**), this result demonstrated that HBV stabilises HIFs under both oxygen tensions, although inhibition of the degradation pathway under 1% oxygen clearly demonstrated increased expression.

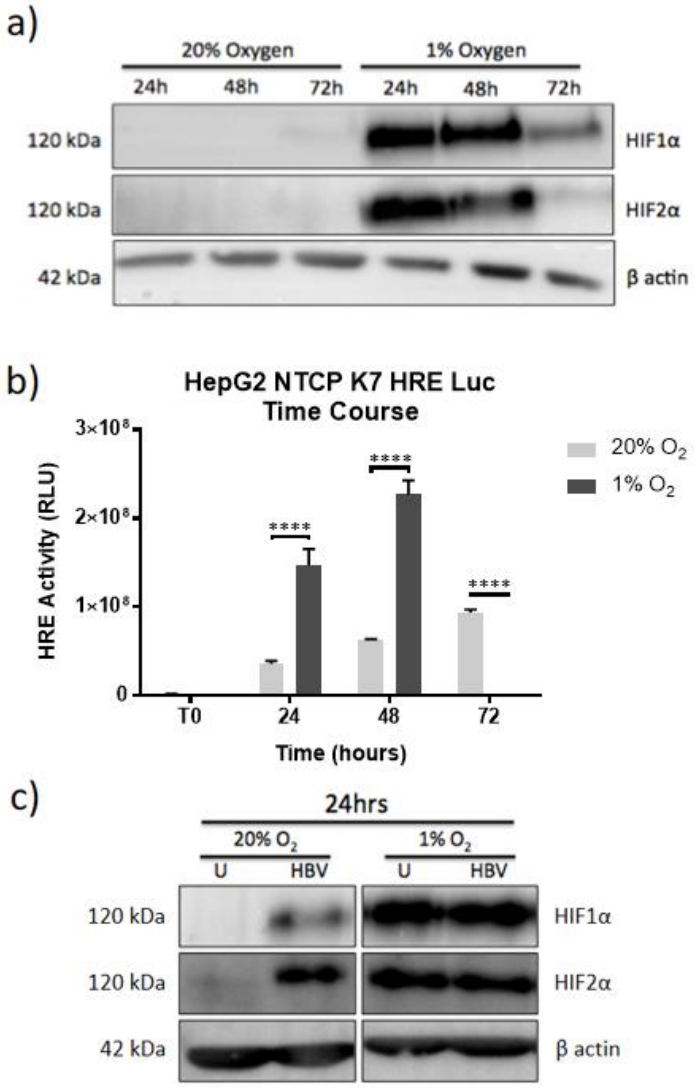

Figure 4.9 HIF kinetics in HepG2-NTCP K7 cells and de novo HBV stabilisation of HIFs

HepG2-NTCP K7 cells were either untransfected (**A**) or transfected with HRE-Luc reporter (**B**). Cells are incubated at 20% or 1% oxygen for 24 hours post transfection. Cells are lysed every 24 hours, over 72 hours with 8M Urea lysis buffer or 1x luciferase lysis buffer for Western blotting (**A**) and HRE-Luc reporter assay (**B**). Multiple t tests (* = P<0.0001). **C)** Western blot demonstrating HIF stabilisation under 20% and 1% oxygen in HBV *de novo* infection. Infected cells are placed under 20% or 1% oxygen over 24 hours. Data represents the means of 6 biological repeats. Error bars show SE of 18 technical repeats.

Following demonstration of HIF stabilisation by HBV infection we examined the effect of infection on HIF transcript expression and HRE activation (**Figure 4.10a,b**). These results demonstrate that infection increases the expression of HIF-1α and VEGF mRNA levels relative to uninfected cells (**Figure 4.10a**). Following these results we examined the expression of CA9 during HBV infection over a 72 hour time course (**Figure 4.10b**). This result demonstrated an increased expression under 20% and 1% oxygen in HBV infected samples, although the difference was only significant at the 1% oxygen tension. This result combined with the previous demonstration of up-regulated hypoxic genes in HepG2.2.15 cells prompted examination of the hypoxic gene expression profile during *de novo* infections (**Figure 4.11b**). We examined the expression of HIF transcripts during early HBV infection by preparing RNA at 24h and 72h post infection. The experiment was performed in this way to compare the response to uninfected HepG2-NTCP K7 cells without adding stress from an extended HBV infection. This result indicated that activation of HIF transcripts occurs after only 24 hours of infection. Interestingly the pattern of expression changes between 24 and 72 hours of infection, suggesting changes in HBV lifecycle. A comparison of gene profiles at 24 and 72 hours demonstrated a profile of up-regulated genes change over time during early infection (**Figure 4.12**). Additionally we compared the levels of up-regulation against 1% oxygen controls from this experiment and HepG2.2.15 results demonstrated in (**Figure 4.6**) in a table (**Supplementary Table 8.1**). The differences noted in this table could reflect the stage of the HBV lifecycle over time and the difference between episomal DNA in the *de novo* infection and integrated HBV genomes in HepG2.2.15 cells.

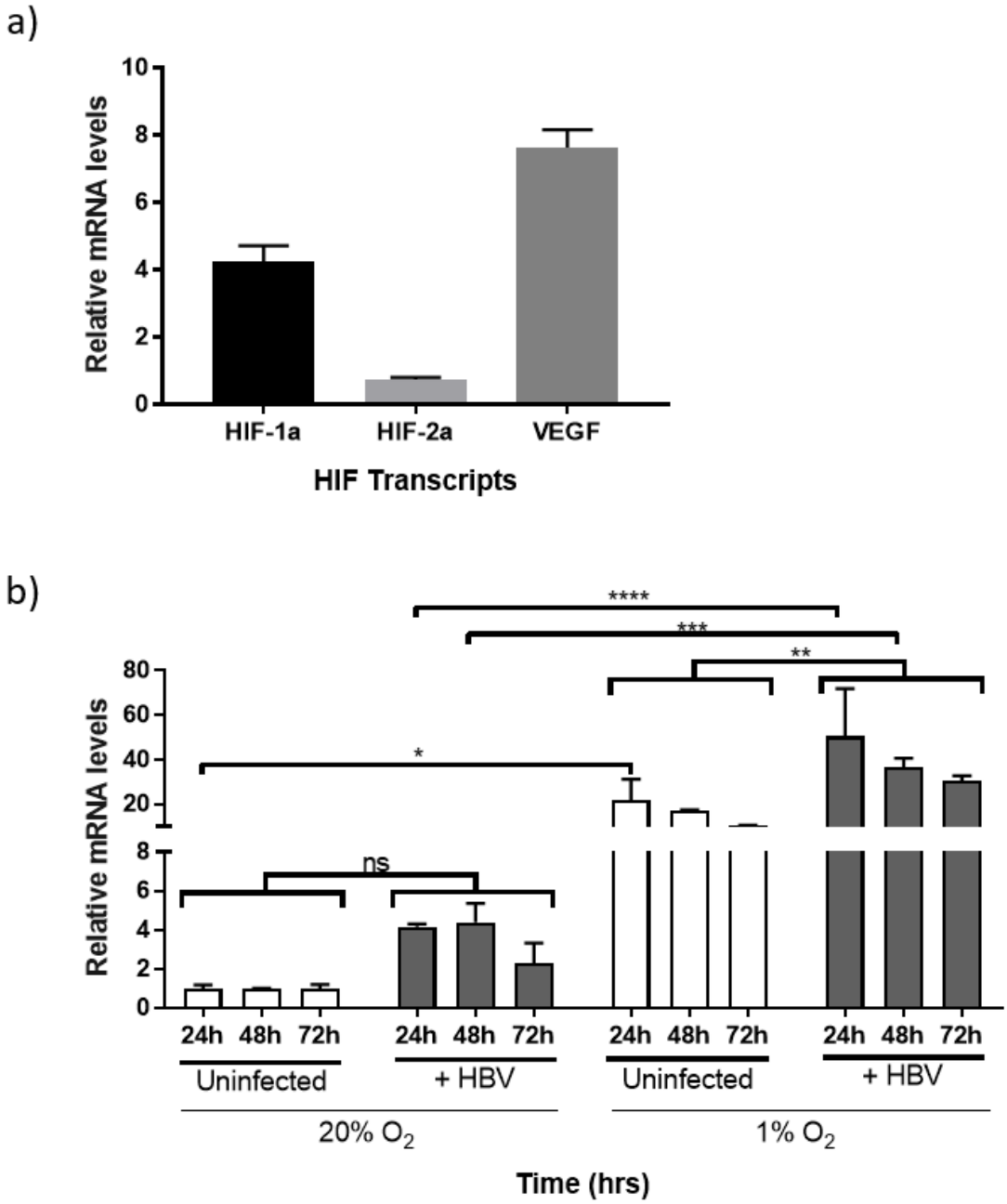

Figure 4.10 HIF transcriptional activity in de novo HBV infection

HepG2-NTCP K7 cells were infected with HBV (MOI 100) over 24 hours. **A)** PCR result demonstrating HIF-1α, HIF-2α and VEGF mRNA expression relative to uninfected controls. **B)** Cells are placed under 20% or 1% oxygen over 72 hours. Graph represents CA9 induction in uninfected and HBV infected cells under 20% and 1% oxygen, Two-Way ANOVA with Tukey's multiple comparison's test. Each graph shows the means of 2 biological repeats. Error bars show SE of 6 technical repeats. Analyses performed using Multiple T Tests (A) and Two-Way ANOVA with Tukey's multiple comparison's test (B).

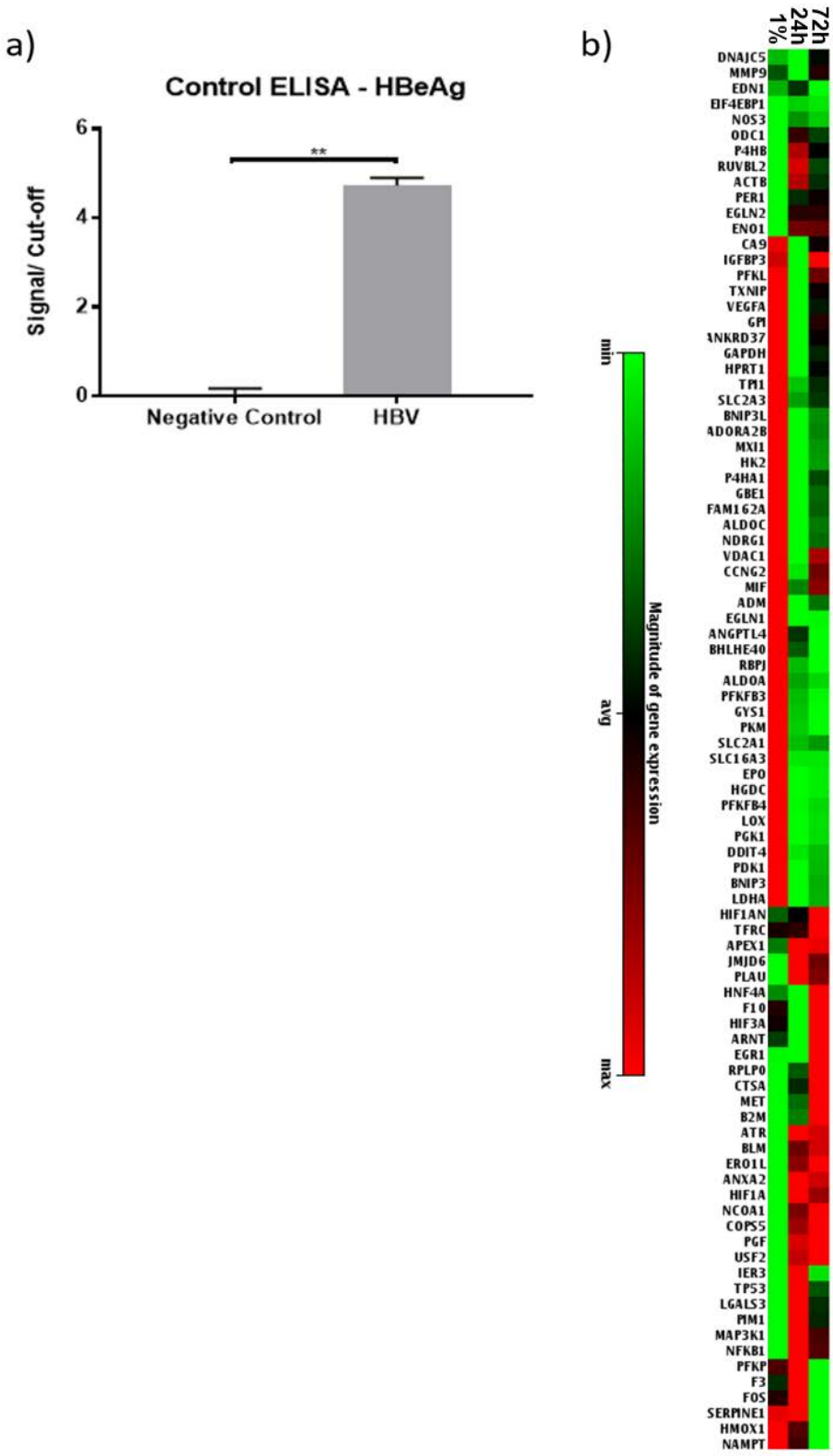

Figure 4.11 De novo HBV infection and HIF transcript activity

Legend on following page.

Figure 4.11 De novo HBV infection and HIF transcript activity (Cont.)

HepG2-NTCP K7 cells were differentiated over 72 hours in 2% DMSO and then infected with HBV (MOI 100). Uninfected cells are seeded 1 day post infection. **A)** Supernatants were collected after 24 hours. Graph represents HBeAg ELISA result to demonstrate successful infection, Unpaired t test (P 0.0014), Error bars show SD of 3 technical repeats. **B)** Samples are lysed 24 and 72 hours post infection for Qiagen RT2 hypoxic gene PCR array. Heatmap was generated by Qiagen RT2 software.

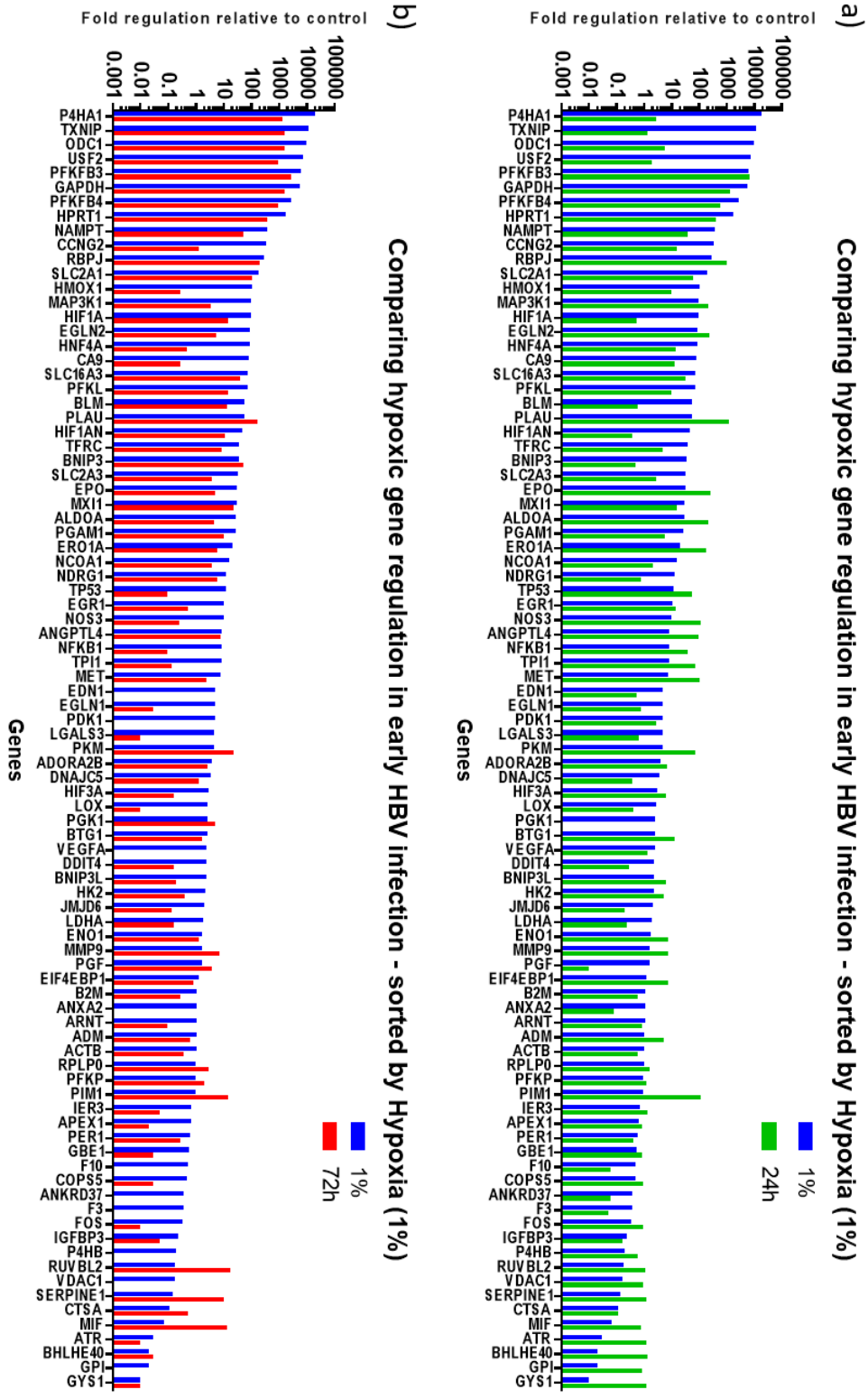

Figure 4.12 Comparisons of de novo infection time points on HIF transcript activity

Legend on following page.

Figure 4.12 Comparisons of de novo infection time points on HIF transcript activity (Cont.)

HepG2-NTCP K7 cells were differentiated over 72 hours in 2% DMSO and then infected with HBV (MOI 100). Uninfected cells are seeded 1 day post infection. **A)** Graph representing HBV samples 24h post-infection compared against hypoxic controls. **B)** Graph representing HBV samples 72h post-infection compared against hypoxic controls.

4.6 Studying HBV-HIF interaction

Having demonstrated that HBV can stabilise HIF and that it is transcriptionally active, we were interested to know whether the viral genome contained any putative HIF binding sites. We identified a conserved HRE binding motif 38 bases upstream from the EnhI and X promoter region that was conserved in diverse HBV genotypes (**Figure 4.13a**). This provided a potential point of direct interaction between the HBV genome and HIFs, we examined the binding of HIF-1α using chromatin immunoprecipitation (ChIP) in combination with a specific HIF-1α antibody, HepG2.2.15 cells and primer pairs that spanned the entire HBV genome. We used HepG2.2.15 cells because 100% of cells contain integrated copies of the HBV genome. This experiment demonstrated an interaction between HIF-1α and the HBV genome between 1580 and 1700 nucleotides (**Figure 4.13c**); this coincides with the EnhI and X promoter regions identified in our bio-informatic screen. It is important to discuss that interaction occurs under both 20% and 1% oxygen (**Figure 4.13b**). Increases under 1% oxygen are likely due to the increased expression of HIF-1α protein under low oxygen, that occurs through normal inhibition of the cellular degradation pathway as observed in **Figure 4.9c**. This data represents relative binding to the HBV genome compared against a non-specific antibody control. We utilised primers against SEMA4B that is known to bind HIF-1α as a positive control for successful chromatin immunoprecipitation of HIF-1α (**Figure 4.13c**) (Schodel *et al*., 2011).

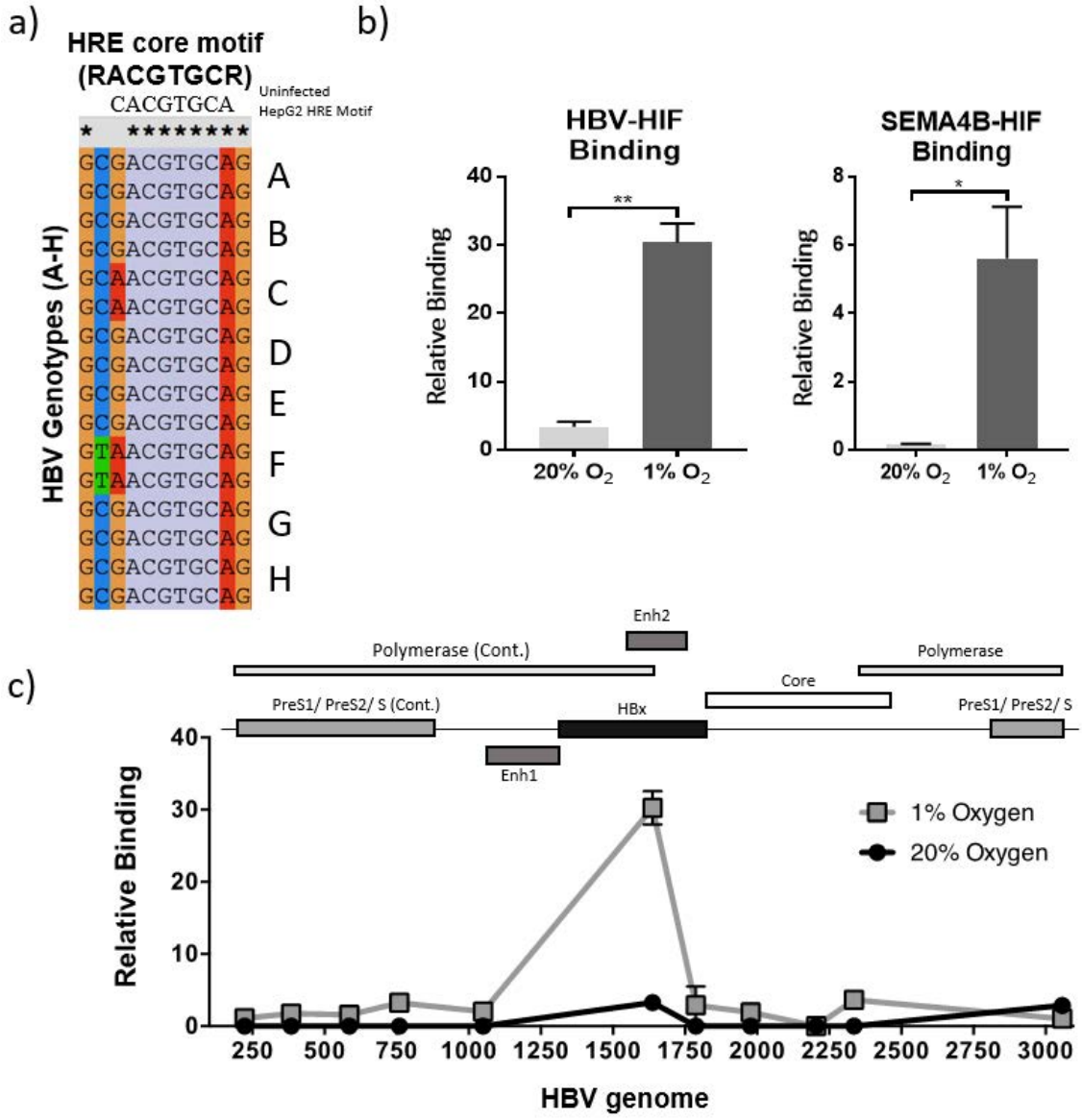

Figure 4.13 Conserved HIF binding site within the HBV genome

HepG2.2.15 cells were placed under 20% and 1% oxygen for 24 hours and used to generate samples for ChIP using the protocol found in section 2.12. **A)** GenBlast search of selected region demonstrates conserved HRE core motif in all HBV genotypes. **B)** Graphs demonstrating HBV-HIF binding and SEMA4B-HIF binding under 20% and 1% oxygen. **C)** PCR results for primers that span HBV genome, graph demonstrates that HIF-1α binds to HBV genome. Data represents means of 2 biological repeats. Error bars show SE of 3 technical repeats. Data analyses performed using Unpaired t test with Welch's corrections (B).

4.7 Discussion

In the previous chapter we established tools for studying low oxygen effects on hepatoma cells. This chapter aimed to examine the effect of HBV infection on the host transcription factor HIF. As discussed, the literature reports an association between HBx and HIF-1α and HIF-2α (Liu *et al*., 2014, Kim, 2014, Yang *et al*., 2017, Hu *et al*., 2016). However, we wanted to pursue this idea further within the context of full replicating HBV. We examined the effect of HBV on HIF stabilisation using multiple models of infection, including plasmid transfections, stable HBV producer cell lines and *de novo* infections. We transfected HepG2-NTCP K7 cells with the HBV genotypes C and D. Genotype D is used frequently in the literature and was the basis for generation of both the stable producer lines. Genotype C is used for comparative purposes, and together these plasmids are used to establish that HBV can stabilize HIFs under normoxic conditions (**Figure 4.3a**). Using plasmids for Genotype D with selected deletions in the X and L genes, or containing a double knock out of X and L showed that HBV stabilisation of HIFs is not dependent on HBx (**Figure 4.4a**). Additionally, this data suggests that the L protein is not involved, this has previously been implicated in facilitating interaction between MDR1 and HBV through HIF-1α (Li *et al*., 2017). Despite demonstrating that HBx and large surface antigen are not essential for HBV HIF stabilisation, there are other HBV proteins that could be involved, perhaps the Core protein. Alternatively, HIF stabilisation could occur as a stress response to HBV infection, which the virus exploits, this however is speculation.

Using a plasmid to express HBx enabled a comparison against the X-minus Genotype D plasmid. Transfection of this plasmid alone under normoxic conditions failed to stabilise HIFs (**Figure 4.4b**). Of course, this does not mean there is no interaction with the HIF pathway; HBx can apparently transactivate a wide range of episomal reporters

by targeting Smc5/6 for degradation.We examined HBx and HRE co-transfections in hepatoma cells following exposure to both 20% and 1% oxygen (**Figure 4.4c**). This demonstrated no significant change in relative HRE activity when compared to HRE alone; this suggests that the pHBx was not functionally active with our reporter (**Figure 4.4d**) However, it is important to note that we were unable to confirm HBx expression in our lab via Western blotting following transfection due to time limitations, instead we relied on HBx reporter activity provided by our collaborators (data not shown). This means that a lack of HRE effect could be due to a lack of HBx protein expression. Previous literature suggests that HBx potentiates HIF stability and increases transcriptional activity following HIF stabilisation under low oxygen (Yoo *et al*., 2003, Liu *et al*., 2014). This data suggests that HBx effects on HIF transcriptional activity could be further downstream in the HIF response pathways rather than a direct interaction with HIF and HRE binding sites.

We confirmed these results using HepG2.2.15 and HepAD38 HBV producer cells by demonstrating HIF stabilisation over a 72 hour time course (**Figure 4.5**). A comparison of CA9 and VEGFA expression under 1% oxygen relative to normoxic controls in HepG2-NTCP K7 and HepG2.2.15 cells (**Figure 4.5**) demonstrated that HBV positive cells expressed higher relative HIF transcript expression. CA9 and VEGFA are both strongly induced by hypoxia (Olive *et al*., 2001, Lin *et al*., 2004) and are therefore commonly used as markers for HIF transcription. In addition, they are associated with poor therapeutic outcomes in cancers because they promote cancer cell survival (McIntyre *et al*., 2012, Ledaki *et al*., 2015). CA9 catalyses the reversible hydration of carbon dioxide and in cancers this enables the maintenance of neutral pH within the tumour microenvironment (Ledaki *et al*., 2015). VEGFA induces angiogenesis and vasculogenesis, which helps oxygenate the tumour microenvironment, promotes cell

migration and inhibits apoptosis (Yang *et al*., 2009, Matsumoto *et al*., 2005). Importantly, a study in our laboratory has shown that CA9 is highly up-regulated in HBV associated HCC and correlates with poor prognosis (Jane McKeating personal communication). This suggests that HBV up-regulated CA9 and VEGFA expression observed in our experiments could be contributing to eventual development of HCC.

We demonstrated that HepG2.2.15 cells under 20% oxygen increase the expression of multiple genes using the hypoxic gene array (**Figure 4.6**). When comparing the profile against uninfected cells under 1% oxygen, we demonstrated differential expression of multiple genes (**Figure 4.7**), whereas FG-4592 treatment exhibits a similar profile for gene expression, but the level of induction is reduced. Interestingly, FG-4592 produces a different response in HepG2 cells when compared against Huh-7 cells, which demonstrated expression beyond 1% oxygen controls. HepG2.2.15 cells do specifically demonstrate increased up-regulation of numerous genes involved in regulating cell growth, proliferation, apoptosis and cellular metabolism often as part of stress responses, examples include; DNA damage-inducible transcript 4 protein (DDIT4) (Sofer *et al*., 2005), N-Myc Downstream Regulated 1 protein (NDRG1) (Kovacevic and Richardson, 2006), Angiopoietin like 4 (ANGPTL4) (Zhu *et al*., 2011) and 6-phosphofructo-2-kinase/ Fructose-2,6-Bisphosphatase 3 (PFKFB3) (Kim *et al*., 2006b) (**Figure 4.7**). These results demonstrate that HBV is stimulating expression of multiple HIF associated genes. However, many of the genes that are up-regulated are stress response genes and could be increased in response to an HBV infection.

We performed a test of HepG2-NTCP K7 cells normal low oxygen responses using Western blotting and the HRE-Luc reporter before further experimentation (**Figure 4.9**). This result demonstrated HIF protein expression from 24 to 72 hours and HRE activation under 1% oxygen at 24 and 48 hours. We observed an increasing activation

of HRE over the 72 hour time course under 20% oxygen, despite declining protein expression. This could be due to cellular stress and activation of the stress response pathways independent of HIFs. Alternatively, the luminometer can detect bright luciferase signals in adjacent wells if the signal is particularly bright. The bars observed at 20% oxygen could be a result of bleeding signal from the 24 and 48 hour signals at 1% oxygen.

Next, we examined the effect of *de novo* infections on HIF stabilisation. HBV infection stabilises HIF-1α and HIF-2α; however, expression was further increased under 1% oxygen. We examined HBV infection effects on downstream HIF transcript expression by demonstrating an increase in HIF-1α, HIF-2α, and VEGFA mRNA levels relative to uninfected cells (**Figure 4.10a**). A time course of CA9 expression in uninfected and HBV infected samples demonstrated that HBV causes an increase in activation under 20% oxygen and 1% oxygen but this is not a significant difference under either condition (**Figure 4.10b**). We examined the effect of *de novo* infections on hypoxic gene expression using the hypoxic gene array (**Figure 4.11**), this result demonstrated expression profiles for early *de novo* infections at 24 and 72 hours post infection. Interestingly, there is a change in the expression of up-regulated genes between 24 and 72 hours. Perhaps reflecting a different stage of the HBV lifecycle. Early infection involves the translocation of rcDNA to the nucleus and formation of cccDNA before transcription of pgRNA begins. This process has been discussed in more detail in the main introduction (**section 1.2.4**). Alterations in gene expression at this time suggest that different stages of the HBV lifecycle differentially regulate HIF expression. Following this result, we tested whether HIF-1α interacted with HBV using anti-HIF-1α targeted chromatin immunoprecipitation (**Figure 4.13a,c**). This result demonstrated that HIF-1α is interacting directly with the HBV genome at an HRE site located within

the EnhI/X promoter region; this result has not been shown previously and has some interesting implications, this suggests that HIF-1α may be directly involved in regulating HBV transcription. Combined, these data provide justification for examining the effect of HIFs and low oxygen on HBV replication.

4.8 Summary

This chapter presents results that establish the effect of HBV infection on HIF stabilisation and transcript activity in two model systems. In addition, these results demonstrate a direct interaction between HIF-1α and the HBV genome. The results obtained here provide a model for understanding HBV-HIF interactions and a justification for further study into low oxygen effects on HBV replication.

5. EXAMINING THE EFFECT OF LOW OXYGEN ON HBV REPLICATION

5.1 Introduction

In the previous chapter we demonstrated that HBV infection stabilised HIF expression and associated transcriptional activity. Furthermore, we showed evidence that HIF binds the viral genome under low oxygen conditions, suggesting a direct role for this transcriptional activator to positively regulate viral replication at the transcriptional level. We noted that HBV infected cells showed increased HIF expression under low oxygen, suggesting additive pathways stabilising HIFs. In this chapter, we investigated the effect of low oxygen on viral specific transcription and replication. HBV transcription is dependent on host cellular transcription factors that bind defined motifs within the promoter and enhancer elements, as represented in **figure 5.1** (Quasdorff and Protzer, 2010). These interactions have been discussed in detail in the main introduction (**section 1.2.5.2**).

In this chapter, we examined the effect of low oxygen on HBV promoter activity using a panel of transcriptional reporter assays (Kim *et al*., 2016, Ko *et al*., 2014) depicted in **figure 5.2.** We followed these studies with experiments to examine the effect of low oxygen on HBV replication using both HepG2.2.15 cells and *de novo* infections to confirm these results in a more authentic infection model (**Figure 5.3**). Finally, we examined the HIF dependency of the effect of low oxygen on HBV replication using siRNAs and the HIF pathway inhibitor NSC.

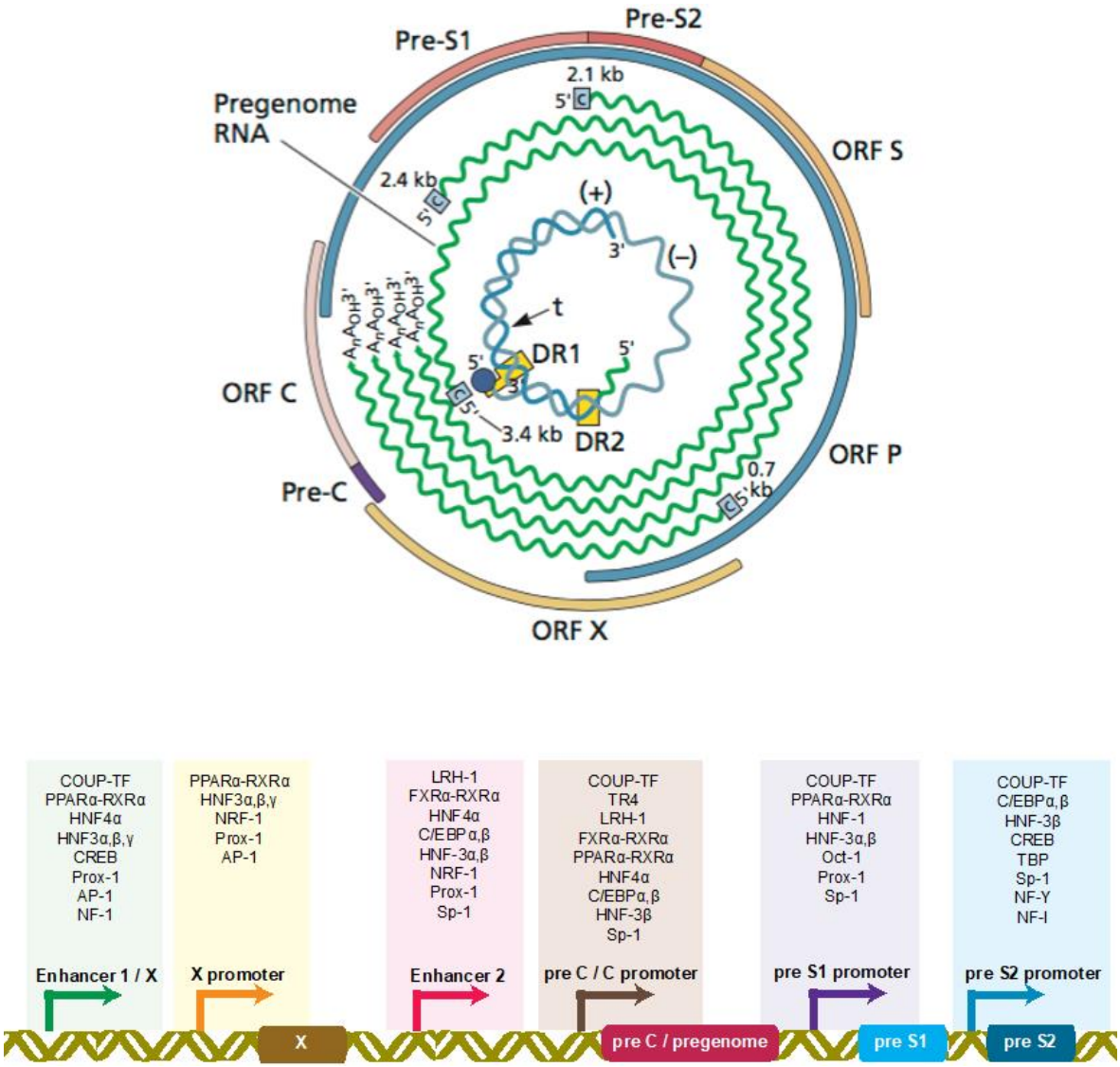

Figure 5.1 HBV genome representations and transcription factor interactions (Lai, A. 2017)

(Top) Schematic representation of HBV partially double-stranded circular genome including open reading frames (ORFs), direct repeats (DR1 and DR2) and viral RNAs. (Bottom) Cartoon representation of linear HBV genome including promoter and enhancer regions, displaying host transcription factor interaction sites.

Results

5.2 Effect of low oxygen on HBV promoter activity

Following the ChIP result in the last chapter, it is clear that HIF-1α interacts with the HBV genome in HepG2.2.15 cells. The HRE site is located close to the X promoter region. This suggests that the host transcription factor interacts with HBV promoters and could stimulate activity. We used the HBV promoter constructs to investigate this further. Following transfection, the cells are placed under normoxic and hypoxic conditions and samples are collected every 24 hours over a 72 hour time period (**Figure 5.2**). These results indicate that low oxygen increases the activity of all promoter constructs. The EnhI/ HBx promoter demonstrated increases under 1% oxygen at all time points, however the only significant difference is observed after 72 hours (**Figure 5.2c**). In comparison, all of the other three HBV promoters demonstrate a significant increase relative to normoxic controls at all time points (**Figure 5.2b,d,e**), demonstrating that low oxygen up-regulates HBV promoter activity. In addition we see significant increases in promoter activity between 24-48 and 24-72 hours (**Figure 5.2b,d,e**). To assess the dependency of the transcription reporters on low oxygen we investigated the effect of HIF stabilising drugs FG-4592 and VH298 previously described in chapters 3 and 4. Following transfection, the cells were either treated with FG-4592 or VH298 and cultured under normoxia.

Our results demonstrate that HIF stabilising drugs increase HBV promoter activity (**Figure 5.3**) significantly compared to 20% oxygen controls. Treatment with VH298 produces similar levels of up-regulation to incubation under 1% oxygen in each of the promoters; whereas treatment with FG-4592 results in a significant increase (**Figure 5.3a-d**). These results were obtained alongside HRE-Luciferase reporter control

demonstrating increased HRE activity under each condition (**Figure 5.3e**). Relative expression of promoter activity against normoxic controls demonstrated that each of the promoters is increased through treatment with FG-4592 and VH298 (**Figure 5.3f-g**). However, under each condition, we saw significantly higher up-regulation of the EnhI/ X promoter activity. This coincided with the ChIP data and suggested that HIF-1α binding caused increased promoter activity. Interestingly, HRE is only present with EnhI/X promoter and yet all promoters show a boost under low oxygen, suggesting direct and indirect effects.

Following these results, we investigated whether viral transcriptional activity is HIF-dependent by co-transfecting promoter plasmids with HIF1a and HIF2a expression vectors. Since over-expression of wild-type HIFs under normoxic conditions are targeted for proteosomal degradation we expressed HIFs containing a double proline mutation within their ODD domains that are stably expressed under normoxia (**Figure 5.4a,b**). We noted increased expression of the double proline HIF mutants and associated activation of HRE-Luc reporter. We therefore investigated the effect of the double proline HIF mutants on HBV reporter activity and observed that EnhI/ X and EnhII/ BCP promoters are significantly increased by co-expressing HIF1α and HIF2α (**Figure 5.4c-f**). Interestingly, the S1 and S2 promoters appear to be primarily regulated by HIF2α, with significant increases observed in promoter activation following co-transfection (**Figure 5.4e,f**). Together these results demonstrate a role for low oxygen and HIFs to up-regulate HBV promoter activity.

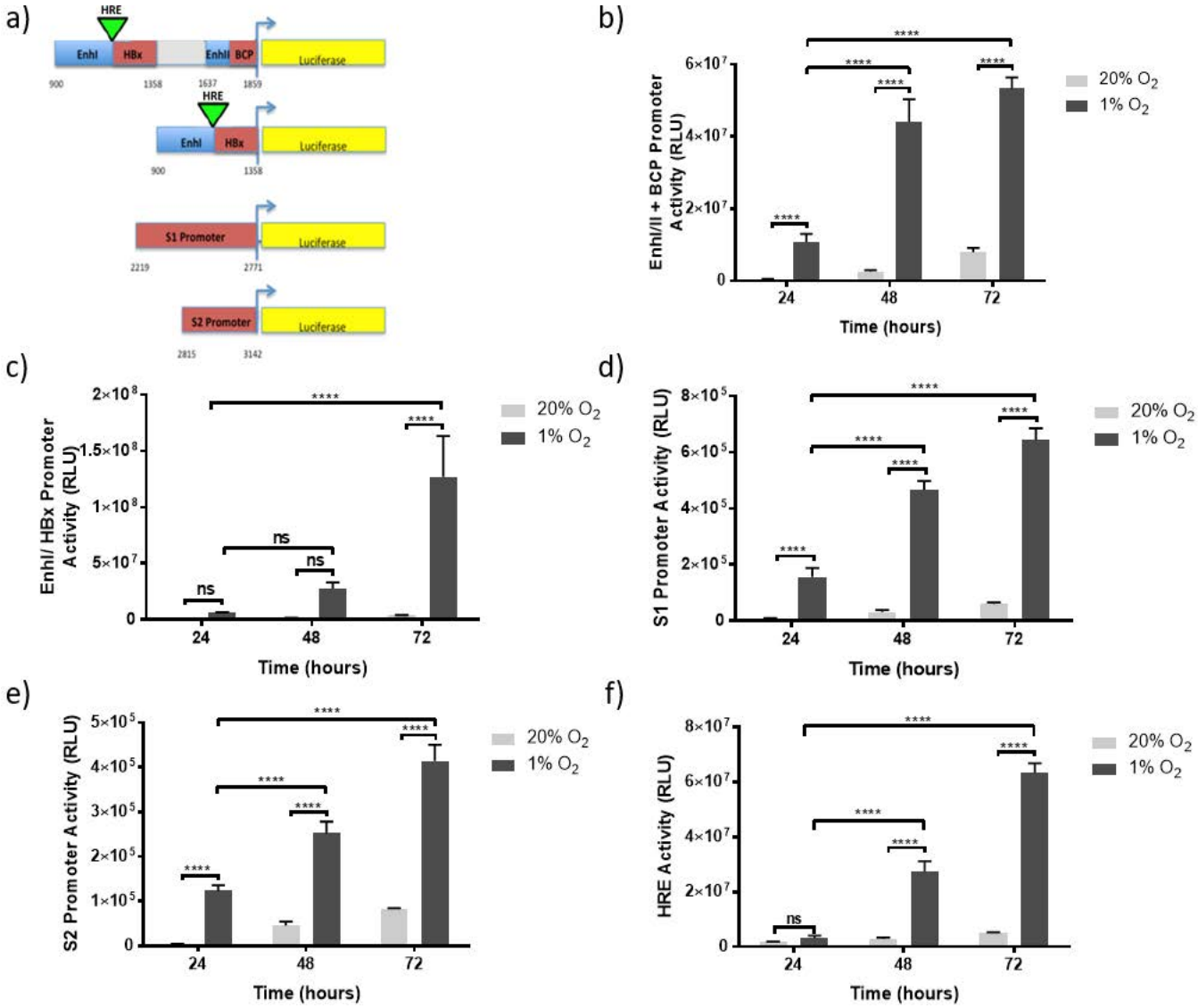

Figure 5.2 HBV promoter activity under 1% oxygen over time

A) HBV reporter constructs for studying promoter activity. From top to bottom: Enhancer 1 and Enhancer 2 with the basal core promoter (EnhI/ II + BCP); Enhancer 1 and HBx (EnhI/ HBx); S1 promoter and S2 promoter. HepG2-NTCP K7 cells were transfected with HBV-promoter-luciferase reporters, after transfection the cells were re-seeded into 96 well plates and placed into hypoxic or normoxic conditions. **B)** Raw RLU values for EnhII/ BCP promoter activation over 72 hours. **C)** Raw RLU values for EnhI/ X promoter activation over 72 hours. **D)** Raw RLU values for S1 promoter activation over 72 hours. **E)** Raw RLU values for S2 promoter activation over 72 hours. **F)** Raw RLU values for HRE activation over 72 hours. Each graph shows the means of 4 biological repeats. Error bars show SE of 12 technical repeats. Data analyses using Two-Way ANOVA with Tukey's multiple comparison's test.

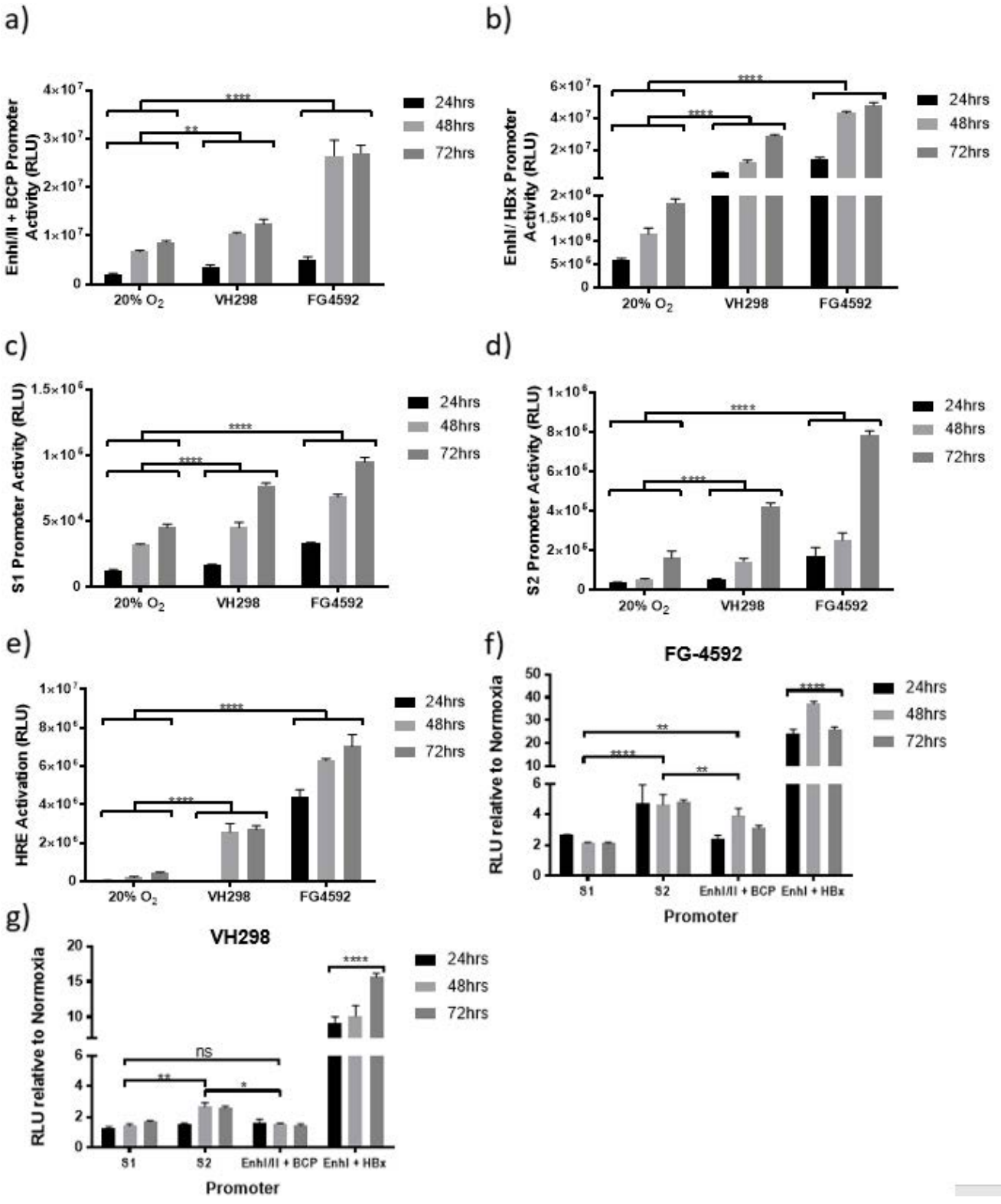

Figure 5.3 HBV promoter activity and HIF stabilising agents

Legend on following page.

Figure 5.3 HBV promoter activity and HIF stabilising agents (Cont.)

HepG2-NTCP K7 cells were transfected with HBV-promoter-luciferase reporters, after transfection the cells were re-seeded into 96 well plates. The cells were then placed into 20% or 1% oxygen. Normoxic samples are either treated with VH298 (100μM) or FG-4592 (1μM) or left untreated. **A)** Raw RLU values for EnhII/ BCP promoter activation over 72 hours. **B)** Raw RLU values for EnhI/ X promoter activation over 72 hours. **C)** Raw RLU values for S1 promoter activation over 72 hours. **D)** Raw RLU values for S2 promoter activation over 72 hours. **E)** Raw RLU values for HRE activation over 72 hours. **F)** Relative activation of HBV promoters following FG-4592 treatment relative to normoxic controls. **G)** Relative activation of HBV promoters following VH298 treatment relative to normoxic controls. Each graph shows the means of 4 biological repeats. Error bars show SE of 12 technical repeats. Data analysed using Two-Way ANOVA with Tukey's multiple comparisons test

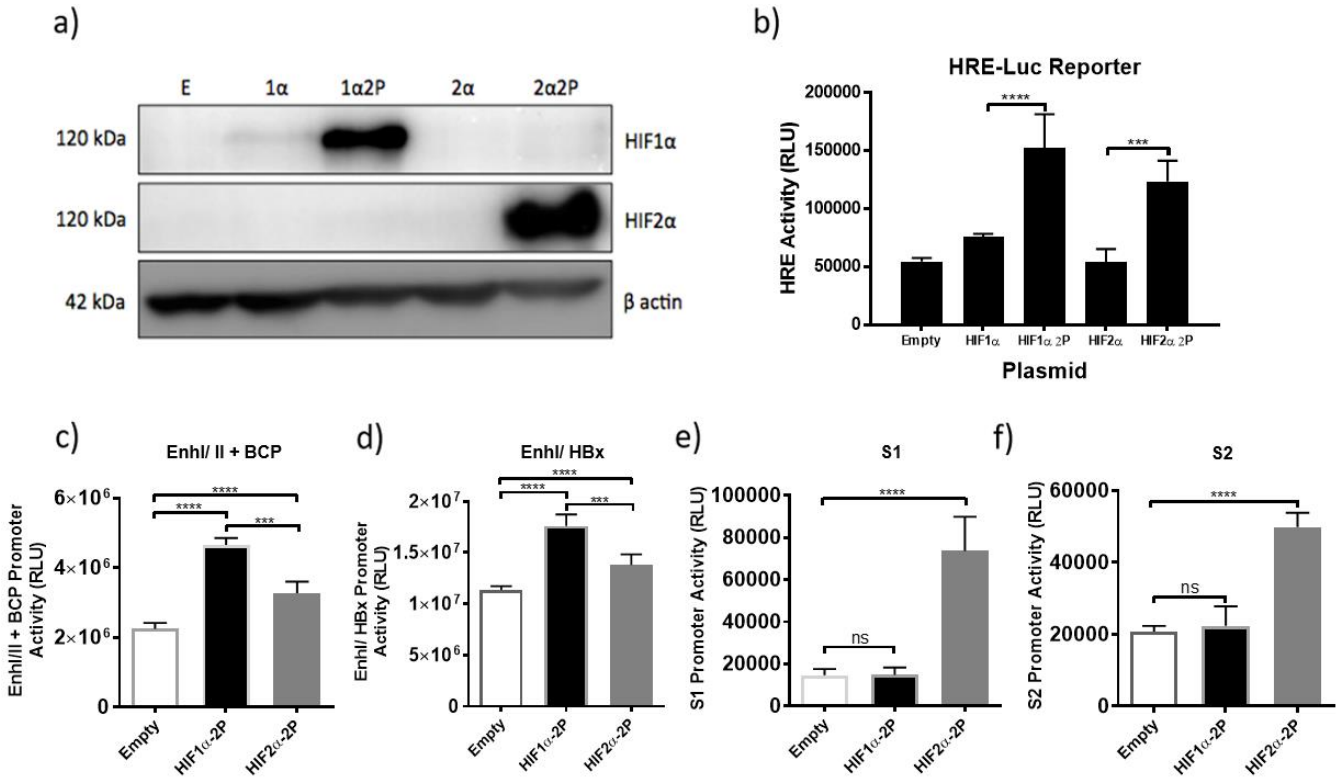

Figure 5.4 Effect of HIF on HBV promoter activity

HepG2-NTCP K7 cells were transfected with pHIF-1α, pHIF-2α, pHIF-1α-2P or pHIF-2α-2P. **A)** Western blot demonstrating HIF over expression under normoxic conditions. **B)** HRE-Luc reporter and the HIF over expression plasmids. **C-F)** HepG2-NTCP K7 cells were co-transfected with an HBV-Luc reporters EnhI/II + BCP (**C**), EnhI/ HBx (**D**), S1 (**E**), S2 (**F**) and the HIF over expression plasmids (double proline mutants); following transfection the cells were reseeded into 96 well plates. Each graph shows the means of 2 biological repeats. Error bars show SE of 6 technical repeats. Data analysed with One-Way ANOVA with Tukey's multiple comparison's test.

5.3 Effect of low oxygen on HBV replication

To investigate the effect of low oxygen on HBV replication we quantified viral pgRNA, rcDNA and cccDNA by PCR. Low oxygen increases HBV pgRNA over a 72 hour time course, with significant increases observed after 48 and 72 hours (**Figure 5.5a**). The increased pgRNA could reflect an increase in promoter activity or an increase in template for transcription. This is important when considering the result in HepG2.2.15 cells, which contain both stably integrated viral genomes and cccDNA. Considering this we examined the expression of cccDNA and demonstrated significant increases under low oxygen (**Figure 5.5b**). This was performed alongside PCRs for HBV rcDNA, which demonstrated a similar pattern of expression, however there was only a significant difference at the 24 and 72 hour time points (**Figure 5.5c**). Interestingly this value appears to have declined from the 24 hour mark, perhaps because intracellular rcDNA has been converted into cccDNA. The pattern of rcDNA expression over 72 hours suggests a possible increased effect of reverse transcription on pgRNA to rcDNA synthesis. Using a PCR designed to amplify secreted and packaged rcDNA we observed no significant change in this parameter under 1% oxygen over any of the time points studied (**Figure 5.5d**). Taken together these results suggest that low oxygen promotes viral transcription. This could also be the result of increased transcription of pgRNA from cccDNA. The increased cccDNA levels under low oxygen could be the result of multiple pathways. Firstly, low oxygen could be increasing infectious spreading, however HepG2.2.15 cells lack NTCP and so this seems unlikely. Alternatively, this could be through an increase in the reimport of encapsidated rcDNA into the nucleus and subsequent conversion into cccDNA. Lastly, this could be the result of reduced Smc5/6 associated degradation of cccDNA through an HBx-HIF interaction.

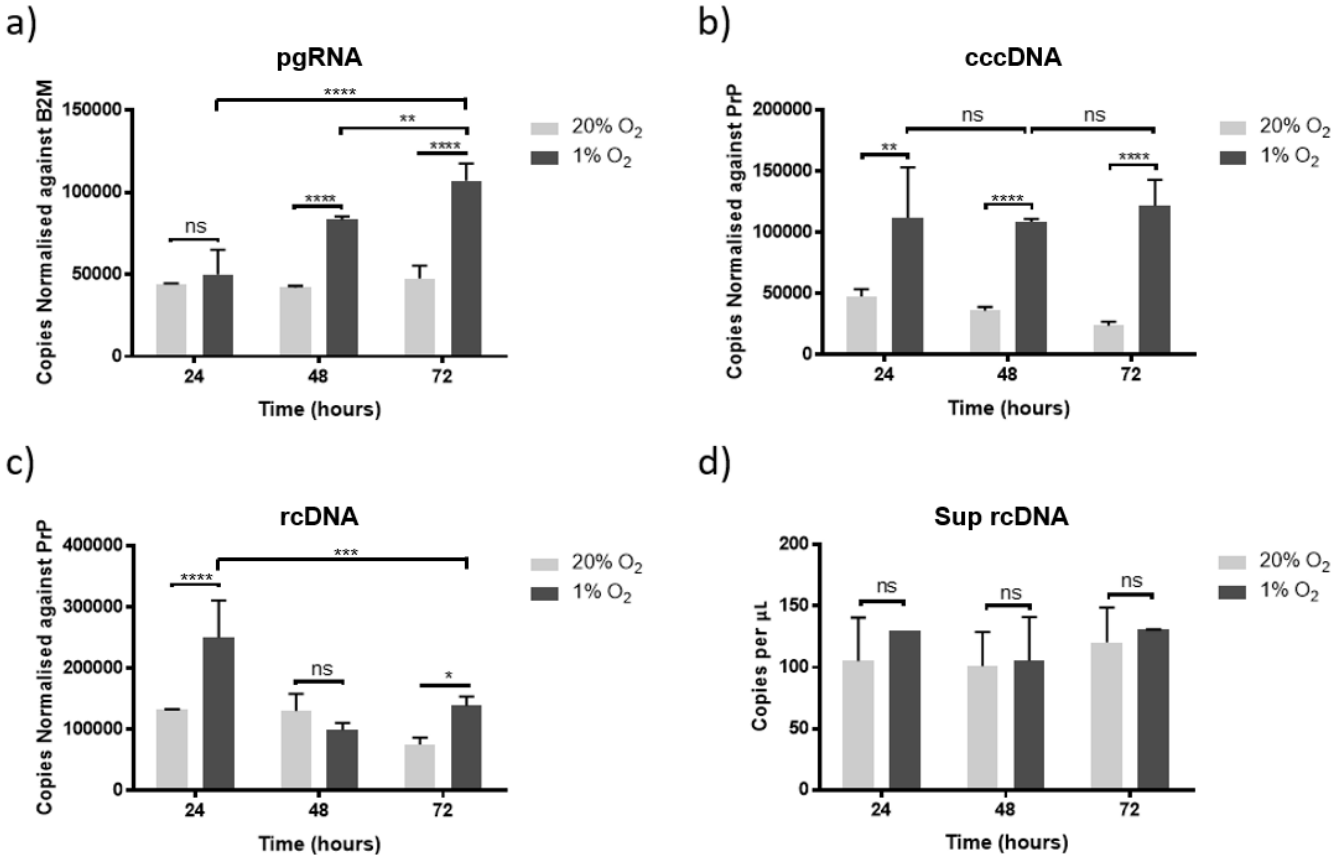

Figure 5.5 Low oxygen effects on HBV replication

HepG2.2.15 cells were placed under 20% or 1% oxygen for 24-72 hours. Samples were lysed every 24hrs for RNA and DNA preparation with RLT+ buffer, supernatants were harvested at every time point for ELISAs and extracellular HBV DNA PCR. qPCR was performed to examine HBV pgRNA **(A)**, cccDNA **(B)**, rcDNA **(C),** and supernatant rcDNA **(D).** Each graph shows means of 3 biological repeats. Error bars show SE of 9 technical repeats. Data analysed using Two-Way ANOVA with Tukey's multiple comparison's test.

5.4 Effect of hepatocellular differentiation on HBV replication under low oxygen

It is important to consider that these experiments with HepG2.2.15 cells that carry integrated copies of HBV are performed in the absence of any DMSO treatment. To confirm these observations with *de novo* infected cells it is necessary to continuously treat the cells with DMSO to establish and maintain a productive infection. Since we previously observed a blunted response to DMSO-differentiated HepG2 cells to low oxygen in terms of HIF signalling (**Figure 3.15**) we were interested to evaluate the impact of DMSO on low oxygen stimulated viral transcription.

We examined the effect of DMSO mediated differentiation on HepG2.2.15 expression of HIF and stimulatory effect of low oxygen on pgRNA and rcDNA levels using Western blotting and quantitative PCR (**Figure 5.6**). Previous studies have demonstrated that DMSO differentiation increases HBV transcription and replication at multiple stages in the viral life cycle (Verrier *et al*., 2016b, Urban *et al*., 2014). Our data showed a significant increase in HBV RNA and DNA levels under 1% oxygen (**Figure 5.6b,c**). DMSO differentiation significantly increased the expression of both pgRNA and rcDNA under normoxic conditions, however it blunts the effect of low oxygen priming of viral transcription. This demonstrated more evidence that pgRNA and rcDNA regulation are regulated by low oxygen, potentially through HIF expression which, we have previously shown is blunted under DMSO differentiation.

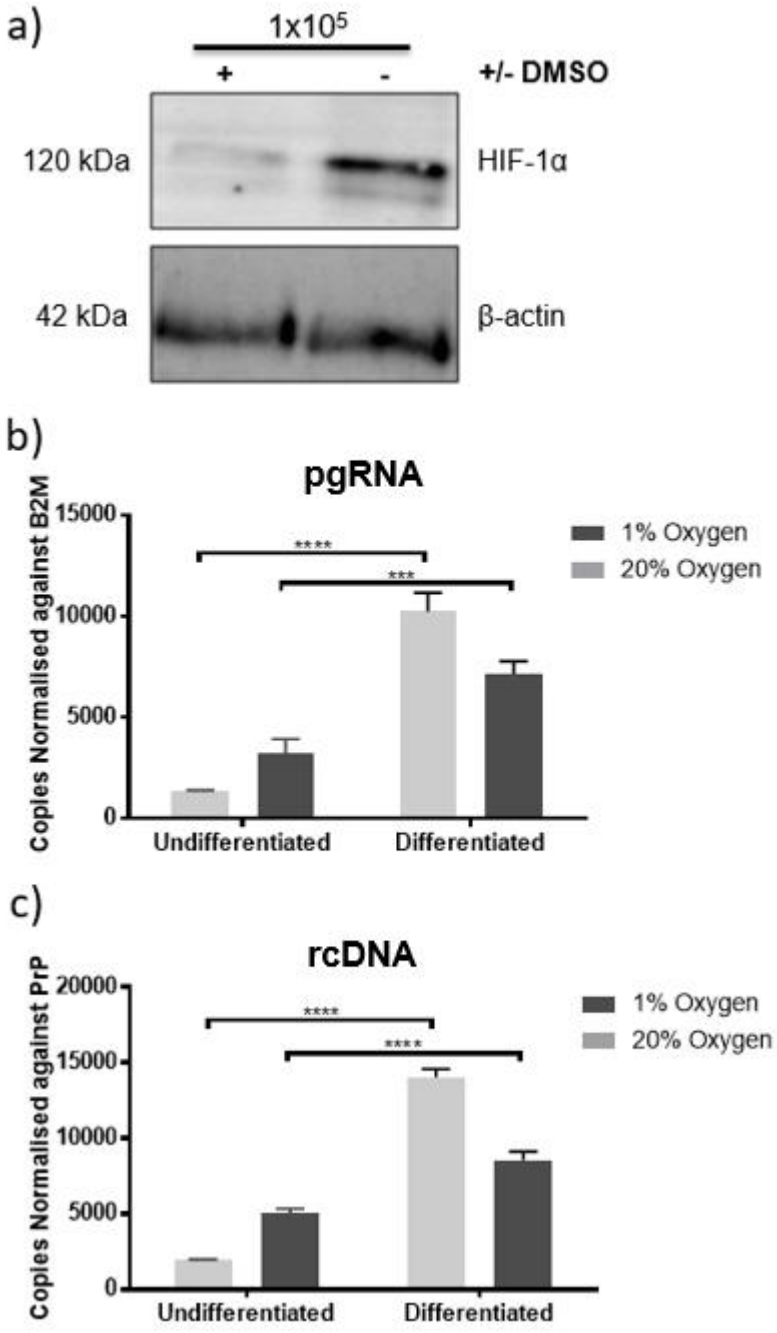

Figure 5.6 Differentiation status of HBV infected cells blunts their response to low oxygen

A) HepG2.2.15 cells were either differentiated using 2% DMSO or untreated and placed under 20% oxygen. Equal protein loading for Western blot determined by counting control wells. qPCR was used to measure HBV pgRNA (**B**) and rcDNA (**C**). Each graph shows the means of 3 biological repeats. Error bars show SE of 9 technical repeats. Two-Way ANOVA with Tukey's multiple comparison's test.

5.5 Removing DMSO from the de novo infection protocol

Considering the effect that DMSO has on HIF expression, the hypoxic gene array and on HBV nucleic acid expression, we decided it was important to remove DMSO from our infection protocols to accurately study the effect of low oxygen on HBV replication. We therefore evaluated the effect of removing DMSO from differentiated HepG2 cells on viral transcripts under normoxic and hypoxic conditions (**Figure 5.7**). Cells were treated or not with 2% DMSO for three days and differentiation media removed and replaced with DMEM. The cells were then incubated under 20% or 1% oxygen and lysed for RNA preparation every 24 hours. A T0 sample was lysed at the point of DMSO removal as a control (**Figure 5.7a**). This experiment shows that non-differentiated cells show an increase in pgRNA levels under low oxygen over 72 hours (**Figure 5.7b**). Interestingly, removing DMSO restores pgRNA expression to levels observed in un-differentiated cells. However, the levels are still elevated initially (**Figure 5.7c**). After 72 hours, we saw pgRNA levels return to those comparable with control cells in **Figure 5.7b** (**Figure 5.7c**). These results were repeated successfully, and it was demonstrated that rcDNA expression responds to DMSO treatment and removal in the same pattern (data not shown). These data provide the justification for developing a *de novo* infection protocol in the absence of DMSO.

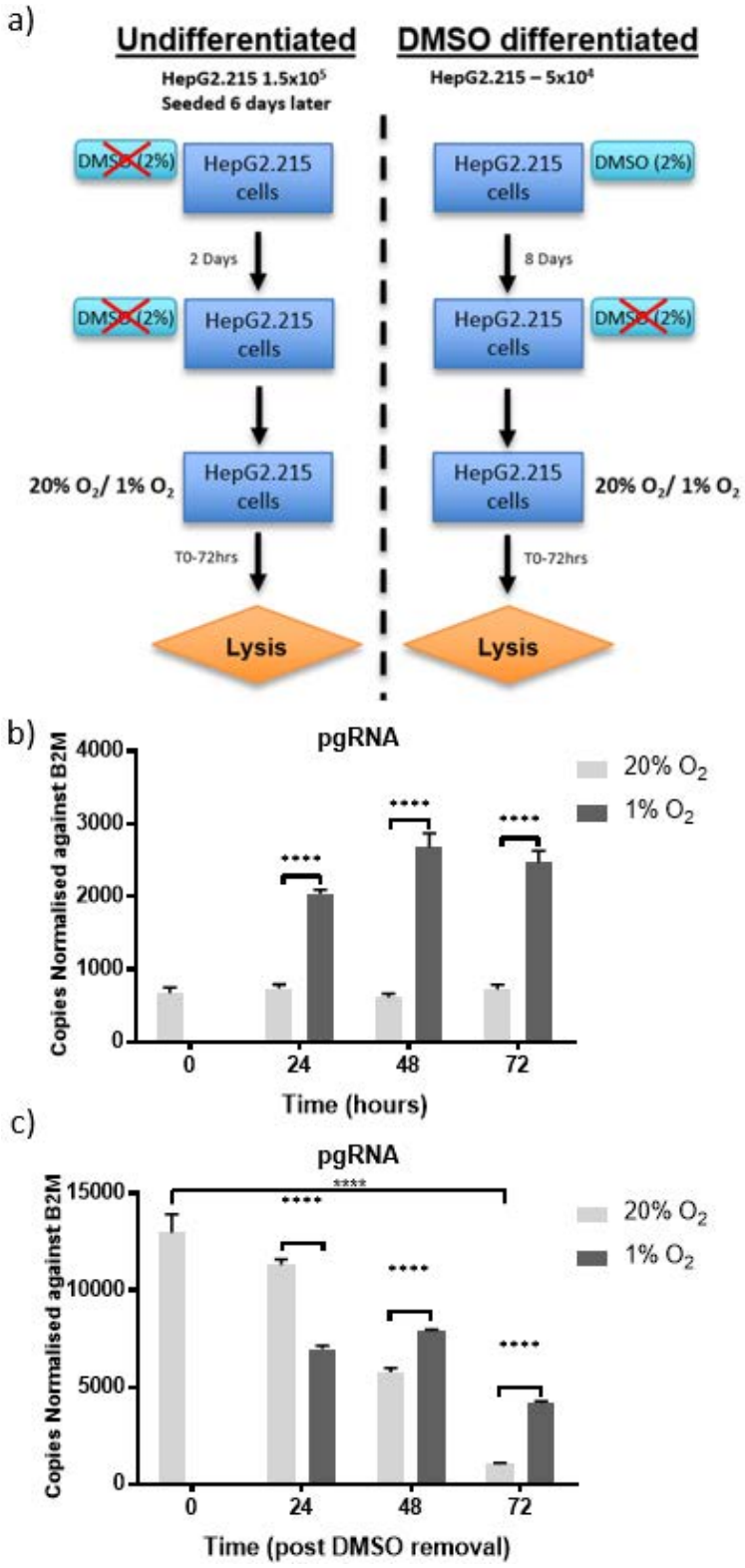

Figure 5.7 HBV nucleic acids expression in the DMSO escape assay

Legend on following page.

Figure 5.7 HBV nucleic acids expression in the DMSO escape assay

A) Schematic representation of DMSO "Escape" assay using HepG2.2.15 cells. Seed cells into 12-well plates $5x10^4$ cells per well. Differentiate in 2% DMSO over 8 days. After 6 days, seed out non-DMSO differentiated controls for confluence on day 8 ($1.5x10^5$ cells per well). After 8-day differentiation, remove DMSO from appropriate samples. Place samples under 20% and 1% oxygen for 72 hours. **B/C)** HepG2.2.15 cells were either differentiated over 72hrs with 2% DMSO or left undifferentiated. **B)** Undifferentiated cells were placed under 20% or 1% oxygen and lysed every 24 hours. **C)** DMSO differentiated cells had media replaced with DMSO free media and placed under 20% or 1% oxygen, samples were lysed every 24 hours following DMSO removal for RNA. T0 controls represent cells at start of incubation. Each graph shows the means of 2 biological repeats. Error bars show SE of 8 technical repeats. Analyses performed using Two-Way ANOVA with Sidak's multiple comparison's test.

5.6 Studying viral replication in de novo infections under low oxygen

Results obtained in chapter 3 combined with results using HepG2.2.15 cells indicate a need to remove DMSO from our infection protocol if we wanted to accurately study the effect of low oxygen on viral replication.

Having demonstrated that pgRNA and rcDNA levels could return to levels observed in un-differentiated cells, we altered the protocol standardly used for *de novo* infections by removing DMSO once the infection has been established (**Figure 5.8a**). Following this protocol, we examined the effect of low oxygen on HBV nucleic acid levels in the absence of DMSO (**Figure 5.8b-d**). These results demonstrate significant increases after 24 hours in pgRNA, cccDNA and rcDNA following exposure to 1% oxygen. This result confirms the previous result obtained using HepG2.2.15 cells.

An independent repeat using a 72 hour time course demonstrated that HBV pgRNA increases under low oxygen (**Figure 5.9a**), up-regulated expression remains constant over 72 hours perhaps indicating an increase in promoter activity or template for transcription. In addition, we demonstrated that cccDNA and rcDNA expression increased significantly over time (**Figure 5.9b,c**). This would suggest an increase in template for viral transcription. As stated previously, this could indicate an increase in virus spread, reimport of rcDNA or inhibition of degradation through Smc5/6. Additionally, we demonstrated that HBsAg levels are increasing over time in a similar manner to viral nucleic acids (**Figure 5.9d**). We confirmed this result using immunofluorescent staining for HBsAg in HepG2-NTCP K7 cells following *de novo* infection (**Figure 5.10a**), counting HBsAg positive cells demonstrated that the percentage of HBs positive cells increases over time and under low oxygen (**Figure**

5.10b) and this effect is not caused by increasing cell number caused by continued proliferation after DMSO removal (**Figure 5.10c**). Together these results confirm data obtained using HepG2.2.15 producer cells, and we conclude that low oxygen promotes HBV replication.

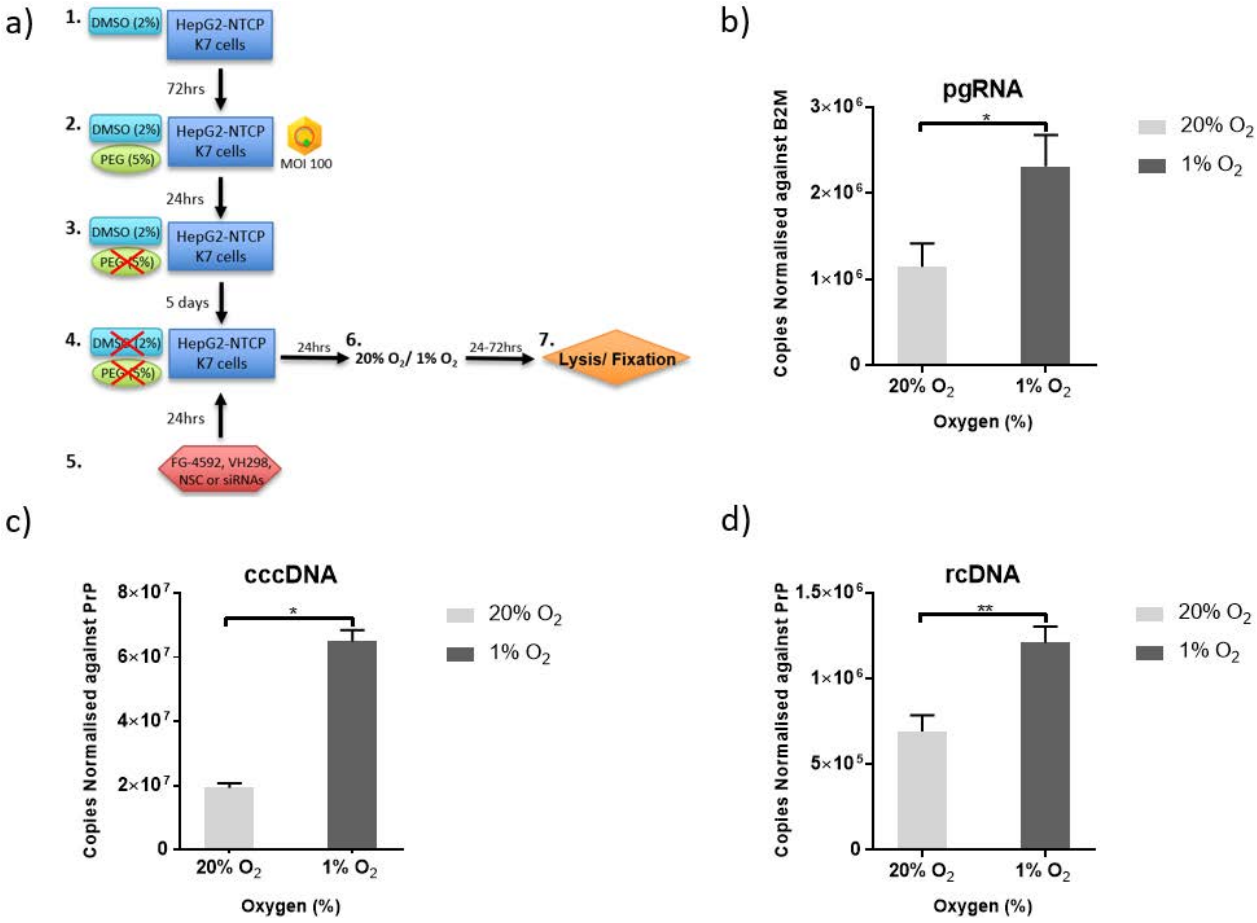

Figure 5.8 Low oxygen effect on HBV replication in de novo infection model

A) Schematic representation of *de novo* infection in HepG2-NTCP K7 cells. HepG2-NTCP K7 cells were differentiated over 72 hours in 2% DMSO. Cells were infected with HBV (MOI 100) over 24 hours in media containing 5% PEG and 2% DMSO. Fresh media without PEG added after 24 hours. Infection is left for 5 days. DMSO is removed from infected cells 5 days post infection. Cells can be treated with drugs and siRNAs at this point. Cells are placed under 20% or 1% oxygen over 24 hours. **B)** Graph demonstrating pgRNA PCR result. **C)** Graph demonstrating cccDNA PCR result. **D)** Graph demonstrating rcDNA PCR result. Each graph represents the means of 6 biological repeats. Error bars show SE of the mean of 18 technical repeats. Data analysed using Unpaired t test with Welch's correction.

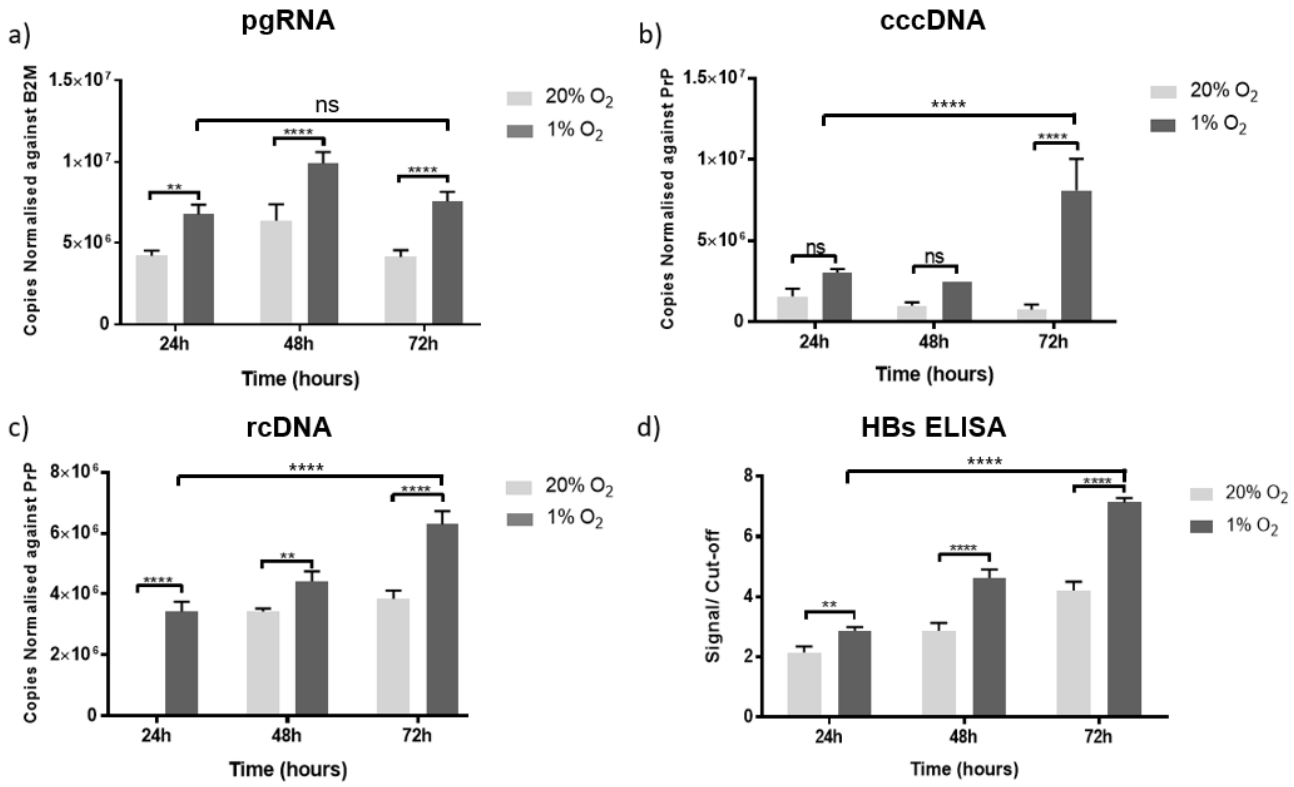

Figure 5.9 Time course of HBV nucleic acid expression under low oxygen

HepG2-NTCP K7 cells were differentiated over 72 hours in 2% DMSO. Cells were infected with HBV (MOI 100). Following infection cells were placed under 20% or 1% oxygen over 72 hours. **A)** Graph demonstrating pgRNA PCR result. **B)** Graph demonstrating cccDNA PCR result. **C)** Graph demonstrating rcDNA PCR result. **D)** Graph demonstrating HBsAg ELISA result as signal/ cut-off (described in methods section). Each graphs shows the means of 6 biological repeats. Error bars show SE of 18 technical repeats. Data analysed using Two-Way ANOVA with Tukey's and Sidak's multiple comparison's tests.

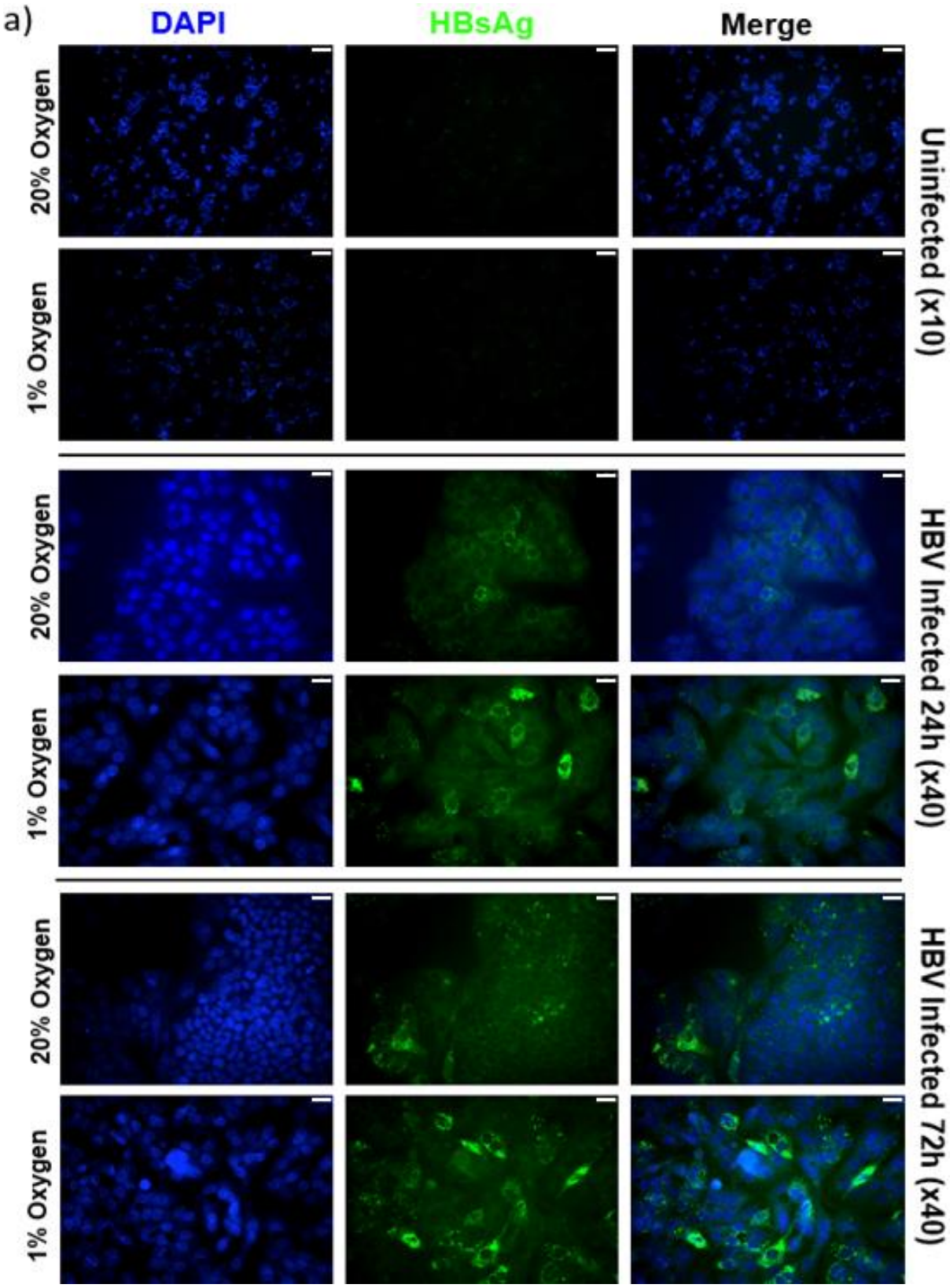

Figure 5.10a Immunofluorescent staining of HBsAg

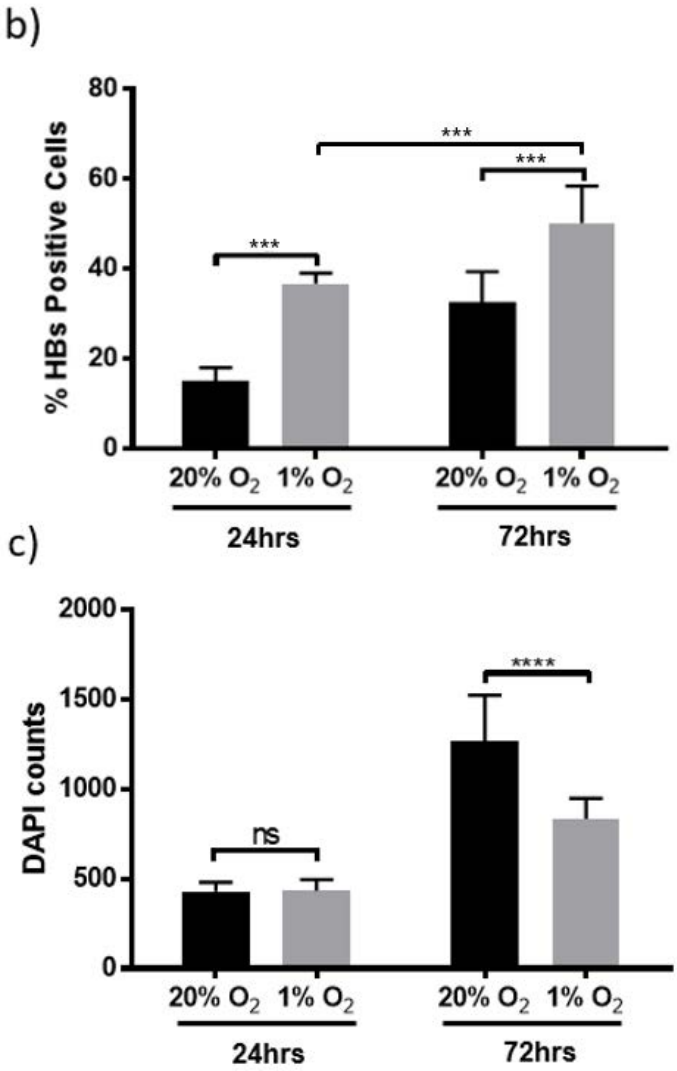

Fig 5.10 Continued

A) HepG2-NTCP K7 cells were infected with HBV (MOI 100) on collagen coated coverslips. Infections were placed under 20% or 1% oxygen over 72 hours. Cells were fixed in 6% PFA and stained with an anti-HBs antibody and DAPI, images taken with a Leica DM6000 microscope. Scale bars represent 100µm in x10 images and 25µm in x40 images. **B)** Graph representing the percentage of HBs positive cells in anti-HBs immunofluorescent stained samples. **C)** Cell counts were determined by counting DAPI stains using ImageJ. HBs counts performed manually. Graph represents average HBs counts obtained from 9 images per condition at 40x magnification. Data analysed using Multiple t tests within time points and Two-Way ANOVA with Tukey's multiple comparison's test between timepoints.

5.7 HBV replication and HIFs

Having demonstrated that low oxygen promotes viral replication using HepG2.2.15 producer cells and a *de novo* infection model, we investigated whether the effect is HIF dependent. Data gathered using ChIP and HBV promoter constructs argues for low oxygen regulation of replication being HIF dependent, however, we have yet to demonstrate this using the *de novo* infection model. Following initial infection, we treated HepG2-NTCP K7 cells with the HIF pathway inhibitor NSC and incubated the cells under 20% and 1% oxygen for 72 hours.

As previously demonstrated in Chapter 3, NSC treatment results in inhibition of HIF expression. This causes a significant reduction in pgRNA, cccDNA, rcDNA and HBsAg expression under 1% oxygen over 72 hours (**Figure 5.11**). A similar experiment utilising siRNAs to reduce expression of HIF-1α and HIF-2α after initial infection confirms this result. We utilised Western blotting to demonstrate effective silencing of protein expression and subsequent PCRs to show that reduced HIF expression causes a reduction in HBV replication; specifically, we saw significantly reduced pgRNA expression following HIF-1α silencing (**Figure 5.12b**) and significant decreases in cccDNA expression using HIF-1α and HIF-2α siRNAs (**Figure 5.12c**). This indicated HIFs are involved in the expression of pgRNA and cccDNA, perhaps through regulation of HBV transcription. However, siRNA treatment did not reduce expression of all nucleic acids. HBV rcDNA levels are decreased following treatment with NSC, but we did not see a decrease in expression following transfection with siRNAs (**Figure 5.11c** and **Figure 5.12d**). This could suggest a HIF independent effect of low oxygen on rcDNA expression.

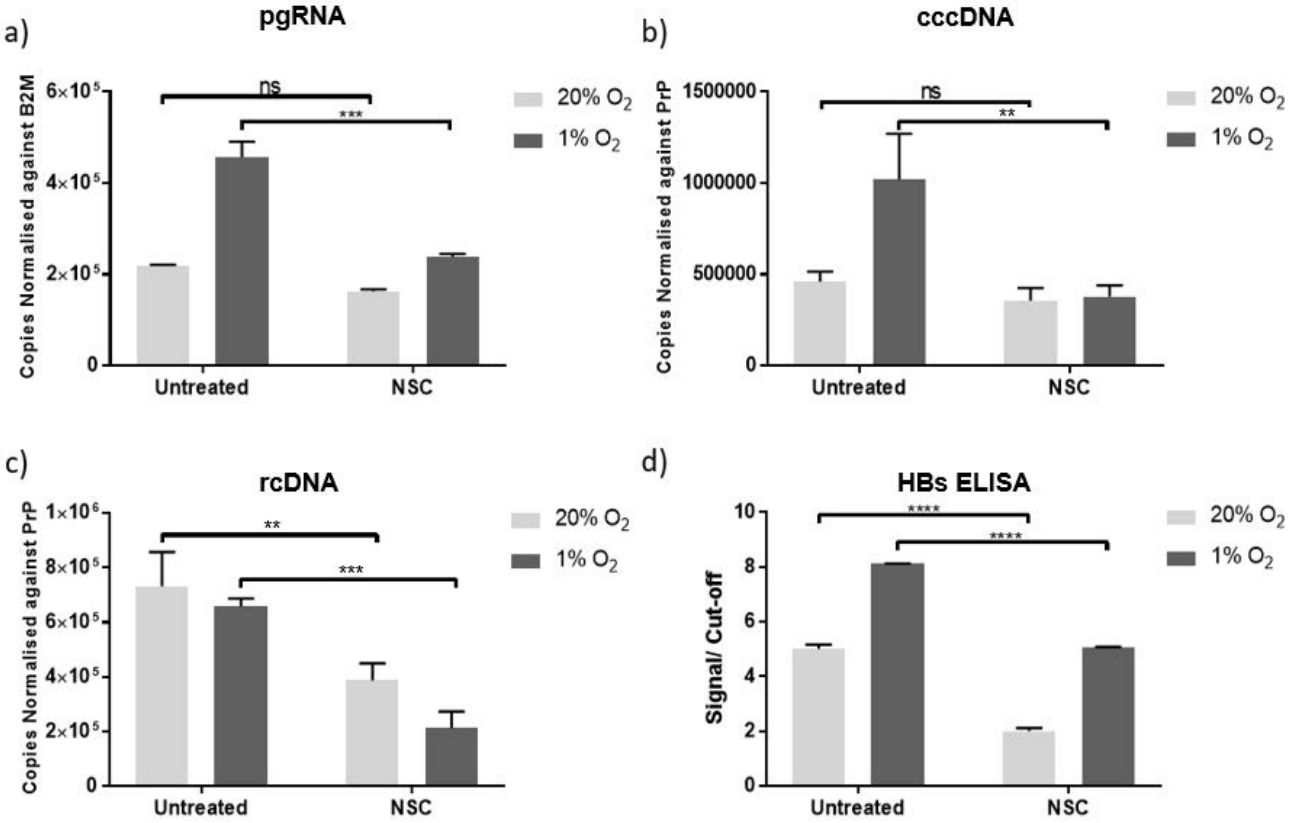

Figure 5.11 Time course of HBV nucleic acid expression with NSC treatment

HepG2-NTCP K7 cells were infected with HBV (MOI 100). Followign infection, cells were treated with 1μM NSC or left untreated. Cells are placed under 20% or 1% oxygen over 72 hours. **A)** Graph demonstrating pgRNA PCR results. **B)** Graph demonstrating cccDNA PCR results. **C)** Graph demonstrating rcDNA PCR results. **D)** Graph demonstrating HBs ELISA results. Each graph shows the means of 2 biological repeats. Error bars show SE of 6 technical repeats. Data analysed using Two-Way ANOVA with Tukey's multiple comparison's test.

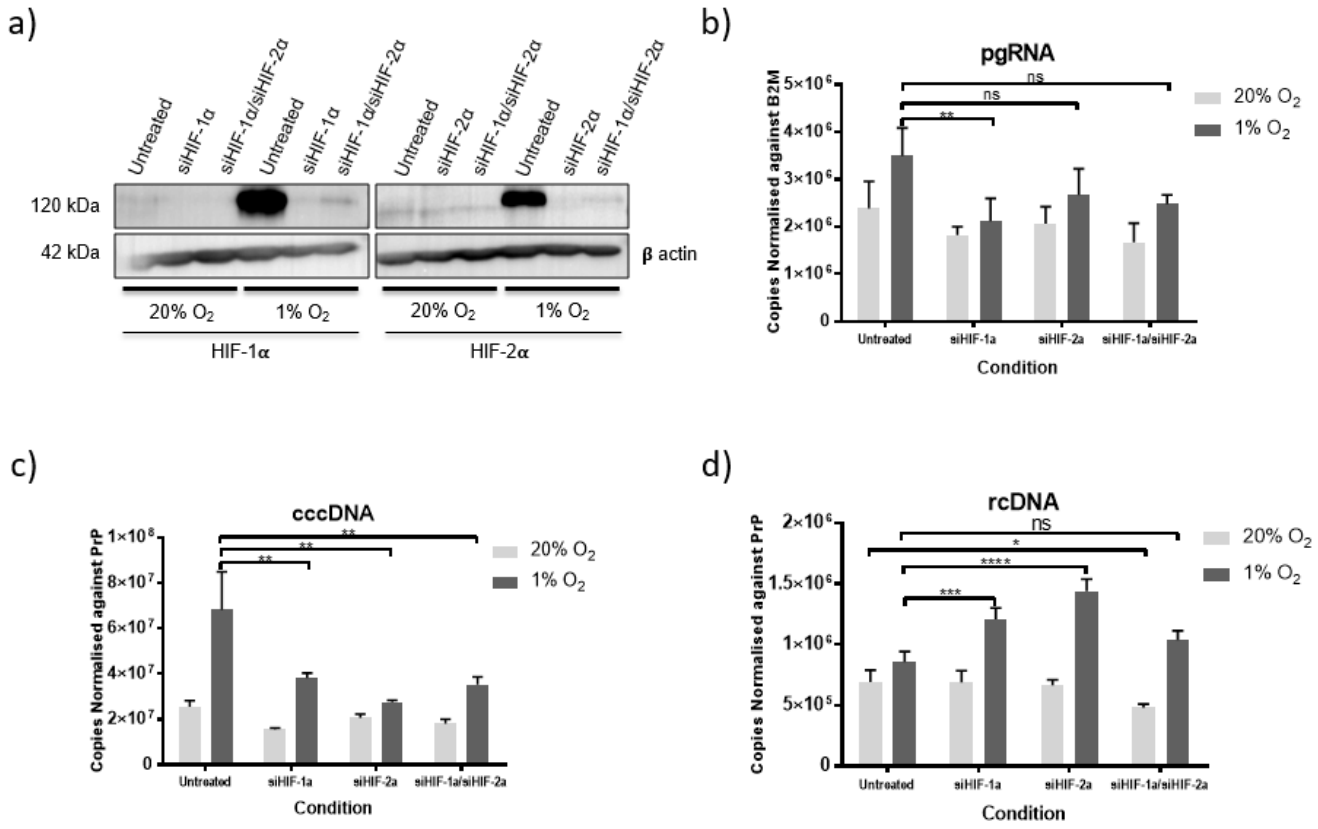

Figure 5.12 Time course of HBV nucleic acid expression with siRNA transfections

HepG2-NTCP K7 cells were infected with HBV (MOI 100). Following infection, cells transfected with siRNAs against HIF-1α or HIF-2α or left untreated. Cells are placed under 20% or 1% oxygen over 72 hours. **A)** Western blot demonstrating HIF stabilisation in infected HepG2-NTCP K7 cells under 20% and 1% oxygen following transfection with siRNAs. **B)** Graph demonstrating pgRNA PCR results. **C)** Graph demonstrating cccDNA PCR results. **D)** Graph demonstrating rcDNA PCR results. Each graph shows the means of 3 biological repeats. Error bars show SE of 9 technical repeats. Data analysed using Two-Way ANOVA with Sidak's multiple comparison's test.

5.8 Discussion

Having established that HBV stabilises HIFs in the previous chapter we moved onto examining the effect of low oxygen effects on viral life cycle. We observed increased activity for all HBV promoters (**Figures 5.2 and 5.3**) using HBV promoter constructs and HIF stabilising agents, which indicated that low oxygen is regulating viral transcription. Treatment with FG-4592 increased promoter activity significantly when compared to 1% oxygen controls. Plotting the data for each condition relative to 20% oxygen controls reveals that increased activity is not dependent on time, just low oxygen and HIF expression. This difference in effect could be due to the method of HIF stabilisation. As discussed previously, VH298 inhibits the VHL protein as part of the proteasomal degradation pathway, whereas FG-4592 inhibits PHDs, perhaps indicating a role for other parts of the low oxygen response in target cells. However, neither of these drugs specifically targets a single HIF isoform. Therefore, we utilised plasmids to over express both HIF-1α and HIF-2α that contain mutations in the double proline residues within the oxygen-dependent degradation (ODD) domain. These mutations prevent hydroxylation by PHDs and therefore prevent degradation. These plasmids were utilised in conjunction with HBV reporter plasmids to demonstrate which isoform was affecting HBV promoter activity (**Figure 5.4**). This result demonstrated that promoter activities are differentially regulated by HIF-1α and HIF-2α. HIF-1α specifically increased activity in the EnhI/ X promoter and EnhII/ BCP promoter. Activation in the EnhII/ BCP promoter could be attributed to the EnhI/ X promoter within the construct. Interestingly, the S1 and S2 promoters see increased activity following HIF-2α stabilisation. Collectively these results indicate that low oxygen has a role in increasing HBV transcription and provide justification for examining different steps in the viral lifecycle more closely. Specifically, this was achieved by exposing HepG2.2.15

cells and *de novo* infections to low oxygen environments. So, we examined the effect of low oxygen on different steps of the replication cycle using PCR and ELISAs.

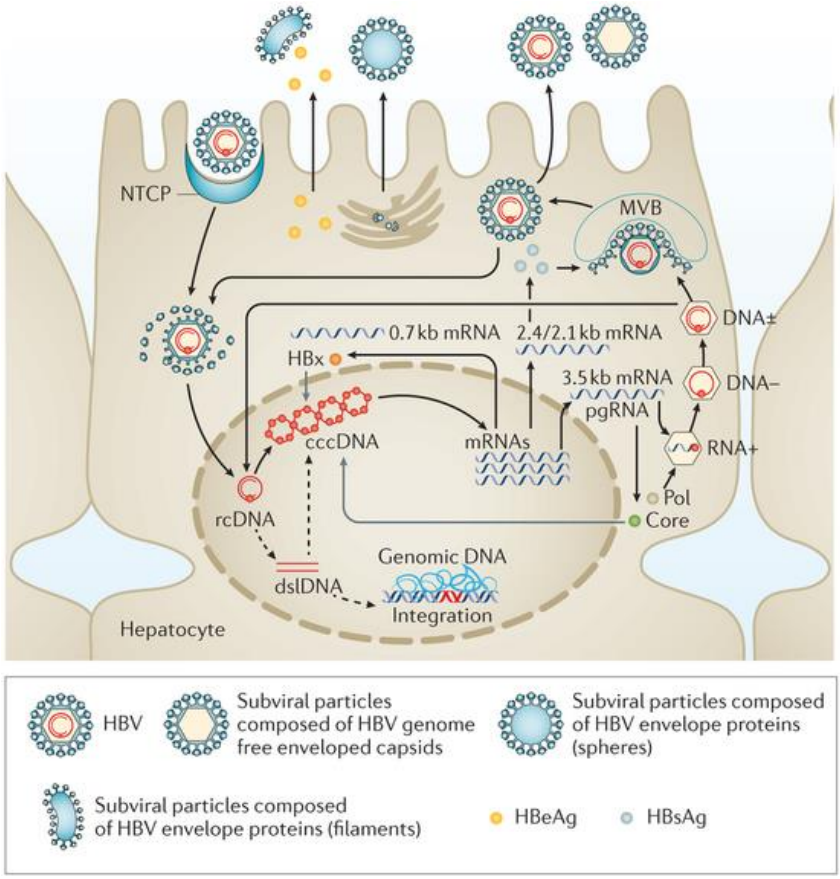

Figure 5.13 HBV lifecycle (Thomas & Liang, 2016)

Initial experiments were conducted using HepG2.2.15 cells, the PCRs demonstrate an increase in pgRNA, cccDNA and rcDNA under low oxygen (**Figure 5.5**). Each of the HBV nucleic acids are increased after 24 hours, although pgRNA is not increased significantly. Increased expression of cccDNA could indicate a couple of different effects under low oxygen (**Figure 5.5b**). First, this could indicate that low oxygen is promoting conversion from rcDNA to cccDNA as shown in **Figure 5.13**. Secondly, this could indicate that low oxygen promotes the re-import of rcDNA into the nucleus rather than secretion following DNA synthesis (Li *et al*., 2010a, Gallucci and Kann, 2017). This possibility is supported by PCR data demonstrating no increase in the secretion of HBV virions following low oxygen exposure, as demonstrated using PCR to test for supernatant rcDNA levels (**Figure 5.5d**). Lastly, increases in cccDNA could indicate an increase in spreading infection and therefore greater percentage of HBV positive cells. However, in HepG2.2.15 cells, each cell contains integrated copies of the HBV genome and lack NTCP. To test this, we utilised immunofluorescent staining of HBs in *de novo* infected HepG2-NTCP K7 cells (**Figure 5.10a**). This result indicated an increase in the percentage of HBs positive cells (**Figure 5.10b**) and provides some support for the increase of spreading infection under low oxygen.

So, increases in pgRNA suggest that low oxygen is promoting HBV transcription from cccDNA, this supports the data we obtained using the HBV reporter plasmids (**Figure 5.2**). Increased pgRNA expression could subsequently increase expression of rcDNA and cccDNA by providing more template for DNA synthesis and increased rcDNA for re-import into the nucleus. Increased levels of cccDNA following re-import of mature virions has been reported previously (Nassal, 2015), and our data suggests that low oxygen causes an increase in this behaviour. HBV pgRNA and cccDNA are increased immediately following 24 hour exposure to hypoxia, this then remains stable and even

increased further over 48 and 72 hours (**Figure 5.5a, b**). HBV rcDNA showed significant increases initially, that diminished over 48 hours and then increased again after 72 hours (**Figure 5.5c**). The implications of this are not fully understood, but it could be the result of reverse transcription from pgRNA and subsequent positive strand synthesis. HBV rcDNA drops as it is converted into cccDNA and then increases again as replication builds up. However, when examining the ratio of expression for rcDNA to pgRNA under each oxygen tension, we saw increased rcDNA expression early on suggesting an increase in production from pgRNA (**Table 5.1**). At this stage, this is just speculation and it is important to consider that HIF signalling is dynamic and fluctuations in activity could change the response in HBV infections.

Table 5.1 Ratios of rcDNA to pgRNA expression

Table detailing the ratio of rcDNA to pgRNA expression under 20% and 1 % oxygen over 72 hours during *de novo* infection experiment.

	20% Oxygen	1% Oxygen
Time (hours)	rcDNA: pgRNA	rcDNA: pgRNA
24h	3:1	5:1
48h	3:1	1.2:1
72h	1.5:1	1.3:1

We demonstrated no difference in supernatant rcDNA expression between 20% and 1% oxygen using PCR. This implies that low oxygen does not affect secretion of virions; this has been shown to occur through MVBs and the ESCRT pathway, discussed in detail in **section 1.2.7**. This provides a possible explanation for observed increased in cccDNA; the rcDNA produced via reverse transcription could be translocated to the nucleus and re-imported for an increased cccDNA pool (Nassal, 2015).

Considering the HBV S1 and S2 promoter data obtained demonstrating increased activity under low oxygen, we would expect an increase in HBsAg expression. We demonstrated that antigen secretion (or expression) is increased under low oxygen using ELISAs against HBs and anti-HBs immunofluorescent staining (**Figure 5.9d** and **Figure 5.10a**), this however does not contradict the supernatant rcDNA result. HBV antigens are secreted via the Golgi general secretory pathway. This implies that low oxygen might play a regulatory role in the endoplasmic reticulum (ER) and Golgi during HBV infections. It has been demonstrated previously that hypoxia inhibits the adaptive unfolded-protein response (UPR) in Beta cells and reduces ER to Golgi trafficking of proteins (Bensellam *et al*., 2016); however another report demonstrated that hypoxia played a role in increasing trafficking of copper through the biosynthesis secretory pathway in the Golgi (White, 2009). If hypoxia typically inhibits secretion then this suggests that HBV can overcome the inhibitory effect of low oxygen.

Having demonstrated the effect of low oxygen on the HepG2.2.15 cells it became important to confirm these results using *de novo* infections. However, as we demonstrated previously, DMSO blunts the HIF response in uninfected cells. This is problematic because the current gold standard *de novo* infection protocols require the differentiation of target cells in 2% DMSO for 72 hours proceeding infection. We

decided to examine the effect of DMSO differentiation on HBV nucleic acids expression and HIF responses in HepG2.2.15 cells. Our data demonstrated that HepG2.2.15 cells exhibit blunted HIF expression and altered pgRNA and rcDNA leves following DMSO differentiation and so we developed the DMSO "escape" assay to test the effects of DMSO removal following differentiation. We demonstrated that removing the DMSO can result in the return of pgRNA and rcDNA expression to levels observed in undifferentiated cells after 72 hours (**Figure 5.7b,c**). This is important when considering the study of HBV in low oxygen environments. This result provided the justification for removal of DMSO from our *de novo* infection protocol following initial infection. Using this protocol, we performed *de novo* infection and examine the effect of 24 hour low oxygen exposure on a more authentic infection model. This confirmed our results in HepG2.2.15 cells, demonstrating significant increases in pgRNA, cccDNA and rcDNA expression after 24 hour incubation under 1% oxygen (**Figure 5.8**). We performed a repeat experiment including a time course of incubation under 1% oxygen, this demonstrated increased cccDNA at all time points, but this was only significant at 72 hours (**Figure 5.9**). HBV pgRNA and rcDNA levels were increased significantly at all time points. These results suggest that low oxygen is up-regulating cccDNA, however the response is delayed. Perhaps suggesting that low oxygen is increasing transcription of pgRNA from cccDNA, which subsequently causes increased rcDNA expression, which is then re-imported. Both models for HBV infection have demonstrated the same effect of low oxygen on viral replication, data demonstrated in earlier chapters showed that HBV stabilised HIFs and treatment with HIF stabilising agents resulted in increased promoter activity. This provides strong evidence that the effects on HBV replication are mediated through HIFs. To confirm this result, we performed a *de novo* infection and treated infected cells with the HIF pathway inhibitor

NSC and siRNAs against HIF-1α or HIF-2α (**Figures 5.11** and **Figure 5.12** respectively) and examined the effect on viral nucleic acids following exposure to low oxygen. A combination of these data suggest that the increased viral replication observed under low oxygen is likely due to HIF-1α specifically.

Taken together the results in this chapter imply that low oxygen boosted HBV replication at several stages in the viral life cycle: transcription and cccDNA genesis. We also establish that differentiation is altering normal hypoxic responses and determined that removing DMSO from the equation post infection is a viable method of maintaining efficient infection but not impairing the hypoxic responses.

5.9 Summary

This chapter presents results demonstrating that low oxygen increased HBV promoter activity. Further experimentation using HIF stabilising agents and over expression plasmids suggests that this effect is mediated primarily through HIF-1α. In addition, we demonstrated that HBV nucleic acids are up-regulated in HepG2.2.15 cells following exposure to low oxygen. We confirmed this result using *de novo* infections and demonstrate that increasing expression under 1% oxygen is indicative of spreading infection rather than re-import and amplification of viral DNA. We further demonstrated the effect of low oxygen on HBV replication and specifically identify HIFs in this process using NSC and siRNAs to down regulate HBV nucleic acid expression.

6. DISCUSSION

In this thesis, we aimed to study the role hypoxia plays in HBV viral replication. To achieve this, we examined the low oxygen responses within target cells and included examination of differentiated cells. These results provided the basis for HBV infection models. We followed this with an examination of HBV and HIF stabilisation using HepG2.2.15 producer cells and *de novo* infection models. Whilst the *de novo* infection protocol we used is considered the "gold standard" for modelling HBV infections, there are some limitations that are important to consider. Firstly, this model is reliant on artificial differentiation using DMSO. Treatment with this chemical could result in multiple off target effects that affect the observed results. Further testing of DMSO effects on HBV infections would be required to be sure no off target effects are occurring. We tested an alternative method of differentiation for hepatocytes and found that HepG2 cells could not tolerate the differentiation process enough for efficient use in experimentation. It would be interesting to consider the use of pluripotent stem cells as progenitors for differentiated hepatocytes as the basis for future models of infection. Secondly, this infection model relies on the overexpression of NTCP and polyethylene glycol treatment to enable efficient infection. This is incredibly artificial and therefore results obtained using this model could be affected by multiple cell manipulations that have occurred. The model system could potentially be improved by trying to remove each of these treatments. However, this could significantly reduce the level of HBV infections. The model could be improved by altering the cell types used for infection. The use of primary human hepatocytes would provide a more realistic model for infections. We established that stabilisation occurs under both 20% and 1% oxygen; and that stabilisation is not dependent upon X and L proteins. Considering this result it

is unclear how HBV infection results in HIF stabilisation, perhaps through HBV induced reactive oxygen species (ROS) accumulation (Mishra *et al.*, 2017). ROS have demonstrated a role in regulation of HIF-1 through altered activity of PHD2 *(Niecknig et al.*, 2012). Further testing revealed an HRE binding motif within the HBV genome, and the use of a ChIP assay demonstrated a direct interaction between HIF-1α and the HBV EnhI/ X promoter. In the final results chapter, we examined the effects of low oxygen on HBV transcription and replication using a combination of HBV-promoter-luciferase constructs and PCRs targeting HBV nucleic acids. These data demonstrated that low oxygen up-regulated viral transcription and replication. Further investigation using the HIF inhibitor NSC and specific siRNAs demonstrated that low oxygen effects on HBV infection are HIF dependent. Together our results argue a role for HIFs in viral transcription that impacts upon replication and demonstrate that this effect is independent of low oxygen. However, the effect is potentially accentuated in hypoxic or inflammatory environments.

The biological relevance of our observations may be reflected in the oxygen gradient associated with normal blood flow in the liver, and inflammation associated with infection, liver disease and hepatocellular carcinoma (Jungermann and Kietzmann, 2000, Gebhardt *et al*., 2007, Wilson *et al*., 2014). These all result in hypoxic environments within the liver of varying oxygen tensions. Our collaborators from the Protzer laboratory at T.U.M in Munich, have demonstrated that HBV will predominantly localize to low oxygen regions in the livers of HBV transgenic mice. Our data suggests a pro-viral role for HIFs in viral replication. These transcription factors are reported to act as part of multiple stress response pathways; and through binding of promoter regions regulate a number of genes involved in glucose metabolism, regulation of lipid

metabolism, liver injury and tumour-associated angiogenesis, metastasis and inflammation. This was discussed in more detail in the main introduction.

A number of reports have demonstrated interactions between HIFs and other viruses. For example, it was demonstrated that the HPV protein E6 inhibits p53, which inhibits HIF-1α expression (Ravi *et al*., 2000). In addition, it has been shown that HPV E7 protein can stabilise HIF-1α through direct interaction with the protein (Bodily *et al*., 2011). Other reports demonstrate that EBV can increase HIF-1α synthesis through LMP-1 protein enhancing the ERK1/2 MAPK signalling pathway (Wakisaka *et al*., 2004). Additionally, EBV proteins EBNA 3 and 5 have been demonstrated to inhibit PHD activity and therefore prevent degradation of HIFs (Darekar *et al*., 2012). Reports also demonstrate KSHV stabilisation of HIF-1α through the vGPCR protein, which stimulates the secretion of multiple cytokines that enhance the synthesis of HIF-1α (Jham *et al*., 2011). Our lab has previously demonstrated a role for HIFs in the lifecycle of HCV and demonstrated that hypoxic exposure results in increased viral replication (Wilson *et al*., 2012). Colleagues within our lab have also recently demonstrated inhibition of HIV-1 replication following exposure to low oxygen (Unpublished, Jane McKeating personal communication). Previous reports have demonstrated a link between HIFs and HBV through the HBx protein (Yoo *et al*., 2003, Yoo *et al*., 2004, Yoo *et al*., 2008). Specifically, these papers demonstrate increased MAPK signalling resulting in increased HIF-1α expression; increased HDAC1 transcription and binding of PHDs/ VHL to prevent HIF-1α degradation. Another study by Li and colleagues demonstrated an interaction between LHB and HIFs resulting in increased MDR1 expression (Li *et al*., 2017). Our data demonstrated that HBV interactions with HIFs are not dependent on HBx or LHB. This was an interesting result and motivated further examination of other interactions. We examined the interaction between HIF-1α and

the HBV genome using anti-HIF-1α ChIP and primers spanning the HBV genome; this revealing a direct interaction between HIF-1α and the viral genome at an HRE motif found in the EnhI/ X promoter region. This interaction has not been previously shown.

This result does not preclude the interaction of viral proteins with HIFs but demonstrated a role for the host transcription factor in regulating viral transcription. Previous studies have shown multiple transcription factors that will interact with the HBV and regulate the virus (Quasdorff and Protzer, 2010), these have been discussed in more detail in the main introduction. We demonstrated low oxygen and HIF effects on HBV promoter activation using the HBV luciferase reporters. These data demonstrate the reverse of previous research, which primarily focuses on HBx regulation of HIF activity. The implication is that HBV is modifying host behaviour. Our models suggest that HBV is actively stabilising HIFs even under 20% oxygen conditions and through interaction with the viral genome stimulate transcription. This in turn results in increased replication. We propose a model in which HBV ordinarily utilises HIFs, and this effect is accentuated under low oxygen or inflammatory conditions.

A study by Song and colleagues examined the effect of inflammation on miR-210 activity under low oxygen during HBV infection. They concluded that low oxygen was reducing viral replication through miR-210 activity (Song *et al*., 2014). These results seem to directly contradict those found in our studies. However, they only use the HepG2.2.15 cell model of infection and only measure the levels of HBsAg, HBeAg and HBV DNA found in harvested supernatants following hypoxic exposure. Our data is based upon multiple models of infections and more stringent experimental techniques that measure the levels of HBV nucleic acid expression harvested from cell lysates of infected cells. Importantly, Song and colleagues suggest that low oxygen and

inflammation increase miR-210 activity, which causes reduced viral replication (Song *et al*., 2014). If our data is correct, then HBV is overcoming this down regulation whilst in low oxygen regions. Zhang and colleagues also demonstrate a role for miR-210 and miR-199a-3p in reducing viral replication following up-regulation during inflammation (Zhang *et al*., 2010), however they do not utilise low oxygen in their study. This result suggests that up-regulation of micro RNAs is part of an anti-viral response that is at least partly controlled through HIF stabilisation.

Our studies highlight the need for further study into low oxygen and inflammatory effects on HBV replication. The data shown in this thesis indicates that cccDNA, rcDNA and pgRNA levels are increased under low oxygen. We have studied the effect of low oxygen on viral entry and demonstrated no change following hypoxic incubation (data not shown). This implies that either low oxygen is promoting nuclear import of virions following infection, or more likely, low oxygen is promoting transcription from cccDNA. This would result in up-regulation of pgRNA and generate more template for rcDNA synthesis. Increased synthesis of rcDNA results in increased levels of re-import and therefore increased cccDNA levels. Especially considering our data suggests that low oxygen was not increasing the level of secreted rcDNA. Multiple repeat infections demonstrated different patterns of viral replication up-regulation. Up-regulation is not consistently at any one timepoint. This suggests that the process is controlled by the virus and that up-regulation is regulated to reflect different stages of infection lifecycles. This could suggest that HBV infections occur preferentially under low oxygen conditions before spreading through the liver. In addition, low oxygen induced expression of viral nucleic acids, perhaps suggesting that HBV pathogenesis is increased under low oxygen environments. Alternatively, this could represent the dynamic nature of HIF signalling. In conclusion, the virus is likely utilising a host

transcription factor to regulate viral transcription and replication. Considering the challenges with treating HBV due to the formation of cccDNA and a reservoir for replication, a better understanding of these host-viral interactions and the effect on infection progression, could reduce the burden of infectious disease on human health. In addition, our findings highlight a potential role for HIF inhibitors as therapeutics in the treatment of HBV.

6.1 Future Work

While these data have uncovered a role for low oxygen in the HBV lifecycle, more investigation is necessary to validate the involvement of HIF-1α and HIF-2α; and determine the circumstances under which each isoform is utilised. It would be valuable to perform additional ChIP experiments to confirm whether all HIF isoforms can bind to the HRE motif within the genome. These interactions have only been demonstrated using the HepG2.2.15 cell model so far, it would be important to expand upon this result and demonstrate interactions using a *de novo* infection model. Additionally, it would be interesting to examine the effect of low oxygen on the epigenetics of cccDNA. It is well known that low oxygen can induce epigenetic changes through the recruitment of HDACs to chromosomes (Kim *et al*., 2007, Liang *et al*., 2006), and previous research has shown that cccDNA behaves as a mini chromosome and undergoes epigenetic changes (Yoo *et al*., 2008, Belloni *et al*., 2009). However, there is no research that examines the role hypoxia might play on cccDNA. It would be interesting to examine epigenetic changes in cccDNA following hypoxic exposure; and investigate the impact of any epigenetic changes on HIF binding to the genome. Additionally, it has been shown that specific PHD activities are determined by the oxygen tension with each PHD being regulated by a different effective K_m (Schofield and Ratcliffe, 2004). This in turn determines the HIF isoform that is expressed depending on the cell type

(Schofield and Ratcliffe, 2004, Berchner-Pfannschmidt *et al*., 2008). It would be interesting to examine whether the oxygen tension can alter the isoform of HIF that bind the HBV genome. We demonstrated that different promoters are regulated through the expression of HIF-1α or HIF-2α using over expression plasmids; promoter activation seems to occur despite only finding an HRE binding site in the EnhI/ X promoter. A study of HIF isoform binding to HBV promoters under varying hypoxic oxygen tensions would be interesting and would complement our data using HIF over expression plasmids.

Although we observed a decrease in viral replication through inhibition of cccDNA, rcDNA and pgRNA levels following transfection with siRNAs or treatment with NSC; the role of HIFs in viral replication could be further studied using knockout cell lines generated with the CRISPR knockout system or perhaps an inducible knockout system. This is important because whilst the siRNAs and HIF inhibitor are effective, their reduction of HIF expression is not 100%. It would be interesting to examine an HBV infection in cells with complete knockout, would an HBV infection be viable independent of HIFs? Having demonstrated that HBV-HIF interactions are not necessarily through HBx and that stabilisation is independent of HBx and LHB, it would be interesting to examine the interaction between HIFs and other viral proteins. Considering the observed increase in replication, it is possible that HIFs are interacting with the Core protein or the viral polymerase. This could be achieved using GST bound agarose affinity beads and a pulldown assay.

Another interesting direction for future study, would be the examination of HBV induced HIF stabilisation on host metabolism and the impact on HBV. Previous reports have demonstrated that HBV alters the hexosamine biosynthetic and phosphatidylcholine pathways (Li *et al*., 2015). Other studies also demonstrate that these pathways are

regulated by low oxygen (Guillaumond *et al*., 2013). Hexosamine is specifically involved in post-translational modifications (Taparra *et al*., 2016, Ferrer *et al*., 2014) and could be utilised by HBV to induce changes in cccDNA structure. In addition, HIFs are strongly associated with glucose metabolism changes, through HRE activation and regulation of genes such as GLUT1 and GLUT3 amongst others (Semenza, 2003, Kim *et al*., 2006a). It would be interesting to study the impact of viral infection on host metabolism and how these changes affect the virus.

HBV is strongly associated with the development of HCC; however, the pathogenesis of HBV-related HCC is currently not clear. Evidence suggests that HBV could induce malignant transformation through direct integration of the viral genome into host chromosome or HBx associated activation of the MAPK pathway and inhibition of the p53 tumour suppressor (Ueda *et al*., 1995, Wang *et al*., 1994). It is also suggested that chronic infections induce HCC formation through cycles of inflammation and regeneration; and as a consequence of cirrhosis development (El-Serag, 2012). HIFs are known to affect most of the hallmarks of cancer (Wigerup *et al*., 2016) and we demonstrated that HBV can stabilise HIF expression over extended time periods. It would be interesting to investigate the contribution of HBV stabilised HIFs on the process of HCC development. In addition, hypoxia induces epigenetic changes through recruitment of HDACs, which modify chromosomes and reportedly cccDNA (Yoo *et al*., 2008). Epigenetic changes are associated with improved infection outcome (Koumbi 2015). These in turn could cumulatively be responsible for the development of HCC in chronic infections.

Our results indicate that low oxygen does not increase secreted rcDNA levels, but we did observe an increase in the percentage of HBs positive cells over time, indicating an increase in the number of infected cells. It would be interesting to examine how low

oxygen is increasing viral replication. This increase could be due to vertical spreading, whilst cells are dividing or perhaps increasing susceptibility to infection. This could be tested through the use of cell cycle inhibitors such as RO-3306 (Vassilev, 2006) or cell cycle arrest using gamma-irradiation (O'Connell *et al*., 1998). Following treatment with each of these methods, examination of viral spread under 20% and 1% oxygen would provide more evidence to determine how low oxygen is affecting spread.

Lastly, this thesis has demonstrated the pro-viral effect of low oxygen in the HBV life cycle, specifically showing a role for HIF-1α and HIF-2α. It will be important to expand this research to include HIF-independent low oxygen signalling pathways because hypoxic responses are dynamic and subject to fluctuation. In addition, it would be interesting to further investigate the role of HIF3α in the viral lifecycle, to date, there are very few studies that investigate the role of this protein in uninfected cells and even less for viral infections.

7. REFERENCES

ABRAHAM, T. M. & LOEB, D. D. 2006. Base Pairing between the 5′ Half of ε and a cis-Acting Sequence, Φ, Makes a Contribution to the Synthesis of Minus-Strand DNA for Human Hepatitis B Virus. *J Virol,* 80**,** 4380-7.

ADAMS, D. H. & EKSTEEN, B. 2006. Aberrant homing of mucosal T cells and extra-intestinal manifestations of inflammatory bowel disease. *Nat Rev Immunol,* 6**,** 244-251.

ADLER, M., TAVALAI, N., MULLER, R. & STAMMINGER, T. 2011. Human cytomegalovirus immediate-early gene expression is restricted by the nuclear domain 10 component Sp100. *J Gen Virol,* 92**,** 1532-8.

AGANI, F. & JIANG, B. H. 2013. Oxygen-independent regulation of HIF-1: novel involvement of PI3K/AKT/mTOR pathway in cancer. *Curr Cancer Drug Targets,* 13**,** 245-51.

ALDER, O., CULLUM, R., LEE, S., KAN, AROHUMAM C., WEI, W., YI, Y., GARSIDE, VICTORIA C., BILENKY, M., GRIFFITH, M., MORRISSY, A. S., ROBERTSON, GORDON A., THIESSEN, N., ZHAO, Y., CHEN, Q., PAN, D., JONES, STEVEN J. M., MARRA, MARCO A. & HOODLESS, PAMELA A. 2014. Hippo Signaling Influences HNF4A and FOXA2 Enhancer Switching during Hepatocyte Differentiation. *Cell Reports,* 9**,** 261-271.

ANDO, H., NATSUME, A., IWAMI, K., OHKA, F., KUCHIMARU, T., KIZAKA-KONDOH, S., ITO, K., SAITO, K., SUGITA, S., HOSHINO, T. & WAKABAYASHI, T. 2013. A hypoxia-inducible factor (HIF)-3alpha splicing variant, HIF-3alpha4 impairs angiogenesis in hypervascular malignant meningiomas with epigenetically silenced HIF-3alpha4. *Biochem Biophys Res Commun,* 433**,** 139-44.

ARAGONES, J., SCHNEIDER, M., VAN GEYTE, K., FRAISL, P., DRESSELAERS, T., MAZZONE, M., DIRKX, R., ZACCHIGNA, S., LEMIEUX, H., JEOUNG, N. H., LAMBRECHTS, D., BISHOP, T., LAFUSTE, P., DIEZ-JUAN, A., HARTEN, S. K., VAN NOTEN, P., DE BOCK, K., WILLAM, C., TJWA, M., GROSFELD, A., NAVET, R., MOONS, L., VANDENDRIESSCHE, T., DEROOSE, C., WIJEYEKOON, B., NUYTS, J., JORDAN, B., SILASI-MANSAT, R., LUPU, F., DEWERCHIN, M., PUGH, C., SALMON, P., MORTELMANS, L., GALLEZ, B., GORUS, F., BUYSE, J., SLUSE, F., HARRIS, R. A., GNAIGER, E., HESPEL, P., VAN HECKE, P., SCHUIT, F., VAN VELDHOVEN, P., RATCLIFFE, P., BAES, M., MAXWELL, P. & CARMELIET, P. 2008. Deficiency or inhibition of oxygen sensor Phd1 induces hypoxia tolerance by reprogramming basal metabolism. *Nat Genet,* 40**,** 170-80.

AUGSTEIN, A., POITZ, D. M., BRAUN-DULLAEUS, R. C., STRASSER, R. H. & SCHMEISSER, A. 2011. Cell-specific and hypoxia-dependent regulation of human HIF-3alpha: inhibition of the expression of HIF target genes in vascular cells. *Cell Mol Life Sci,* 68**,** 2627-42.

BAKER, L. C. J., BOULT, J. K. R., WALKER-SAMUEL, S., CHUNG, Y., JAMIN, Y., ASHCROFT, M. & ROBINSON, S. P. 2012. The HIF-pathway inhibitor NSC-134754 induces metabolic changes and anti-tumour activity while maintaining vascular function. *Br J Cancer,* 106**,** 1638-47.

BARDOS, J. I. & ASHCROFT, M. 2004. Hypoxia-inducible factor-1 and oncogenic signalling. *Bioessays,* 26**,** 262-9.

BASAGOUDANAVAR, S. H., PERLMAN, D. H. & HU, J. 2007. Regulation of Hepadnavirus Reverse Transcription by Dynamic Nucleocapsid Phosphorylation. *J Virol,* 81**,** 1641-9.

BAYARSAIHAN, D. 2011. Epigenetic Mechanisms in Inflammation. *J Dent Res,* 90**,** 9-17.

BEISEL, C. & PARO, R. 2011. Silencing chromatin: comparing modes and mechanisms. *Nat Rev Genet,* 12**,** 123-35.

BELLONI, L., ALLWEISS, L., GUERRIERI, F., PEDICONI, N., VOLZ, T., POLLICINO, T., PETERSEN, J., RAIMONDO, G., DANDRI, M. & LEVRERO, M. 2012. IFN-α inhibits HBV transcription and replication in cell culture and in humanized mice by targeting the

epigenetic regulation of the nuclear cccDNA minichromosome. *The Journal of Clinical Investigation,* 122**,** 529-537.

BELLONI, L., POLLICINO, T., DE NICOLA, F., GUERRIERI, F., RAFFA, G., FANCIULLI, M., RAIMONDO, G. & LEVRERO, M. 2009. Nuclear HBx binds the HBV minichromosome and modifies the epigenetic regulation of cccDNA function. *Proc Natl Acad Sci U S A,* 106**,** 19975-9.

BENHENDA, S., DUCROUX, A., RIVIERE, L., SOBHIAN, B., WARD, M. D., DION, S., HANTZ, O., PROTZER, U., MICHEL, M. L., BENKIRANE, M., SEMMES, O. J., BUENDIA, M. A. & NEUVEUT, C. 2013. Methyltransferase PRMT1 is a binding partner of HBx and a negative regulator of hepatitis B virus transcription. *J Virol,* 87**,** 4360-71.

BENSELLAM, M., MAXWELL, E. L., CHAN, J. Y., LUZURIAGA, J., WEST, P. K., JONAS, J. C., GUNTON, J. E. & LAYBUTT, D. R. 2016. Hypoxia reduces ER-to-Golgi protein trafficking and increases cell death by inhibiting the adaptive unfolded protein response in mouse beta cells. *Diabetologia,* 59**,** 1492-502.

BERCHNER-PFANNSCHMIDT, U., TUG, S., TRINIDAD, B., OEHME, F., YAMAC, H., WOTZLAW, C., FLAMME, I. & FANDREY, J. 2008. Nuclear Oxygen Sensing: Induction of Endogenous Prolyl-hydroxylase 2 Activity by Hypoxia and Nitric Oxide. *Journal of Biological Chemistry,* 283**,** 31745-31753.

BERRA, E., BENIZRI, E., GINOUVES, A., VOLMAT, V., ROUX, D. & POUYSSEGUR, J. 2003. HIF prolyl-hydroxylase 2 is the key oxygen sensor setting low steady-state levels of HIF-1alpha in normoxia. *Embo j,* 22**,** 4082-90.

BERTOUT, J. A., MAJMUNDAR, A. J., GORDAN, J. D., LAM, J. C., DITSWORTH, D., KEITH, B., BROWN, E. J., NATHANSON, K. L. & SIMON, M. C. 2009. HIF2α inhibition promotes p53 pathway activity, tumor cell death, and radiation responses. *Proc Natl Acad Sci U S A,* 106**,** 14391-6.

BERTOUT, J. A., PATEL, S. A. & SIMON, M. C. 2008. The impact of O2 availability on human cancer. *Nat Rev Cancer,* 8**,** 967-75.

BILL, C. A. & SUMMERS, J. 2004. Genomic DNA double-strand breaks are targets for hepadnaviral DNA integration. *Proc Natl Acad Sci U S A,* 101**,** 11135-40.

BISHOP, N. & WOODMAN, P. 2000. ATPase-defective Mammalian VPS4 Localizes to Aberrant Endosomes and Impairs Cholesterol Trafficking. *Mol Biol Cell,* 11**,** 227-39.

BLIGHT, K. J., MCKEATING, J. A. & RICE, C. M. 2002. Highly permissive cell lines for subgenomic and genomic hepatitis C virus RNA replication. *J Virol,* 76**,** 13001-14.

BODILY, J. M., MEHTA, K. P. & LAIMINS, L. A. 2011. Human papillomavirus E7 enhances hypoxia-inducible factor 1-mediated transcription by inhibiting binding of histone deacetylases. *Cancer Res,* 71**,** 1187-95.

BOGOMOLSKI-YAHALOM, V., KLEIN, A., GREENBLAT, I., HAVIV, Y. & TUR-KASPA, R. 1997. The TATA-less promoter of hepatitis B virus S gene contains a TBP binding site and an active initiator. *Virus Res,* 49**,** 1-7.

BOREGOWDA, R. K., ADAMS, C. & HU, J. 2012. TP-RT Domain Interactions of Duck Hepatitis B Virus Reverse Transcriptase in cis and in trans during Protein-Primed Initiation of DNA Synthesis In Vitro. *J Virol,* 86**,** 6522-36.

BRUSS, V. 2007. Hepatitis B virus morphogenesis. *World J Gastroenterol,* 13**,** 65-73.

CARROLL, V. A. & ASHCROFT, M. 2006. Role of hypoxia-inducible factor (HIF)-1alpha versus HIF-2alpha in the regulation of HIF target genes in response to hypoxia, insulin-like growth factor-I, or loss of von Hippel-Lindau function: implications for targeting the HIF pathway. *Cancer Res,* 66**,** 6264-70.

CHANDEL, N. S., MCCLINTOCK, D. S., FELICIANO, C. E., WOOD, T. M., MELENDEZ, J. A., RODRIGUEZ, A. M. & SCHUMACKER, P. T. 2000. Reactive oxygen species generated at mitochondrial complex III stabilize hypoxia-inducible factor-1alpha during hypoxia: a mechanism of O2 sensing. *J Biol Chem,* 275**,** 25130-8.

CHANG , M.-H., CHEN , C.-J., LAI , M.-S., HSU , H.-M., WU , T.-C., KONG , M.-S., LIANG , D.-C., SHAU , W.-Y. & CHEN , D.-S. 1997. Universal Hepatitis B Vaccination in Taiwan and the Incidence of Hepatocellular Carcinoma in Children. *New England Journal of Medicine,* 336**,** 1855-1859.

CHANG, T. T., GISH, R. G., DE MAN, R., GADANO, A., SOLLANO, J., CHAO, Y. C., LOK, A. S., HAN, K. H., GOODMAN, Z., ZHU, J., CROSS, A., DEHERTOGH, D., WILBER, R., COLONNO, R. & APELIAN, D. 2006. A comparison of entecavir and lamivudine for HBeAg-positive chronic hepatitis B. *N Engl J Med,* 354**,** 1001-10.

CHANG, T. T., LAI, C. L., KEW YOON, S., LEE, S. S., COELHO, H. S., CARRILHO, F. J., POORDAD, F., HALOTA, W., HORSMANS, Y., TSAI, N., ZHANG, H., TENNEY, D. J., TAMEZ, R. & ILOEJE, U. 2010. Entecavir treatment for up to 5 years in patients with hepatitis B e antigen-positive chronic hepatitis B. *Hepatology,* 51**,** 422-30.

CHEN, A. & BROWN, C. 2012. Distinct families of cis-acting RNA replication elements epsilon from hepatitis B viruses. *RNA Biol,* 9**,** 130-6.

CHEN, M., HIENG, S., QIAN, X., COSTA, R. & OU, J. H. 1994. Regulation of hepatitis B virus ENI enhancer activity by hepatocyte-enriched transcription factor HNF3. *Virology,* 205**,** 127-32.

CHEN, N., QIAN, J., CHEN, J., YU, X., MEI, C., HAO, C., JIANG, G., LIN, H., ZHANG, X., ZUO, L., HE, Q., FU, P., LI, X., NI, D., HEMMERICH, S., LIU, C., SZCZECH, L., BESARAB, A., NEFF, T. B., PEONY YU, K. H. & VALONE, F. H. 2017. Phase 2 studies of oral hypoxia-inducible factor prolyl hydroxylase inhibitor FG-4592 for treatment of anemia in China. *Nephrol Dial Transplant*.

CHEN, X., EL GAZZAR, M., YOZA, B. K. & MCCALL, C. E. 2009. The NF-κB Factor RelB and Histone H3 Lysine Methyltransferase G9a Directly Interact to Generate Epigenetic Silencing in Endotoxin Tolerance. *J Biol Chem,* 284**,** 27857-65.

CHEN, Y., GOTTE, M., LIU, J. & PARK, P. W. 2008. Microbial subversion of heparan sulfate proteoglycans. *Mol Cells,* 26**,** 415-26.

CHEN, Y. & MARION, P. L. 1996. Amino acids essential for RNase H activity of hepadnaviruses are also required for efficient elongation of minus-strand viral DNA. *J Virol,* 70**,** 6151-6.

CHENG, X., XIA, Y., SERTI, E., BLOCK, P. D., CHUNG, M., CHAYAMA, K., REHERMANN, B. & LIANG, T. J. 2017. Hepatitis B virus evades innate immunity of hepatocytes but activates cytokine production by macrophages. *Hepatology,* 66**,** 1779-1793.

CHOI, B. H., PARK, C. J. & RHO, H. M. 1998. Insulin activates the hepatitis B virus X gene through the activating protein-1 binding site in HepG2 cells. *DNA Cell Biol,* 17**,** 951-6.

CHOISY, M., KEOMALAPHET, S., XAYDALASOUK, K., QUET, F., LATTHAPHASAVANG, V. & BUISSON, Y. 2017. Prevalence of Hepatitis B Virus Infection among Pregnant Women Attending Antenatal Clinics in Vientiane, Laos, 2008–2014. *Hepat Res Treat,* 2017.

COLEMAN, W. B., WENNERBERG, A. E., SMITH, G. J. & GRISHAM, J. W. 1993. Regulation of the differentiation of diploid and some aneuploid rat liver epithelial (stemlike) cells by the hepatic microenvironment. *Am J Pathol,* 142**,** 1373-82.

COLGROVE, R., SIMON, G. & GANEM, D. 1989. Transcriptional activation of homologous and heterologous genes by the hepatitis B virus X gene product in cells permissive for viral replication. *J Virol,* 63**,** 4019-26.

COLPITTS, C. C., VERRIER, E. R. & BAUMERT, T. F. 2015. Targeting Viral Entry for Treatment of Hepatitis B and C Virus Infections. *ACS Infectious Diseases,* 1**,** 420-427.

COOPER, A. & SHAUL, Y. 2006. Clathrin-mediated endocytosis and lysosomal cleavage of hepatitis B virus capsid-like core particles. *J Biol Chem,* 281**,** 16563-9.

CORTES LEDESMA, F., EL KHAMISY, S. F., ZUMA, M. C., OSBORN, K. & CALDECOTT, K. W. 2009. A human 5'-tyrosyl DNA phosphodiesterase that repairs topoisomerase-mediated DNA damage. *Nature,* 461**,** 674-8.

COSTA, R. H., KALINICHENKO, V. V., HOLTERMAN, A.-X. L. & WANG, X. 2003. Transcription factors in liver development, differentiation, and regeneration. *Hepatology,* 38**,** 1331-1347.

COSTANTINI, S., DI BERNARDO, G., CAMMAROTA, M., CASTELLO, G. & COLONNA, G. 2013. Gene expression signature of human HepG2 cell line. *Gene,* 518**,** 335-45.

COUGOT, D., WU, Y., CAIRO, S., CARAMEL, J., RENARD, C. A., LEVY, L., BUENDIA, M. A. & NEUVEUT, C. 2007. The hepatitis B virus X protein functionally interacts with CREB-binding protein/p300 in the regulation of CREB-mediated transcription. *J Biol Chem,* 282**,** 4277-87.

CREYGHTON, M. P., CHENG, A. W., WELSTEAD, G. G., KOOISTRA, T., CAREY, B. W., STEINE, E. J., HANNA, J., LODATO, M. A., FRAMPTON, G. M., SHARP, P. A., BOYER, L. A., YOUNG, R. A. & JAENISCH, R. 2010. Histone H3K27ac separates active from poised enhancers and predicts developmental state. *Proc Natl Acad Sci U S A,* 107**,** 21931-6.

CUI, X., GUO, J. T. & HU, J. 2015. Hepatitis B Virus Covalently Closed Circular DNA Formation in Immortalized Mouse Hepatocytes Associated with Nucleocapsid Destabilization. *J Virol,* 89**,** 9021-8.

CURSIO, R., MIELE, C., FILIPPA, N., VAN OBBERGHEN, E. & GUGENHEIM, J. 2008. Liver HIF-1 alpha induction precedes apoptosis following normothermic ischemia-reperfusion in rats. *Transplant Proc,* 40**,** 2042-5.

DABEVA, M. D., ALPINI, G., HURSTON, E. & SHAFRITZ, D. A. 1993. Models for hepatic progenitor cell activation. *Proc Soc Exp Biol Med,* 204**,** 242-52.

DAREKAR, S., GEORGIOU, K., YURCHENKO, M., YENAMANDRA, S. P., CHACHAMI, G., SIMOS, G., KLEIN, G. & KASHUBA, E. 2012. Epstein-Barr Virus Immortalization of Human B-Cells Leads to Stabilization of Hypoxia-Induced Factor 1 Alpha, Congruent with the Warburg Effect. *PLoS ONE,* 7**,** e42072.

DECORSIERE, A., MUELLER, H., VAN BREUGEL, P. C., ABDUL, F., GEROSSIER, L., BERAN, R. K., LIVINGSTON, C. M., NIU, C., FLETCHER, S. P., HANTZ, O. & STRUBIN, M. 2016. Hepatitis B virus X protein identifies the Smc5/6 complex as a host restriction factor. *Nature,* 531**,** 386-9.

DELMAS, J., SCHORR, O., JAMARD, C., GIBBS, C., TREPO, C., HANTZ, O. & ZOULIM, F. 2002. Inhibitory effect of adefovir on viral DNA synthesis and covalently closed circular DNA formation in duck hepatitis B virus-infected hepatocytes in vivo and in vitro. *Antimicrob Agents Chemother,* 46**,** 425-33.

DOITSH, G. & SHAUL, Y. 2003. A long HBV transcript encoding pX is inefficiently exported from the nucleus. *Virology,* 309**,** 339-49.

DONATO, M. T., TOLOSA, L. & GOMEZ-LECHON, M. J. 2015. Culture and Functional Characterization of Human Hepatoma HepG2 Cells. *Methods Mol Biol,* 1250**,** 77-93.

EBLE, B. E., LINGAPPA, V. R. & GANEM, D. 1990. The N-terminal (pre-S2) domain of a hepatitis B virus surface glycoprotein is translocated across membranes by downstream signal sequences. *J Virol,* 64**,** 1414-9.

EL-SERAG, H. B. 2012. Epidemiology of Viral Hepatitis and Hepatocellular Carcinoma. *Gastroenterology,* 142**,** 1264-1273.e1.

ELGOUHARI, H. M., ABU-RAJAB TAMIMI, T. I. & CAREY, W. D. 2008. Hepatitis B virus infection: understanding its epidemiology, course, and diagnosis. *Cleve Clin J Med,* 75**,** 881-9.

ESSANI, N. A., FISHER, M. A. & JAESCHKE, H. 1997. Inhibition of NF-kappa B activation by dimethyl sulfoxide correlates with suppression of TNF-alpha formation, reduced ICAM-1 gene transcription, and protection against endotoxin-induced liver injury. *Shock,* 7**,** 90-6.

ESTEBAN, M. A., TRAN, M. G., HARTEN, S. K., HILL, P., CASTELLANOS, M. C., CHANDRA, A., RAVAL, R., O'BRIEN T, S. & MAXWELL, P. H. 2006. Regulation of E-cadherin expression by VHL and hypoxia-inducible factor. *Cancer Res,* 66**,** 3567-75.

EVANS, A. J., RUSSELL, R. C., ROCHE, O., BURRY, T. N., FISH, J. E., CHOW, V. W., KIM, W. Y., SARAVANAN, A., MAYNARD, M. A., GERVAIS, M. L., SUFAN, R. I., ROBERTS, A. M., WILSON, L. A., BETTEN, M., VANDEWALLE, C., BERX, G., MARSDEN, P. A., IRWIN, M. S., TEH, B. T., JEWETT, M. A. & OHH, M. 2007. VHL promotes E2 box-dependent E-cadherin transcription by HIF-mediated regulation of SIP1 and snail. *Mol Cell Biol,* 27**,** 157-69.

EVARTS, R. P., NAGY, P., MARSDEN, E. & THORGEIRSSON, S. S. 1987. A precursor-product relationship exists between oval cells and hepatocytes in rat liver. *Carcinogenesis,* 8**,** 1737-40.

EVARTS, R. P., NAGY, P., NAKATSUKASA, H., MARSDEN, E. & THORGEIRSSON, S. S. 1989. In vivo differentiation of rat liver oval cells into hepatocytes. *Cancer Res,* 49**,** 1541-7.

EVERETT, R. D. 2006. Interactions between DNA viruses, ND10 and the DNA damage response. *Cell Microbiol,* 8**,** 365-74.
FALLOT, G., NEUVEUT, C. & BUENDIA, M. A. 2012. Diverse roles of hepatitis B virus in liver cancer. *Curr Opin Virol,* 2**,** 467-73.
FAUSTO, N. 1990. Hepatocyte differentiation and liver progenitor cells. *Current Opinion in Cell Biology,* 2**,** 1036-1042.
FAUSTO, N. & CAMPBELL, J. S. 2003. The role of hepatocytes and oval cells in liver regeneration and repopulation. *Mechanisms of Development,* 120**,** 117-130.
FAUSTO, N., CAMPBELL, J. S. & RIEHLE, K. J. 2006. Liver regeneration. *Hepatology,* 43**,** S45-S53.
FERRER, C. M., LYNCH, T. P., SODI, V. L., FALCONE, J. N., SCHWAB, L. P., PEACOCK, D. L., VOCADLO, D. J., SEAGROVES, T. N. & REGINATO, M. J. 2014. O-GlcNAcylation regulates cancer metabolism and survival stress signaling via regulation of HIF-1 pathway. *Molecular cell,* 54**,** 820-831.
FIORE, M., ZANIER, R. & DEGRASSI, F. 2002. Reversible G(1) arrest by dimethyl sulfoxide as a new method to synchronize Chinese hamster cells. *Mutagenesis,* 17**,** 419-24.
FOUREL, I., SAPUTELLI, J., SCHAFFER, P. & MASON, W. S. 1994. The carbocyclic analog of 2'-deoxyguanosine induces a prolonged inhibition of duck hepatitis B virus DNA synthesis in primary hepatocyte cultures and in the liver. *J Virol,* 68**,** 1059-65.
FRANOVIC, A., HOLTERMAN, C. E., PAYETTE, J. & LEE, S. 2009. Human cancers converge at the HIF-2α oncogenic axis. *Proceedings of the National Academy of Sciences,* 106**,** 21306-21311.
FROST, J., GALDEANO, C., SOARES, P., GADD, M. S., GRZES, K. M., ELLIS, L., EPEMOLU, O., SHIMAMURA, S., BANTSCHEFF, M., GRANDI, P., READ, K. D., CANTRELL, D. A., ROCHA, S. & CIULLI, A. 2016. Potent and selective chemical probe of hypoxic signalling downstream of HIF-α hydroxylation via VHL inhibition. 7**,** 13312.
FUJITA, H., YAMANAKA, M., IMAMURA, K., TANAKA, Y., NARA, A., YOSHIMORI, T., YOKOTA, S. & HIMENO, M. 2003. A dominant negative form of the AAA ATPase SKD1/VPS4 impairs membrane trafficking out of endosomal/lysosomal compartments: class E vps phenotype in mammalian cells. *J Cell Sci,* 116**,** 401-14.
FULL, F., JUNGNICKL, D., REUTER, N., BOGNER, E., BRULOIS, K., SCHOLZ, B., STURZL, M., MYOUNG, J., JUNG, J. U., STAMMINGER, T. & ENSSER, A. 2014. Kaposi's sarcoma associated herpesvirus tegument protein ORF75 is essential for viral lytic replication and plays a critical role in the antagonization of ND10-instituted intrinsic immunity. *PLoS Pathog,* 10**,** e1003863.
FURUSYO, N., NAKASHIMA, H., KASHIWAGI, K., KUBO, N., HAYASHIDA, K., USUDA, S., MISHIRO, S., KASHIWAGI, S. & HAYASHI, J. 2002. Clinical outcomes of hepatitis B virus (HBV) genotypes B and C in Japanese patients with chronic HBV infection. *Am J Trop Med Hyg,* 67**,** 151-7.
GALLINA, A., BONELLI, F., ZENTILIN, L., RINDI, G., MUTTINI, M. & MILANESI, G. 1989. A recombinant hepatitis B core antigen polypeptide with the protamine-like domain deleted self-assembles into capsid particles but fails to bind nucleic acids. *J Virol,* 63**,** 4645-52.
GALLUCCI, L. & KANN, M. 2017. Nuclear Import of Hepatitis B Virus Capsids and Genome. *Viruses,* 9.
GANE, E. J. 2017. Future anti-HBV strategies. *Liver International,* 37**,** 40-44.
GARCIA, A. D., OSTAPCHUK, P. & HEARING, P. 1993. Functional interaction of nuclear factors EF-C, HNF-4, and RXR alpha with hepatitis B virus enhancer I. *J Virol,* 67**,** 3940-50.
GEBHARDT, R., BALDYSIAK-FIGIEL, A., KRUGEL, V., UEBERHAM, E. & GAUNITZ, F. 2007. Hepatocellular expression of glutamine synthetase: an indicator of morphogen actions as master regulators of zonation in adult liver. *Prog Histochem Cytochem,* 41**,** 201-66.
GENTILE, I., ZAPPULO, E., BUONOMO, A. R. & BORGIA, G. 2014. Prevention of mother-to-child transmission of hepatitis B virus and hepatitis C virus. *Expert Rev Anti Infect Ther,* 12**,** 775-82.

GERLICH, W. H. 2013. Medical virology of hepatitis B: how it began and where we are now. *Virol J,* 10**,** 239.
GHAVAMI, A., VAN DER GIESSEN, E. & ONCK, P. R. 2016. Energetics of Transport through the Nuclear Pore Complex. *PLoS One,* 11.
GILBERT, R. J. C., BEALES, L., BLOND, D., SIMON, M. N., LIN, B. Y., CHISARI, F. V., STUART, D. I. & ROWLANDS, D. J. 2005. Hepatitis B small surface antigen particles are octahedral. *Proc Natl Acad Sci U S A,* 102**,** 14783-8.
GILMORE, T. D. 2006. Introduction to NF-kappaB: players, pathways, perspectives. *Oncogene,* 25**,** 6680-4.
GINGRAS, A. C., KENNEDY, S. G., O'LEARY, M. A., SONENBERG, N. & HAY, N. 1998. 4E-BP1, a repressor of mRNA translation, is phosphorylated and inactivated by the Akt(PKB) signaling pathway. *Genes Dev,* 12**,** 502-13.
GLEBE, D. & URBAN, S. 2007. Viral and cellular determinants involved in hepadnaviral entry. *World J Gastroenterol,* 13**,** 22-38.
GODA, N. & KANAI, M. 2012. Hypoxia-inducible factors and their roles in energy metabolism. *Int J Hematol,* 95**,** 457-63.
GORDAN, J. D., BERTOVRT, J. A., HU, C. J., DIEHL, J. A. & SIMON, M. C. 2007a. HIF-2α promotes hypoxic cell proliferation by enhancing c-Myc transcriptional activity. *Cancer Cell,* 11**,** 335-47.
GORDAN, J. D., THOMPSON, C. B. & SIMON, M. C. 2007b. HIF and c-Myc: sibling rivals for control of cancer cell metabolism and proliferation. *Cancer Cell,* 12**,** 108-13.
GRIPON, P., CANNIE, I. & URBAN, S. 2005. Efficient Inhibition of Hepatitis B Virus Infection by Acylated Peptides Derived from the Large Viral Surface Protein. *J Virol,* 79**,** 1613-22.
GRISHAM, J. W. 1962. A Morphologic Study of Deoxyribonucleic Acid Synthesis and Cell Proliferation in Regenerating Rat Liver; Autoradiography with Thymidine-H<sup>3</sup&gt. *Cancer Research,* 22**,** 842.
GUERQUIN, M. J., RUGGIU, M., RONSIN, O., ROBERT, N., OLIVERA-MARTINEZ, I., NOURISSAT, G., LU, Y., KADLER, K. E., HAVIS, E., DUPREZ, D., DOURSOUNIAN, L., CHARVET, B., BONNIN, M. A., BERENBAUM, F. & BAUMBERGER, T. 2013. Transcription factor EGR1 directs tendon differentiation and promotes tendon repair. 123**,** 3564-76.
GUILLAUMOND, F., LECA, J., OLIVARES, O., LAVAUT, M.-N., VIDAL, N., BERTHEZÈNE, P., DUSETTI, N. J., LONCLE, C., CALVO, E., TURRINI, O., IOVANNA, J. L., TOMASINI, R. & VASSEUR, S. 2013. Strengthened glycolysis under hypoxia supports tumor symbiosis and hexosamine biosynthesis in pancreatic adenocarcinoma. *Proceedings of the National Academy of Sciences of the United States of America,* 110**,** 3919-3924.
GUO, H., XU, C., ZHOU, T., BLOCK, T. M. & GUO, J. T. 2012. Characterization of the Host Factors Required for Hepadnavirus Covalently Closed Circular (ccc) DNA Formation. *PLoS One,* 7.
GUO, Y., LI, Y., MU, S., ZHANG, J. & YAN, Z. 2009. Evidence that methylation of hepatitis B virus covalently closed circular DNA in liver tissues of patients with chronic hepatitis B modulates HBV replication. *J Med Virol,* 81**,** 1177-83.
GUZY, R. D., HOYOS, B., ROBIN, E., CHEN, H., LIU, L., MANSFIELD, K. D., SIMON, M. C., HAMMERLING, U. & SCHUMACKER, P. T. 2005. Mitochondrial complex III is required for hypoxia-induced ROS production and cellular oxygen sensing. *Cell Metab,* 1**,** 401-8.
HALPERN, M. S., ENGLAND, J. M., DEERY, D. T., PETCU, D. J., MASON, W. S. & MOLNAR-KIMBER, K. L. 1983. Viral nucleic acid synthesis and antigen accumulation in pancreas and kidney of Pekin ducks infected with duck hepatitis B virus. *Proc Natl Acad Sci U S A,* 80**,** 4865-9.
HANCOCK, R. L., DUNNE, K., WALPORT, L. J., FLASHMAN, E. & KAWAMURA, A. 2015. Epigenetic regulation by histone demethylases in hypoxia. *Epigenomics,* 7**,** 791-811.
HARRIS, R. S., PETERSEN-MAHRT, S. K. & NEUBERGER, M. S. 2002. RNA editing enzyme APOBEC1 and some of its homologs can act as DNA mutators. *Mol Cell,* 10**,** 1247-53.

HATTON, T., ZHOU, S. & STANDRING, D. N. 1992. RNA- and DNA-binding activities in hepatitis B virus capsid protein: a model for their roles in viral replication. *J Virol,* 66**,** 5232-41.

HAY, D. C., ZHAO, D., FLETCHER, J., HEWITT, Z. A., MCLEAN, D., URRUTICOECHEA-URIGUEN, A., BLACK, J. R., ELCOMBE, C., ROSS, J. A., WOLF, R. & CUI, W. 2008. Efficient differentiation of hepatocytes from human embryonic stem cells exhibiting markers recapitulating liver development in vivo. *Stem Cells,* 26**,** 894-902.

HEERMANN, K. H., GOLDMANN, U., SCHWARTZ, W., SEYFFARTH, T., BAUMGARTEN, H. & GERLICH, W. H. 1984. Large surface proteins of hepatitis B virus containing the pre-s sequence. *J Virol,* 52**,** 396-402.

HEIKKILA, M., PASANEN, A., KIVIRIKKO, K. I. & MYLLYHARJU, J. 2011. Roles of the human hypoxia-inducible factor (HIF)-3alpha variants in the hypoxia response. *Cell Mol Life Sci,* 68**,** 3885-901.

HELENIUS, A. & AEBI, M. 2001. Intracellular functions of N-linked glycans. *Science,* 291**,** 2364-9.

HERZIG, S., HEDRICK, S., MORANTTE, I., KOO, S. H., GALIMI, F. & MONTMINY, M. 2003. CREB controls hepatic lipid metabolism through nuclear hormone receptor PPAR-gamma. *Nature,* 426**,** 190-3.

HERZIG, S., LONG, F., JHALA, U. S., HEDRICK, S., QUINN, R., BAUER, A., RUDOLPH, D., SCHUTZ, G., YOON, C., PUIGSERVER, P., SPIEGELMAN, B. & MONTMINY, M. 2001. CREB regulates hepatic gluconeogenesis through the coactivator PGC-1. *Nature,* 413**,** 179-83.

HESS, J., ANGEL, P. & SCHORPP-KISTNER, M. 2004. AP-1 subunits: quarrel and harmony among siblings. *J Cell Sci,* 117**,** 5965-73.

HILDT, E., SAHER, G., BRUSS, V. & HOFSCHNEIDER, P. H. 1996. The hepatitis B virus large surface protein (LHBs) is a transcriptional activator. *Virology,* 225**,** 235-9.

HOFFMANN, J., BOEHM, C., HIMMELSBACH, K., DONNERHAK, C., ROETTGER, H., WEISS, T. S., PLOEN, D. & HILDT, E. 2013. Identification of alpha-taxilin as an essential factor for the life cycle of hepatitis B virus. *J Hepatol,* 59**,** 934-41.

HOLOTNAKOVA, T., TYLKOVA, L., TAKACOVA, M., KOPACEK, J., PETRIK, J., PASTOREKOVA, S. & PASTOREK, J. 2010. Role of the HBx oncoprotein in carbonic anhydrase 9 induction. *J Med Virol,* 82**,** 32-40.

HOLTZINGER, A., STREETER, P. R., SARANGI, F., HILLBORN, S., NIAPOUR, M., OGAWA, S. & KELLER, G. 2015. New markers for tracking endoderm induction and hepatocyte differentiation from human pluripotent stem cells. *Development,* 142**,** 4253-65.

HOU, J., LIU, Z. & GU, F. 2005. Epidemiology and Prevention of Hepatitis B Virus Infection. *Int J Med Sci,* 2**,** 50-7.

HU, C. J., WANG, L. Y., CHODOSH, L. A., KEITH, B. & SIMON, M. C. 2003. Differential Roles of Hypoxia-Inducible Factor 1α (HIF-1α) and HIF-2α in Hypoxic Gene Regulation. *Mol Cell Biol,* 23**,** 9361-74.

HU, J. & BOYER, M. 2006. Hepatitis B Virus Reverse Transcriptase and ε RNA Sequences Required for Specific Interaction In Vitro. *J Virol,* 80**,** 2141-50.

HU, J. & SEEGER, C. 1996. Hsp90 is required for the activity of a hepatitis B virus reverse transcriptase. *Proc Natl Acad Sci U S A,* 93**,** 1060-4.

HU, J. & SEEGER, C. 2015. Hepadnavirus Genome Replication and Persistence. *Cold Spring Harb Perspect Med,* 5.

HU, J., TOFT, D. O. & SEEGER, C. 1997. Hepadnavirus assembly and reverse transcription require a multi-component chaperone complex which is incorporated into nucleocapsids. *Embo j,* 16**,** 59-68.

HU, J. L., LIU, L. P., YANG, S. L., FANG, X., WEN, L., REN, Q. G. & YU, C. 2016. Hepatitis B virus induces hypoxia-inducible factor-2alpha expression through hepatitis B virus X protein. *Oncol Rep,* 35**,** 1443-8.

HUANG, H. C., CHEN, C. C., CHANG, W. C., TAO, M. H. & HUANG, C. 2012. Entry of hepatitis B virus into immortalized human primary hepatocytes by clathrin-dependent endocytosis. *J Virol,* 86**,** 9443-53.

HUANG, Y. Q., WANG, L. W., YAN, S. N. & GONG, Z. J. 2004. Effects of cell cycle on telomerase activity and on hepatitis B virus replication in HepG2 2.2.15 cells. *Hepatobiliary Pancreat Dis Int,* 3**,** 543-7.

HUNG, C. M., HUANG, W. C., PAN, H. L., CHIEN, P. H., LIN, C. W., CHEN, L. C., CHIEN, Y. F., LIN, C. C., LEOW, K. H., CHEN, W. S., CHEN, J. Y., HO, C. Y., HOU, P. S. & CHEN, Y. J. 2014. Hepatitis B virus X upregulates HuR protein level to stabilize HER2 expression in hepatocellular carcinoma cells. *Biomed Res Int,* 2014**,** 827415.

HUOVILA, A. P., EDER, A. M. & FULLER, S. D. 1992. Hepatitis B surface antigen assembles in a post-ER, pre-Golgi compartment. *J Cell Biol,* 118**,** 1305-20.

IMTIYAZ, H. Z. & SIMON, M. C. 2010. Hypoxia-inducible factors as essential regulators of inflammation. *Curr Top Microbiol Immunol,* 345**,** 105-20.

IMTIYAZ, H. Z., YUAN, L. J., WILLIAMS, E. P., SIMON, M. C., PATEL, S. A., KEITH, B., HICKEY, M. M., HAMMOND, R., GIMOTTY, P. A. & DURHAM, A. C. 2010. Hypoxia-inducible factor 2α regulates macrophage function in mouse models of acute and tumor inflammation. 120**,** 2699-714.

ISAACS, J. S., JUNG, Y. J., MOLE, D. R., LEE, S., TORRES-CABALA, C., CHUNG, Y. L., MERINO, M., TREPEL, J., ZBAR, B., TORO, J., RATCLIFFE, P. J., LINEHAN, W. M. & NECKERS, L. 2005. HIF overexpression correlates with biallelic loss of fumarate hydratase in renal cancer: novel role of fumarate in regulation of HIF stability. *Cancer Cell,* 8**,** 143-53.

ISORCE, N., LUCIFORA, J., ZOULIM, F. & DURANTEL, D. 2015. Immune-modulators to combat hepatitis B virus infection: From IFN-alpha to novel investigational immunotherapeutic strategies. *Antiviral Res,* 122**,** 69-81.

JENH, A. M., THIO, C. L. & PHAM, P. A. 2009. Tenofovir for the treatment of hepatitis B virus. *Pharmacotherapy,* 29**,** 1212-27.

JHAM, B. C., MA, T., HU, J., CHAISUPARAT, R., FRIEDMAN, E. R., PANDOLFI, P. P., SCHNEIDER, A., SODHI, A. & MONTANER, S. 2011. Amplification of the Angiogenic Signal through the Activation of the TSC/mTOR/HIF Axis by the KSHV vGPCR in Kaposi's Sarcoma. *PLoS ONE,* 6**,** e19103.

JIA, X., CHEN, J., MEGGER, D. A., ZHANG, X., KOZLOWSKI, M., ZHANG, L., FANG, Z., LI, J., CHU, Q., WU, M., LI, Y., SITEK, B. & YUAN, Z. 2017. Label-free Proteomic Analysis of Exosomes Derived from Inducible Hepatitis B Virus-Replicating HepAD38 Cell Line. *Mol Cell Proteomics,* 16**,** S144-s160.

JIANG, B., HIMMELSBACH, K., REN, H., BOLLER, K. & HILDT, E. 2016. Subviral Hepatitis B Virus Filaments, like Infectious Viral Particles, Are Released via Multivesicular Bodies. *J Virol,* 90**,** 3330-41.

JILBERT, A. R., FREIMAN, J. S., GOWANS, E. J., HOLMES, M., COSSART, Y. E. & BURRELL, C. J. 1987. Duck hepatitis B virus DNA in liver, spleen, and pancreas: analysis by in situ and Southern blot hybridization. *Virology,* 158**,** 330-8.

JOKILEHTO, T. & JAAKKOLA, P. M. 2010. The role of HIF prolyl hydroxylases in tumour growth. *Journal of Cellular and Molecular Medicine,* 14**,** 758-770.

JONES, S. A., BOREGOWDA, R., SPRATT, T. E. & HU, J. 2012. In Vitro Epsilon RNA-Dependent Protein Priming Activity of Human Hepatitis B Virus Polymerase. *Journal of Virology,* 86**,** 5134-5150.

JONES, S. A., CLARK, D. N., CAO, F., TAVIS, J. E. & HU, J. 2014. Comparative Analysis of Hepatitis B Virus Polymerase Sequences Required for Viral RNA Binding, RNA Packaging, and Protein Priming. *J Virol,* 88**,** 1564-72.

JONES, S. A. & HU, J. 2013. Hepatitis B virus reverse transcriptase: diverse functions as classical and emerging targets for antiviral intervention. *Emerging Microbes & Infections,* 2**,** e56.

JUNGERMANN, K. & KIETZMANN, T. 2000. Oxygen: Modulator of metabolic zonation and disease of the liver. *Hepatology,* 31**,** 255-260.

KAELIN, W. G., JR. 2008. The von Hippel-Lindau tumour suppressor protein: O2 sensing and cancer. *Nat Rev Cancer,* 8**,** 865-73.

KAELIN, W. G., JR. & RATCLIFFE, P. J. 2008. Oxygen sensing by metazoans: the central role of the HIF hydroxylase pathway. *Mol Cell,* 30**,** 393-402.
KANNO, T., BERTA, D. G. & SJOGREN, C. 2015. The Smc5/6 Complex Is an ATP-Dependent Intermolecular DNA Linker. *Cell Rep,* 12**,** 1471-82.
KAWANAKA, T., KUBO, A., IKUSHIMA, H., SANO, T., TAKEGAWA, Y. & NISHITANI, H. 2008. Prognostic significance of HIF-2alpha expression on tumor infiltrating macrophages in patients with uterine cervical cancer undergoing radiotherapy. *J Med Invest,* 55**,** 78-86.
KEITH, B., JOHNSON, R. S. & SIMON, M. C. 2011. HIF1α and HIF2α: sibling rivalry in hypoxic tumor growth and progression. 12**,** 9-22.
KIM, B. K., LIM, S. O. & PARK, Y. G. 2008. Requirement of the cyclic adenosine monophosphate response element-binding protein for hepatitis B virus replication. *Hepatology,* 48**,** 361-73.
KIM, C. H. 2014. Hidden secret in hepatitis B viral X protein mutation and hypoxia-inducible factor-1alpha in hepatocarcinoma cancer. *Hepatobiliary Surg Nutr,* 3**,** 115-7.
KIM, H. R., LEE, S. H. & JUNG, G. 2010a. The hepatitis B viral X protein activates NF-kappaB signaling pathway through the up-regulation of TBK1. *FEBS Lett,* 584**,** 525-30.
KIM, J. W., TCHERNYSHYOV, I., SEMENZA, G. L. & DANG, C. V. 2006a. HIF-1-mediated expression of pyruvate dehydrogenase kinase: a metabolic switch required for cellular adaptation to hypoxia. *Cell Metab,* 3**,** 177-85.
KIM, S., WANG, H. & RYU, W. S. 2010b. Incorporation of Eukaryotic Translation Initiation Factor eIF4E into Viral Nucleocapsids via Interaction with Hepatitis B Virus Polymerase. *J Virol,* 84**,** 52-8.
KIM, S. G., MANES, N. P., EL-MAGHRABI, M. R. & LEE, Y. H. 2006b. Crystal structure of the hypoxia-inducible form of 6-phosphofructo-2-kinase/fructose-2,6-bisphosphatase (PFKFB3): a possible new target for cancer therapy. *J Biol Chem,* 281**,** 2939-44.
KIM, S. H., JEONG, J. W., PARK, J. A., LEE, J. W., SEO, J. H., JUNG, B. K., BAE, M. K. & KIM, K. W. 2007. Regulation of the HIF-1alpha stability by histone deacetylases. *Oncol Rep,* 17**,** 647-51.
KIM, W., LEE, S., SON, Y., KO, C. & RYU, W. S. 2016. DDB1 Stimulates Viral Transcription of Hepatitis B Virus via HBx-Independent Mechanisms. *J Virol,* 90**,** 9644-53.
KIM, W. Y., PERERA, S., ZHOU, B., CARRETERO, J., YEH, J. J., HEATHCOTE, S. A., JACKSON, A. L., NIKOLINAKOS, P., OSPINA, B., NAUMOV, G., BRANDSTETTER, K. A., WEIGMAN, V. J., ZAGHLUL, S., HAYES, D. N., PADERA, R. F., HEYMACH, J. V., KUNG, A. L., SHARPLESS, N. E., KAELIN, W. G., JR. & WONG, K. K. 2009. HIF2alpha cooperates with RAS to promote lung tumorigenesis in mice. *J Clin Invest,* 119**,** 2160-70.
KIMATA, T., NAGAKI, M., TSUKADA, Y., OGISO, T. & MORIWAKI, H. 2006. Hepatocyte nuclear factor-4alpha and -1 small interfering RNA inhibits hepatocyte differentiation induced by extracellular matrix. *Hepatol Res,* 35**,** 3-9.
KING, A., SELAK, M. A. & GOTTLIEB, E. 2006. Succinate dehydrogenase and fumarate hydratase: linking mitochondrial dysfunction and cancer. *Oncogene,* 25**,** 4675-82.
KO, C., LEE, S., WINDISCH, M. P. & RYU, W. S. 2014. DDX3 DEAD-box RNA helicase is a host factor that restricts hepatitis B virus replication at the transcriptional level. *J Virol,* 88**,** 13689-98.
KOCK, J. & SCHLICHT, H. J. 1993. Analysis of the earliest steps of hepadnavirus replication: genome repair after infectious entry into hepatocytes does not depend on viral polymerase activity. *J Virol,* 67**,** 4867-74.
KOLIOS, G., VALATAS, V. & KOUROUMALIS, E. 2006. Role of Kupffer cells in the pathogenesis of liver disease. *World J Gastroenterol,* 12**,** 7413-20.
KOUMBI, L. & KARAYIANNIS, P. 2015. The Epigenetic Control of Hepatitis B Virus Modulates the Outcome of Infection. *Frontiers in Microbiology,* 6**,** 1491.
KOVACEVIC, Z. & RICHARDSON, D. R. 2006. The metastasis suppressor, Ndrg-1: a new ally in the fight against cancer. *Carcinogenesis,* 27**,** 2355-66.

KRAINC, D., BAI, G., OKAMOTO, S., CARLES, M., KUSIAK, J. W., BRENT, R. N. & LIPTON, S. A. 1998. Synergistic activation of the N-methyl-D-aspartate receptor subunit 1 promoter by myocyte enhancer factor 2C and Sp1. *J Biol Chem,* 273**,** 26218-24.

KRISHNAMACHARY, B., ZAGZAG, D., NAGASAWA, H., RAINEY, K., OKUYAMA, H., BAEK, J. H. & SEMENZA, G. L. 2006. Hypoxia-inducible factor-1-dependent repression of E-cadherin in von Hippel-Lindau tumor suppressor-null renal cell carcinoma mediated by TCF3, ZFHX1A, and ZFHX1B. *Cancer Res,* 66**,** 2725-31.

KUMAR, V., JAYASURYAN, N. & KUMAR, R. 1996. A truncated mutant (residues 58-140) of the hepatitis B virus X protein retains transactivation function. *Proc Natl Acad Sci U S A,* 93**,** 5647-52.

KWON, S. Y. & LEE, C. H. 2011. Epidemiology and prevention of hepatitis B virus infection. *Korean J Hepatol,* 17**,** 87-95.

LADNER, S. K., OTTO, M. J., BARKER, C. S., ZAIFERT, K., WANG, G. H., GUO, J. T., SEEGER, C. & KING, R. W. 1997. Inducible expression of human hepatitis B virus (HBV) in stably transfected hepatoblastoma cells: a novel system for screening potential inhibitors of HBV replication. *Antimicrob Agents Chemother,* 41**,** 1715-20.

LAMBERT, C., DÖRING, T. & PRANGE, R. 2007. Hepatitis B Virus Maturation Is Sensitive to Functional Inhibition of ESCRT-III, Vps4, and γ2-Adaptin. *J Virol,* 81**,** 9050-60.

LAMONTAGNE, R. J., BAGGA, S. & BOUCHARD, M. J. 2016. Hepatitis B virus molecular biology and pathogenesis. *Hepatoma Research,* 2**,** 163-186.

LEBOSSÉ, F., TESTONI, B., FRESQUET, J., FACCHETTI, F., GALMOZZI, E., FOURNIER, M., HERVIEU, V., BERTHILLON, P., BERBY, F., BORDES, I., DURANTEL, D., LEVRERO, M., LAMPERTICO, P. & ZOULIM, F. 2016. Intrahepatic innate immune response pathways are downregulated in untreated chronic hepatitis B. *Journal of Hepatology,* 66**,** 897-909.

LEDAKI, I., MCINTYRE, A., WIGFIELD, S., BUFFA, F., MCGOWAN, S., BABAN, D., LI, J. & HARRIS, A. L. 2015. Carbonic anhydrase IX induction defines a heterogeneous cancer cell response to hypoxia and mediates stem cell-like properties and sensitivity to HDAC inhibition. *Oncotarget,* 6**,** 19413-27.

LEEK, R. D., TALKS, K. L., PEZZELLA, F., TURLEY, H., CAMPO, L., BROWN, N. S., BICKNELL, R., TAYLOR, M., GATTER, K. C. & HARRIS, A. L. 2002. Relation of hypoxia-inducible factor-2 alpha (HIF-2 alpha) expression in tumor-infiltrative macrophages to tumor angiogenesis and the oxidative thymidine phosphorylase pathway in Human breast cancer. *Cancer Res,* 62**,** 1326-9.

LEISTNER, C. M., GRUEN-BERNHARD, S. & GLEBE, D. 2008. Role of glycosaminoglycans for binding and infection of hepatitis B virus. *Cell Microbiol,* 10**,** 122-33.

LEMPP, F. A. & URBAN, S. 2014. Inhibitors of hepatitis B virus attachment and entry. *Intervirology,* 57**,** 151-7.

LEVRERO, M., POLLICINO, T., PETERSEN, J., BELLONI, L., RAIMONDO, G. & DANDRI, M. 2009. Control of cccDNA function in hepatitis B virus infection. *J Hepatol,* 51**,** 581-92.

LI, F., SHI, W., CAPURRO, M. & FILMUS, J. 2011. Glypican-5 stimulates rhabdomyosarcoma cell proliferation by activating Hedgehog signaling. *J Cell Biol,* 192**,** 691-704.

LI, H., ZHU, W., ZHANG, L., LEI, H., WU, X., GUO, L., CHEN, X., WANG, Y. & TANG, H. 2015. The metabolic responses to hepatitis B virus infection shed new light on pathogenesis and targets for treatment. *Scientific Reports,* 5**,** 8421.

LI, H. C., HUANG, E. Y., SU, P. Y., WU, S. Y., YANG, C. C., LIN, Y. S., CHANG, W. C. & SHIH, C. 2010a. Nuclear Export and Import of Human Hepatitis B Virus Capsid Protein and Particles. *PLoS Pathog,* 6.

LI, J. & OU, J. H. 2001. Differential regulation of hepatitis B virus gene expression by the Sp1 transcription factor. *J Virol,* 75**,** 8400-6.

LI, M., XIE, Y., WU, X., KONG, Y. & WANG, Y. 1995. HNF3 binds and activates the second enhancer, ENII, of hepatitis B virus. *Virology,* 214**,** 371-8.

LI, S., YANG, Y., DING, X., YANG, M., SHE, S., PENG, H., XU, X., RAN, X., LI, S., HU, P., HU, H., ZHANG, D. & REN, H. 2017. LHBs can elevate the expression of MDR1 through

HIF-1alpha in patients with CHB infection: a comparative proteomic study. *Oncotarget,* 8**,** 4549-4562.
LI, T., ROBERT, E. I., VAN BREUGEL, P. C., STRUBIN, M. & ZHENG, N. 2010b. A promiscuous alpha-helical motif anchors viral hijackers and substrate receptors to the CUL4-DDB1 ubiquitin ligase machinery. *Nat Struct Mol Biol,* 17**,** 105-11.
LI, W. & URBAN, S. 2016. Entry of hepatitis B and hepatitis D virus into hepatocytes: Basic insights and clinical implications. *J Hepatol,* 64**,** S32-40.
LIANG, D., KONG, X. & SANG, N. 2006. Effects of Histone Deacetylase Inhibitors on HIF-1. *Cell cycle (Georgetown, Tex.),* 5**,** 2430-2435.
LIANG, T. J. 2009. Hepatitis B: the virus and disease. *Hepatology,* 49**,** S13-21.
LIM, R. Y., FAHRENKROG, B., KOSER, J., SCHWARZ-HERION, K., DENG, J. & AEBI, U. 2007. Nanomechanical basis of selective gating by the nuclear pore complex. *Science,* 318**,** 640-3.
LIN, C., MCGOUGH, R., ASWAD, B., BLOCK, J. A. & TEREK, R. 2004. Hypoxia induces HIF-1alpha and VEGF expression in chondrosarcoma cells and chondrocytes. *J Orthop Res,* 22**,** 1175-81.
LIN, J., GU, C., SHEN, Z., LIU, Y., WANG, W., TAO, S., CUI, X., LIU, J. & XIE, Y. 2017. Hepatocyte nuclear factor 1alpha downregulates HBV gene expression and replication by activating the NF-kappaB signaling pathway. *PLoS One,* 12**,** e0174017.
LIN, T.-Y., CHOU, C.-F., CHUNG, H.-Y., CHIANG, C.-Y., LI, C.-H., WU, J.-L., LIN, H.-J., PAI, T.-W., HU, C.-H. & TZOU, W.-S. 2014. Hypoxia-Inducible Factor 2 Alpha Is Essential for Hepatic Outgrowth and Functions via the Regulation of leg1 Transcription in the Zebrafish Embryo. *PLOS ONE,* 9**,** e101980.
LIN, Y. C., HSU, E. C. & TING, L. P. 2009. Repression of hepatitis B viral gene expression by transcription factor nuclear factor-kappaB. *Cell Microbiol,* 11**,** 645-60.
LIU, J., AHIEKPOR, A., LI, L., LI, X., ARBUTHNOT, P., KEW, M. & FEITELSON, M. A. 2009. Increased expression of ErbB-2 in liver is associated with hepatitis B x antigen and shorter survival in patients with liver cancer. *Int J Cancer,* 125**,** 1894-901.
LIU, L. P., HU, B. G., YE, C., HO, R. L., CHEN, G. G. & LAI, P. B. 2014. HBx mutants differentially affect the activation of hypoxia-inducible factor-1alpha in hepatocellular carcinoma. *Br J Cancer,* 110**,** 1066-73.
LIU, P., FANG, X., SONG, Y., JIANG, J., HE, Q. & LIU, X. 2016. Expression of hypoxia-inducible factor 3α in hepatocellular carcinoma and its association with other hypoxia-inducible factors. *Exp Ther Med,* 11**,** 2470-6.
LIVINGSTON, C. M., RAMAKRISHNAN, D., STRUBIN, M., FLETCHER, S. P. & BERAN, R. K. 2017. Identifying and Characterizing Interplay between Hepatitis B Virus X Protein and Smc5/6. *Viruses,* 9.
LOEB, D. D., HIRSCH, R. C. & GANEM, D. 1991. Sequence-independent RNA cleavages generate the primers for plus strand DNA synthesis in hepatitis B viruses: implications for other reverse transcribing elements. *Embo j,* 10**,** 3533-40.
LOEB, D. D. & TIAN, R. 1995. Transfer of the minus strand of DNA during hepadnavirus replication is not invariable but prefers a specific location. *J Virol,* 69**,** 6886-91.
LU, F. M., LI, T., LIU, S. & ZHUANG, H. 2010. Epidemiology and prevention of hepatitis B virus infection in China. *Journal of Viral Hepatitis,* 17**,** 4-9.
LU, X., LU, Y., GESCHWINDT, R., DWEK, R. A. & BLOCK, T. M. 2001. Hepatitis B virus MHBs antigen is selectively sensitive to glucosidase-mediated processing in the endoplasmic reticulum. *DNA Cell Biol,* 20**,** 647-56.
LUANGSAY, S., GRUFFAZ, M., ISORCE, N., TESTONI, B., MICHELET, M., FAURE-DUPUY, S., MAADADI, S., AIT-GOUGHOULTE, M., PARENT, R., RIVOIRE, M., JAVANBAKHT, H., LUCIFORA, J., DURANTEL, D. & ZOULIM, F. 2015. Early inhibition of hepatocyte innate responses by hepatitis B virus. *Journal of Hepatology,* 63**,** 1314-1322.
LUCIFORA, J., ARZBERGER, S., DURANTEL, D., BELLONI, L., STRUBIN, M., LEVRERO, M., ZOULIM, F., HANTZ, O. & PROTZER, U. 2011. Hepatitis B virus X protein is essential to initiate and maintain virus replication after infection. *J Hepatol,* 55**,** 996-1003.

LUCIFORA, J. P., U. 2012. 'Hepatitis B Virus X Protein: A Key Regulator of the Virus Life Cycle'. *In:* GARCIA, M. L. R., V (ed.) *Viral Genomes—Molecular Structure, Diversity, Gene Expression Mechanisms and Host-Virus Interactions.*

LUTGEHETMANN, M., MANCKE, L. V., VOLZ, T., HELBIG, M., ALLWEISS, L., BORNSCHEUER, T., POLLOK, J. M., LOHSE, A. W., PETERSEN, J., URBAN, S. & DANDRI, M. 2012. Humanized chimeric uPA mouse model for the study of hepatitis B and D virus interactions and preclinical drug evaluation. *Hepatology,* 55**,** 685-94.

LUTGEHETMANN, M., VOLZ, T., KOPKE, A., BROJA, T., TIGGES, E., LOHSE, A. W., FUCHS, E., MURRAY, J. M., PETERSEN, J. & DANDRI, M. 2010. In vivo proliferation of hepadnavirus-infected hepatocytes induces loss of covalently closed circular DNA in mice. *Hepatology,* 52**,** 16-24.

MACDONALD, R. A. 1961. "lifespan" of liver cells: Autoradiographic study using tritiated thymidine in normal, cirrhotic, and partially hepatectomized rats. *Archives of Internal Medicine,* 107**,** 335-343.

MAHONEY, F. J. 1999. Update on Diagnosis, Management, and Prevention of Hepatitis B Virus Infection. *Clin Microbiol Rev,* 12**,** 351-66.

MAJMUNDAR, A. J., SKULI, N., MESQUITA, R. C., KIM, M. N., YODH, A. G., NGUYEN-MCCARTY, M. & SIMON, M. C. 2012. O(2) Regulates Skeletal Muscle Progenitor Differentiation through Phosphatidylinositol 3-Kinase/AKT Signaling. *Mol Cell Biol,* 32**,** 36-49.

MAJMUNDAR, A. J., WONG, W. J. & SIMON, M. C. 2010. Hypoxia inducible factors and the response to hypoxic stress. *Mol Cell,* 40**,** 294-309.

MAK, P., LEAV, I., PURSELL, B., BAE, D., YANG, X., TAGLIENTI, C. A., GOUVIN, L. M., SHARMA, V. M. & MERCURIO, A. M. 2010. ERβ Impedes Prostate Cancer EMT by Destabilizing HIF-1α and Inhibiting VEGF-Mediated Snail Nuclear Localization: Implications for Gleason Grading. *Cancer Cell,* 17**,** 319-32.

MANYAHI, J., MSIGWA, Y., MHIMBIRA, F. & MAJIGO, M. 2017. High sero-prevalence of hepatitis B virus and human immunodeficiency virus infections among pregnant women attending antenatal clinic at Temeke municipal health facilities, Dar es Salaam, Tanzania: a cross sectional study. *BMC Pregnancy Childbirth,* 17.

MASTROGIANNAKI, M., VAULONT, S., SIMON, M. C., PEYSSONNAUX, C., MATAK, P. & KEITH, B. 2009. HIF-2α, but not HIF-1α, promotes iron absorption in mice. 119**,** 1159-66.

MATSUMOTO, T., BOHMAN, S., DIXELIUS, J., BERGE, T., DIMBERG, A., MAGNUSSON, P., WANG, L., WIKNER, C., QI, J. H., WERNSTEDT, C., WU, J., BRUHEIM, S., MUGISHIMA, H., MUKHOPADHYAY, D., SPURKLAND, A. & CLAESSON-WELSH, L. 2005. VEGF receptor-2 Y951 signaling and a role for the adapter molecule TSAd in tumor angiogenesis. *Embo j,* 24**,** 2342-53.

MAXWELL, P. H. & ECKARDT, K.-U. 2016. HIF prolyl hydroxylase inhibitors for the treatment of renal anaemia and beyond. *Nat Rev Nephrol,* 12**,** 157-168.

MAYNARD, M. A., QI, H., CHUNG, J., LEE, E. H., KONDO, Y., HARA, S., CONAWAY, R. C., CONAWAY, J. W. & OHH, M. 2003. Multiple splice variants of the human HIF-3 alpha locus are targets of the von Hippel-Lindau E3 ubiquitin ligase complex. *J Biol Chem,* 278**,** 11032-40.

MCINTYRE, A., PATIAR, S., WIGFIELD, S., LI, J. L., LEDAKI, I., TURLEY, H., LEEK, R., SNELL, C., GATTER, K., SLY, W. S., VAUGHAN-JONES, R. D., SWIETACH, P. & HARRIS, A. L. 2012. Carbonic anhydrase IX promotes tumor growth and necrosis in vivo and inhibition enhances anti-VEGF therapy. *Clin Cancer Res,* 18**,** 3100-11.

MEIER, A., MEHRLE, S., WEISS, T. S., MIER, W. & URBAN, S. 2013. Myristoylated PreS1-domain of the hepatitis B virus L-protein mediates specific binding to differentiated hepatocytes. *Hepatology,* 58**,** 31-42.

MEREDITH, L. W., HU, K., CHENG, X., HOWARD, C. R., BAUMERT, T. F., BALFE, P., VAN DE GRAAF, K. F., PROTZER, U. & MCKEATING, J. A. 2016. Lentiviral hepatitis B pseudotype entry requires sodium taurocholate co-transporting polypeptide and additional hepatocyte-specific factors. *J Gen Virol,* 97**,** 121-7.

MICHALIK, L., AUWERX, J., BERGER, J. P., CHATTERJEE, V. K., GLASS, C. K., GONZALEZ, F. J., GRIMALDI, P. A., KADOWAKI, T., LAZAR, M. A., O'RAHILLY, S., PALMER, C. N., PLUTZKY, J., REDDY, J. K., SPIEGELMAN, B. M., STAELS, B. & WAHLI, W. 2006. International Union of Pharmacology. LXI. Peroxisome proliferator-activated receptors. *Pharmacol Rev,* 58**,** 726-41.

MILICH, D. & LIANG, T. J. 2003. Exploring the biological basis of hepatitis B e antigen in hepatitis B virus infection. *Hepatology,* 38**,** 1075-1086.

MILICH, D. R., PETERSON, D. L., SCHÖDEL, F., JONES, J. E. & HUGHES, J. L. 1995. Preferential recognition of hepatitis B nucleocapsid antigens by Th1 or Th2 cells is epitope and major histocompatibility complex dependent. *J Virol,* 69**,** 2776-85.

MISHRA, A. K., PANT, K., PRADHAN, S. M. & VENUGOPAL, S. K. 2017. Reactive Oxygen Species Produced by HBV Help in Replication and Autophagy in Host Cells. *Journal of Clinical and Experimental Hepatology,* 7**,** S18.

MONTERO, H., GARCÍA-ROMÁN, R. & MORA, S. I. 2015. eIF4E as a Control Target for Viruses. *Viruses,* 7**,** 739-50.

MOON, E. J., JEONG, C. H., JEONG, J. W., KIM, K. R., YU, D. Y., MURAKAMI, S., KIM, C. W. & KIM, K. W. 2004. Hepatitis B virus X protein induces angiogenesis by stabilizing hypoxia-inducible factor-1alpha. *Faseb j,* 18**,** 382-4.

MOON, J. O., WELCH, T. P., GONZALEZ, F. J. & COPPLE, B. L. 2009. Reduced liver fibrosis in hypoxia-inducible factor-1alpha-deficient mice. *Am J Physiol Gastrointest Liver Physiol,* 296**,** G582-92.

MORALEDA, G., SAPUTELLI, J., ALDRICH, C. E., AVERETT, D., CONDREAY, L. & MASON, W. S. 1997. Lack of effect of antiviral therapy in nondividing hepatocyte cultures on the closed circular DNA of woodchuck hepatitis virus. *J Virol,* 71**,** 9392-9.

MORIKAWA, K., SUDA, G. & SAKAMOTO, N. 2016. Viral life cycle of hepatitis B virus: Host factors and druggable targets. *Hepatology Research,* 46**,** 871-877.

MURAKAMI, S. 1999. Hepatitis B virus X protein: structure, function and biology. *Intervirology,* 42**,** 81-99.

MURAKAMI, S. 2001. Hepatitis B virus X protein: a multifunctional viral regulator. *J Gastroenterol,* 36**,** 651-60.

MURDOCH, C., GIANNOUDIS, A. & LEWIS, C. E. 2004. Mechanisms regulating the recruitment of macrophages into hypoxic areas of tumors and other ischemic tissues. *Blood,* 104**,** 2224-34.

MURPHY, C. M., XU, Y., LI, F., NIO, K., RESZKA-BLANCO, N., LI, X., WU, Y., YU, Y., XIONG, Y. & SU, L. 2016. Hepatitis B Virus X protein promotes degradation of SMC5/6 to enhance HBV replication. *Cell Rep,* 16**,** 2846-54.

NASSAL, M. 2015. HBV cccDNA: viral persistence reservoir and key obstacle for a cure of chronic hepatitis B. *Gut,* 64**,** 1972-84.

NATH, B. & SZABO, G. 2012. Hypoxia and Hypoxia Inducible Factors: Diverse Roles in Liver Diseases. *Hepatology,* 55**,** 622-33.

NI, Y., LEMPP, F. A., MEHRLE, S., NKONGOLO, S., KAUFMAN, C., FALTH, M., STINDT, J., KONIGER, C., NASSAL, M., KUBITZ, R., SULTMANN, H. & URBAN, S. 2014. Hepatitis B and D viruses exploit sodium taurocholate co-transporting polypeptide for species-specific entry into hepatocytes. *Gastroenterology,* 146**,** 1070-83.

NICOLL, A. J., ANGUS, P. W., CHOU, S. T., LUSCOMBE, C. A., SMALLWOOD, R. A. & LOCARNINI, S. A. 1997. Demonstration of duck hepatitis B virus in bile duct epithelial cells: implications for pathogenesis and persistent infection. *Hepatology,* 25**,** 463-9.

NIECKNIG, H., TUG, S., REYES, B. D., KIRSCH, M., FANDREY, J. & BERCHNER-PFANNSCHMIDT, U. 2012. Role of reactive oxygen species in the regulation of HIF-1 by prolyl hydroxylase 2 under mild hypoxia. *Free Radic Res,* 46**,** 705-17.

NISHIYAMA, Y., GODA, N., KANAI, M., NIWA, D., OSANAI, K., YAMAMOTO, Y., SENOO-MATSUDA, N., JOHNSON, R. S., MIURA, S., KABE, Y. & SUEMATSU, M. 2012. HIF-1alpha induction suppresses excessive lipid accumulation in alcoholic fatty liver in mice. *J Hepatol,* 56**,** 441-7.

NIU, C., LIVINGSTON, C. M., LI, L., BERAN, R. K., DAFFIS, S., RAMAKRISHNAN, D., BURDETTE, D., PEISER, L., SALAS, E., RAMOS, H., YU, M., CHENG, G., STRUBIN, M., DELANEY IV, W. E. & FLETCHER, S. P. 2017. The Smc5/6 Complex Restricts HBV when Localized to ND10 without Inducing an Innate Immune Response and Is Counteracted by the HBV X Protein Shortly after Infection. *PLoS One,* 12**,** e0169648.

O'CONNELL, A. C., LILLIBRIDGE, C. D., ZHENG, C., BAUM, B. J., O'CONNELL, B. C. & AMBUDKAR, I. S. 1998. Gamma-irradiation-induced cell cycle arrest and cell death in a human submandibular gland cell line: effect of E2F1 expression. *J Cell Physiol,* 177**,** 264-73.

ODOM, D. T., ZIZLSPERGER, N., GORDON, D. B., BELL, G. W., RINALDI, N. J., MURRAY, H. L., VOLKERT, T. L., SCHREIBER, J., ROLFE, P. A., GIFFORD, D. K., FRAENKEL, E., BELL, G. I. & YOUNG, R. A. 2004. Control of pancreas and liver gene expression by HNF transcription factors. *Science,* 303**,** 1378-81.

OGSTON, C. W., SCHECHTER, E. M., HUMES, C. A. & PRANIKOFF, M. B. 1989. Extrahepatic replication of woodchuck hepatitis virus in chronic infection. *Virology,* 169**,** 9-14.

OLIVE, P. L., AQUINO-PARSONS, C., MACPHAIL, S. H., LIAO, S. Y., RALEIGH, J. A., LERMAN, M. I. & STANBRIDGE, E. J. 2001. Carbonic anhydrase 9 as an endogenous marker for hypoxic cells in cervical cancer. *Cancer Res,* 61**,** 8924-9.

OLSAVSKY GOYAK, K. M., LAURENZANA, E. M. & OMIECINSKI, C. J. 2010. Hepatocyte Differentiation. *In:* MAUREL, P. (ed.) *Hepatocytes: Methods and Protocols.* Totowa, NJ: Humana Press.

ORI, A., ATZMONY, D., HAVIV, I. & SHAUL, Y. 1994. An NF1 motif plays a central role in hepatitis B virus enhancer. *Virology,* 204**,** 600-8.

ORTEGA-PRIETO, A. M. & DORNER, M. 2017. Immune Evasion Strategies during Chronic Hepatitis B and C Virus Infection. *Vaccines (Basel),* 5.

PALUMBO, G. A., SCISCIANI, C., PEDICONI, N., LUPACCHINI, L., ALFALATE, D., GUERRIERI, F., CALVO, L., SALERNO, D., DI COCCO, S., LEVRERO, M. & BELLONI, L. 2015. IL6 Inhibits HBV Transcription by Targeting the Epigenetic Control of the Nuclear cccDNA Minichromosome. *PLoS One,* 10.

PAPANDREOU, I., CAIRNS, R. A., FONTANA, L., LIM, A. L. & DENKO, N. C. 2006. HIF-1 mediates adaptation to hypoxia by actively downregulating mitochondrial oxygen consumption. *Cell Metab,* 3**,** 187-97.

PATEL, N., WHITE, S. J., THOMPSON, R. F., BINGHAM, R., WEIß, E. U., MASKELL, D. P., ZLOTNICK, A., DYKEMAN, E. C., TUMA, R., TWAROCK, R., RANSON, N. A. & STOCKLEY, P. G. 2017. HBV RNA pre-genome encodes specific motifs that mediate interactions with the viral core protein that promote nucleocapsid assembly. 2**,** 17098.

PATIENT, R., HOURIOUX, C. & ROINGEARD, P. 2009. Morphogenesis of hepatitis B virus and its subviral envelope particles. *Cellular Microbiology,* 11**,** 1561-1570.

PATIENT, R., HOURIOUX, C., SIZARET, P. Y., TRASSARD, S., SUREAU, C. & ROINGEARD, P. 2007. Hepatitis B Virus Subviral Envelope Particle Morphogenesis and Intracellular Trafficking. *J Virol,* 81**,** 3842-51.

PATZER, E. J., NAKAMURA, G. R., SIMONSEN, C. C., LEVINSON, A. D. & BRANDS, R. 1986. Intracellular assembly and packaging of hepatitis B surface antigen particles occur in the endoplasmic reticulum. *J Virol,* 58**,** 884-92.

PERLMAN, D. H., BERG, E. A., O'CONNOR, P. B., COSTELLO, C. E. & HU, J. 2005. Reverse transcription-associated dephosphorylation of hepadnavirus nucleocapsids. *Proc Natl Acad Sci U S A,* 102**,** 9020-5.

PERRILLO, R. 2009. Benefits and risks of interferon therapy for hepatitis B. *Hepatology,* 49**,** S103-11.

PERSING, D. H., VARMUS, H. E. & GANEM, D. 1987. The preS1 protein of hepatitis B virus is acylated at its amino terminus with myristic acid. *J Virol,* 61**,** 1672-7.

PERSSON, B. & ARGOS, P. 1994. Prediction of transmembrane segments in proteins utilising multiple sequence alignments. *J Mol Biol,* 237**,** 182-92.

PETERSON, D. L., NATH, N. & GAVILANES, F. 1982. Structure of hepatitis B surface antigen. Correlation of subtype with amino acid sequence and location of the carbohydrate moiety. *J Biol Chem,* 257**,** 10414-20.

PILARSKY, C., WENZIG, M., SPECHT, T., SAEGER, H. D. & GRÜTZMANN, R. 2004. Identification and Validation of Commonly Overexpressed Genes in Solid Tumors by Comparison of Microarray Data. *Neoplasia,* 6**,** 744-50.

POLLICINO, T., BELLONI, L., RAFFA, G., PEDICONI, N., SQUADRITO, G., RAIMONDO, G. & LEVRERO, M. 2006. Hepatitis B virus replication is regulated by the acetylation status of hepatitis B virus cccDNA-bound H3 and H4 histones. *Gastroenterology,* 130**,** 823-37.

PONTOGLIO, M., BARRA, J., HADCHOUEL, M., DOYEN, A., KRESS, C., BACH, J. P., BABINET, C. & YANIV, M. 1996. Hepatocyte nuclear factor 1 inactivation results in hepatic dysfunction, phenylketonuria, and renal Fanconi syndrome. *Cell,* 84**,** 575-85.

PRICKAERTS, P., ADRIAENS, M. E., BEUCKEN, T. V. D., KOCH, E., DUBOIS, L., DAHLMANS, V. E. H., GITS, C., EVELO, C. T. A., CHAN-SENG-YUE, M., WOUTERS, B. G. & VONCKEN, J. W. 2016. Hypoxia increases genome-wide bivalent epigenetic marking by specific gain of H3K27me3. *Epigenetics & Chromatin,* 9**,** 46.

PROVENZANO, R., BESARAB, A., SUN, C. H., DIAMOND, S. A., DURHAM, J. H., CANGIANO, J. L., AIELLO, J. R., NOVAK, J. E., LEE, T., LEONG, R., ROBERTS, B. K., SAIKALI, K. G., HEMMERICH, S., SZCZECH, L. A., YU, K. H. & NEFF, T. B. 2016. Oral Hypoxia-Inducible Factor Prolyl Hydroxylase Inhibitor Roxadustat (FG-4592) for the Treatment of Anemia in Patients with CKD. *Clin J Am Soc Nephrol,* 11**,** 982-91.

QI, Y., GAO, Z., XU, G., PENG, B., LIU, C., YAN, H., YAO, Q., SUN, G., LIU, Y., TANG, D., SONG, Z., HE, W., SUN, Y., GUO, J. T. & LI, W. 2016. DNA Polymerase κ Is a Key Cellular Factor for the Formation of Covalently Closed Circular DNA of Hepatitis B Virus. *PLoS Pathog,* 12.

QU, A., TAYLOR, M., XUE, X., MATSUBARA, T., METZGER, D., CHAMBON, P., GONZALEZ, F. J. & SHAH, Y. M. 2011. Hypoxia-Inducible Transcription Factor 2α Promotes Steatohepatitis Through Augmenting Lipid Accumulation, Inflammation and Fibrosis. *Hepatology,* 54**,** 472-83.

QUASDORFF, M., HOSEL, M., ODENTHAL, M., ZEDLER, U., BOHNE, F., GRIPON, P., DIENES, H. P., DREBBER, U., STIPPEL, D., GOESER, T. & PROTZER, U. 2008. A concerted action of HNF4alpha and HNF1alpha links hepatitis B virus replication to hepatocyte differentiation. *Cell Microbiol,* 10**,** 1478-90.

QUASDORFF, M. & PROTZER, U. 2010. Control of hepatitis B virus at the level of transcription. *Journal of Viral Hepatitis,* 17**,** 527-536.

RABE, B., VLACHOU, A., PANTÉ, N., HELENIUS, A. & KANN, M. 2003. Nuclear import of hepatitis B virus capsids and release of the viral genome. *Proceedings of the National Academy of Sciences,* 100**,** 9849-9854.

RADZIWILL, G., TUCKER, W. & SCHALLER, H. 1990. Mutational analysis of the hepatitis B virus P gene product: domain structure and RNase H activity. *J Virol,* 64**,** 613-20.

RAFTY, L. A., SANTIAGO, F. S. & KHACHIGIAN, L. M. 2002. NF1/X represses PDGF A-chain transcription by interacting with Sp1 and antagonizing Sp1 occupancy of the promoter. *Embo j,* 21**,** 334-43.

RANEY, A. K., EASTON, A. J., MILICH, D. R. & MCLACHLAN, A. 1991. Promoter-specific transactivation of hepatitis B virus transcription by a glutamine- and proline-rich domain of hepatocyte nuclear factor 1. *J Virol,* 65**,** 5774-81.

RANEY, A. K., JOHNSON, J. L., PALMER, C. N. & MCLACHLAN, A. 1997. Members of the nuclear receptor superfamily regulate transcription from the hepatitis B virus nucleocapsid promoter. *J Virol,* 71**,** 1058-71.

RANEY, A. K., LE, H. B. & MCLACHLAN, A. 1992. Regulation of transcription from the hepatitis B virus major surface antigen promoter by the Sp1 transcription factor. *J Virol,* 66**,** 6912-21.

RANEY, A. K. & MCLACHLAN, A. 1995. Characterization of the hepatitis B virus large surface antigen promoter Sp1 binding site. *Virology,* 208**,** 399-404.

RANEY, A. K., ZHANG, P. & MCLACHLAN, A. 1995. Regulation of transcription from the hepatitis B virus large surface antigen promoter by hepatocyte nuclear factor 3. *J Virol,* 69**,** 3265-72.

RANKIN, E. B., RHA, J., SELAK, M. A., UNGER, T. L., KEITH, B., LIU, Q. & HAASE, V. H. 2009. Hypoxia-inducible factor 2 regulates hepatic lipid metabolism. *Molecular and Cellular Biology,* 29**,** 4527-4538.

RAVI, R., MOOKERJEE, B., BHUJWALLA, Z. M., SUTTER, C. H., ARTEMOV, D., ZENG, Q., DILLEHAY, L. E., MADAN, A., SEMENZA, G. L. & BEDI, A. 2000. Regulation of tumor angiogenesis by p53-induced degradation of hypoxia-inducible factor 1α. *Genes & Development,* 14**,** 34-44.

REN, J. H., TAO, Y., ZHANG, Z. Z., CHEN, W. X., CAI, X. F., CHEN, K., KO, B. C., SONG, C. L., RAN, L. K., LI, W. Y., HUANG, A. L. & CHEN, J. 2014. Sirtuin 1 regulates hepatitis B virus transcription and replication by targeting transcription factor AP-1. *J Virol,* 88**,** 2442-51.

RHIM, J. A., SANDGREN, E. P., DEGEN, J. L., PALMITER, R. D. & BRINSTER, R. L. 1994. Replacement of Diseased Mouse Liver by Hepatic Cell Transplantation. *Science,* 263**,** 1149-1152.

RIEGER, A. & NASSAL, M. 1996. Specific hepatitis B virus minus-strand DNA synthesis requires only the 5' encapsidation signal and the 3'-proximal direct repeat DR1. *J Virol,* 70**,** 585-9.

RIJCKBORST, V. & JANSSEN, H. L. A. 2010. The Role of Interferon in Hepatitis B Therapy. *Curr Hepat Rep,* 9**,** 231-8.

RIVIERE, L., GEROSSIER, L., DUCROUX, A., DION, S., DENG, Q., MICHEL, M. L., BUENDIA, M. A., HANTZ, O. & NEUVEUT, C. 2015. HBx relieves chromatin-mediated transcriptional repression of hepatitis B viral cccDNA involving SETDB1 histone methyltransferase. *J Hepatol,* 63**,** 1093-102.

RODRIGUEZ-INIGO, E., MARISCAL, L., BARTOLOME, J., CASTILLO, I., NAVACERRADA, C., ORTIZ-MOVILLA, N., PARDO, M. & CARRENO, V. 2003. Distribution of hepatitis B virus in the liver of chronic hepatitis C patients with occult hepatitis B virus infection. *J Med Virol,* 70**,** 571-80.

ROINGEARD, P. & SUREAU, C. 1998. Ultrastructural analysis of hepatitis B virus in HepG2-transfected cells with special emphasis on subviral filament morphogenesis. *Hepatology,* 28**,** 1128-33.

ROST, M., MANN, S., LAMBERT, C., DORING, T., THOME, N. & PRANGE, R. 2006. Gamma-adaptin, a novel ubiquitin-interacting adaptor, and Nedd4 ubiquitin ligase control hepatitis B virus maturation. *J Biol Chem,* 281**,** 29297-308.

RYU, D. K., AHN, B. Y. & RYU, W. S. 2010. Proximity between the cap and 5' epsilon stem-loop structure is critical for the suppression of pgRNA translation by the hepatitis B viral polymerase. *Virology,* 406**,** 56-64.

RYU, D. K., KIM, S. & RYU, W. S. 2008. Hepatitis B virus polymerase suppresses translation of pregenomic RNA via a mechanism involving its interaction with 5' stem-loop structure. *Virology,* 373**,** 112-23.

SAEED, U., WAHEED, Y. & ASHRAF, M. 2014. Hepatitis B and hepatitis C viruses: a review of viral genomes, viral induced host immune responses, genotypic distributions and worldwide epidemiology. *Asian Pacific Journal of Tropical Disease,* 4**,** 88-96.

SANG, N., STIEHL, D. P., BOHENSKY, J., LESHCHINSKY, I., SRINIVAS, V. & CARO, J. 2003. MAPK signaling up-regulates the activity of hypoxia-inducible factors by its effects on p300. *J Biol Chem,* 278**,** 14013-9.

SANTOS-ROSA, H., SCHNEIDER, R., BANNISTER, A. J., SHERRIFF, J., BERNSTEIN, B. E., EMRE, N. C., SCHREIBER, S. L., MELLOR, J. & KOUZARIDES, T. 2002. Active genes are tri-methylated at K4 of histone H3. *Nature,* 419**,** 407-11.

SARRAZIN, S., LAMANNA, W. C. & ESKO, J. D. 2011. Heparan sulfate proteoglycans. *Cold Spring Harb Perspect Biol,* 3.

SCHÄDLER, S. & HILDT, E. 2009. HBV Life Cycle: Entry and Morphogenesis. *Viruses,* 1.

SCHODEL, J., OIKONOMOPOULOS, S., RAGOUSSIS, J., PUGH, C. W., RATCLIFFE, P. J. & MOLE, D. R. 2011. High-resolution genome-wide mapping of HIF-binding sites by ChIP-seq. *Blood,* 117**,** e207-17.

SCHOFIELD, C. J. & RATCLIFFE, P. J. 2004. Oxygen sensing by HIF hydroxylases. *Nat Rev Mol Cell Biol,* 5**,** 343-354.

SCHREINER, S. & NASSAL, M. 2017. A Role for the Host DNA Damage Response in Hepatitis B Virus cccDNA Formation—and Beyond? *Viruses,* 9.

SCHREM, H., KLEMPNAUER, J. & BORLAK, J. 2002. Liver-enriched transcription factors in liver function and development. Part I: the hepatocyte nuclear factor network and liver-specific gene expression. *Pharmacol Rev,* 54**,** 129-58.

SCHULZE, A., GRIPON, P. & URBAN, S. 2007. Hepatitis B virus infection initiates with a large surface protein-dependent binding to heparan sulfate proteoglycans. *Hepatology,* 46**,** 1759-68.

SCHULZE, A., MILLS, K., WEISS, T. S. & URBAN, S. 2012. Hepatocyte polarization is essential for the productive entry of the hepatitis B virus. *Hepatology,* 55**,** 373-83.

SCHWEITZER, A., HORN, J., MIKOLAJCZYK, R. T., KRAUSE, G. & OTT, J. J. 2015. Estimations of worldwide prevalence of chronic hepatitis B virus infection: a systematic review of data published between 1965 and 2013. *Lancet,* 386**,** 1546-55.

SCORTEGAGNA, M., DING, K., OKTAY, Y., GAUR, A., THURMOND, F., YAN, L. J., MARCK, B. T., MATSUMOTO, A. M., SHELTON, J. M., RICHARDSON, J. A., BENNETT, M. J. & GARCIA, J. A. 2003. Multiple organ pathology, metabolic abnormalities and impaired homeostasis of reactive oxygen species in Epas1-/- mice. *Nat Genet,* 35**,** 331-40.

SEEGER, C., GANEM, D. & VARMUS, H. E. 1986. Biochemical and genetic evidence for the hepatitis B virus replication strategy. *Science,* 232**,** 477-84.

SEEGER, C. & MASON, W. S. 2000. Hepatitis B Virus Biology. *Microbiology and Molecular Biology Reviews,* 64**,** 51-68.

SEEGER, C. & MASON, W. S. 2015. Molecular biology of hepatitis B virus infection. *Virology,* 479-480**,** 672-86.

SELAK, M. A., ARMOUR, S. M., MACKENZIE, E. D., BOULAHBEL, H., WATSON, D. G., MANSFIELD, K. D., PAN, Y., SIMON, M. C., THOMPSON, C. B. & GOTTLIEB, E. 2005. Succinate links TCA cycle dysfunction to oncogenesis by inhibiting HIF-alpha prolyl hydroxylase. *Cancer Cell,* 7**,** 77-85.

SELLS, M. A., CHEN, M. L. & ACS, G. 1987. Production of hepatitis B virus particles in Hep G2 cells transfected with cloned hepatitis B virus DNA. *Proc Natl Acad Sci U S A,* 84**,** 1005-9.

SEMENZA, G. L. 2003. Targeting HIF-1 for cancer therapy. *Nat Rev Cancer,* 3**,** 721-32.

SEVERI, T., YING, C., VERMEESCH, J. R., CASSIMAN, D., CNOPS, L., VERSLYPE, C., FEVERY, J., ARCKENS, L., NEYTS, J. & VAN PELT, J. F. 2006. Hepatitis B virus replication causes oxidative stress in HepAD38 liver cells. *Mol Cell Biochem,* 290**,** 79-85.

SHAMAY, M., AGAMI, R. & SHAUL, Y. 2001. HBV integrants of hepatocellular carcinoma cell lines contain an active enhancer. *Oncogene,* 20**,** 6811-9.

SHARIFI, Z. 2014. Natural History of Chronic Hepatitis B Virus Infection Based on Laboratory Testing. *Iran J Public Health,* 43**,** 990-3.

SHARMA, S. K., SAINI, N. & CHWLA, Y. 2005. Hepatitis B Virus: Inactive carriers. *Virol J,* 2**,** 82.

SHAUL, Y., BEN-LEVY, R. & DE-MEDINA, T. 1986. High affinity binding site for nuclear factor I next to the hepatitis B virus S gene promoter. *Embo j,* 5**,** 1967-71.

SHI, Y. H. & SHI, C. H. 2009. Molecular characteristics and stages of chronic hepatitis B virus infection. *World J Gastroenterol,* 15**,** 3099-105.

SHIM, H., DOLDE, C., LEWIS, B. C., WU, C. S., DANG, G., JUNGMANN, R. A., DALLA-FAVERA, R. & DANG, C. V. 1997. c-Myc transactivation of LDH-A: Implications for tumor metabolism and growth. *Proc Natl Acad Sci U S A,* 94**,** 6658-63.

SIMON, M. C. 2006. Coming up for air: HIF-1 and mitochondrial oxygen consumption. *Cell Metab,* 3**,** 150-1.

SIMS, K. A. & WOODLAND, A. M. 2006. Entecavir: a new nucleoside analog for the treatment of chronic hepatitis B infection. *Pharmacotherapy,* 26**,** 1745-57.
SIRMA, H., WEIL, R., ROSMORDUC, O., URBAN, S., ISRAEL, A., KREMSDORF, D. & BRECHOT, C. 1998. Cytosol is the prime compartment of hepatitis B virus X protein where it colocalizes with the proteasome. *Oncogene,* 16**,** 2051-63.
SITTERLIN, D., BERGAMETTI, F., TIOLLAIS, P., TENNANT, B. C. & TRANSY, C. 2000a. Correct binding of viral X protein to UVDDB-p127 cellular protein is critical for efficient infection by hepatitis B viruses. *Oncogene,* 19**,** 4427-31.
SITTERLIN, D., BERGAMETTI, F. & TRANSY, C. 2000b. UVDDB p127-binding modulates activities and intracellular distribution of hepatitis B virus X protein. *Oncogene,* 19**,** 4417-26.
SITTERLIN, D., LEE, T. H., PRIGENT, S., TIOLLAIS, P., BUTEL, J. S. & TRANSY, C. 1997. Interaction of the UV-damaged DNA-binding protein with hepatitis B virus X protein is conserved among mammalian hepadnaviruses and restricted to transactivation-proficient X-insertion mutants. *J Virol,* 71**,** 6194-9.
SOFER, A., LEI, K., JOHANNESSEN, C. M. & ELLISEN, L. W. 2005. Regulation of mTOR and Cell Growth in Response to Energy Stress by REDD1. *Mol Cell Biol,* 25**,** 5834-45.
SOHN, J. A., LITWIN, S. & SEEGER, C. 2009. Mechanism for CCC DNA Synthesis in Hepadnaviruses. *PLoS One,* 4.
SOLAINI, G., BARACCA, A., LENAZ, G. & SGARBI, G. 2010. Hypoxia and mitochondrial oxidative metabolism. *Biochimica et Biophysica Acta (BBA) - Bioenergetics,* 1797**,** 1171-1177.
SONG, B. C., KIM, H., KIM, S. H., CHA, C. Y., KOOK, Y. H. & KIM, B. J. 2005. Comparison of full length sequences of hepatitis B virus isolates in hepatocellular carcinoma patients and asymptomatic carriers of Korea. *J Med Virol,* 75**,** 13-9.
SONG, G., JIA, H., XU, H., LIU, W., ZHU, H., LI, S., SHI, J., LI, Z., HE, J. & CHEN, Z. 2014. Studying the association of microRNA-210 level with chronic hepatitis B progression. *J Viral Hepat,* 21**,** 272-80.
SONG, Y. M., SONG, S. O., JUNG, Y. K., KANG, E. S., CHA, B. S., LEE, H. C. & LEE, B. W. 2012. Dimethyl sulfoxide reduces hepatocellular lipid accumulation through autophagy induction. *Autophagy,* 8**,** 1085-97.
SPANDAU, D. F. & LEE, C. H. 1988. trans-activation of viral enhancers by the hepatitis B virus X protein. *J Virol,* 62**,** 427-34.
SPANDAU, D. F. & LEE, C. H. 1992. Repression of the hepatitis B virus enhancer by a cellular factor. *J Gen Virol,* 73 (Pt 1)**,** 131-7.
STIELER, J. T. & PRANGE, R. 2014. Involvement of ESCRT-II in Hepatitis B Virus Morphogenesis. *PLoS One,* 9.
STOLZE, I. P., MOLE, D. R. & RATCLIFFE, P. J. 2006. Regulation of HIF: prolyl hydroxylases. *Novartis Found Symp,* 272**,** 15-25; discussion 25-36.
SU, H. & YEE, J. K. 1992. Regulation of hepatitis B virus gene expression by its two enhancers. *Proc Natl Acad Sci U S A,* 89**,** 2708-12.
SUREAU, C. & SALISSE, J. 2013. A conformational heparan sulfate binding site essential to infectivity overlaps with the conserved hepatitis B virus a-determinant. *Hepatology,* 57**,** 985-94.
TACKE, F., LIEDTKE, C., BOCKLAGE, S., MANNS, M. P. & TRAUTWEIN, C. 2005. CREB/PKA sensitive signalling pathways activate and maintain expression levels of the hepatitis B virus pre-S2/S promoter. *Gut,* 54**,** 1309-17.
TAKASHIMA, H., ARAKI, K., MIYAZAKI, J., YAMAMURA, K. & KIMOTO, M. 1992. Characterization of T-cell tolerance to hepatitis B virus (HBV) antigen in transgenic mice. *Immunology,* 75**,** 398-405.
TALKS, K. L., TURLEY, H., GATTER, K. C., MAXWELL, P. H., PUGH, C. W., RATCLIFFE, P. J. & HARRIS, A. L. 2000. The Expression and Distribution of the Hypoxia-Inducible Factors HIF-1α and HIF-2α in Normal Human Tissues, Cancers, and Tumor-Associated Macrophages. *Am J Pathol,* 157**,** 411-21.

TANAKA, Y., KANAI, F., ICHIMURA, T., TATEISHI, K., ASAOKA, Y., GULENG, B., JAZAG, A., OHTA, M., IMAMURA, J., IKENOUE, T., IJICHI, H., KAWABE, T., ISOBE, T. & OMATA, M. 2005. The hepatitis B virus X protein enhances AP-1 activation through interaction with Jab1. *Oncogene,* 25**,** 633-642.

TANG, H., BANKS, K. E., ANDERSON, A. L. & MCLACHLAN, A. 2001. Hepatitis B virus transcription and replication. *Drug News Perspect,* 14**,** 325-34.

TANG, H. & MCLACHLAN, A. 2001. Transcriptional regulation of hepatitis B virus by nuclear hormone receptors is a critical determinant of viral tropism. *Proc Natl Acad Sci U S A,* 98**,** 1841-6.

TANG, H. & MCLACHLAN, A. 2002. Mechanisms of inhibition of nuclear hormone receptor-dependent hepatitis B virus replication by hepatocyte nuclear factor 3beta. *J Virol,* 76**,** 8572-81.

TAPARRA, K., TRAN, P. T. & ZACHARA, N. E. 2016. Hijacking the Hexosamine Biosynthetic Pathway to Promote EMT-Mediated Neoplastic Phenotypes. *Frontiers in Oncology,* 6**,** 85.

TENNANT, D. A., FREZZA, C., MACKENZIE, E. D., NGUYEN, Q. D., ZHENG, L., SELAK, M. A., ROBERTS, D. L., DIVE, C., WATSON, D. G., ABOAGYE, E. O. & GOTTLIEB, E. 2009. Reactivating HIF prolyl hydroxylases under hypoxia results in metabolic catastrophe and cell death. *Oncogene,* 28**,** 4009-21.

THOMAS, E. & LIANG, T. J. 2016. Experimental models of hepatitis B and C [mdash] new insights and progress. *Nat Rev Gastroenterol Hepatol,* 13**,** 362-374.

THORGEIRSSON, S. S. 1996. Hepatic stem cells in liver regeneration. *The FASEB Journal,* 10**,** 1249-56.

THORGEIRSSON, S. S., EVARTS, R. P., BISGAARD, H. C., FUJIO, K. & HU, Z. 1993. Hepatic Stem Cell Compartment: Activation and Lineage Commitment. *Proceedings of the Society for Experimental Biology and Medicine,* 204**,** 253-260.

TRAN, E. J. & WENTE, S. R. 2006. Dynamic nuclear pore complexes: life on the edge. *Cell,* 125**,** 1041-53.

TRIERWEILER, C., HOCKENJOS, B., ZATLOUKAL, K., THIMME, R., BLUM, H. E., WAGNER, E. F. & HASSELBLATT, P. 2016. The transcription factor c-JUN/AP-1 promotes HBV-related liver tumorigenesis in mice. *Cell Death Differ,* 23**,** 576-82.

TROPBERGER, P., MERCIER, A., ROBINSON, M., ZHONG, W., GANEM, D. E. & HOLDORF, M. 2015. Mapping of histone modifications in episomal HBV cccDNA uncovers an unusual chromatin organization amenable to epigenetic manipulation. *Proc Natl Acad Sci U S A,* 112**,** E5715-24.

TROPBERGER, P., POTT, S., KELLER, C., KAMIENIARZ-GDULA, K., CARON, M., RICHTER, F., LI, G., MITTLER, G., LIU, E. T., BUHLER, M., MARGUERON, R. & SCHNEIDER, R. 2013. Regulation of transcription through acetylation of H3K122 on the lateral surface of the histone octamer. *Cell,* 152**,** 859-72.

TSAI, K. N., CHONG, C. L., CHOU, Y. C., HUANG, C. C., WANG, Y. L., WANG, S. W., CHEN, M. L., CHEN, C. H. & CHANG, C. 2015. Doubly Spliced RNA of Hepatitis B Virus Suppresses Viral Transcription via TATA-Binding Protein and Induces Stress Granule Assembly. *J Virol,* 89**,** 11406-19.

TSAI, S. L., CHEN, P. J., LAI, M. Y., YANG, P. M., SUNG, J. L., HUANG, J. H., HWANG, L. H., CHANG, T. H. & CHEN, D. S. 1992. Acute exacerbations of chronic type B hepatitis are accompanied by increased T cell responses to hepatitis B core and e antigens. Implications for hepatitis B e antigen seroconversion. *J Clin Invest,* 89**,** 87-96.

TSAI, Y. P. & WU, K. J. 2014. Epigenetic regulation of hypoxia-responsive gene expression: Focusing on chromatin and DNA modifications. *International Journal of Cancer,* 134**,** 249-256.

TSUGE, M., HIRAGA, N., AKIYAMA, R., TANAKA, S., MATSUSHITA, M., MITSUI, F., ABE, H., KITAMURA, S., HATAKEYAMA, T., KIMURA, T., MIKI, D., MORI, N., IMAMURA, M., TAKAHASHI, S., HAYES, C. N. & CHAYAMA, K. 2010. HBx protein is indispensable for development of viraemia in human hepatocyte chimeric mice. *J Gen Virol,* 91**,** 1854-64.

TU, T., BUDZINSKA, M. A., SHACKEL, N. A. & URBAN, S. 2017. HBV DNA Integration: Molecular Mechanisms and Clinical Implications. *Viruses,* 9.
TUR-KASPA, R., BURK, R. D., SHAUL, Y. & SHAFRITZ, D. A. 1986. Hepatitis B virus DNA contains a glucocorticoid-responsive element. *Proc Natl Acad Sci U S A,* 83**,** 1627-31.
TUTTLEMAN, J. S., PUGH, J. C. & SUMMERS, J. W. 1986. In vitro experimental infection of primary duck hepatocyte cultures with duck hepatitis B virus. *J Virol,* 58**,** 17-25.
TWU, J. S. & SCHLOEMER, R. H. 1987. Transcriptional trans-activating function of hepatitis B virus. *J Virol,* 61**,** 3448-53.
UEDA, H., ULLRICH, S. J., GANGEMI, J. D., KAPPEL, C. A., NGO, L., FEITELSON, M. A. & JAY, G. 1995. Functional inactivation but not structural mutation of p53 causes liver cancer. *Nat Genet,* 9**,** 41-7.
UEDA, K., TSURIMOTO, T. & MATSUBARA, K. 1991. Three envelope proteins of hepatitis B virus: large S, middle S, and major S proteins needed for the formation of Dane particles. *J Virol,* 65**,** 3521-9.
UNIACKE, J., HOLTERMAN, C. E., LACHANCE, G., FRANOVIC, A., JACOB, M. D., FABIAN, M. R., PAYETTE, J., HOLCIK, M., PAUSE, A. & LEE, S. 2012. An oxygen-regulated switch in the protein synthesis machinery. *Nature,* 486**,** 126-9.
URBAN, S., BARTENSCHLAGER, R., KUBITZ, R. & ZOULIM, F. 2014. Strategies to inhibit entry of HBV and HDV into hepatocytes. *Gastroenterology,* 147**,** 48-64.
URBAN, S. & GRIPON, P. 2002. Inhibition of Duck Hepatitis B Virus Infection by a Myristoylated Pre-S Peptide of the Large Viral Surface Protein. *J Virol,* 76**,** 1986-90.
URBAN, S., SCHULZE, A., DANDRI, M. & PETERSEN, J. 2010. The replication cycle of hepatitis B virus. *Journal of Hepatology,* 52**,** 282-284.
VAN BREUGEL, P. C., ROBERT, E. I., MUELLER, H., DECORSIERE, A., ZOULIM, F., HANTZ, O. & STRUBIN, M. 2012. Hepatitis B virus X protein stimulates gene expression selectively from extrachromosomal DNA templates. *Hepatology,* 56**,** 2116-24.
VAN HEMERT, F. J., VAN DE KLUNDERT, M. A., LUKASHOV, V. V., KOOTSTRA, N. A., BERKHOUT, B. & ZAAIJER, H. L. 2011. Protein X of hepatitis B virus: origin and structure similarity with the central domain of DNA glycosylase. *PLoS One,* 6**,** e23392.
VASSILEV, L. T. 2006. Cell cycle synchronization at the G2/M phase border by reversible inhibition of CDK1. *Cell Cycle,* 5**,** 2555-6.
VECCHI, C., MONTOSI, G. & PIETRANGELO, A. 2010. Huh-7: a human "hemochromatotic" cell line. *Hepatology,* 51**,** 654-9.
VERRIER, E. R., COLPITTS, C. C., BACH, C., HEYDMANN, L., WEISS, A., RENAUD, M., DURAND, S. C., HABERSETZER, F., DURANTEL, D., ABOU-JAOUDE, G., LOPEZ LEDESMA, M. M., FELMLEE, D. J., SOUMILLON, M., CROONENBORGHS, T., POCHET, N., NASSAL, M., SCHUSTER, C., BRINO, L., SUREAU, C., ZEISEL, M. B. & BAUMERT, T. F. 2016a. A targeted functional RNA interference screen uncovers glypican 5 as an entry factor for hepatitis B and D viruses. *Hepatology,* 63**,** 35-48.
VERRIER, E. R., COLPITTS, C. C., SCHUSTER, C., ZEISEL, M. B. & BAUMERT, T. F. 2016b. Cell Culture Models for the Investigation of Hepatitis B and D Virus Infection. *Viruses,* 8.
VILLAGRA, A., SOTOMAYOR, E. M. & SETO, E. 2010. Histone deacetylases and the immunological network: implications in cancer and inflammation. *Oncogene,* 29**,** 157-73.
VOLZ, T., ALLWEISS, L., BEN, M. M., WARLICH, M., LOHSE, A. W., POLLOK, J. M., ALEXANDROV, A., URBAN, S., PETERSEN, J., LUTGEHETMANN, M. & DANDRI, M. 2013. The entry inhibitor Myrcludex-B efficiently blocks intrahepatic virus spreading in humanized mice previously infected with hepatitis B virus. *J Hepatol,* 58**,** 861-7.
VON APPEN, A. & BECK, M. 2016. Structure Determination of the Nuclear Pore Complex with Three-Dimensional Cryo electron Microscopy. *J Mol Biol,* 428**,** 2001-10.
WAKISAKA, N., KONDO, S., YOSHIZAKI, T., MURONO, S., FURUKAWA, M. & PAGANO, J. S. 2004. Epstein-Barr Virus Latent Membrane Protein 1 Induces Synthesis of Hypoxia-Inducible Factor 1α. *Molecular and Cellular Biology,* 24**,** 5223-5234.
WANG, G. H. & SEEGER, C. 1992. The reverse transcriptase of hepatitis B virus acts as a protein primer for viral DNA synthesis. *Cell,* 71**,** 663-70.

WANG, S., CHEN, Z., HU, C., QIAN, F., CHENG, Y., WU, M., SHI, B., CHEN, J., HU, Y. & YUAN, Z. 2013. Hepatitis B virus surface antigen selectively inhibits TLR2 ligand-induced IL-12 production in monocytes/macrophages by interfering with JNK activation. *J Immunol,* 190**,** 5142-51.

WANG, X., MA, J., FU, Q., ZHU, L., ZHANG, Z., ZHANG, F., LU, N. & CHEN, A. 2017. Role of hypoxiainducible factor1alpha in autophagic cell death in microglial cells induced by hypoxia. *Mol Med Rep,* 15**,** 2097-2105.

WANG, X. W., FORRESTER, K., YEH, H., FEITELSON, M. A., GU, J. R. & HARRIS, C. C. 1994. Hepatitis B virus X protein inhibits p53 sequence-specific DNA binding, transcriptional activity, and association with transcription factor ERCC3. *Proceedings of the National Academy of Sciences of the United States of America,* 91**,** 2230-2234.

WATANABE, T., SORENSEN, E. M., NAITO, A., SCHOTT, M., KIM, S. & AHLQUIST, P. 2007. Involvement of host cellular multivesicular body functions in hepatitis B virus budding. *Proceedings of the National Academy of Sciences,* 104**,** 10205-10210.

WATASHI, K., URBAN, S., LI, W. & WAKITA, T. 2014. NTCP and Beyond: Opening the Door to Unveil Hepatitis B Virus Entry. *Int J Mol Sci,* 15**,** 2892-905.

WEI, C., NI, C., SONG, T., LIU, Y., YANG, X., ZHENG, Z., JIA, Y., YUAN, Y., GUAN, K., XU, Y., CHENG, X., ZHANG, Y., YANG, X., WANG, Y., WEN, C., WU, Q., SHI, W. & ZHONG, H. 2010. The hepatitis B virus X protein disrupts innate immunity by downregulating mitochondrial antiviral signaling protein. *J Immunol,* 185**,** 1158-68.

WERLE-LAPOSTOLLE, B., BOWDEN, S., LOCARNINI, S., WURSTHORN, K., PETERSEN, J., LAU, G., TREPO, C., MARCELLIN, P., GOODMAN, Z., DELANEY, W. E. T., XIONG, S., BROSGART, C. L., CHEN, S. S., GIBBS, C. S. & ZOULIM, F. 2004. Persistence of cccDNA during the natural history of chronic hepatitis B and decline during adefovir dipivoxil therapy. *Gastroenterology,* 126**,** 1750-8.

WHITE, C. 2009. Copper transport into the secretory pathway is regulated by oxygen in. 122**,** 1315-21.

WHO. 2017. *Hepatitis B* [Online]. World Health Organization. Available: http://www.who.int/mediacentre/factsheets/fs204/en/ [Accessed 11 July 2017 2017].

WIGERUP, C., PÅHLMAN, S. & BEXELL, D. 2016. Therapeutic targeting of hypoxia and hypoxia-inducible factors in cancer. *Pharmacology & Therapeutics,* 164**,** 152-169.

WILSON, G. K., BRIMACOMBE, C. L., ROWE, I. A., REYNOLDS, G. M., FLETCHER, N. F., STAMATAKI, Z., BHOGAL, R. H., SIMÕES, M. L., ASHCROFT, M., AFFORD, S. C., MITRY, R. R., DHAWAN, A., MEE, C. J., HÜBSCHER, S. G., BALFE, P. & MCKEATING, J. A. 2012. A dual role for hypoxia inducible factor-1α in the hepatitis C virus lifecycle and hepatoma migration. *Journal of Hepatology,* 56**,** 803-809.

WILSON, G. K., TENNANT, D. A. & MCKEATING, J. A. 2014. Hypoxia inducible factors in liver disease and hepatocellular carcinoma: Current understanding and future directions. *Journal of Hepatology,* 61**,** 1397-1406.

XIANG, A., REN, F., LEI, X., ZHANG, J., GUO, R., LU, Z. & GUO, Y. 2015. The hepatitis B virus (HBV) core protein enhances the transcription activation of CRE via the CRE/CREB/CBP pathway. *Antiviral Res,* 120**,** 7-15.

YAN, H., PENG, B., LIU, Y., XU, G., HE, W., REN, B., JING, Z., SUI, J. & LI, W. 2014. Viral entry of hepatitis B and D viruses and bile salts transportation share common molecular determinants on sodium taurocholate cotransporting polypeptide. *J Virol,* 88**,** 3273-84.

YAN, H., ZHONG, G., XU, G., HE, W., JING, Z., GAO, Z., HUANG, Y., QI, Y., PENG, B., WANG, H., FU, L., SONG, M., CHEN, P., GAO, W., REN, B., SUN, Y., CAI, T., FENG, X., SUI, J. & LI, W. 2012. Sodium taurocholate cotransporting polypeptide is a functional receptor for human hepatitis B and D virus. *eLife,* 1.

YANG, J. C., TENG, C. F., WU, H. C., TSAI, H. W., CHUANG, H. C., TSAI, T. F., HSU, Y. H., HUANG, W., WU, L. W. & SU, I. J. 2009. Enhanced expression of vascular endothelial growth factor-A in ground glass hepatocytes and its implication in hepatitis B virus hepatocarcinogenesis. *Hepatology,* 49**,** 1962-71.

YANG, M. H., WU, M. Z., CHIOU, S. H., CHEN, P. M., CHANG, S. Y., LIU, C. J., TENG, S. C. & WU, K. J. 2008. Direct regulation of TWIST by HIF-1alpha promotes metastasis. *Nat Cell Biol,* 10**,** 295-305.

YANG, S. L., REN, Q. G., ZHANG, T., PAN, X., WEN, L., HU, J. L., YU, C. & HE, Q. J. 2017. Hepatitis B virus X protein and hypoxiainducible factor-1alpha stimulate Notch gene expression in liver cancer cells. *Oncol Rep,* 37**,** 348-356.

YANG, W., MASON, W. S. & SUMMERS, J. 1996. Covalently closed circular viral DNA formed from two types of linear DNA in woodchuck hepatitis virus-infected liver. *J Virol,* 70**,** 4567-75.

YANG, W. & SUMMERS, J. 1995. Illegitimate replication of linear hepadnavirus DNA through nonhomologous recombination. *J Virol,* 69**,** 4029-36.

YANG, W. & SUMMERS, J. 1998. Infection of Ducklings with Virus Particles Containing Linear Double-Stranded Duck Hepatitis B Virus DNA: Illegitimate Replication and Reversion. *J Virol,* 72**,** 8710-7.

YEE, J. K. 1989. A liver-specific enhancer in the core promoter region of human hepatitis B virus. *Science,* 246**,** 658-61.

YEH, C. T., CHIU, H. T., CHU, C. M. & LIAW, Y. F. 1998. G1 phase dependent nuclear localization of relaxed-circular hepatitis B virus DNA and aphidicolin-induced accumulation of covalently closed circular DNA. *J Med Virol,* 55**,** 42-50.

YOO, Y. G., CHO, S., PARK, S. & LEE, M. O. 2004. The carboxy-terminus of the hepatitis B virus X protein is necessary and sufficient for the activation of hypoxia-inducible factor-1alpha. *FEBS Lett,* 577**,** 121-6.

YOO, Y. G., NA, T. Y., SEO, H. W., SEONG, J. K., PARK, C. K., SHIN, Y. K. & LEE, M. O. 2008. Hepatitis B virus X protein induces the expression of MTA1 and HDAC1, which enhances hypoxia signaling in hepatocellular carcinoma cells. *Oncogene,* 27**,** 3405-13.

YOO, Y. G., OH, S. H., PARK, E. S., CHO, H., LEE, N., PARK, H., KIM, D. K., YU, D. Y., SEONG, J. K. & LEE, M. O. 2003. Hepatitis B virus X protein enhances transcriptional activity of hypoxia-inducible factor-1alpha through activation of mitogen-activated protein kinase pathway. *J Biol Chem,* 278**,** 39076-84.

YU, X. & MERTZ, J. E. 1996. Promoters for synthesis of the pre-C and pregenomic mRNAs of human hepatitis B virus are genetically distinct and differentially regulated. *J Virol,* 70**,** 8719-26.

YU, X. & MERTZ, J. E. 1997. Differential regulation of the pre-C and pregenomic promoters of human hepatitis B virus by members of the nuclear receptor superfamily. *J Virol,* 71**,** 9366-74.

YU, X. & MERTZ, J. E. 2003. Distinct modes of regulation of transcription of hepatitis B virus by the nuclear receptors HNF4alpha and COUP-TF1. *J Virol,* 77**,** 2489-99.

YUEN, M.-F. & LAI, C.-L. 2015. Hepatitis B in 2014: HBV research moves forward[mdash]receptors and reactivation. *Nat Rev Gastroenterol Hepatol,* 12**,** 70-72.

ZARET, K. S. & GROMPE, M. 2008. Generation and Regeneration of Cells of the Liver and Pancreas. *Science,* 322**,** 1490.

ZHANG, G. L., LI, Y. X., ZHENG, S. Q., LIU, M., LI, X. & TANG, H. 2010. Suppression of hepatitis B virus replication by microRNA-199a-3p and microRNA-210. *Antiviral Res,* 88**,** 169-75.

ZHANG, P., RANEY, A. K. & MCLACHLAN, A. 1993. Characterization of functional Sp1 transcription factor binding sites in the hepatitis B virus nucleocapsid promoter. *J Virol,* 67**,** 1472-81.

ZHANG, S., MA, K., LIU, Y., PAN, X., CHEN, Q., QI, L. & LI, S. 2016. Stabilization of Hypoxia-inducible Factor by DMOG Inhibits Development of Chronic Hypoxia-Induced Right Ventricular Remodeling. *J Cardiovasc Pharmacol,* 67**,** 68-75.

ZHANG, S. M., SUN, D. C., LOU, S., BO, X. C., LU, Z., QIAN, X. H. & WANG, S. Q. 2005. HBx protein of hepatitis B virus (HBV) can form complex with mitochondrial HSP60 and HSP70. *Arch Virol,* 150**,** 1579-90.

ZHAO, T., ZHU, Y., MORINIBU, A., KOBAYASHI, M., SHINOMIYA, K., ITASAKA, S., YOSHIMURA, M., GUO, G., HIRAOKA, M. & HARADA, H. 2014. HIF-1-mediated

metabolic reprogramming reduces ROS levels and facilitates the metastatic colonization of cancers in lungs. 4**,** 3793.

ZHOU, D. X. & YEN, T. S. 1991. The ubiquitous transcription factor Oct-1 and the liver-specific factor HNF-1 are both required to activate transcription of a hepatitis B virus promoter. *Mol Cell Biol,* 11**,** 1353-9.

ZHU, M., GUO, J., LI, W., LU, Y., FU, S., XIE, X., XIA, H., DONG, X., CHEN, Y., QUAN, M., ZHENG, S., XIE, K. & LI, M. 2015a. Hepatitis B virus X protein induces expression of alpha-fetoprotein and activates PI3K/mTOR signaling pathway in liver cells. *Oncotarget,* 6**,** 12196-208.

ZHU, M., GUO, J., LI, W., XIA, H., LU, Y., DONG, X., CHEN, Y., XIE, X., FU, S. & LI, M. 2015b. HBx induced AFP receptor expressed to activate PI3K/AKT signal to promote expression of Src in liver cells and hepatoma cells. *BMC Cancer,* 15.

ZHU, P., TAN, M. J., HUANG, R. L., TAN, C. K., CHONG, H. C., PAL, M., LAM, C. R., BOUKAMP, P., PAN, J. Y., TAN, S. H., KERSTEN, S., LI, H. Y., DING, J. L. & TAN, N. S. 2011. Angiopoietin-like 4 protein elevates the prosurvival intracellular O2(-):H2O2 ratio and confers anoikis resistance to tumors. *Cancer Cell,* 19**,** 401-15.

ZLOTNICK, A., CHENG, N., STAHL, S. J., CONWAY, J. F., STEVEN, A. C. & WINGFIELD, P. T. 1997. Localization of the C terminus of the assembly domain of hepatitis B virus capsid protein: Implications for morphogenesis and organization of encapsidated RNA. *Proc Natl Acad Sci U S A,* 94**,** 9556-61.

8. SUPPLEMENTARY FIGURES

		Fold Up-regulation				
Genes	Cellular Function	1% O2	HepG2.215	HBV 24h	HBV 72h	Fold Change (24-72h)
ADM	Preprohormone which is cleaved to form two biologically active peptides, adrenomedullin and proadrenomedullin	1.05	4.0242	5.15	0.64	-8.046875
ADORA2B	Member of the G protein-coupled receptor superfamily	3.88	0.5502	7.07	2.73	-2.58974359
ALDOA	Glycolytic enzyme that catalyses the reversible conversion of fructose-1,6-bisphosphate to glyceraldehyde 3-phosphate and dihydroxyacetone phosphate	28.12	1.3095	221.02	4.64	-47.63362069
ANGPTL4	Functions as a serum hormone that regulates glucose homeostasis, lipid metabolism, and insulin sensitivity	8.33	14.4141	92.40	7.58	-12.18997361
ATR	Kinase that is activated by DNA damage	0.03	0.2298	1.22	0.01	-1.22
BHLHE40	Transcriptional repressor involved in the regulation of the circadian rhythm by negatively regulating the activity of the clock genes	0.02	2.325	1.29	0.03	-43
BLM	DNA-stimulated ATPase and ATP-dependent DNA helicase activities	55.86	0.3114	0.59	13.04	22.10169492
BNIP3	Mitochondrial protein that contains a BH3 domain and acts as a pro-apoptotic factor	34.29	4.759	0.48	52.86	110.125
BNIP3L	Homologue of BNIP3. Inhibits apoptosis induced by BNIP3.	2.32	3.1765	6.19	0.19	-32.57894737
BTG1	Anti-proliferative gene family that regulates cell growth and differentiation	2.57	2.3231	12.43	1.60	-7.76875
CA9	Catalyse the reversible hydration of carbon dioxide	82.00	171.4307	12.31	0.28	-43.96428571
CCNG2	Regulator of cyclin-dependent protein kinases	335.72	1.1431	16.21	1.31	-12.3740458
DNAJC5	Involved in the calcium-mediated control of a late stage of exocytosis	3.46	0.4959	0.38	1.26	3.315789474
EGLN2	Transcriptional complex that is involved in oxygen homeostasis	88.29	0.3262	233.84	5.31	-44.03766478
EGR1	Transcriptional regulator of genes required for differentitation and mitogenesis	10.37	0.3656	14.64	0.53	-27.62264151
EIF4EBP1	Repressor of translation initiation that regulates EIF4E activity	1.24	0.553	7.42	0.81	-9.160493827
ENO1	Role in glycolysis, growth control, hypoxia tolerance and allergic responses	1.70	1.2238	7.39	1.24	-5.959677419
EPO	Regulates red cell production by promoting erythroid differentiation and initiating haemoglobin synthesis	31.12	0.7522	258.13	5.10	-50.61372549
ERO1A	Oxidoreductase involved in disulphide bond formation in the endoplasmic reticulum	20.00	1.7043	185.04	6.09	-30.38423645
GAPDH	Catalyses the sixth step of glycolysis	5460.59	1.7002	1300.92	1643.36	1.263229099
GYS1	Catalyses the addition of glucose monomers to the growing glycogen molecule	0.01	1.7439	1.24	0.01	-124
HIF1A	Transcriptional complex that is involved in oxygen homeostasis	94.98	0.213	0.53	15.05	28.39622642
HIF1AN	Functions as an oxygen sensor and hydroxylates HIF1A	47.72	0.4145	0.39	11.49	29.46153846
HIF3A	Transcriptional complex that is involved in oxygen homeostasis	2.98	1.0543	6.47	0.16	-40.4375
HK2	Hexokinases phosphorylate glucose to produce glucose-6-phosphate	2.20	1.6371	5.25	0.39	-13.46153846
HMOX1	Mediates the first step of heme catabolism	105.16	0.4484	10.07	0.27	-37.2962963
HNF4A	Nuclear transcription factor which binds DNA as a homodimer	85.45	0.3605	14.54	0.46	-31.60869565
HPRT1	Catalyses conversion of hypoxanthine to inosine monophosphate and guanine to guanosine monophosphate	1720.50	0.6466	409.09	382.45	-1.069656164
IER3	Role in the ERK signalling pathway by inhibiting the dephosphorylation of ERK by phosphatase PP2A-PPP2R5C holoenzyme	0.71	1.1243	1.30	0.05	-1.3
MAP3K1	Serine/threonine kinase	95.34	0.3138	221.57	3.39	-65.35988201
MET	Prototypical receptor tyrosine kinase	7.81	0.372	100.37	2.39	41.9958159
MIF	Pro-inflammatory cytokine, involved in the innate immune response to bacterial pathogens	0.07	0.8749	0.79	12.78	16.17721519

Figure 8.1A Comparison of up-regulated hypoxic genes in HBV de novo infection

Genes	Cellular Function	Fold Up-regulation				Fold Change (24-72h)
		1% O2	HepG2.215	HBV 24h	HBV 72h	
MMP9	Involved in the breakdown of extracellular matrix in normal physiological processes	1.64	1.6806	7.34	7.37	1.004087193
MXI1	Transcriptional repressor thought to negatively regulate MYC function	29.25	1.3517	15.83	23.75	1.500315856
NAMPT	Enzyme in the Nicotinamide adenine dinucleotide (NAD+) salvage pathway	364.13	0.5562	38.11	52.74	1.383888743
NCOA1	Transcriptional coactivator for steroid and nuclear hormone receptors	15.78	0.434	2.16	3.69	1.708333333
NDRG1	Cytoplasmic protein involved in stress responses, hormone responses, cell growth, and differentiation. necessary for p53-mediated caspase activation and apoptosis	12.59	11.221	0.81	6.09	7.518518519
NFKB1	Subunit of NF-κB transcription factor	8.33	0.2933	38.03	0.09	-422.5555556
NOS3	Nitric Oxide Synthase 3 - mediates VEGF-induced angiogenesis	9.89	0.2492	113.91	0.26	-438.1153846
ODC1	Enzyme of the polyamine biosynthesis pathway	9822.77	0.2286	5.42	1647.04	303.8819188
PDK1	Mitochondrial multienzyme complex that catalyses the oxidative decarboxylation of pyruvate	4.79	1.9415	2.76	0.01	-276
PFKFB3	Activator of 6-phosphofructokinase-1 (PFK-1), stimulating glycolysis	6356.55	5.9067	6539.44	2842.06	-2.300950719
PFKFB4	Regulates the steady-state concentration of fructose 2,6-bisphosphate	2766.72	6.611	609.25	902.42	1.481198195
PFKL	Catalyses the conversion of D-fructose 6-phosphate to D-fructose 1,6-bisphosphate	73.17	0.8318	9.94	14.09	1.41750503
PFKP	Catalyses the phosphorylation of D-fructose 6-phosphate to fructose 1,6-bisphosphate by ATP	0.95	0.7191	1.23	1.96	1.593495935
PGAM1	Mutase that catalyses the reversible reaction of 3-phosphoglycerate (3-PGA) to 2-phosphoglycerate (2-PGA) in the glycolytic pathway	27.34		5.48	10.53	1.921532847
PGF	Growth factor found in placenta which is homologous to vascular endothelial growth factor	1.63	0.5946	0.01	3.63	363
PGK1	Glycolytic enzyme that catalyses the conversion of 1,3-diphosphoglycerate to 3-phosphoglycerate	2.59	6.1333	0.01	4.99	499
P4HA1	Component of prolyl 4-hydroxylase - enzyme involved in collagen synthesis	19232.08	1.4625	2.85	1359.28	476.9403509
PIM1	Serine/threonine kinase that controls cell growth, differentiation and apoptosis	0.94	0.4505	115.36	15.22	-7.579500657
PKM	Pyruvate kinase that catalyses the transfer of a phosphoryl group from phosphoenolpyruvate to ADP, generating ATP and pyruvate	4.56	1.0944	70.06	23.22	-3.017226529
PLAU	Serine protease that converts plasminogen to plasmin	55.35	0.2552	1270.03	163.69	-7.758751298
RBPJ	Transcriptional regulator important in the Notch signalling pathway	295.92	0.7585	1045.30	207.02	-5.049270602
RPLP0	Subunit of ribosomes that catalyse protein synthesis	0.97	0.6416	1.65	2.78	1.684848485
RUVBL2	Gene product has both ATPase and DNA helicase activities	0.18	0.4643	1.13	17.63	15.60176991
SERPINE1	Serine protease inhibitor	0.14	4.0525	1.22	10.08	8.262295082
SLC16A3	Lactic acid and pyruvate transport across plasma membranes	75.23	1.7449	31.12	38.17	1.226542416
SLC2A1	Transport of glucose across the plasma membranes	191.64	0.4744	61.98	103.50	1.669893514
SLC2A3	Transport of glucose across the plasma membranes	32.18	2.4128	2.87	3.81	1.327526132
TFRC	Cell surface receptor necessary for cellular iron uptake	37.23	0.5062	4.86	8.15	1.676954733
TP53	Tumour suppressor protein that regulates cell cycle arrest, apoptosis, senescence, DNA repair, or changes in metabolism	11.72	0.3532	54.06	0.09	-600.6666667
TPI1	Catalyses the isomerization of glyceraldehydes 3-phosphate (G3P) and dihydroxy-acetone phosphate (DHAP) in glycolysis and gluconeogenesis	8.29	1.1862	68.94	0.13	-530.3076923
TXNIP	Regulator of Hepatic Glucose Production	11689.70	1.0508	1.35	1544.26	1143.896296
USF2	Member of the basic helix-loop-helix leucine zipper family	7154.94	0.4413	1.98	941.90	475.7070707
VEGFA	Growth factor active in angiogenesis, vasculogenesis and endothelial cell growth	2.51	4.4281	1.28	0.01	-128

Figure 8.1B Comparison of up-regulated hypoxic genes in HBV de novo infection (Cont.)

Legend on next page

Figure 8.1B Comparison of up-regulated hypoxic genes in HBV de novo infection (Cont.)

A/B) Table summarising up-regulated genes on hypoxic gene array and comparing changes between 24 and 72 hours of early infection. *De novo* infection of HepG2-NTCP K7 cells with HBV (MOI 100). For comparison, table includes genes up-regulated by hypoxic control (1% oxygen) and HepG2.2.15 cells.

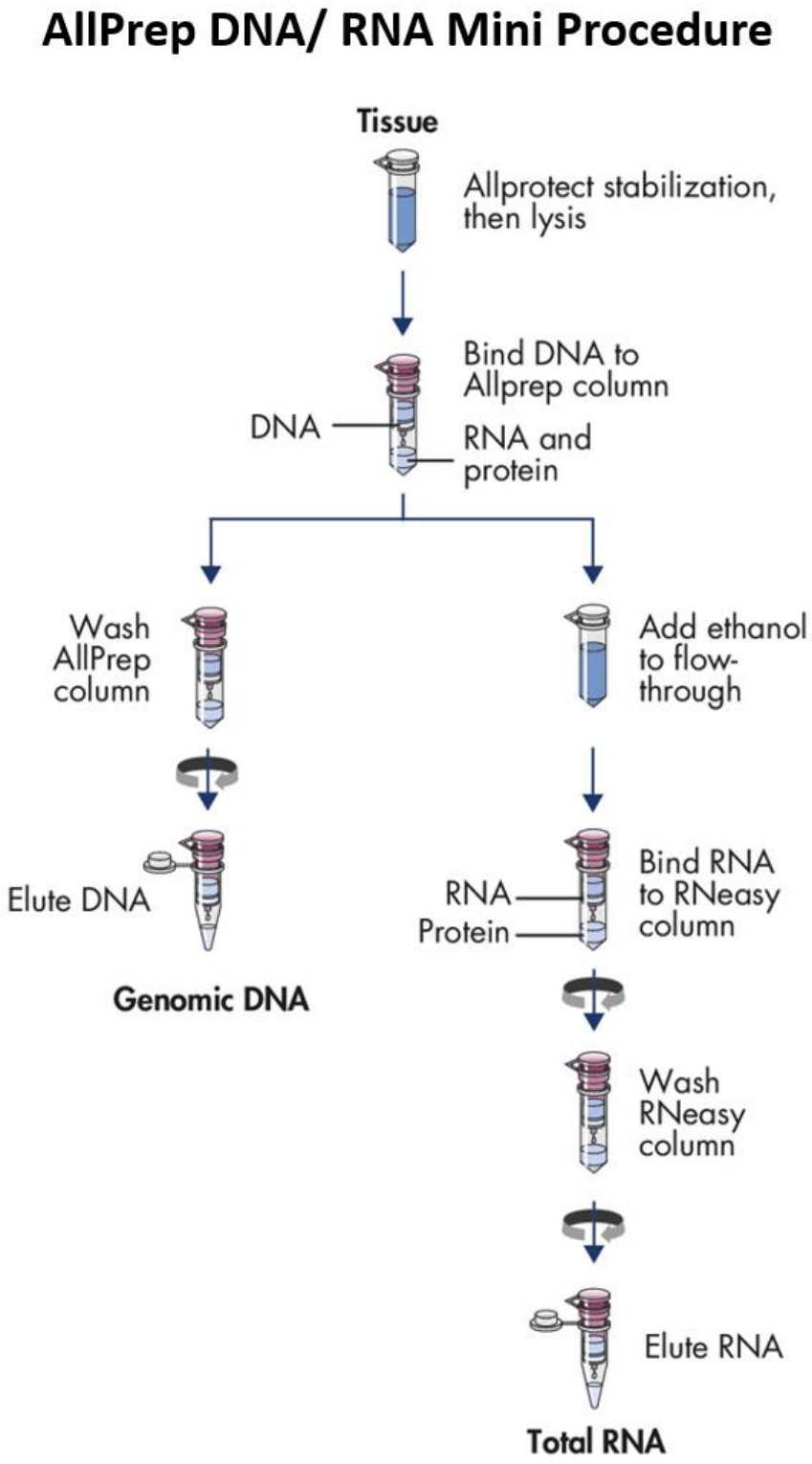

Figure 8.2 Cartoon representation of DNA/ RNA purification process (adapted from Qiagen, USA)